SFERA-III

Solar Facilities for the European Research Area

Training for industries
9-12th July 2019, Odeillo, France

Presentation of the SFERA-III project
Emmanuel Guillot, CNRS-PROMES

NETWORKING

THIS PROJECT HAS RECEIVED FUNDING FROM THE EUROPEAN UNION’S HORIZON 2020 RESEARCH AND INNOVATION PROGRAMME UNDER GRANT AGREEMENT NO **823802**

SFERA-III

Solar Facilities for the European Research Area

No	Name	Short name	Country
1	CENTRO DE INVESTIGACIONES ENERGETICAS, MEDIOAMBIENTALES Y TECNOLOGICAS-CIEMAT	CIEMAT	Spain
2	CENTRE NATIONAL DE LA RECHERCHE SCIENTIFIQUE CNRS	CNRS	France
3	AGENZIA NAZIONALE PER LE NUOVE TECNOLOGIE, L'ENERGIA E LO SVILUPPO ECONOMICO SOSTENIBILE	ENEA	Italy
4	DEUTSCHES ZENTRUM FUER LUFT - UND RAUMFAHRT EV	DLR	Germany
5	COMMISSARIAT A L ENERGIE ATOMIQUE ET AUX ENERGIES ALTERNATIVES	CEA	France
6	UNIVERSIDADE DE EVORA	UEVORA	Portugal
7	EIDGENOESSISCHE TECHNISCHE HOCHSCHULE ZUERICH	ETHZ	Switzerland
8	Fundacion IMDEA Energia	IMDEA	Spain
9	THE CYPRUS INSTITUTE	CYI	Cyprus
10	FRAUNHOFER GESELLSCHAFT ZUR FOERDERUNG DER ANGEWANDTEN FORSCHUNG E.V.	Fraunhofer	Germany
11	Laboratorio Nacional de Energia e Geologia I.P.	LNEG	Portugal
12	MIDDLE EAST TECHNICAL UNIVERSITY	METU	Turkey
13	UNIVERSIDAD DE ALMERIA	UAL	Spain
14	EURONOVIA	EURO	France
15	EUROPEAN SOLAR THERMAL ELECTRICITY ASSOCIATION	ESTELA	Belgium

- 2019-2022
- 9 countries
- 15 partners
- 915 person months
- Grant: 9.1 M€
- 3 activities:
  - Transnational Access
  - Networking (includes this action)
  - Joint Research

Solar Facilities for the European Research Area

WP13	Management and Coordination	CIEMAT

Who we are?

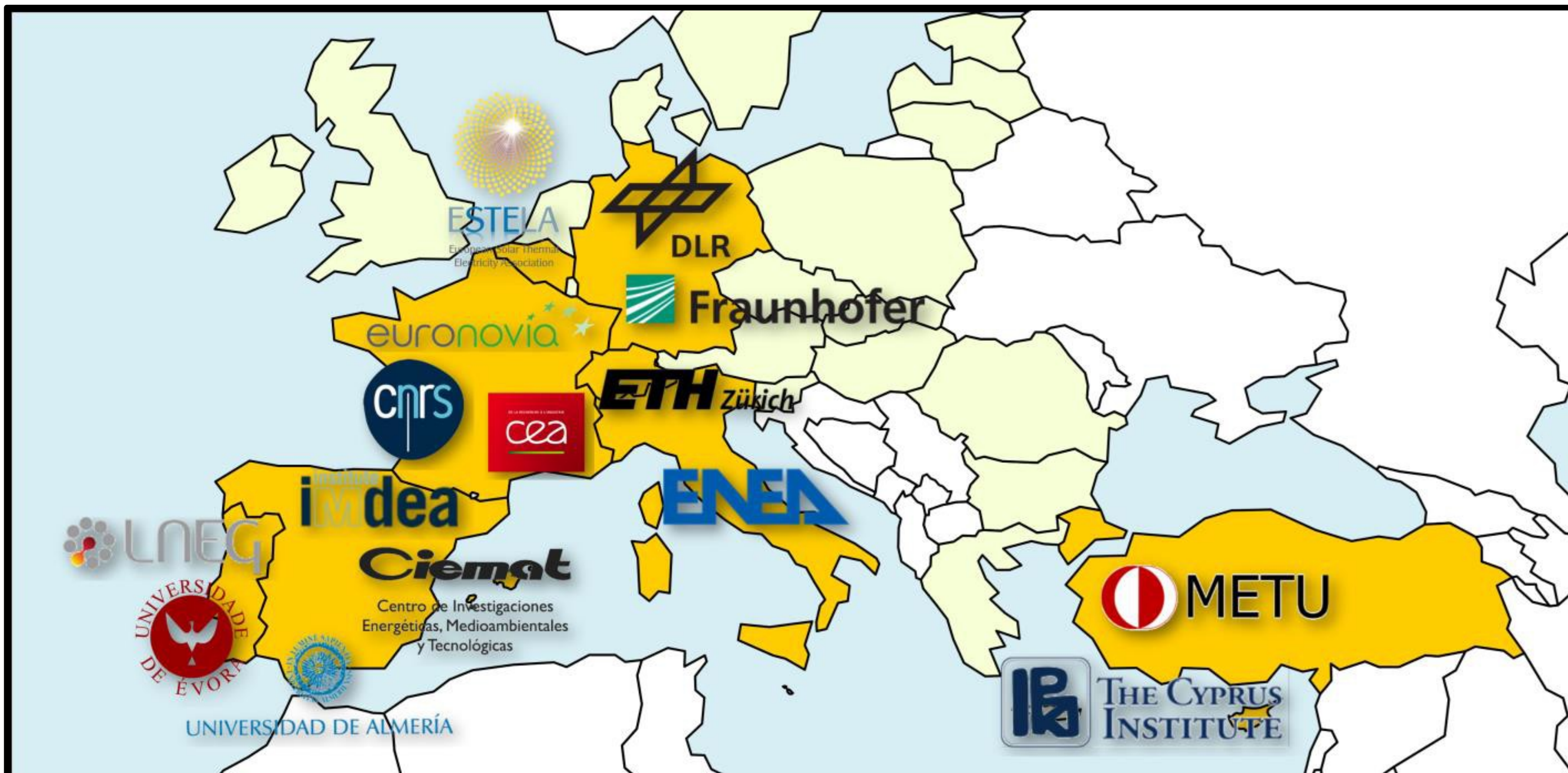

WP13	Management and Coordination	CIEMAT

What are we implementing?

Transnational Access Activities

- 4 access campaigns to our RIs
- 9 partners participating for the very first time
- 11 European advanced solar laboratories and 2 advanced solar laboratories located in two neighbouring countries
- A total of 15 RIs (**11 new RIs**)
- With a total of 47 installations (**31 new installations**)
- 452 weeks of access to the RIs
- 357 Users accessing the RIs

*What follows is a short and random selection of facilities available thru Transnational Access for **Industry** and/or Academy:*

- Hosting of **selected** projects
- On-site **1 or 2 persons** teams
- For **1 to ~3 weeks**
- For industry: IP is **yours**
- 1 campaign per year, ~May
- Travel, accommodation AND operation of the facility **INCLUDED**

https://sfera3.sollab.eu/access/#call

WP5	Provision of the TA Activity	

Site of Odeillo

WP5	Provision of the TA Activity	CIEMAT

WP5	Provision of the TA Activity	CIEMAT

Installation short name: CRS

- Thermal power: 2.1 MW
- 92-heliostat field.
- 43 m-high tower with two testing platforms.
- Heliostats communication by cabling and radio with the control room
- Cryogenic installation (Up to 200 kg/h N2)
- Steam Generator (20 kg/h)
  - Refrigeration Tower
  - Water at 50 m^3/h at 9 bar (Capacity 700 kW)
- Air Pressure Circuit (1.5 m^3/min at 7 – 8 bar)
- Analytical equipment
  - Micro-GC Varian
  - IR cabinet
- Flux measurement system
  - Moving bar (CCD camera)

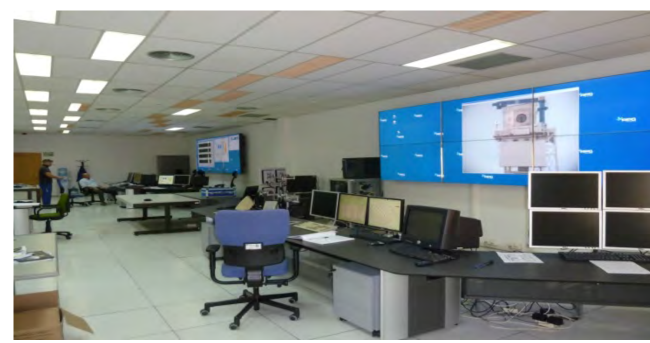

WP5	Provision of the TA Activity	CIEMAT

Installation short name: SOLFU

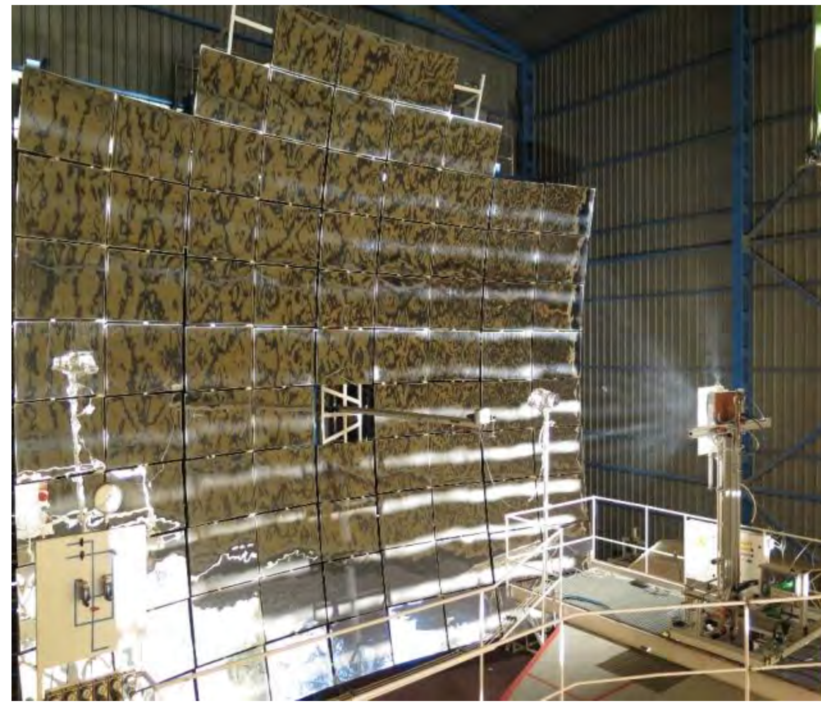

WP5	Synlight	DLR

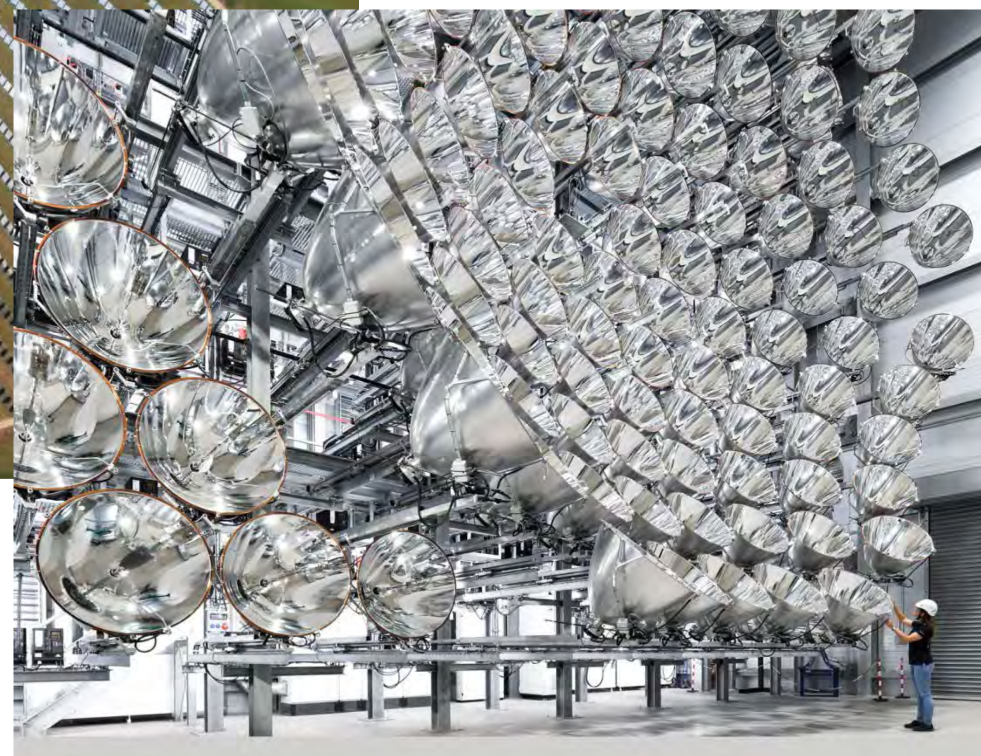

WP5	Provision of the Transnational Access Activity	IMDEA

WP5	Provision of the TA Activity	ENEA

PCS – plant

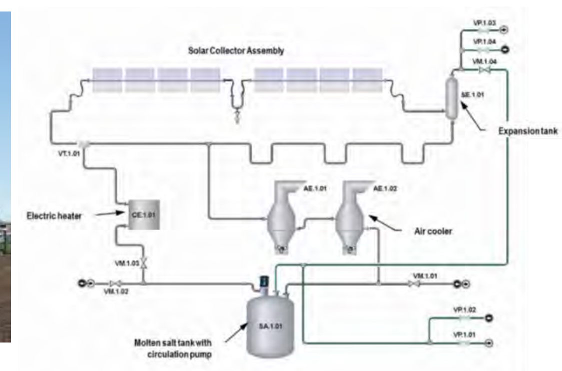

WP5	Provision of the TA Activity	cnrs

5 weeks of MicroSol'R

3 heliostats, 150 kWth, 300 suns
Complete oil+steam process including a thermocline.

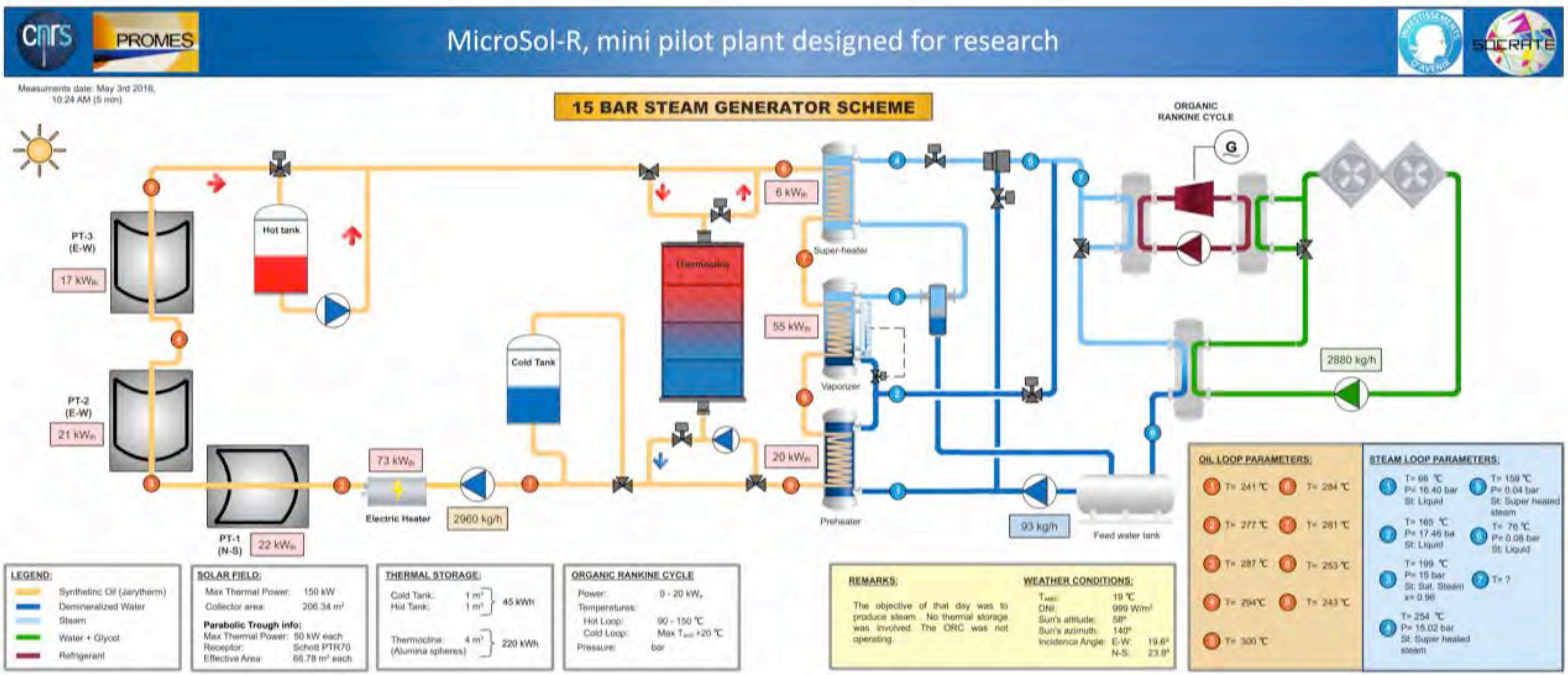

The values here were for a specific test,
they are neither nominal nor representative.

WP5	Provision of the TA Activity	UEVORA

- The **PECS** is a two-axis platform (test bench dimensions: $18*13m^2$) with an oil loop to test concentrator collectors and promote collector development, as well as certification purposes. There are two circuits, one operating with thermal oil up to 400ºC and the other with pressurized water.

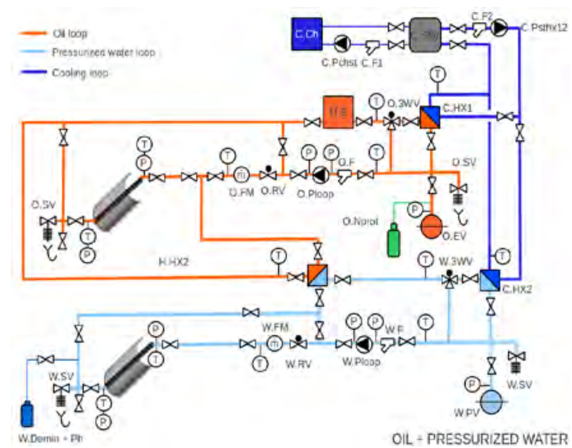

WP5	Provision of the TA Activity	Fraunhofer

C-lab: Concentrator optics laboratory with indoor facilities for surface characterization and optical simulation of materials and CSP systems.

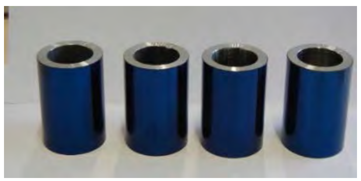

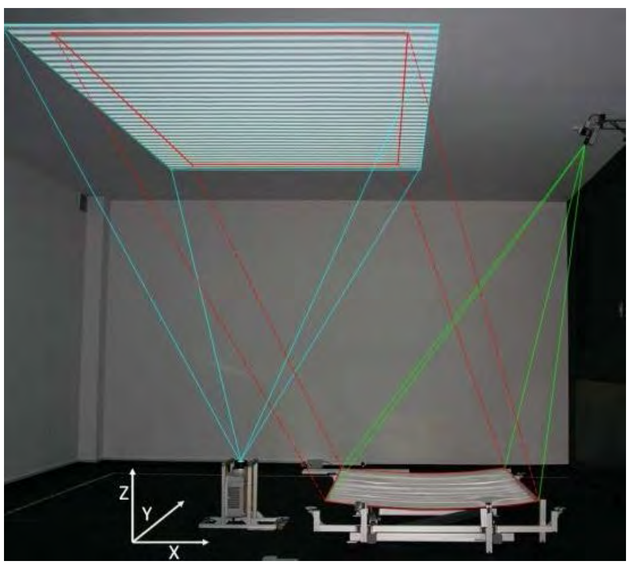

WP5	Provision of the TA Activity	CEA

Optical Characterisation of Materials (Opti-Lab)

Hemispherical absorptance of Flat Samples & tubes

PerkinElmer Lambda 950
\+ 150mm integrating sphere

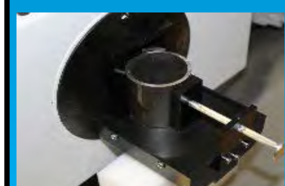

Flat Samples
& **Tubes**

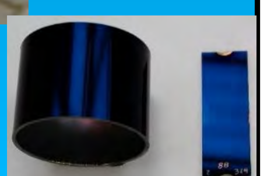

FTIR Bruker Tensor 27
\+ 150 mm integrating sphere

Certified Reference Tubes

spectral emittance in temperatur

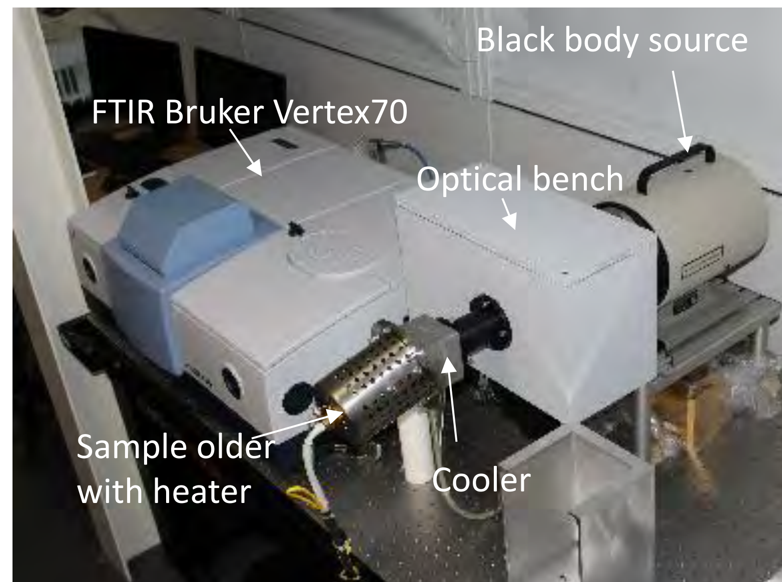

WP5	Provision of the TA Activity	CEA

Optical Characterisation of Systems (Shape)

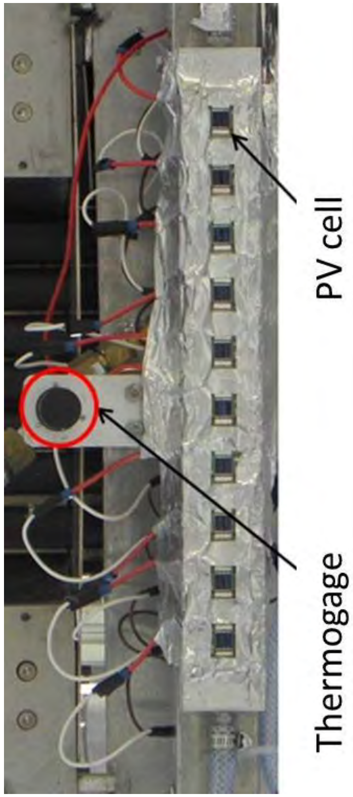

WP5	Provision of the TA Activity	CEA

Accelerated Ageing under Controlled Conditions (Indoor)

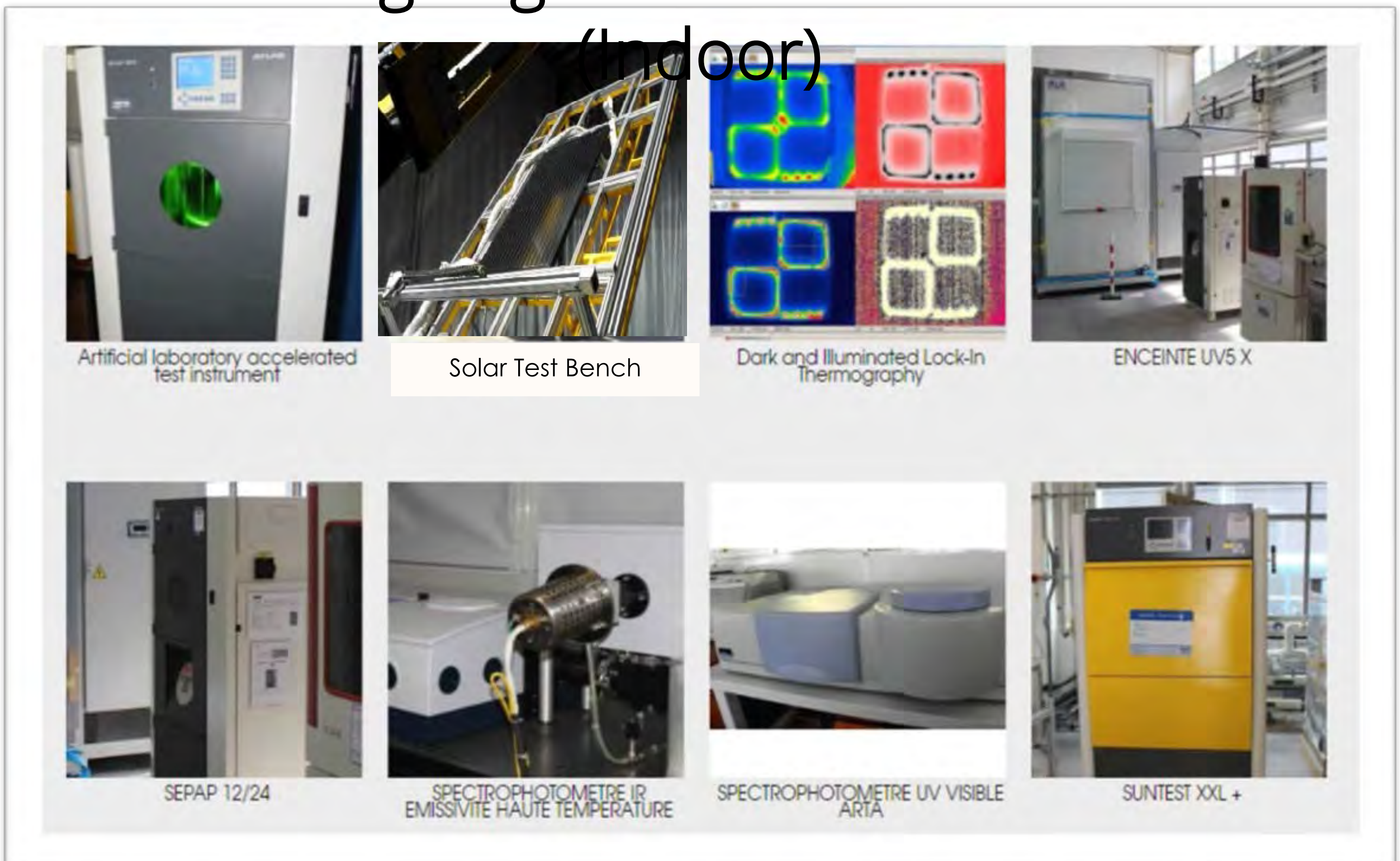

WP5	Provision of the TA Activity	LNEG

Laboratory of Materials and Coatings (LMR):

Durability of materials by exposure in two Outdoor Exposure Testing (OET) Sites:

- ➢ an European reference test site for UV radiation with corrosivity C2/C3 – *Lumiar/Lisboa*
- ➢ a marine/industrial test site with very high/extreme corrosivity C5/CX – *Sines*

Monitored parameters:
- Temperature
- Relative humidity
- Wetness time
- Radiation
- Rain
- Chloride, Sulphur dioxide and Nitrogen oxides in atmosphere

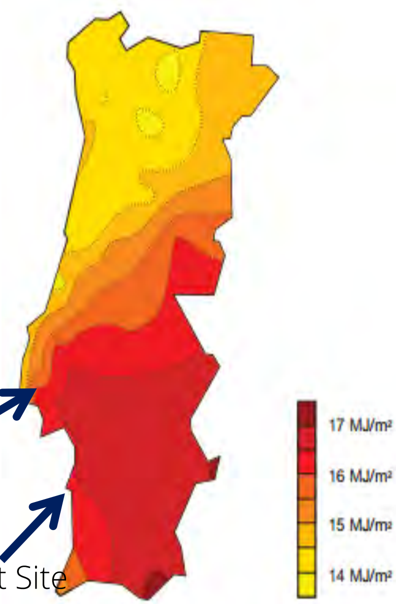

Lumiar/Lisboa
Urban Test Site
Corrosivity C2/C3

Sines
Marine/industrial Test Site
Corrosivity C5/CX

Pilot plants for water treatment by solar photocatalysis

WP13	Management and Coordination	CIEMAT

What are we implementing?

Joint Research Activities

- Improvement of the services offered by the RIs
- Design of an e-Infrastructure for data, computing and networking
- Support of the definition of common standards and protocols
- Curation, preservation and provision of access to data collected or produced under the project

WP 7	Development and Testing of New Technological Concepts for Solar Desalination and Water Treatment Facilities	CyI

Main Expected Outputs:

- Guidelines for reporting on DWT systems
- Testing procedures for new components for DWT processes
- Increased capacity development of participating RIs
- Increased modelling capabilities for DWT
- Enhance recover and market penetration of exploitable products from wastewater treatment processes

Solar Facilities for the European Research Area

WP 8	JRA3 Dynamic control and diagnostics of integrated systems for the production of solar fuels.	ETHZ

Main Expected Outputs: Improved research techniques, diagnostics and control tools in three key areas;

a) Performance testing of materials used in solar fuel production reactors, in terms of stability, thermodynamic and kinetic performance.

b) Solar fuel reactor performance monitoring and evaluation according to; fuel composition, long term stability, specific fuel conversion, and efficiency.

c) Automation and dynamic control of reactors under intermittent solar conditions.

WP 9	Monitoring physical properties of receiver materials at focal point of concentrated solar facilities	cnrs

Main Expected Outputs:

1. Method and setup for **thermomechanical behaviour** in-situ monitoring of real solar receiver
2. Improvement of laboratory **emissivity** measurements
3. Improvement of in-situ **emittance** measurements for the determination of solar receivers **temperature**
4. Improvement of **aerial platforms** for the in-situ determination of linear and point solar receivers **temperature**
5. Improvement of accelerated ageing setups

WP 10	Sensor calibrations Performance parameters	DLR

Main Expected Outputs (1):

- Increased accuracy and comparability of sensor measurements and test bench results
  - Reflectometer/soiling measurements
  - Dynamometer to measure forces/moments on collectors and REPAs Parabolic trough receiver heat loss measurements
- Intra-hour solar DNI forecasting to increase useful on-sun experimental time in solar concentrating RIs
- Answer the question, if we need sky imagers to increase the accuracy of performance parameters
- Increased accuracy of transient on-sun tests of Fresnel & PTC collectors
- Increased robustness of CYI Fresnel research infrastructure against DNI variations

WP 10	Sensor calibrations Performance parameters	DLR

Main Expected Outputs (2):

- Increased quality of shape measurements of heliostats and parabolic troughs
- Increased quality of the pointing accuracy measurements in facilities with low cost small-size heliostats

  → VHCST heliostat field at IMDEA (Spain) and PROTEAS (Cyprus)

WP 11	**Towards an European e-Infrastructure on CST technologies**	CIEMAT

Main Expected Outputs:

1. Definition of the hardware and software required for initial implementation of the e-infrastructure (i.e., the central node at PSA connected to peripheral nodes at DLR, CNRS and ENEA)
2. Definition of the budget needed for the initial implementation of the e-infrastructure
3. Definition of the technical requirements (hardware and software) to be fulfilled by others R+D centres to become a node of the e-infrastructure
4. Definition of the tools and options to be offered by the e-infrastructure
5. Preparation of a Data Management Plan and Access Policy for the e-infrastructure

THANK YOU FOR YOUR ATTENTION!
ANY QUESTIONS?

SFERA III: Training on central receivers

Infrared measurements from a flying drone (UAV)

LABORATOIRE
PROCÉDÉS, MATÉRIAUX et ENERGIE SOLAIRE
.UPR 8521 du CNRS.
conventionnée avec l'université de Perpignan

PROCESSES, MATERIALS and SOLAR ENERGY LABORATORY

Solar Facilities for the European Research Area

Training course
July 10, 2019

Alex Le Gal, *PhD*
Benjamin Grange, *PhD*
Antoine Perez

PROMES-CNRS

Why to measure the surface temperature of a central receiver ?

- Necessary to evaluate heat exchange in the solar receiver (thermal efficiency calculation)

- Important to preserve constitutive materials

- Usefull to detect hot points (which can highlight a malfunction)

Constraints

On central solar receiver :

- High solar flux (from 200 to 800 kW/m²)
- High surface temperature (until 1100°C)
- Complex 3D geometry (surface receivers or volumetric receivers)
- Large thermal scene (several square meters)
- Far from operators (at height about 100 meters except beam down solar tower)
- Intense heat exchanges between the absorber and the heat transfer fluid
- Converging concentrated solar rays all around the focal point

↳ **Infrared measurement from a flying drone**

- Solar receiver : 3m x 2.6m – placed at 87 meters high
- 40 tubes coated with Pyromark absorbing black paint
- Under concentrated solar flux (from 100kW/m² to 600 kW/m²)
- Solar receiver temperature instrumentation: 91 thermocouples
  - 49 inside tubes
  - 14 on tube back side
  - 4 in the insulation
  - **24 on tube front surface (welded)**
- Poor spatial resolution of temperature measurements
- **Local hot points (T>1000°C) must be avoided !**
  - Alloy thermal limit
  - Active heliostat defocusing in case of overheating

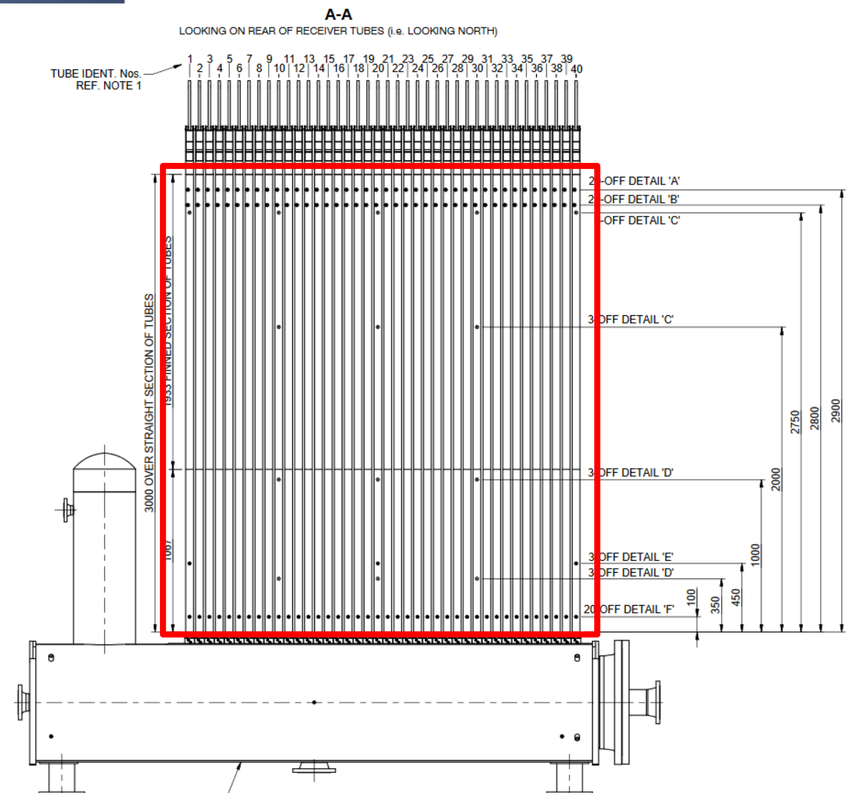

Next-CSP solar receiver

Observation of the solar receiver during the experimentation

- With good spatial resolution
- Hot point detection over the total surface of the solar receiver
- On-sun temperature measurement uncertainty estimation

How to measure a temperature of a surface under concentrated solar flux ?

- Thermocouple

- Pyrometer, Pyroreflectometer

- IR camera

Thermocouple

- Thermocouple (welded)
  - K-type could be used under concentrated solar flux but they indicate a wrong value with an important uncertainty.
  - Over-estimation because of the thermal resistance of the welding, Tc oxidation state, thermal stress & the solar flux.

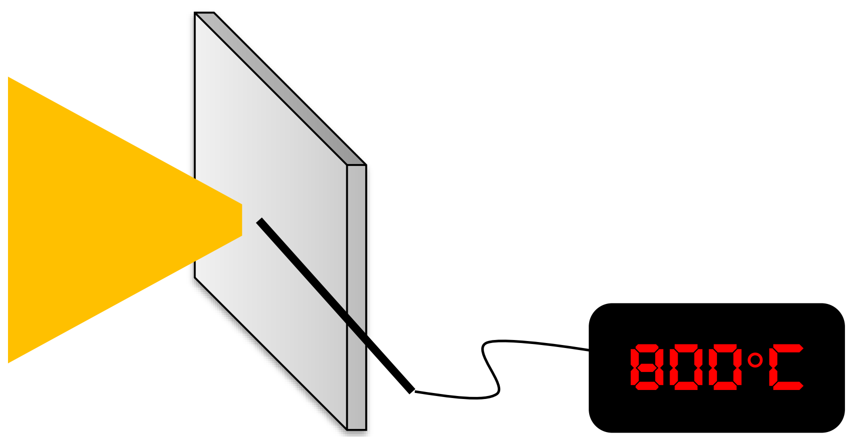

Thermocouple

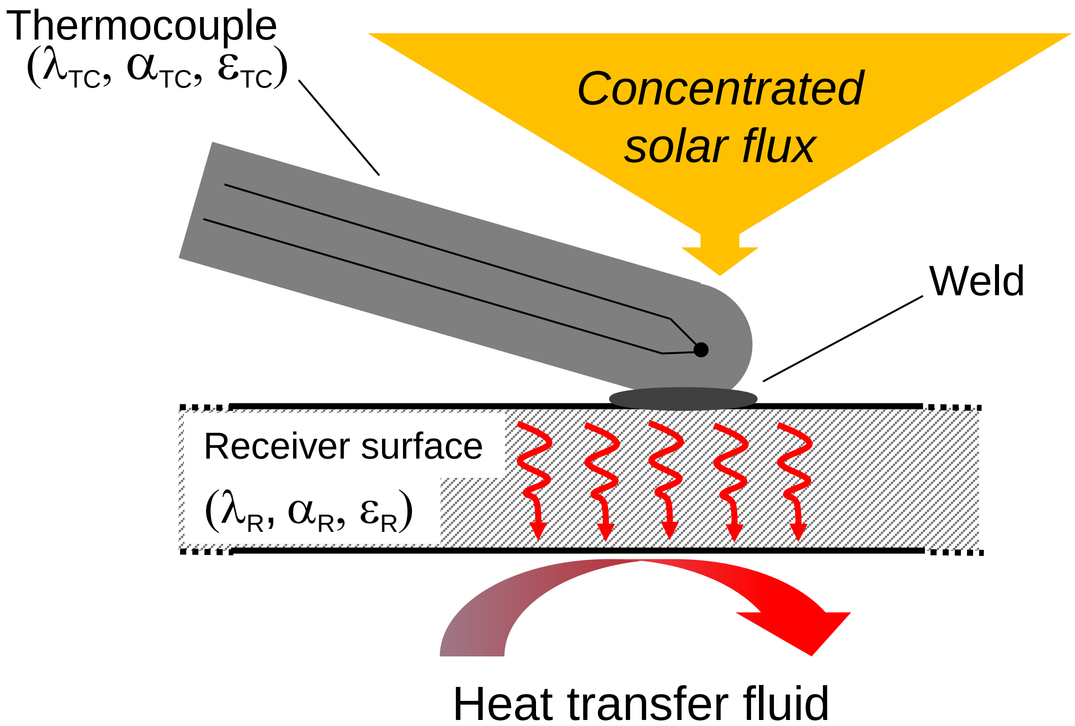

Thermal equilibrium = Power absorbed - Power re-radiated - Power transmitted (conduction + convection)

$$\lambda_{TC} \neq \lambda_{R},\ \alpha_{TC} \neq \alpha_{R},\ \varepsilon_{TC} \neq \varepsilon_{R},$$

A thermal resistance is induced by the welding so the convective heat exchange is different.

The temperature of the thermocouple is different from the temperature of the receiver’s surface

Thermocouple

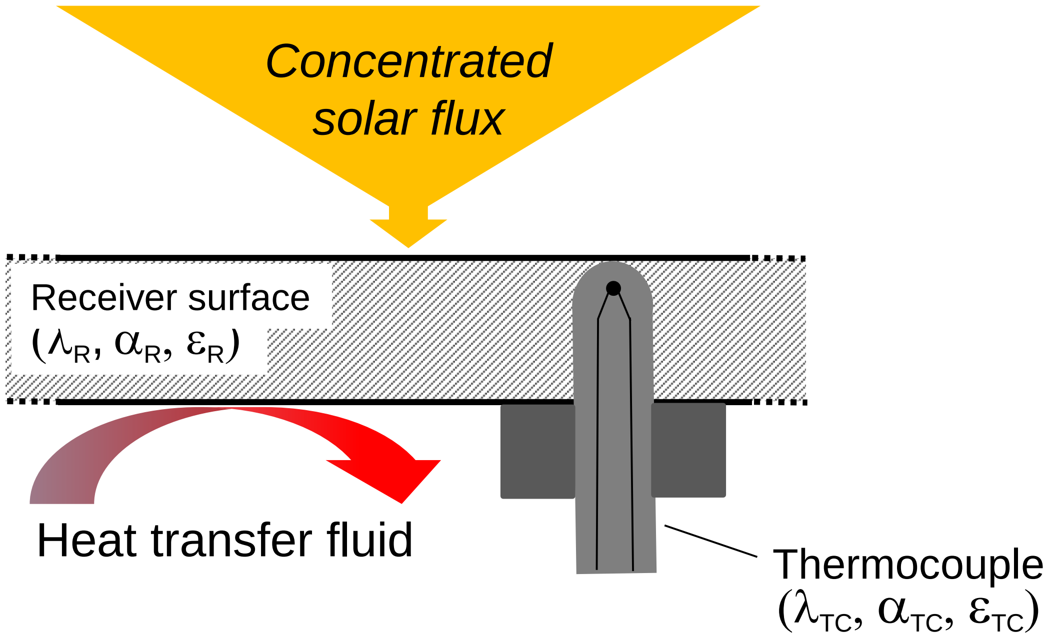

Thermal equilibrium = Power absorbed - Power re-radiated - Power transmitted (conduction + convection)

Only embedded thermocouple could provide correct temperature measurement of a surface under concentrated solar flux

Pyrometer - Pyroreflectometer

Pyrometer

- Temperature measured from IR radiation (not solar blind)
- The emissivity of the sample must be known
- For local temperature measurements (point measurement)

Pyroreflectometer

- Temperature measured from IR radiation (not solar blind)
- The method is based on thermal radiation and reflectivity measurement at two close wavelengths
- The reflectivity is measured in-situ (do not need to know the emissivity)
- For local temperature measurements (point measurement)
- For high temperature (>500°C)

IR camera

Principle :

- Thermal electromagnetic radiation measurement
- Based on the Planck's law
  (for black body, $\alpha=\varepsilon=1$)

$$L_{(\lambda,T)} = \frac{2hc^2}{\lambda^5}\frac{1}{e^{hc/(\lambda kBT)}-1}$$

With,
- L : the luminance
- h : the Planck constant
- c : the speed of light
- λ : the wavelength
- k_B : the Boltzmann constant
- T : the temperature

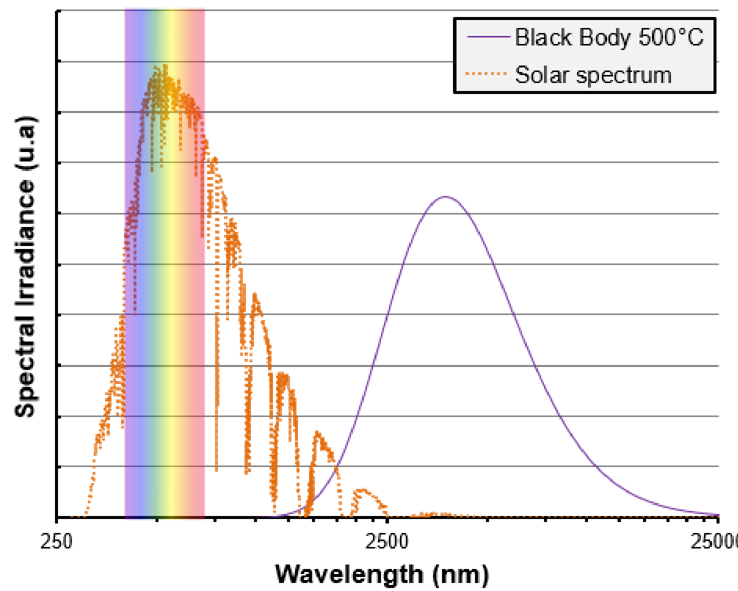

-The luminance of a surface is correlated to the luminance of a black body via the emissivity of the surface (Kirchhoff law)

➥ <u>the emissivity of the surface must be known !</u>

IR camera

Emissivity measurement

In situ reflectivity measurements are not possible, IR Spectrophotometer must be used

The emissivity is calculated over the range of the camera at different temperature from ambient temperature reflectivity measurement.

$$\varepsilon(T) = \frac{\int_{7.5\mu m}^{13\mu m} \left[1 - R(\lambda, T_a)\right] \cdot P(\lambda, T) \cdot d\lambda}{\int_{7.5\mu m}^{13\mu m} P(\lambda, T) \cdot d\lambda}$$

With, $\varepsilon(T)$: the sample thermal emittance at temperature T

λ: the wavelength

$R(\lambda, T_a)$: the sample spectral reflectance measured at room temperature T_a

$P(\lambda, T)$: Planck's law of blackbody emission irradiance at temperature T

Hemispherical directional reflectivity of aged Pyromark coated on inconel

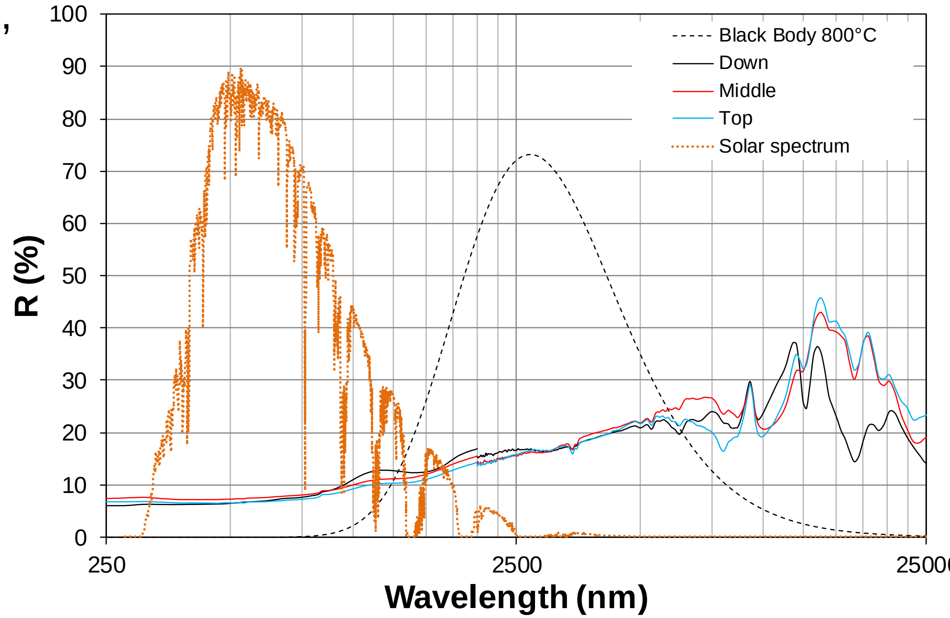

The temperature measurement using IR camera is accurate if only the emissivity is well known. Reflectivity evolution with aging must be followed through measurements in the absence of proven aging model.

IR camera

Emissivity measurement

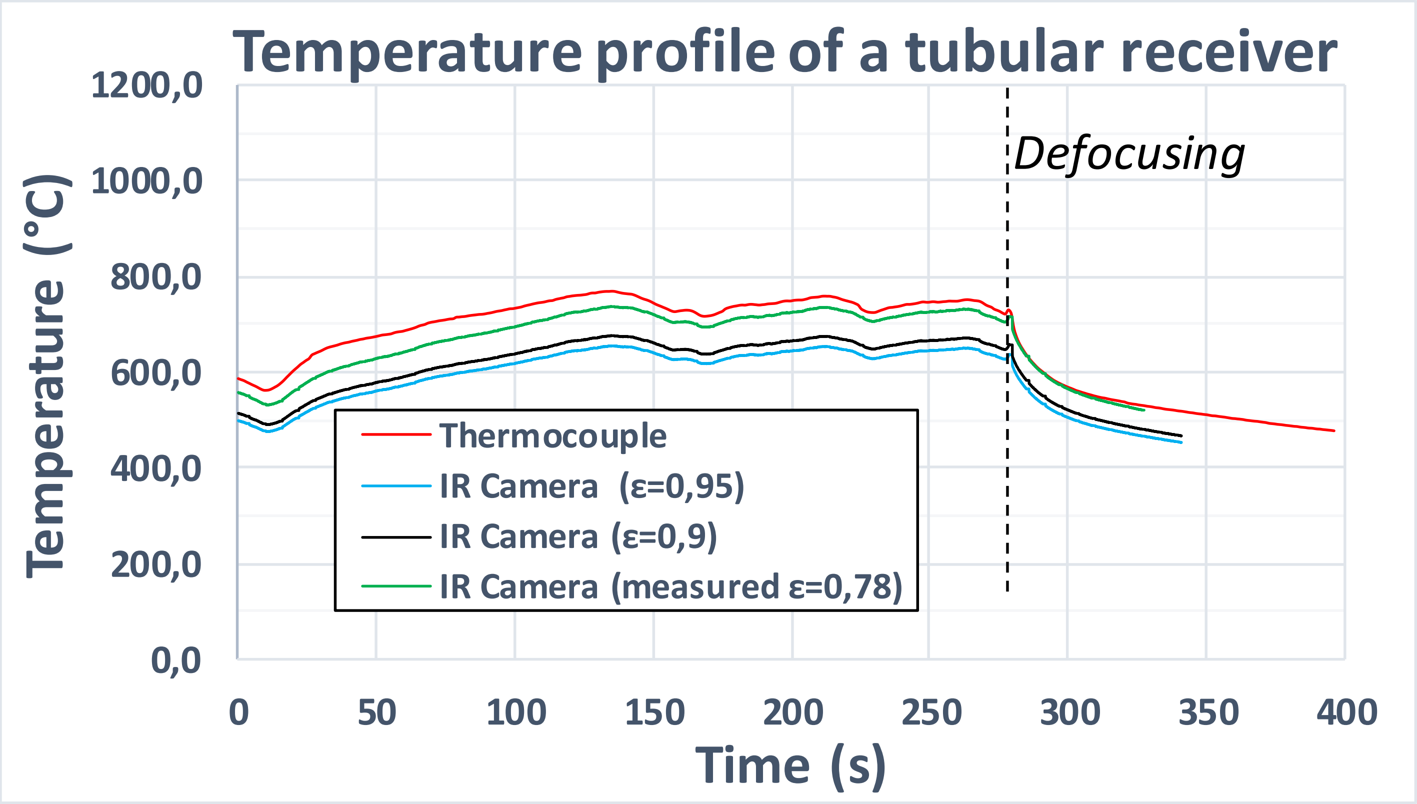

Until 80°C of temperature difference from ε=0.95 to ε=0.78

IR camera

How to choose the good IR camera ?

Several trademarks exist :

- Optris
- Workswell
- FLIR
- …

Selection parameters :

- Temperature range
- Spectral measurement range
- Lens
- Optical resolution

	Trademark	Model	Lens	Optical resolution	Temperature range	Spectral range	Prize	Comments
	FLIR	Vue pro 640	32°x26°	640x512	-40 to 550°C	7.5-13.5 µm	~ 4k€	±5°C
	Optris	Pi640	33°x25° 15°x10° 60°x45°	640x480	-20 to 900°C (200 to 1500°C optional)	7.5-13.5 µm	~ 7k€	±2°C Automatic hot point detection
	Workswell	WIRIS pro	18°x14° 35°x27° 69°x56°	640x512	400 to 1500°C (optional high temperature filter)	7.5-13.5 µm	~ 6 k€	±2°C Digital zoom x14 (IR camera) Autofocus optical visual camera

IR camera

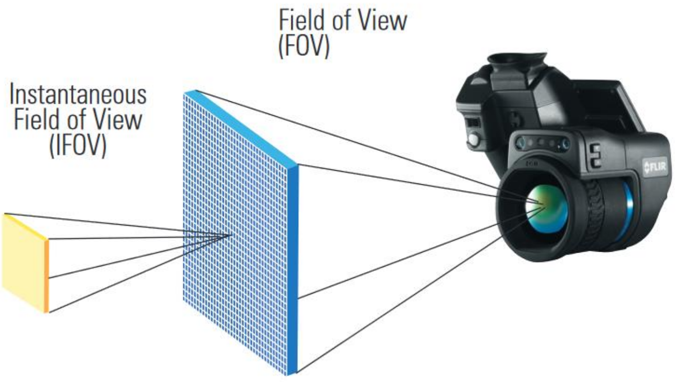

IFOV is an angular projection of just one of the detector's pixels in the IR image. The area each pixel can see depends on your target distance for a given lens.

Field Of View

The **IFOV** is the angular projection of a pixel. IFOV is function of the distance, the lens and the optical resolution.

Example:
Lens : 35°x 27°
Resolution : 640 x 512 pixel
Distance : 20 meters

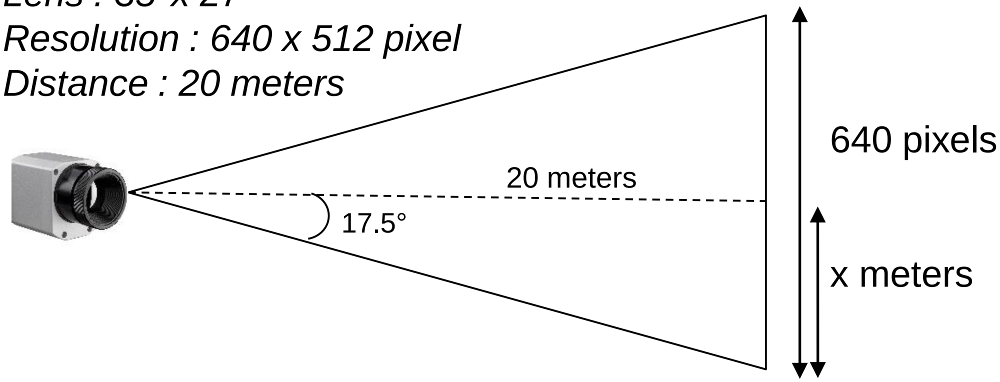

Tan(17.5)=x/20	Pixel size= 2x/nb pixels
X= tan(17.5)x20	Pixel size = 12.6/640
X= 6.3 m	Pixel size = 19.7 mm/pixel

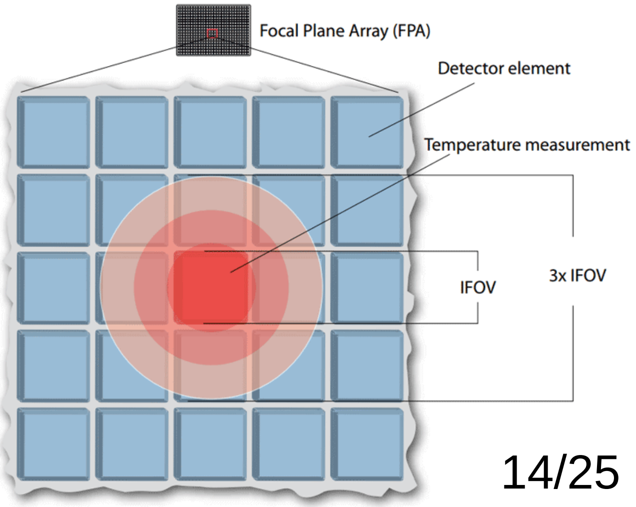

Due to a phenomenon called optical dispersion, radiation from a very small area will not give one detector element enough energy for correct value.
The **MFOV** correspond to 3xIFOV and gives an accurate temperature measurement.

IR camera

Field Of View *(simulation)*

	Optris Pi640	*Wiris pro*
Hot point detection resolution (IFOV)	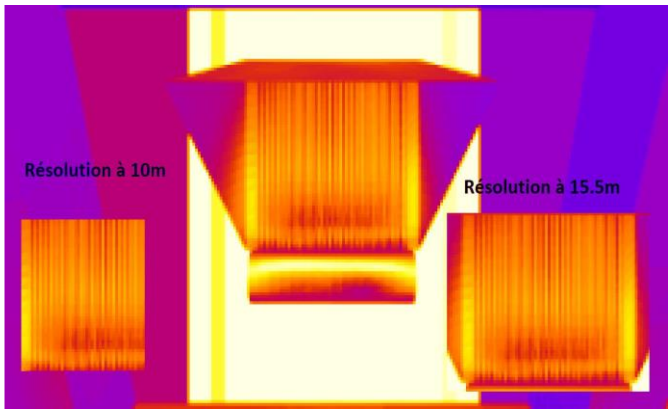	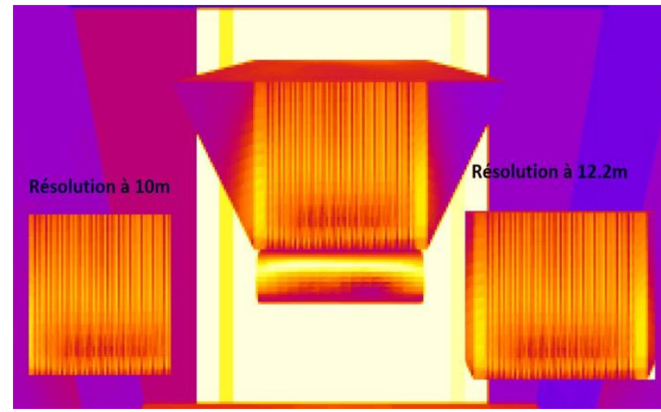
Temperature measurement resolution (MFOV)	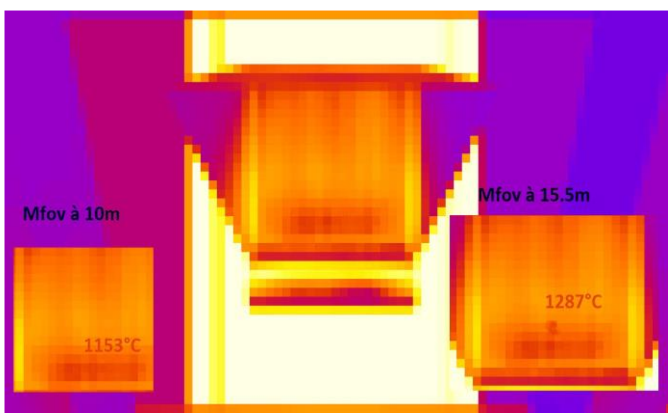	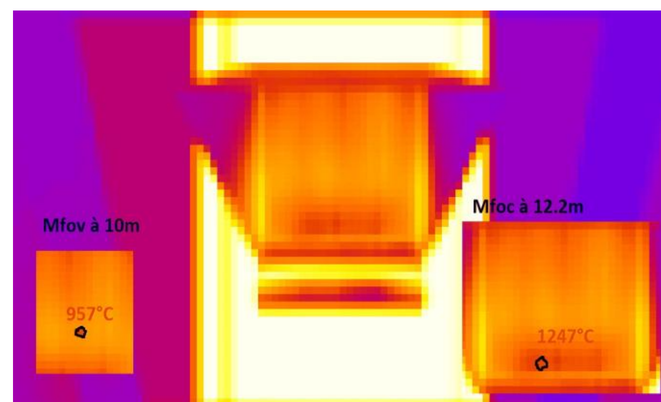

IR camera

<u>The infrared camera is not solar blind</u>

The spectral range of the IR camera is 7.5-13.5 µm.
The irradiance of the solar spectrum in this range is very low but not null.

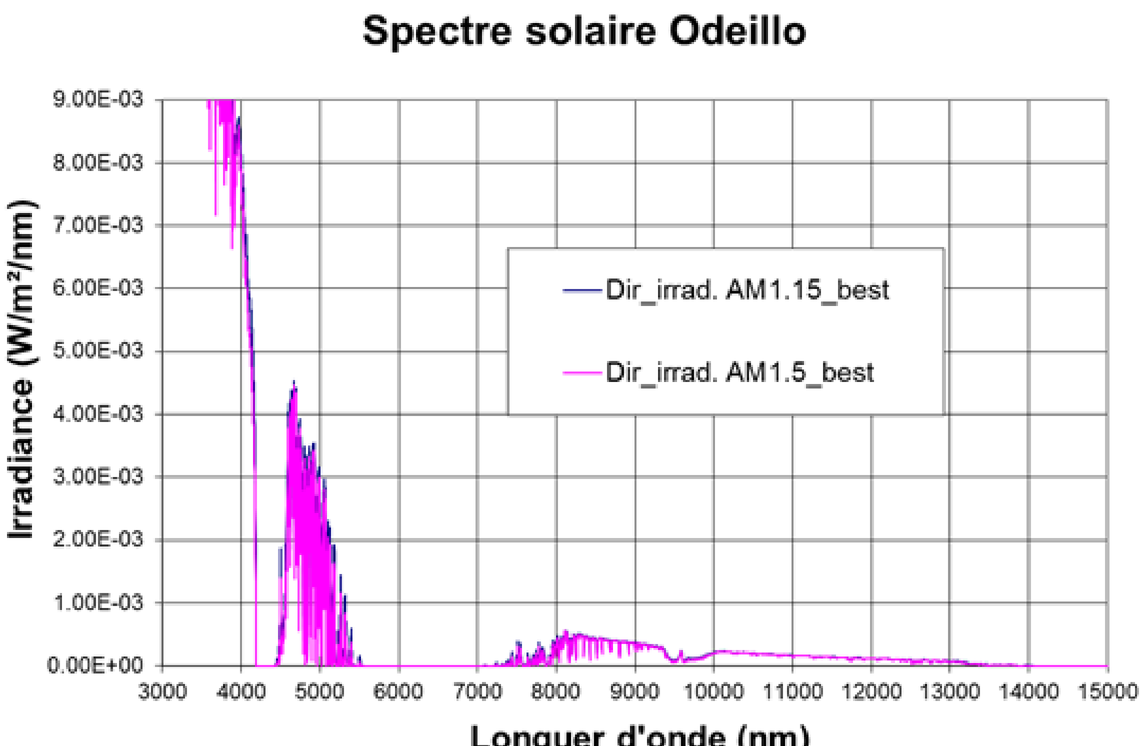

IR camera

The infrared camera is not solar blind

Reflexion of the concentrated solar flux on the receiver could lead to wrong temperature measurement. Calculation must be done to check if it is negligible or not.

1. *Integrate the solar spectrum irradiance in the range of the camera*
2. *Multiply this value by the mirror reflectivity in the same range*
3. *Multiply by the concentration factor*
4. *Multiply by the receiver reflectivity in the same range*
5. *Calculate the thermal radiation emmited by the receiver*
6. *Compare both radiation densities to conclude*

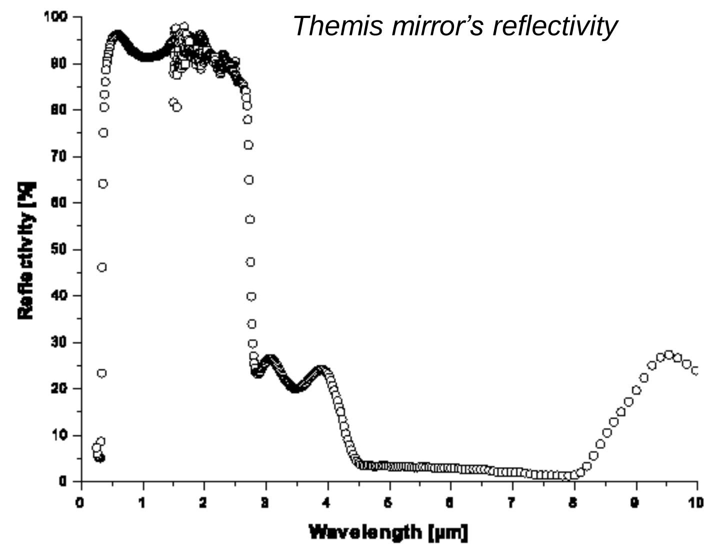

Example:
Integration of the solar spectrum between 7.5 and 13.5 µm give 1.1 W/m²
Themis mirror's reflectivity is 0.25 (mean - same range), the receiver reflectivity (Pyromark) is 0.1
*With a concentration factor of 1000, the solar contribution is **27.5 W/m²***
*At 500°C with an emissivity of 0.95 (Pyromark) the receiver emits about **3.9 kW/m²***

IR camera

Camera software

- The emissivity of the surface can be changed locally
  (several zones could be defined)
- Temperature profiles can be plotted (2 axis)
- Digital zoom can be applied
- Post treatment can be done
- Alarm can be set

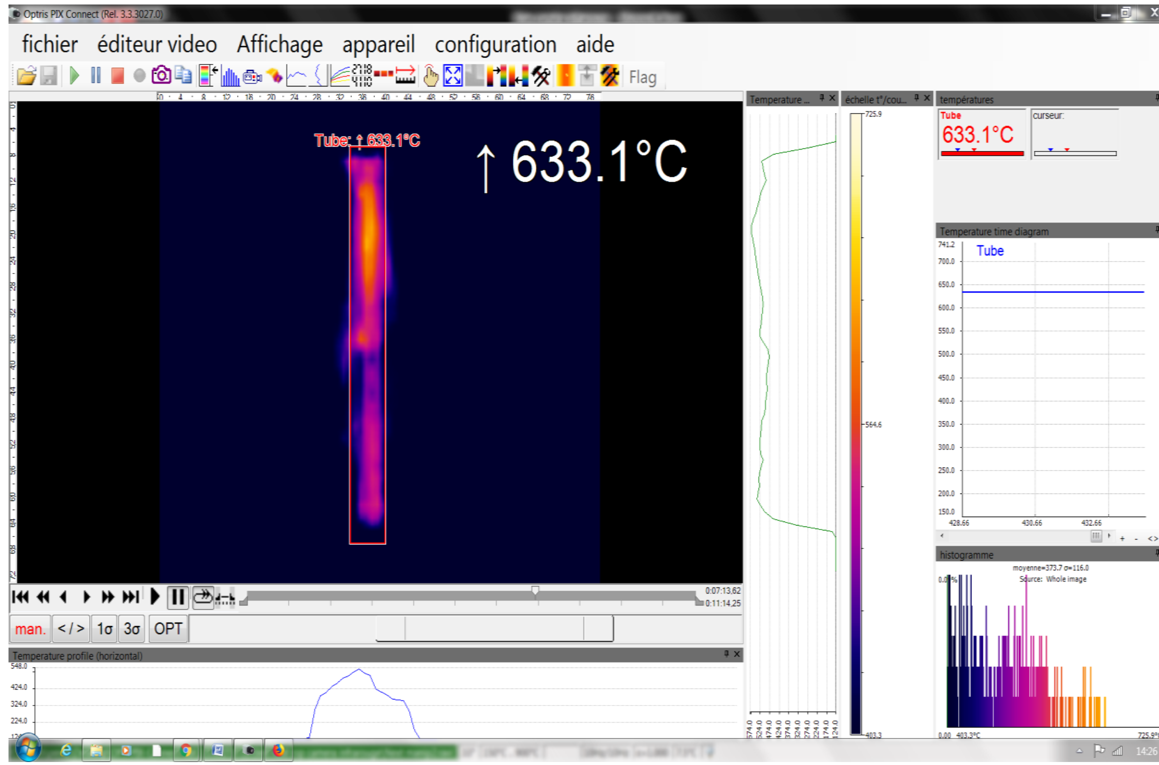

Pix Connect (Optris)

IR camera

Test at the big furnace

- No bright glare from concentrated solar reflexion

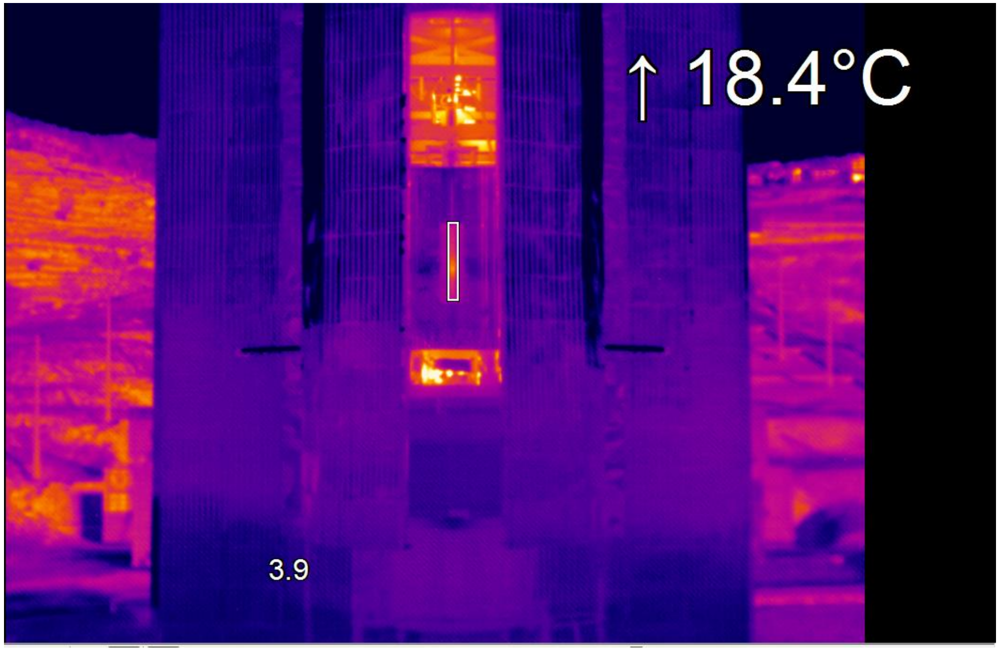

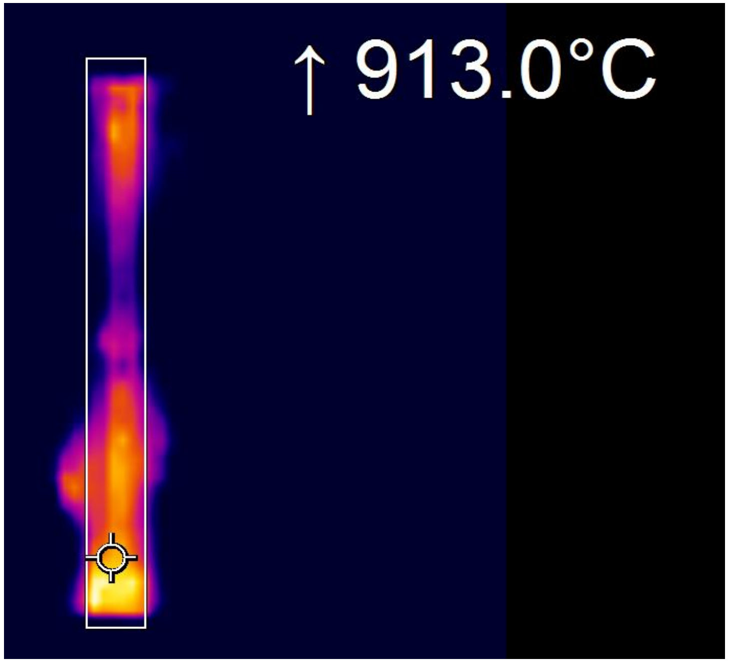

video camera infrarouge tube four 1000Kw.wmv

IR camera

Test at the 1 MW furnace

Comparison with thermocouple measurements :

From 45°C to 75°C temperature difference
IR camera gives lower values than thermocouples

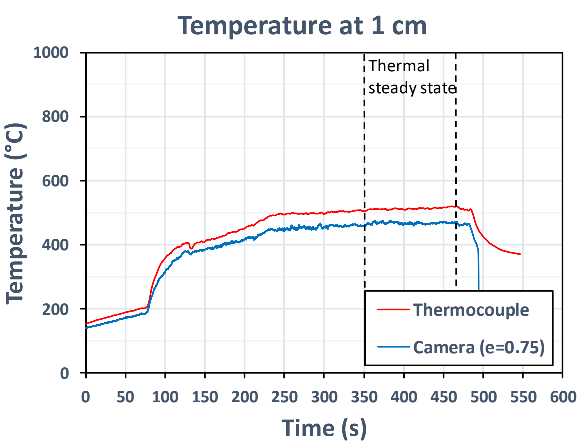

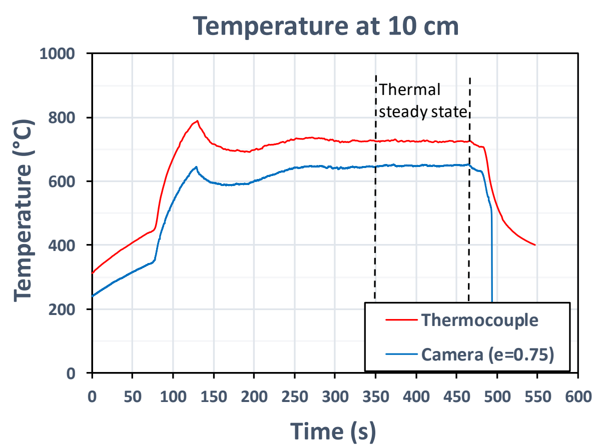

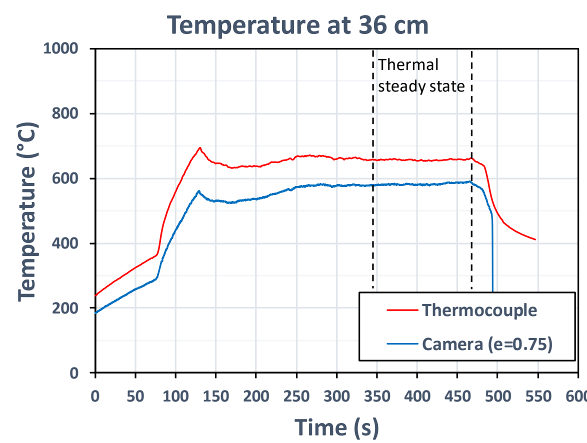

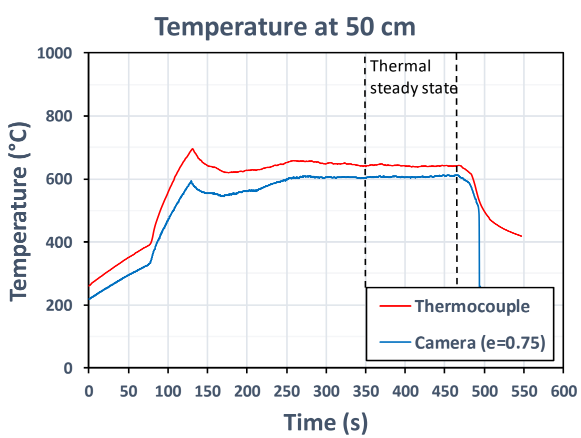

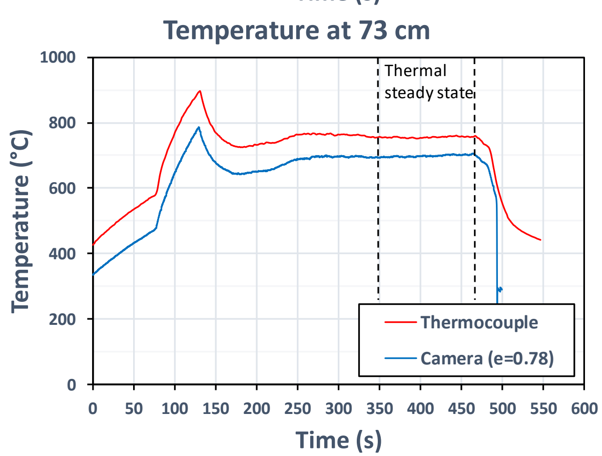

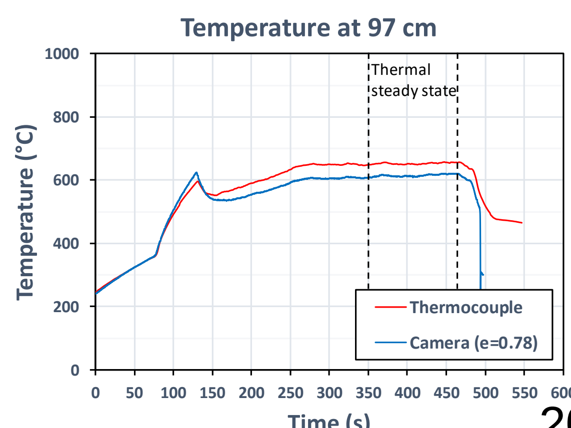

UAV

Unmanned Aircraft Vehicle (flying drone)

Choice criteria

- Mass load
- Battery load (time of flight)
- Camera gimbal
- Software
- Remote control

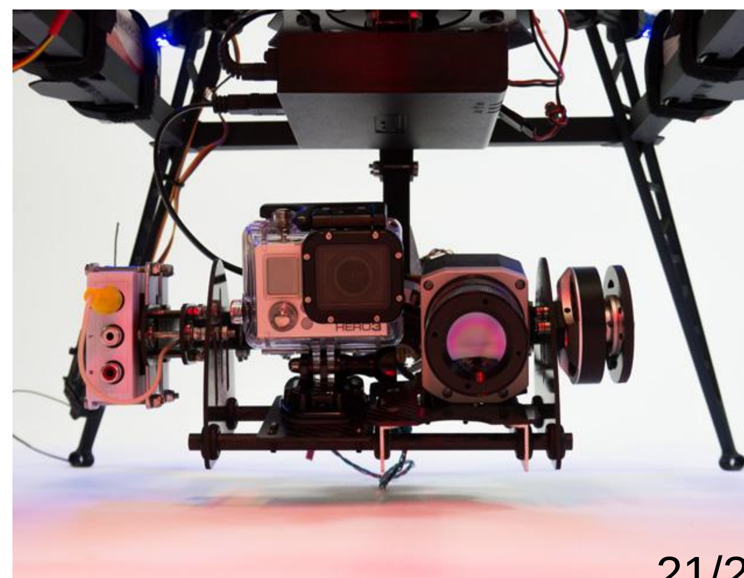

UAV

Optical simulation

[video](#)

SOLSTICE simulation to define « no fly zones » and preset waypoints (flight path).

At 10m front of the receiver (@ 900°C), thermal radiation are about 300 W/m²

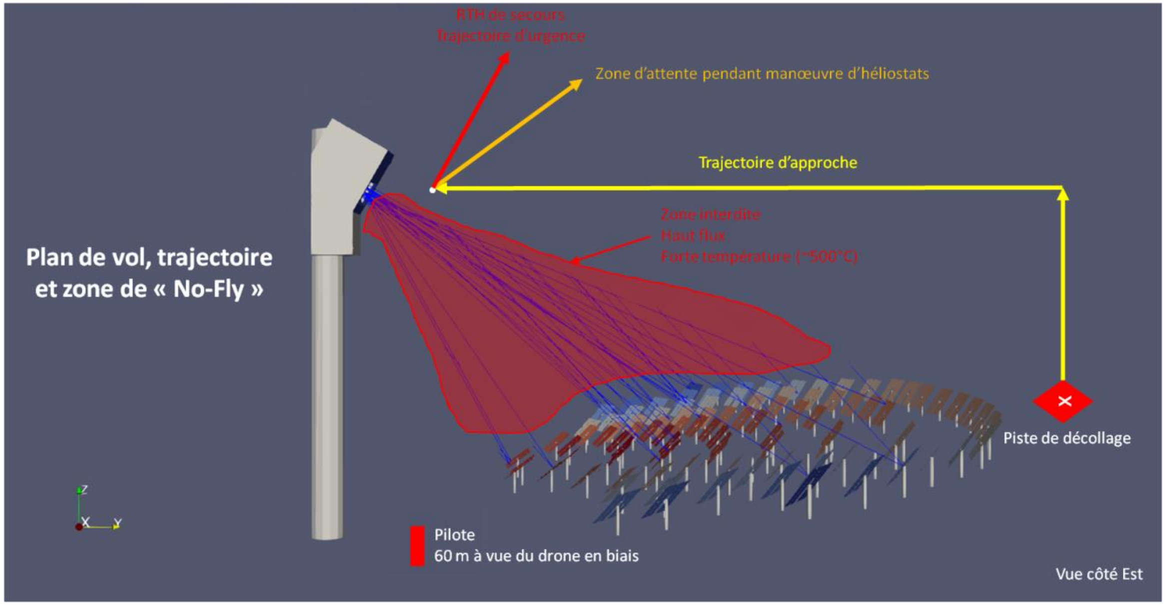

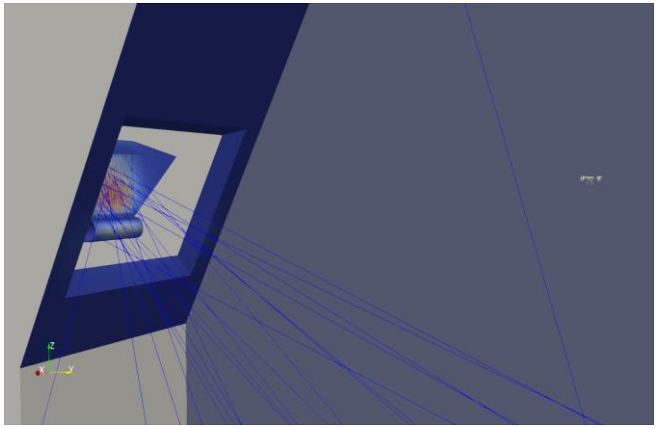

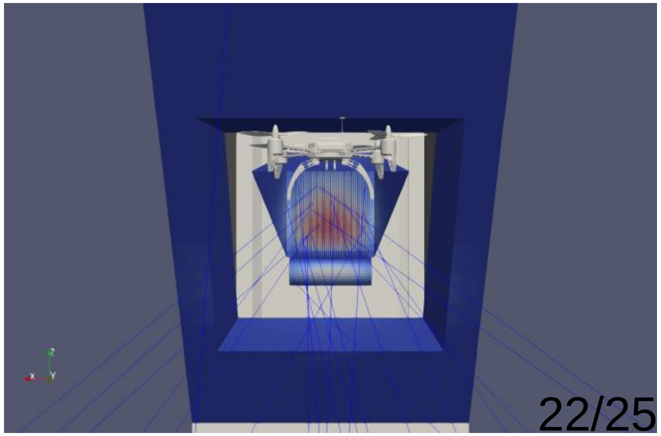

UAV

Operation

- An automated procedure can be defined with several preset waypoints.

- Each waypoint is a set of coordinate managed through GPS

- « No fly zones » are pre-registered on the drone software to avoid any incident

- In France, UAV professional pilots must have a licence to fly

flylitchi software

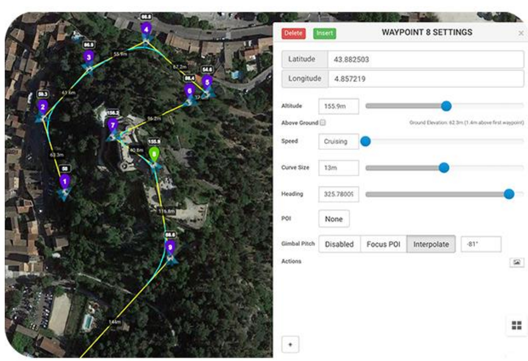

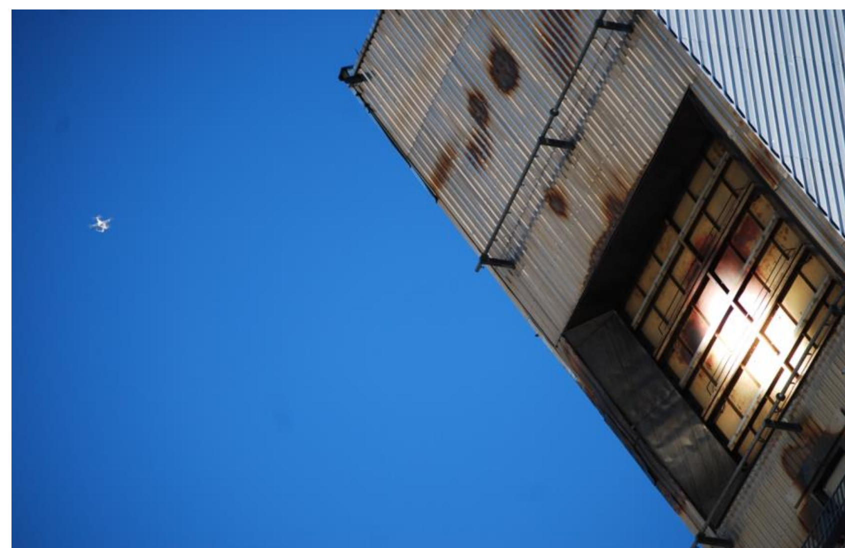

To conclude

- IR measurement from a flying drone is very useful to detect hot points on central receiver
- A large thermal scene can be observed
- Temperature measurement implies the knowledge of emissivity
- IR camera are not solar blind but in the range 7.5-13.5 µm, the concentrated solar flux reflections are negligibles.
- UAV flights are safe and can be totally automated

SFERA

Solar Facilities for the European Research Area

The SFERA-III project has received funding from the European Union's Horizon 2020 research and innovation programme under grant agreement No 823802.

http://sfera3.sollab.eu/

HELIOSTAT FIELD OPTICAL MEASUREMENTS

Gregor Bern

Fraunhofer Institute for Solar Energy Systems ISE

SFERA III Workshop

Training on Central Receivers

Odeillo, July 9-12

www.ise.fraunhofer.de

Fraunhofer ISE

3D Laser Scanning of Heliostat Shape

Preparation of the surface for the measurement

Covering the reflective surface with removable chalk spray for diffuse reflection

The prepared heliostat. Markers in the corners allow the automatic referencing of measurements in different positions

SFERA
Fraunhofer ISE

3D Laser Scanning of Heliostat Shape
The Measurement

3D Laser Scanner, elevated to allow for measurement at various heliostat positions

Fraunhofer ISE

3D Laser Scanning of Heliostat Shape

The Evaluation – Shape and Surface Slope from 3D Pointclouds

Height map along the heliostat surface normal

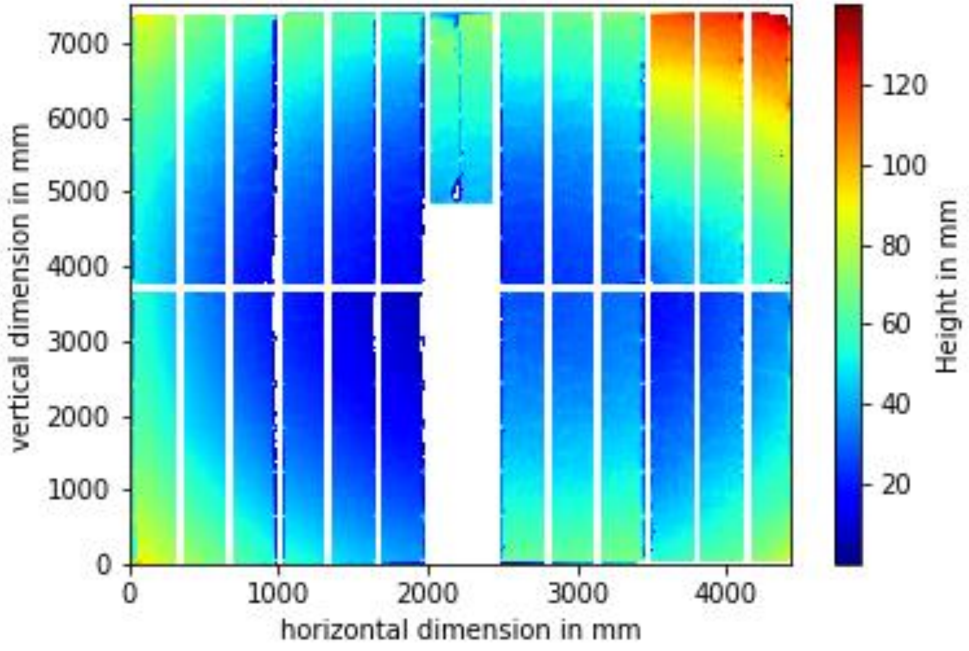

Gradient map (surface slope) along the vertical dimension

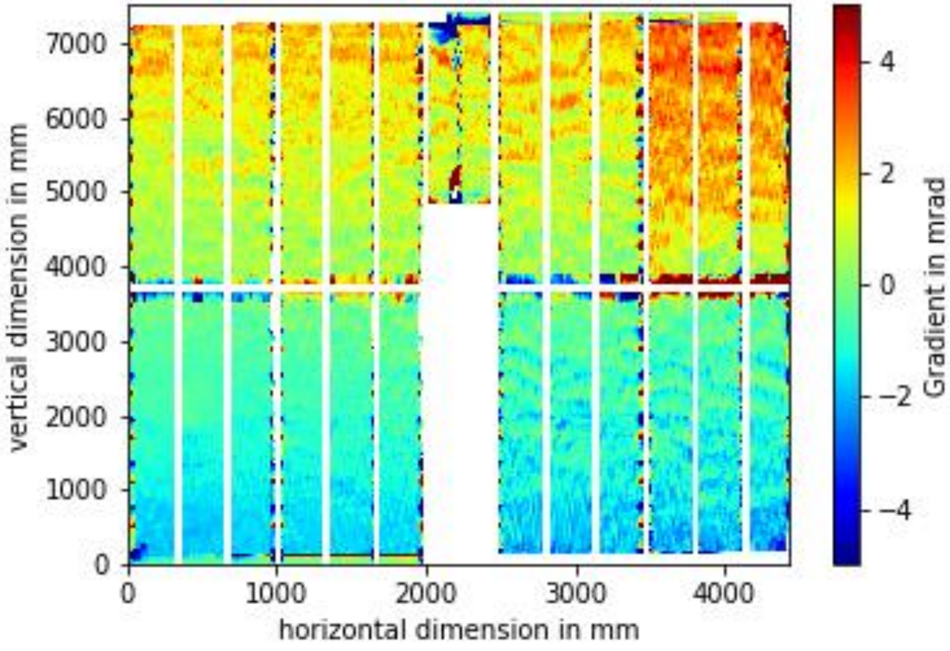

Reflectance and Cleanliness
Measurement in the Field

- Portable devices, eg:
  pFlex (what we used at Themis)
  →automatic storage via Bluetooth
  →simple handling in the field
- Acceptance angle in measurement
  - Important parameter for comparability
  - Standard for parabolic trough 12.5 mrad (relevant for e.g. EuroTrough collector)
  - For central receiver systems much smaller acceptance angles are relevant →3-8 mrad
- Further information e.g. [1],[2]

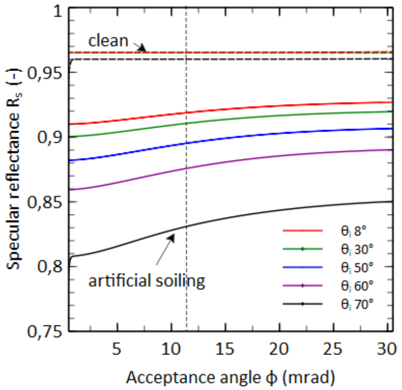

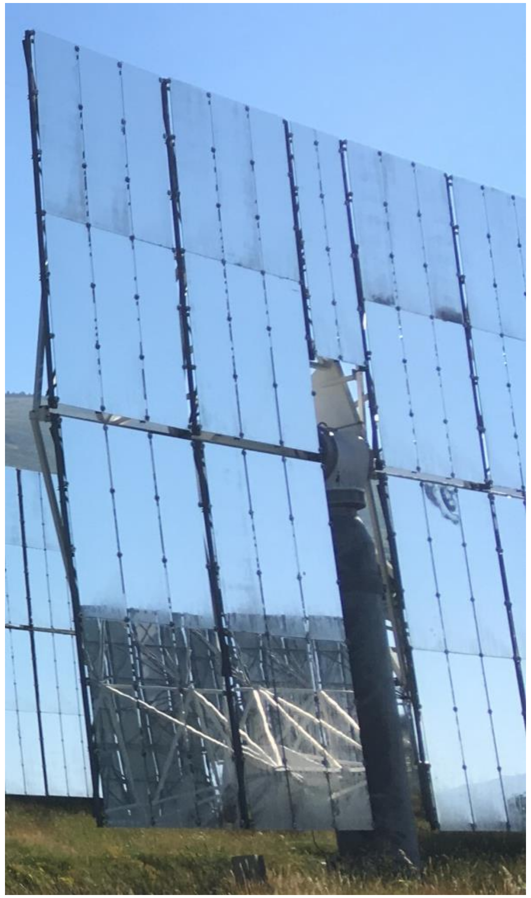

The pFlex device with Bluetooth interface as presented at Themis

[1] A. Heimsath et. al, *Automated Monitoring of Soiling with AVUS Instrument for Improved Solar Site Assessment* (2017).

[2] A. Heimsath et. al, "The effect of soiling on the reflectance of solar reflector materials - Model for prediction of incidence angle dependent reflectance and attenuation due to dust deposition," Sol Energ Mat Sol C **195**, 258–268 (2019).

Fraunhofer ISE

Thank you for your Attendance!



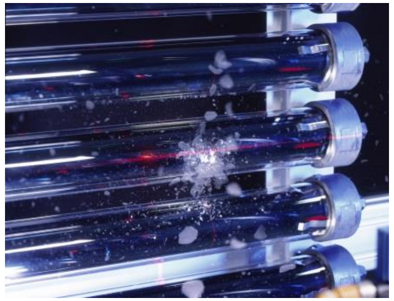
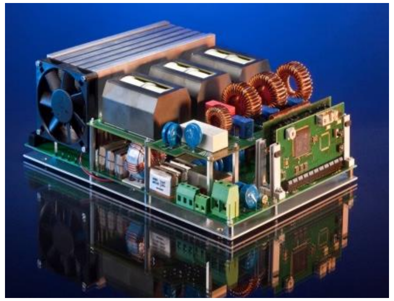
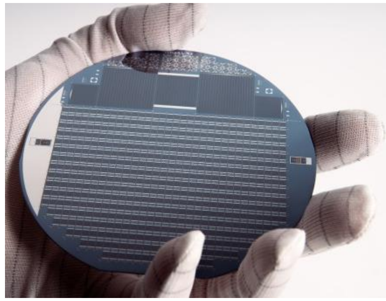


Fraunhofer Institute for Solar Energy Systems ISE

In case of questions, don’t hesitate to contact

Gregor Bern

www.ise.fraunhofer.de

gregor.bern@ise.fraunhofer.de

Solar Facilities for the European Research Area

Fraunhofer ISE

SURROUNDING VERSUS NORTH FIELDS

Solar Facilities for the European Research Area

Heliostats fields, understanding the influence of latitude

Gregor Bern, Peter Schöttl

Fraunhofer Institute for Solar Energy Systems ISE

SFERA III Workshop

Training on Central Receivers

Odeillo, July 9-12

www.ise.fraunhofer.de

AGENDA

- Interactive
  - Summer/winter solstice sun position
  - Calculation of cosine losses
- Latitude effects on surround/polar heliostat fields
  - Reference scenarios
  - Methodology recap
  - Result discussion

Summer/winter solstice sun position

- Location: Odeillo, France
- www.suncalc.org
- Summer (S) solstice: solar zenith $\theta_{s,S} = 19.1°$, solar elevation $\alpha_{s,S} = 70.9°$
- Winter (W) solstice: solar zenith $\theta_{s,W} = 65.9°$, solar elevation $\alpha_{s,S} = 24.1°$

Calculation of cosine losses

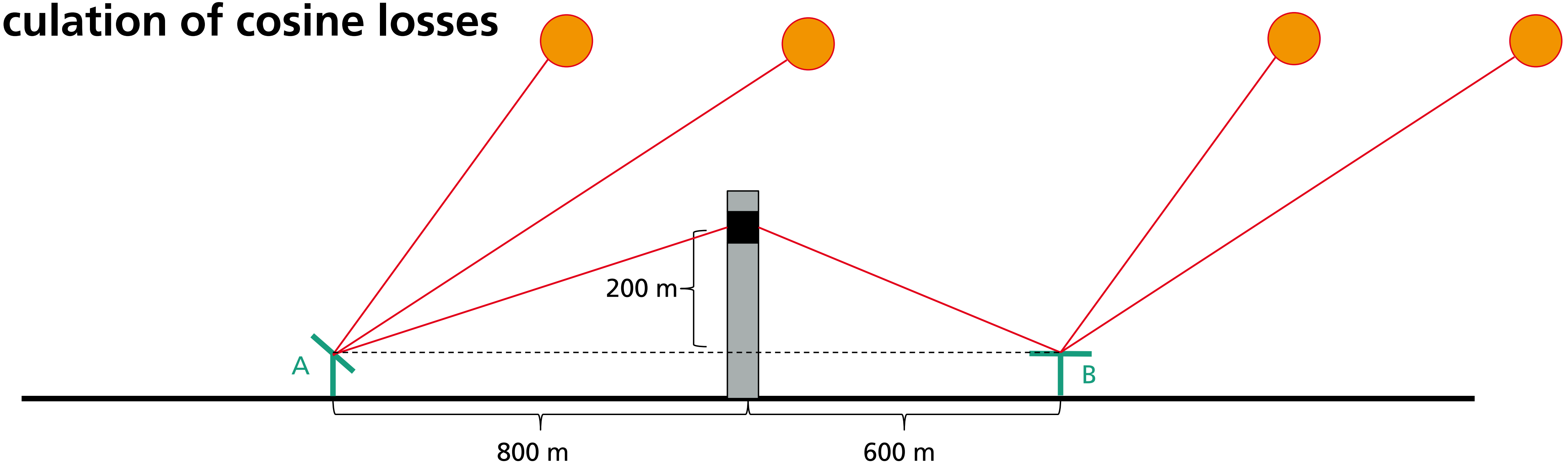

- Heliostat-tower angles: $\beta_A = \tan^{-1}\frac{200}{800} = 14.0°\,, \beta_B = \tan^{-1}\frac{200}{600} = 18.4°$
- Summer solstice: $\theta_{inc,A} = \frac{|\alpha_{s,S}-\beta_A|}{2} = \frac{|70.9°-14.0°|}{2} = 28.5°, \theta_{inc,B} = \frac{|180°-\alpha_{s,S}-\beta_B|}{2} = 45.4°$
  Cosine losses: $1 - \cos\theta_{inc,A} = 0.12\,, 1 - \cos\theta_{inc,B} = 0.30$
- Winter solstice: $\theta_{inc,A} = 5.1°, \theta_{inc,B} = 68.8°$
  Cosine losses: $1 - \cos\theta_{inc,A} = 0\,, 1 - \cos\theta_{inc,B} = 0.64$

Reference scenarios
Sites

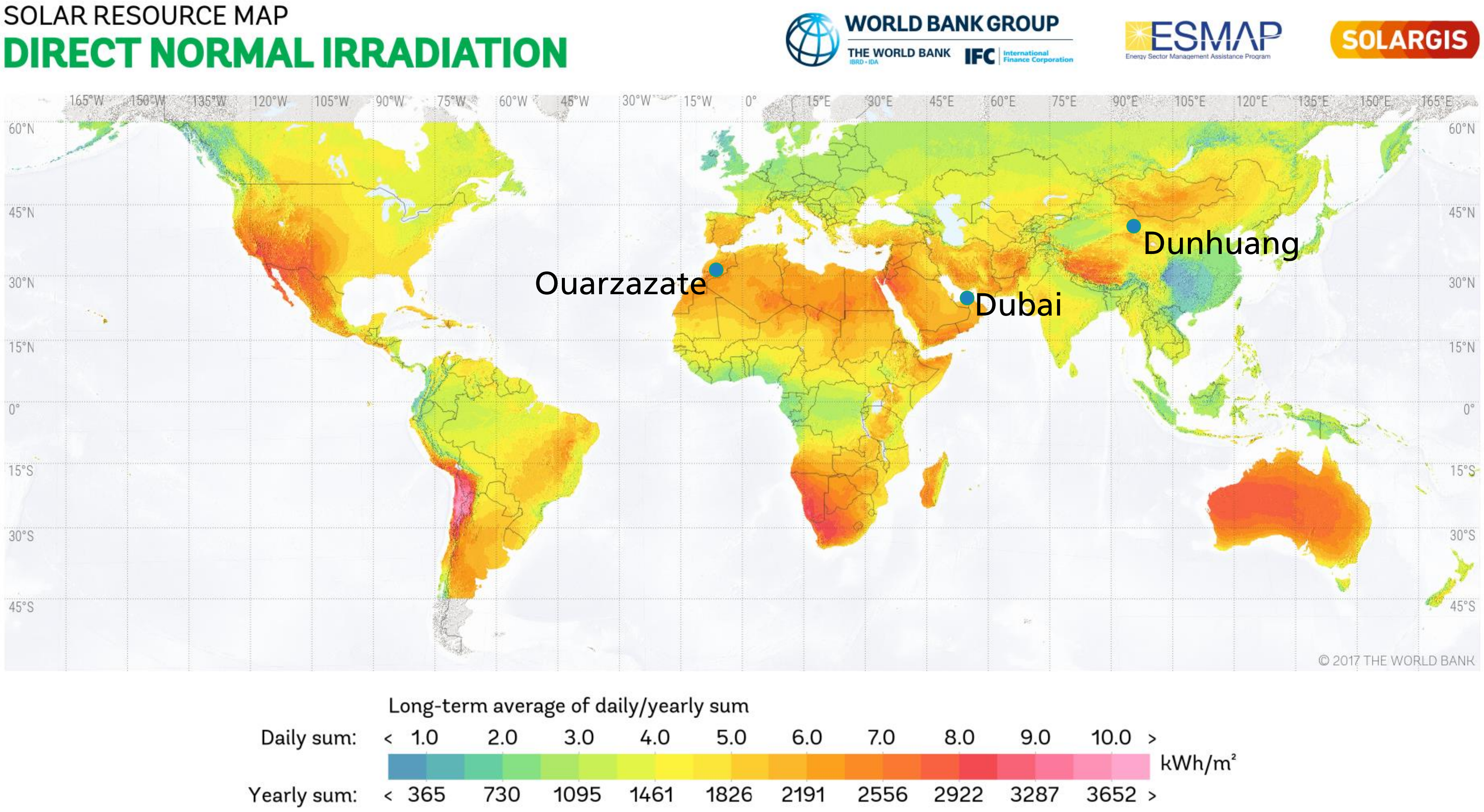

This map is published by the World Bank Group, funded by ESMAP, and prepared by Solargis. For more information and terms of use, please visit http://globalsolaratlas.info.

Reference scenarios
Parameters

	Dubai	Ouarzazate	Dunhuang
Location	24.8 °N, 55.4 °E	31.0 °N, 6.9 °W	39.8 °, 92.7 °E
Annual DNI	2.15 MWh/m²a	2.92 MWh/m²a	2.13 MWh/m²a
Design point DNI	800 W/m² at summer solstice		
Tower height	140 m		
Receiver design power	120 MW_{th}		
Receiver absorber area	521.5 m² (cavity), 260.8 m² (external)		
Heliostat mirror area	115.7 m²		
Heliostat beam quality	3 mrad		
Heliostat reflectance	93%		

Reference scenarios
External vs cavity

- Cavities combined with higher towers than external receivers
  - ignored
- Cavities larger than external receivers
  - $A_{abs,cavity} = A_{abs,external} \cdot 2$
  - Higher costs!

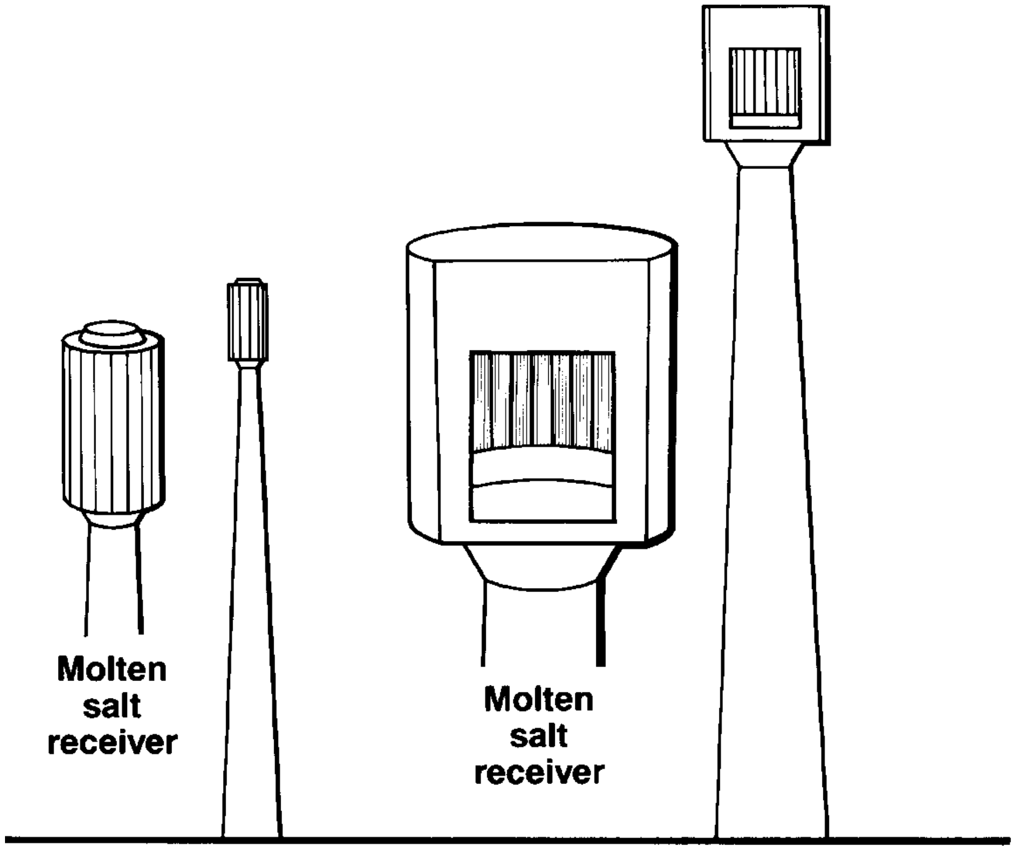

Source: P. K. Falcone, *A HANDBOOK FOR SOLAR CENTRAL RECEIVER DESIGN*. SAND-86-8009. Livermore, CA (USA), 1986.

Methodology recap

1. Create oversized MUEEN field
2. Assess heliostat annual efficiencies with Raytrace3D
3. Assess heliostat design point efficiencies with Raytrace3D
4. Select best-performing heliostats with polygon-based approach

Result discussion
Dubai: selected fields

Cavity

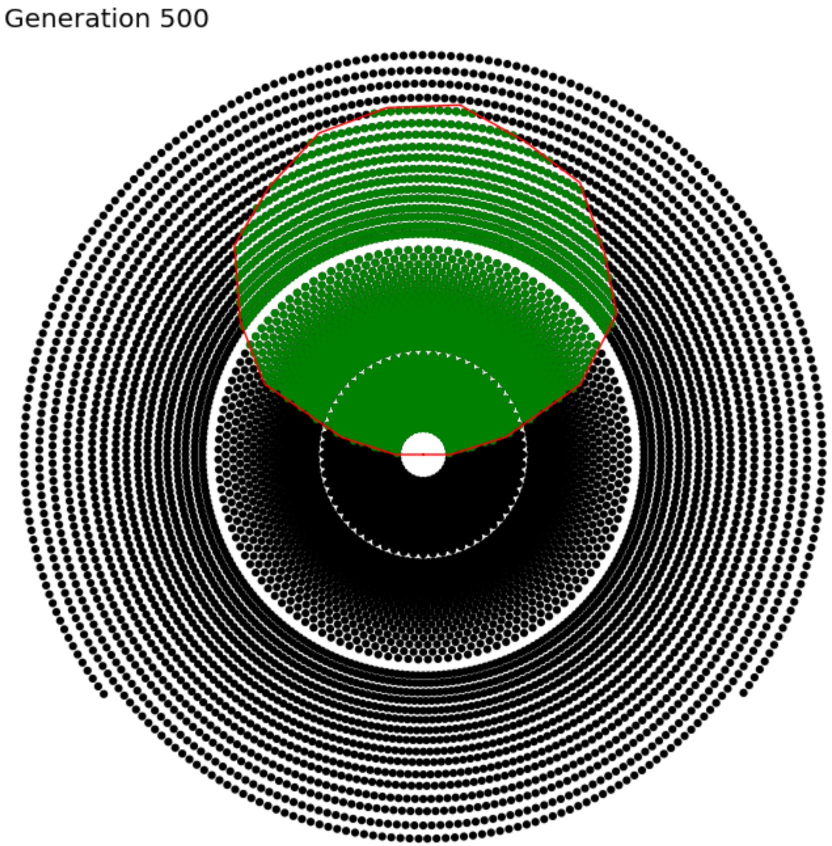

External

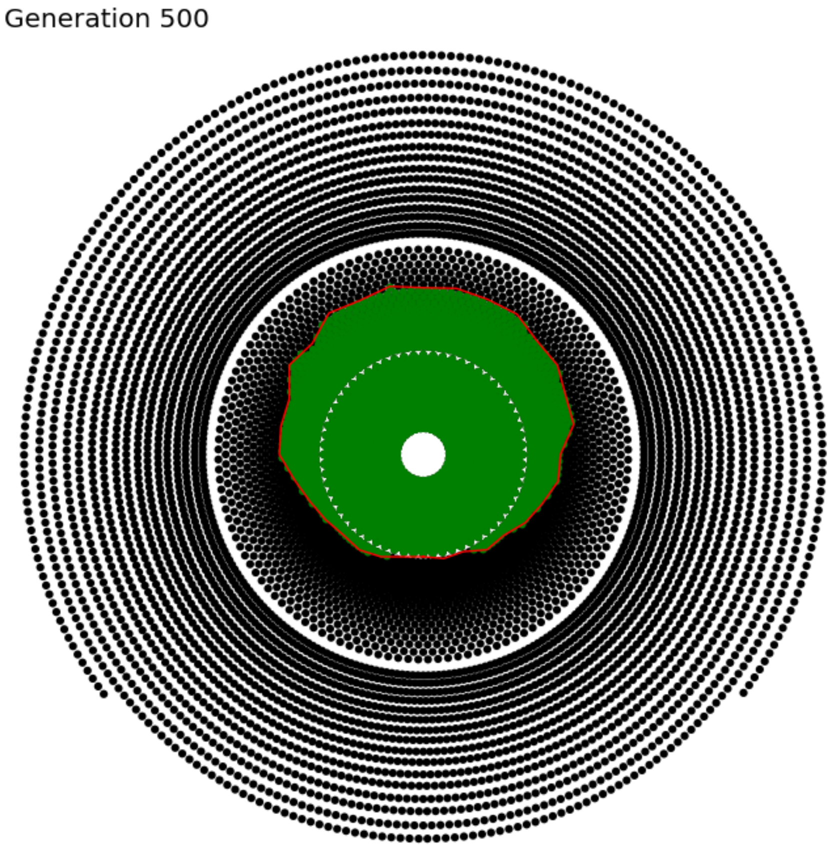

Result discussion

Ouarzazate: selected fields

Cavity

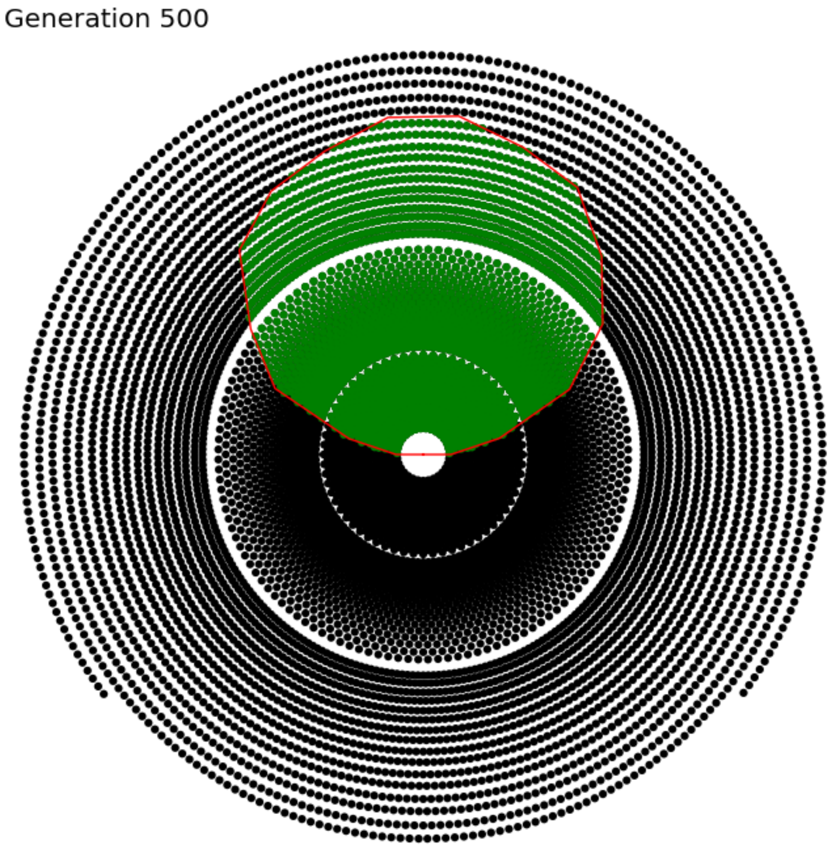

External

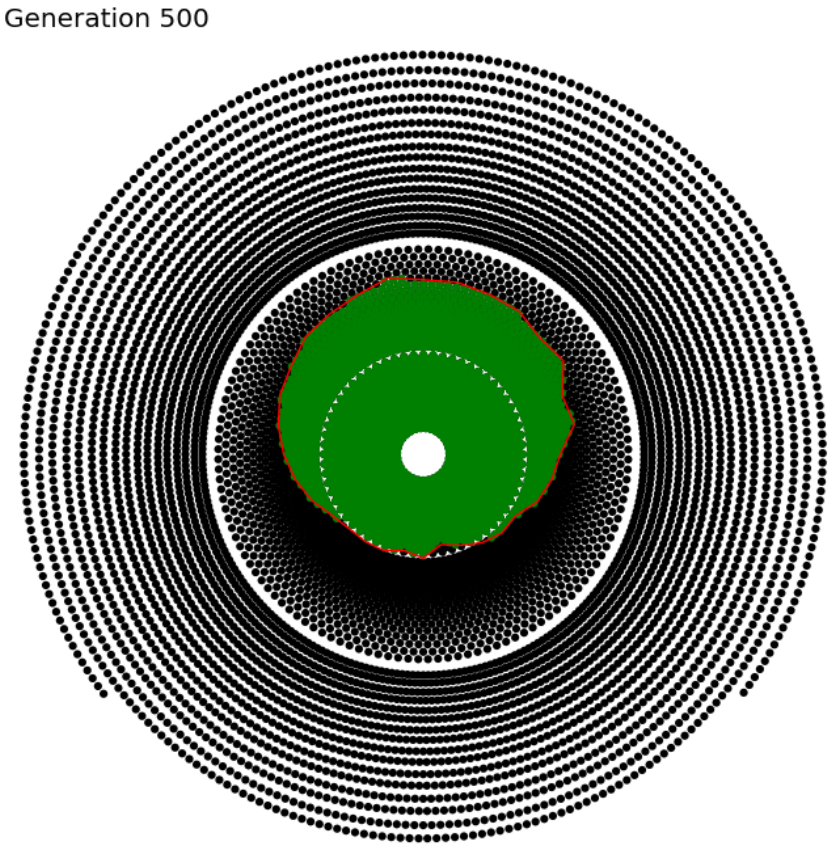

Result discussion

Dunhuang: selected fields

Cavity

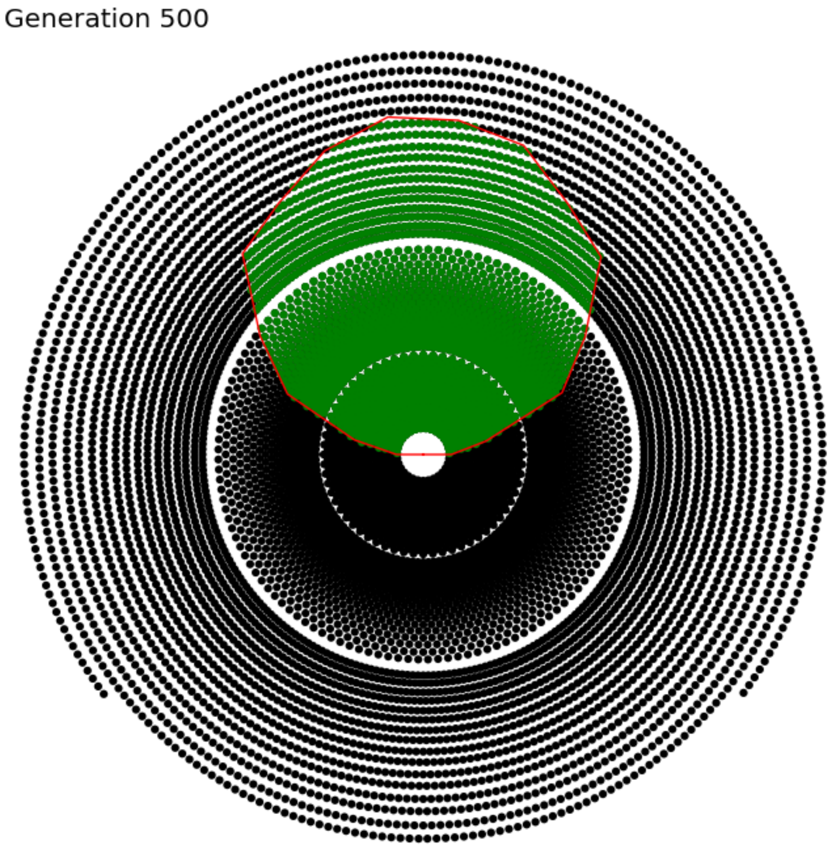

External

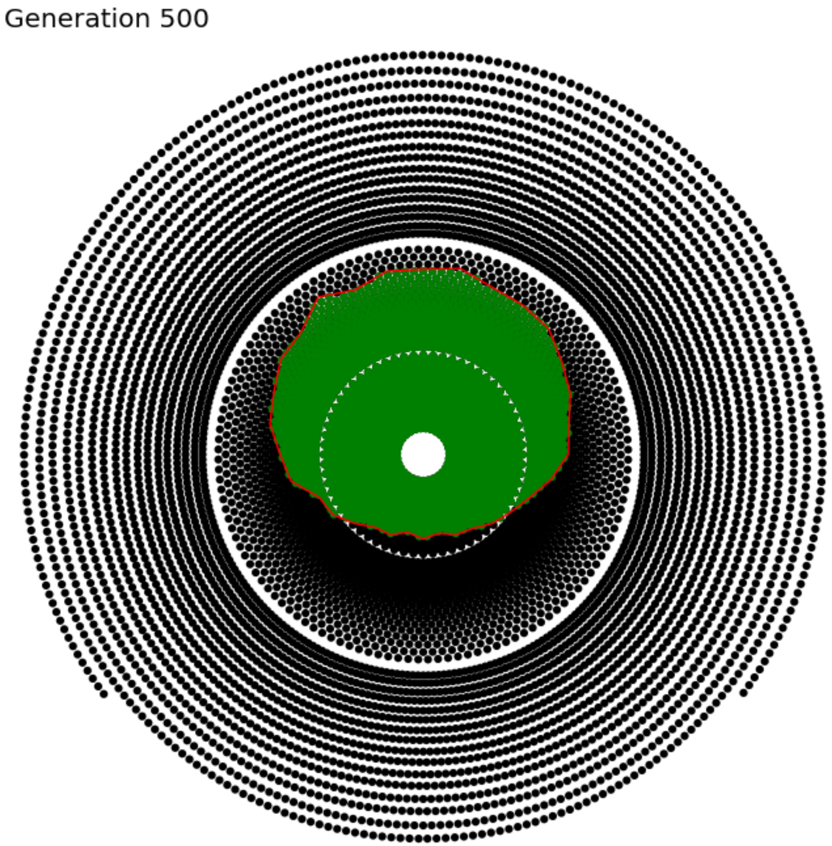

Result discussion
Dubai: optical losses

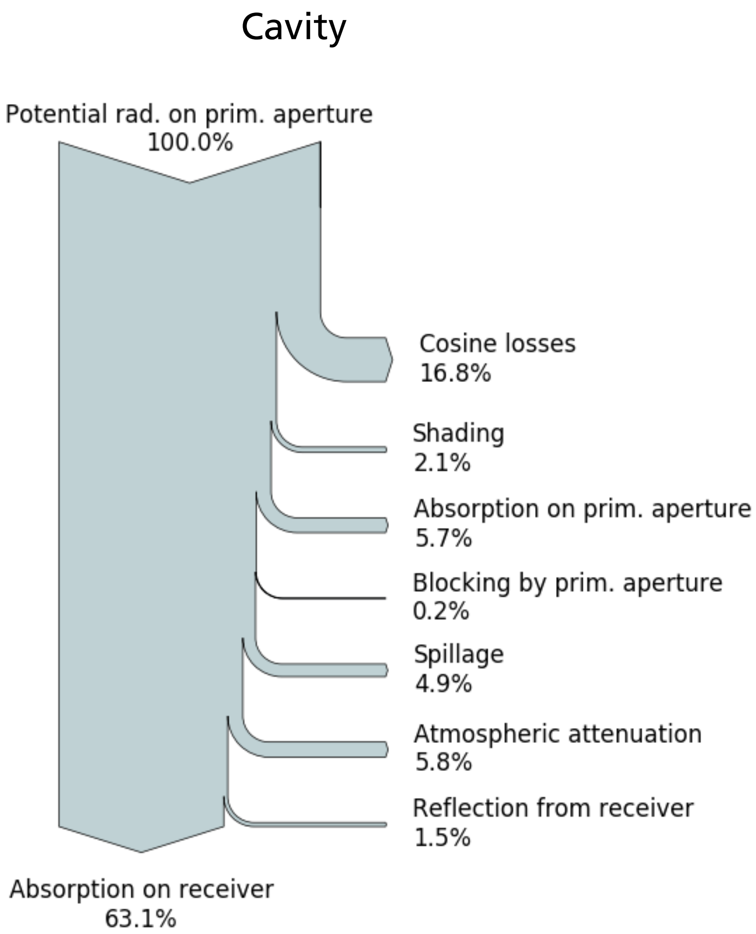

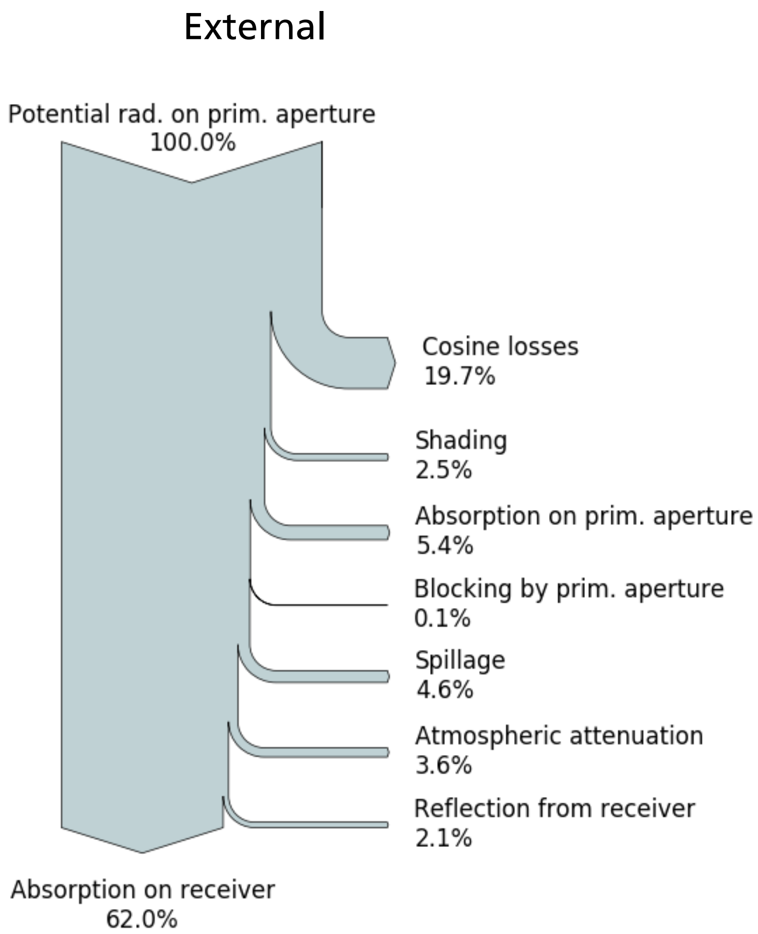

Result discussion
Ouarzazate: optical losses

Cavity

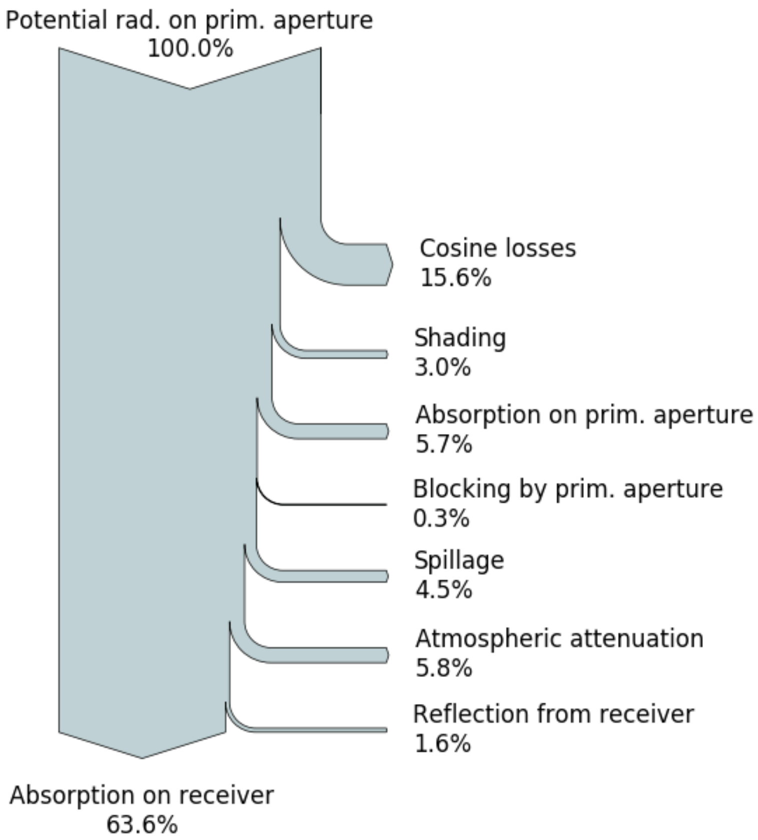

External

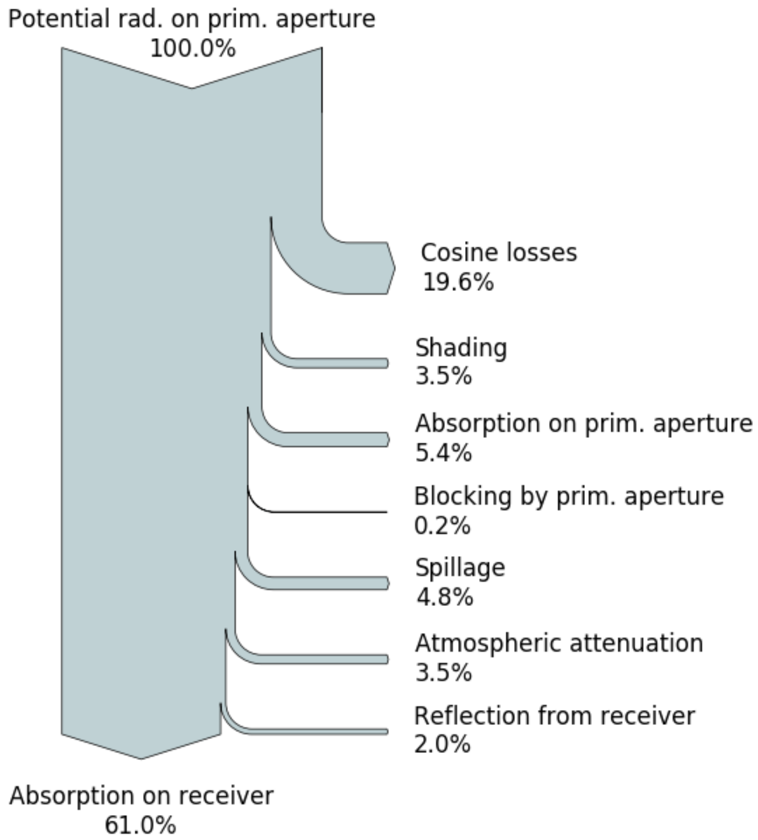

Result discussion
Dunhuang: optical losses

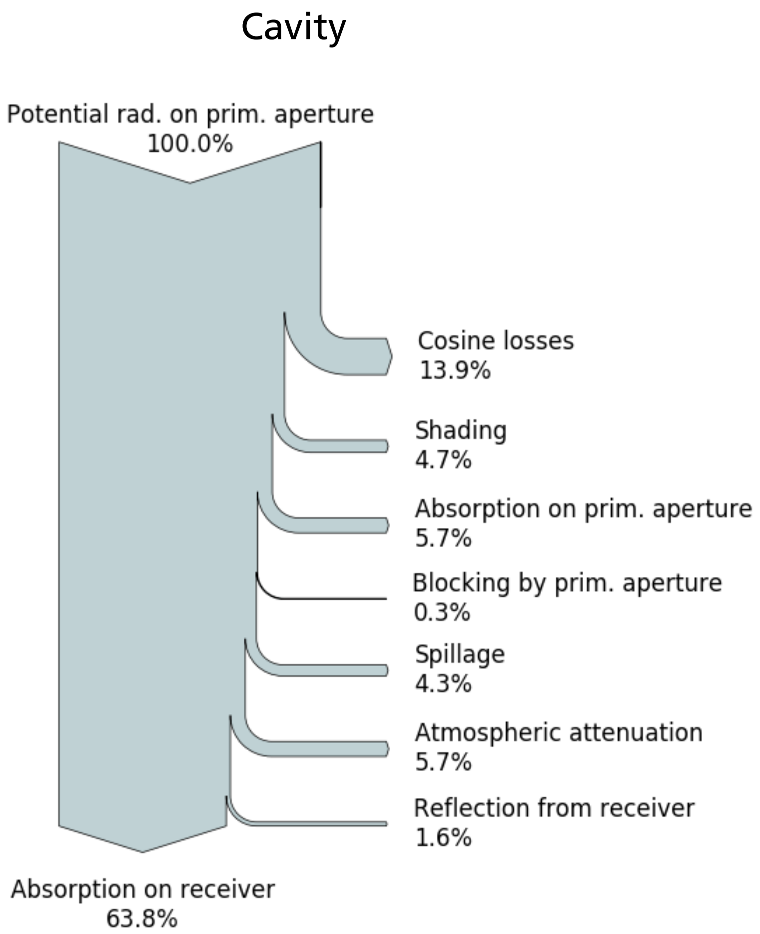

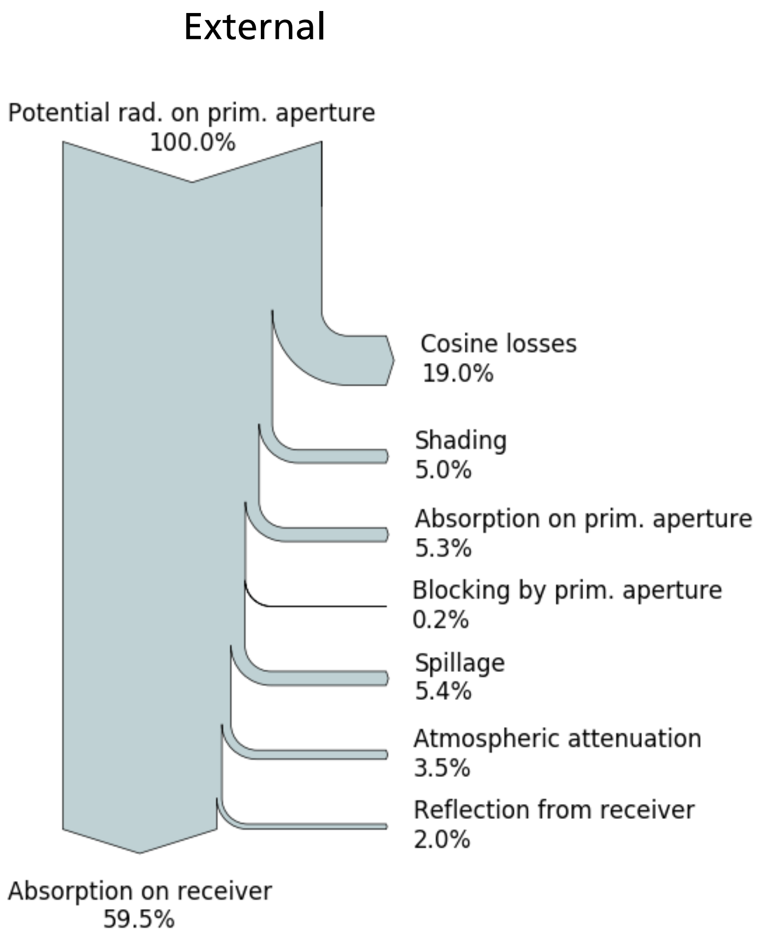

Result discussion
Summer/winter solstice

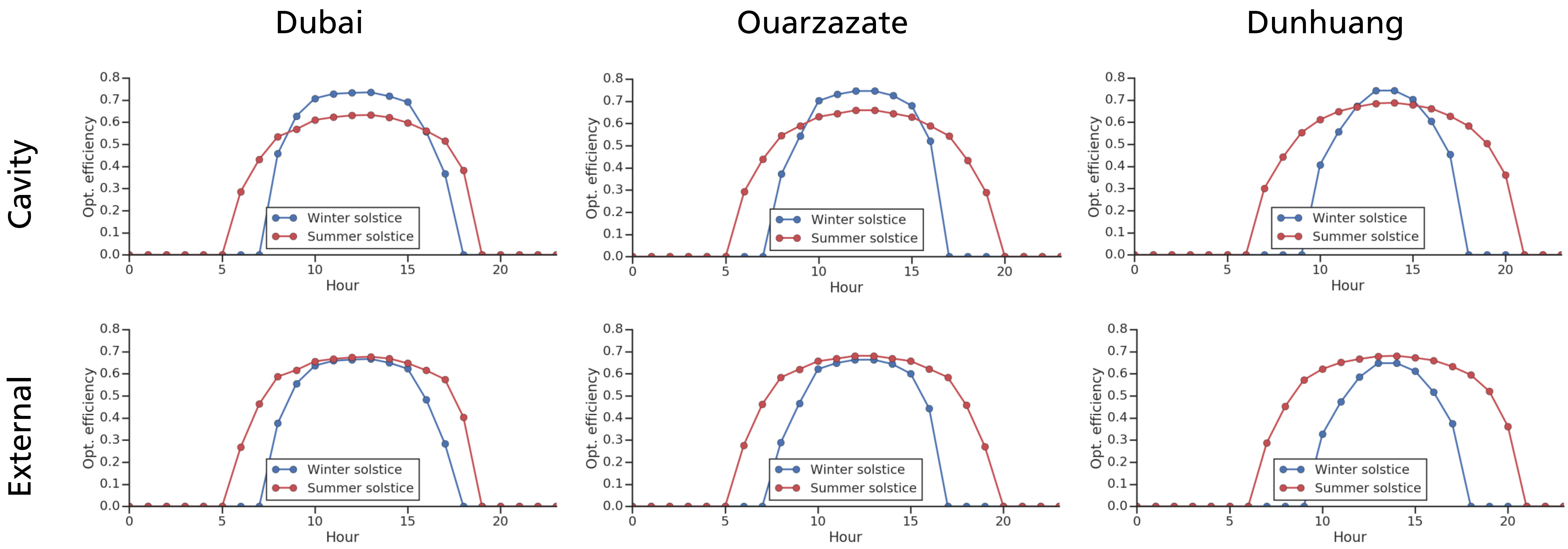

Result discussion
Annual optical efficiency

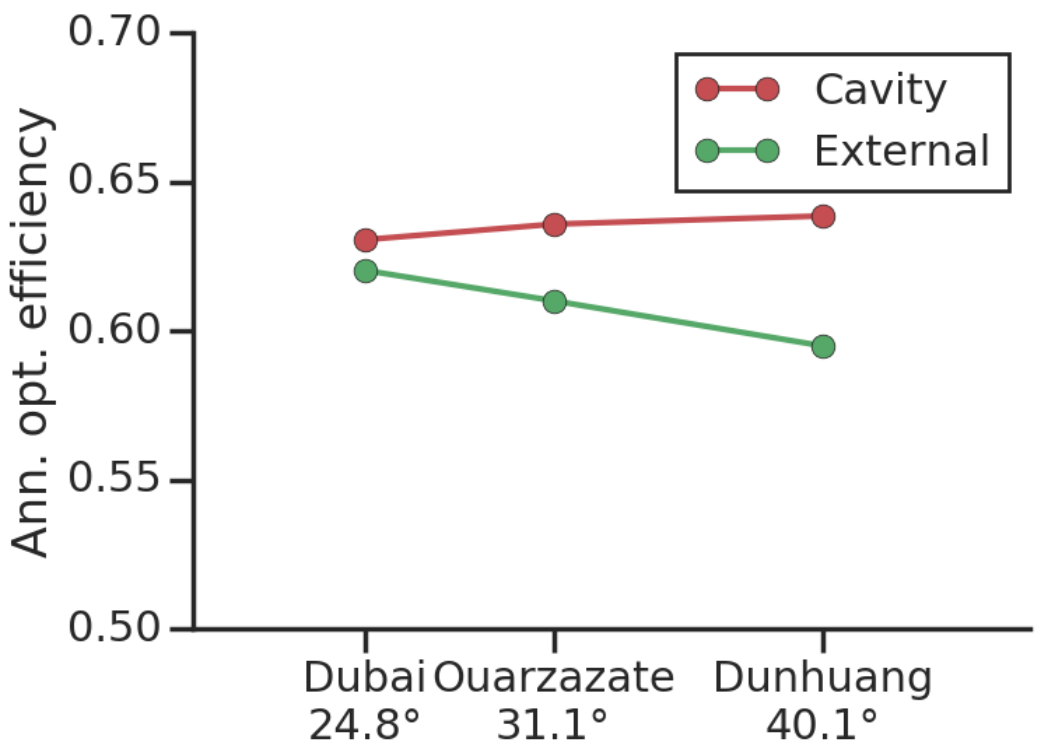

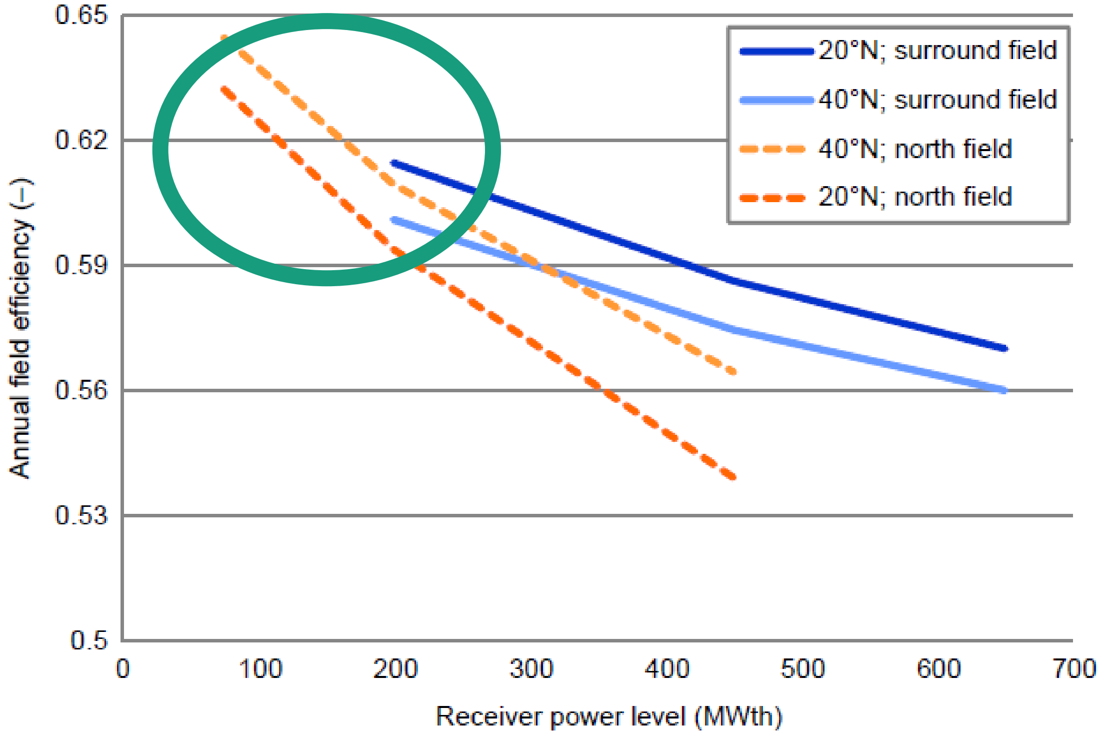

Source: R. Buck and P. Schwarzbözl, "4.17 Solar Tower Systems," in *Comprehensive Energy Systems*: Elsevier, 2018, pp. 692–732.

Thank you for your Attention!



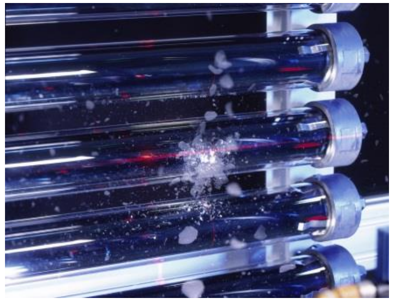
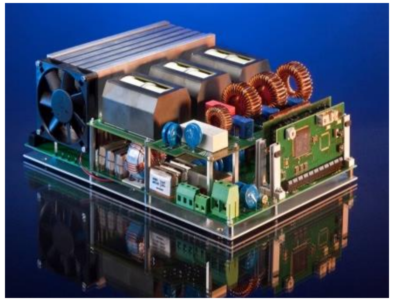
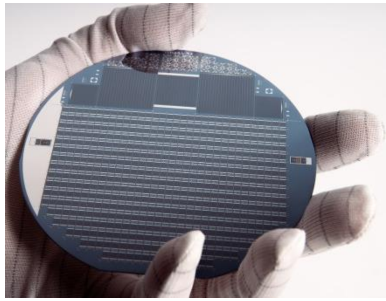


Fraunhofer Institute for Solar Energy Systems ISE

Gregor Bern, Peter Schöttl

www.ise.fraunhofer.de

gregor.bern@ise.fraunhofer.de
peter.schoettl@ise.fraunhofer.de

DESIGN ASPECTS OF FUTURE HYBRID PLANTS

Gregor Bern

Fraunhofer Institute for Solar Energy Systems ISE

SFERA III Workshop

Training on Central Receivers

Odeillo, July 9-12

www.ise.fraunhofer.de

AGENDA

- Hybrid CSP Plants Introduction
  - Classification of hybrid CSP plants
  - Exemplary Overview
    (CSP Co-fired, CSP+Biomass, CSP+Wind)
- CSP+PV hybridization prinziples
- CSP+PV – what to expect in the near future
- Discussion, discussion, discussion

CSP Hybrid Systems
Hybrid technology categories

Internal hybridization

Integration of CSP technology into power cycle of existing (CSP add-on) and new power plants

- Integration into power cycles driven by RE sources
  - CSP-biomass hybrids
  - CSP-geothermal hybrids
- Integration into power cycles using fossil fuel
  - Solar-aided coal-fired power generation (SACPG) hybrids
  - Integrated solar combined cycle (ISCC) natural gas fueled hybrids

External hybridization

Combination of CSP technology with independent RE systems

- Hybridization by use of joint electrical infrastructure
  - CSP-wind hybrids
  - CSP-PV hybrids

CSP Hybrid Systems

Hybrid technology categories

Internal hybridization

Integration of CSP technology into power cycle of existing (CSP add-on) and new power plants

- **Integration into power cycles driven by RE sources**
  - CSP-biomass hybrids
  - CSP-geothermal hybrids
- **Integration into power cycles using fossil fuel**
  - Solar-aided coal-fired power generation (SACPG) hybrids
  - Integrated solar combined cycle (ISCC) natural gas fueled hybrids

External hybridization

Combination of CSP technology with independent RE systems

- **Hybridization by use of joint electrical infrastructure**
  - CSP-wind hybrids
  - CSP-PV hybrids

Internal hybridization

Integration of RE systems with CSP

- **Optimization by common operation strategy**
  - CSP-PV hybrids

CSP Hybrid Systems

Hybrid technology classification regarding solar / RE share

Classification of hybrids based on the RE component share of generated power [1]:

- **High** – hybrids of CSP with wind, PV, biomass, and geothermal energy resources
  ➔ Highest potential for mitigating global warming

- **Medium** – solar plants that use supplementary firing of fossil fuels to enhance plant output
  ➔ Use of backup fossil fuel (usually limited to about 25%)

- **Low** – conventional fossil fuel plants incorporating solar energy for auxiliary functions
  ➔ Solar share usually less than 20%

CSP Hybrid Systems
General strategy

- Hybridization / hybrid power plants?
  ➔ combine CSP with other RE
- Goal:
  - Dispatchability of electricity generation
  - Reduce supply fluctuations
  - Minimize LCOE / maximize capacity factor
  - Establish CSP plants in regions with moderate DNI (<2000 kWh/m²a)
  - Technological bridge towards energy sustainability / “carbon-neutral” PP

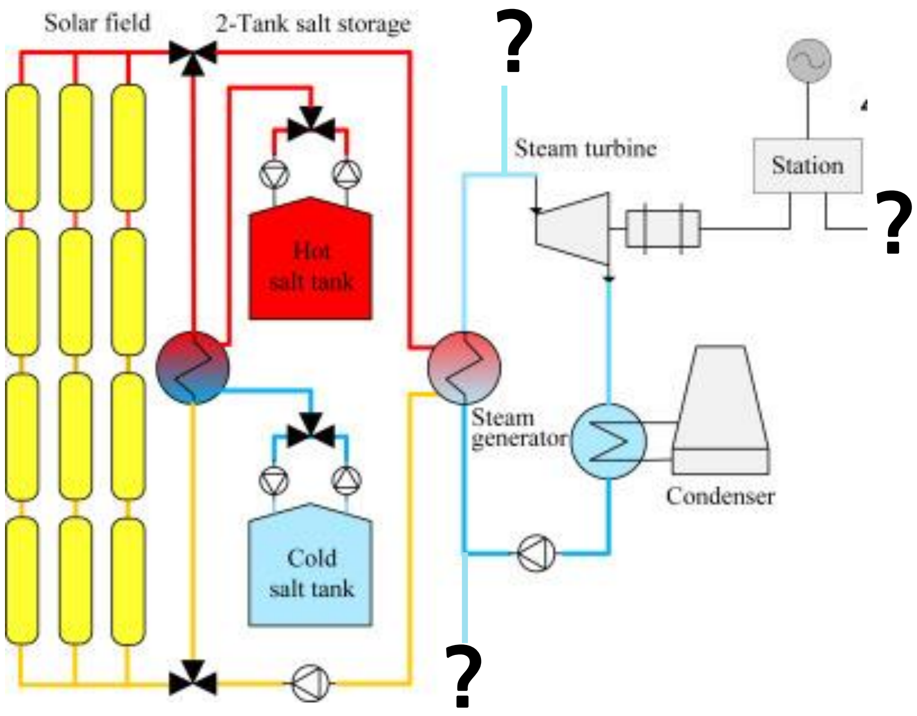

Different possible configuration for CSP hybridization adapted from [2]

ISCC Hybrid Systems

Integrated solar combined cycle (ISCC) hybrid systems

Integrated solar combined cycle (ISCC) natural gas fueled hybrids

Concept description and features:

- Integrated solar combined cycle (ISCC):
  - into topping (Brayton) or bottoming (Rankine) cycle (mostly applied)

  ➔ integration into bottoming cycle yields higher overall efficiency [3]
- CSP integration into topping cycle yields higher solar-to-electric-efficiency [4]
- CSP integration into bottoming cycle possible on high (option A) or low pressure (option B) side (see ***Figure***)
- Solar capacity share in ISCC hybrids: usually < 20%

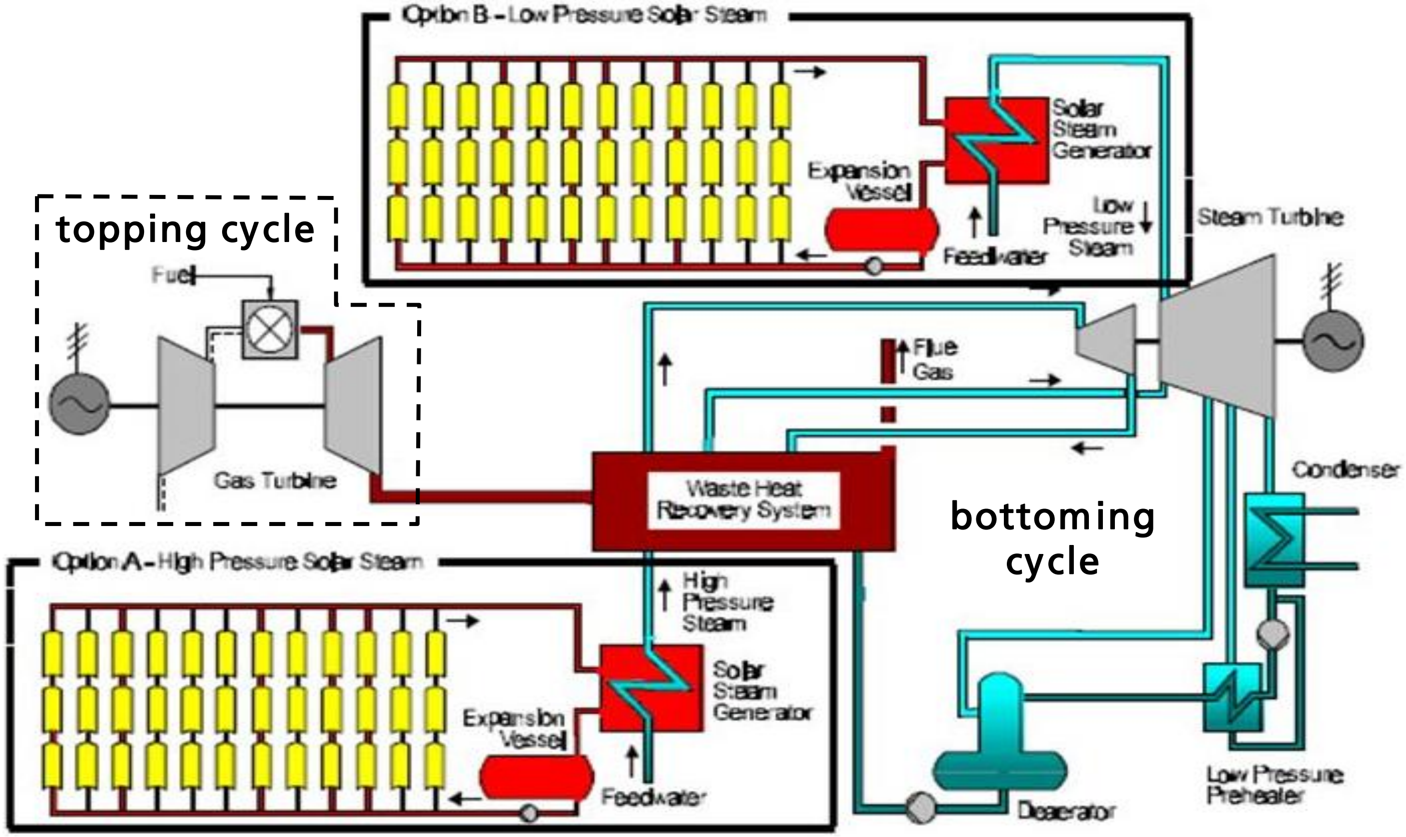

Options for CSP integration into the bottoming cycle of a combined cycle gas-fired power plant

ISCC Hybrid Systems

ISCC hybrid systems: Solar integration into topping cycle

- Solar integration into topping cycle ➔ air heating for combustor, gas turbine exhaust used to generate steam for bottoming cycle in heat recovery steam gen. (HRSG)
- PT integrating by generating steam for injection into combustion chamber (steam injection gas turbine – STIG [5]) ➔ overall STIG system efficiency: 40-55%, corresponding solar-to-electrical efficiency of 15-24%

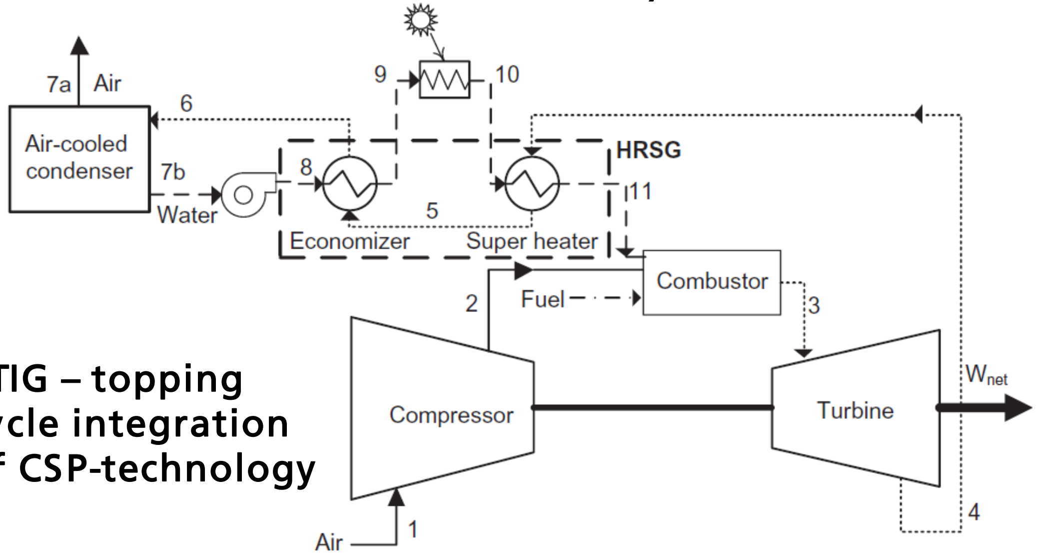

STIG – topping cycle integration of CSP-technology

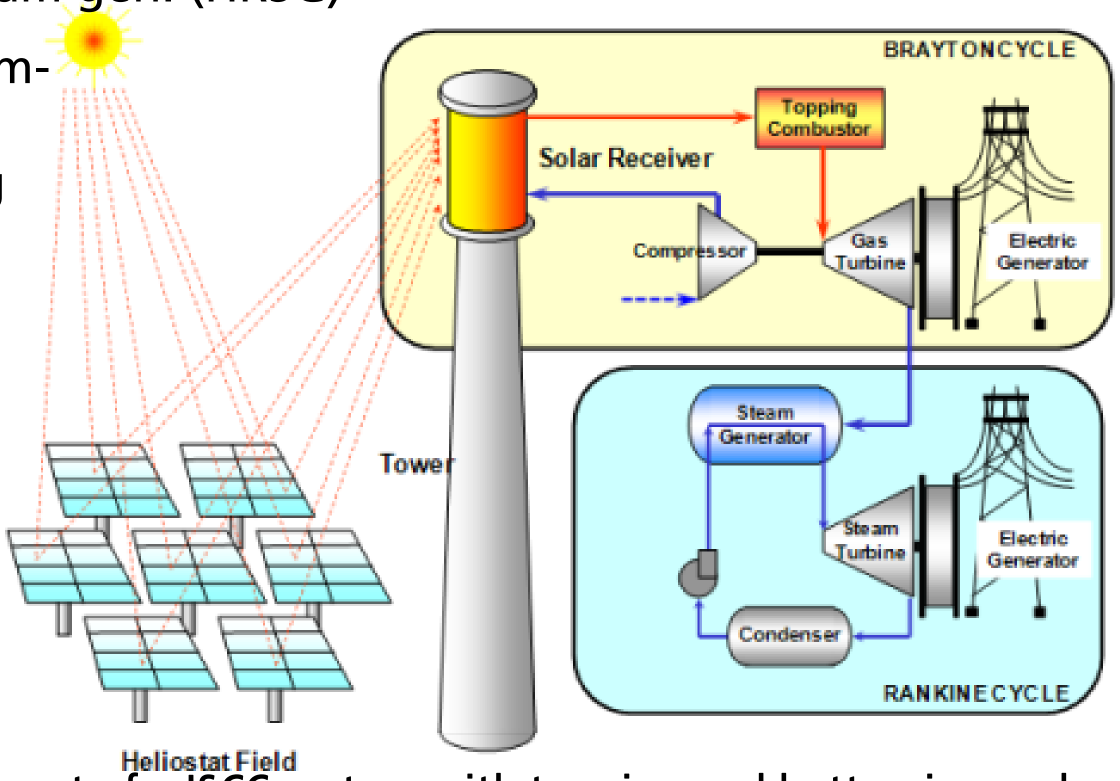

Layout of a ISCC system with topping and bottoming cycle

ISCC Hybrid Systems

ISCC hybrid systems: Solar integration into bottoming cycle

- CSP integration into bottoming cycle similar to *solar-aided coal-fired plants* (SACPG) ➔ instead of using coal, exhaust heat of topping gas turbine + CSP generates steam for the bottoming cycle
- All existing / planned ISCC plants incorporate CSP in the bottoming cycle ➔ integration is technologically mature, offering high reliability and low financial risk compared to topping cycle integration ➔ technology for high-temperature high-pressure solar receivers for topping cycle integration is not well developed yet

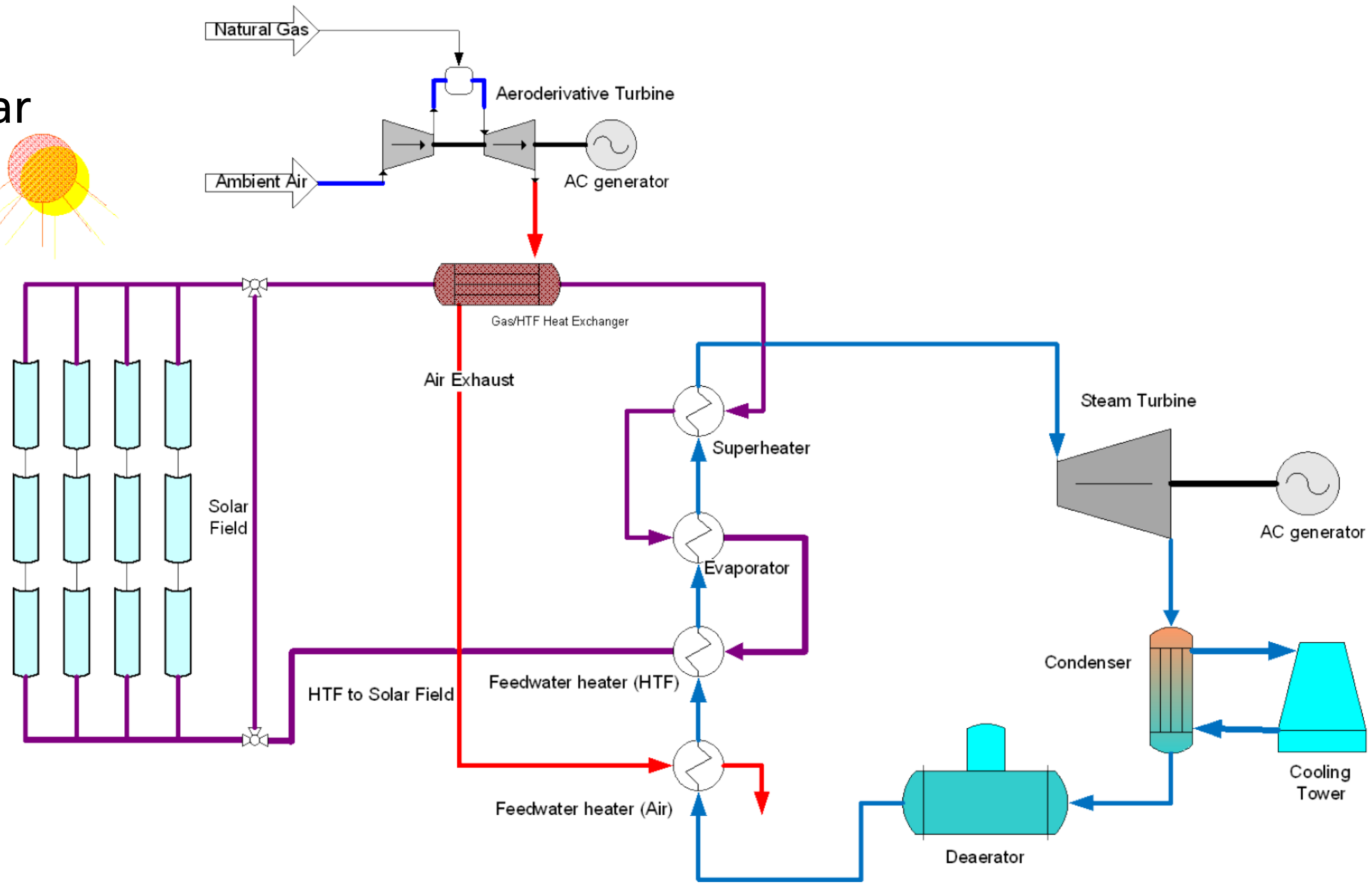

Simplified schematic of gas turbine backup for a PTC plant [6]

ISCC Hybrid Systems
Operating ISCC hybrid system examples [7]

Integrated solar combined cycle (ISCC) natural gas fueled hybrids

Name:	ISCC Hassi R'mel	ISCC Kuraymat	Martin Next Gen. Solar
Country:	Algeria	Egypt	Florida / USA
Start year:	2011	2011	2010
Technology:	Parabolic trough	Parabolic trough	Parabolic trough
Solar-based capacity:	20 MW	20 MW	75 MW
Solar-Field Aperture Area:	183,860 m²	130,800 m²	464,908 m²
Heat transfer fluid (HTF):	thermal oil (th.o.)	th.o. "Therminol VP-1"	th.o. "Dowtherm A"
SF inlet / outlet temp.:	293°C / 393°C	293°C /	393°C

Photos of operational ISCC hybrid power plants

Fraunhofer ISE

CSP-Biomass Hybrid Systems

Integration into power cycles driven by RE sources

Concept description:

- CSP integrated into power cycle of fuel-based plant
- Parallel or additional thermal energy input

Advantages:

- Electricity generation during low / no solar radiation (without TES)
- Continuous steam turbine operation (without TES)
- Maximum overall energy efficiency: approx. 33% [8]
- Capacity of biomass plant approx. 5 - 50 MW_{el}
  ➔ economy of scale benefits
  ➔ limited by feedstock transportation
  i.e. cost- increase for large plants

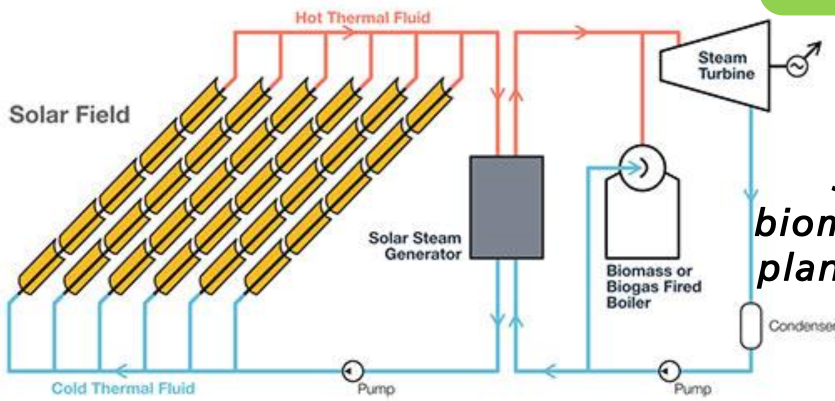

Solar-aided biomass power plant [SkyFuel]

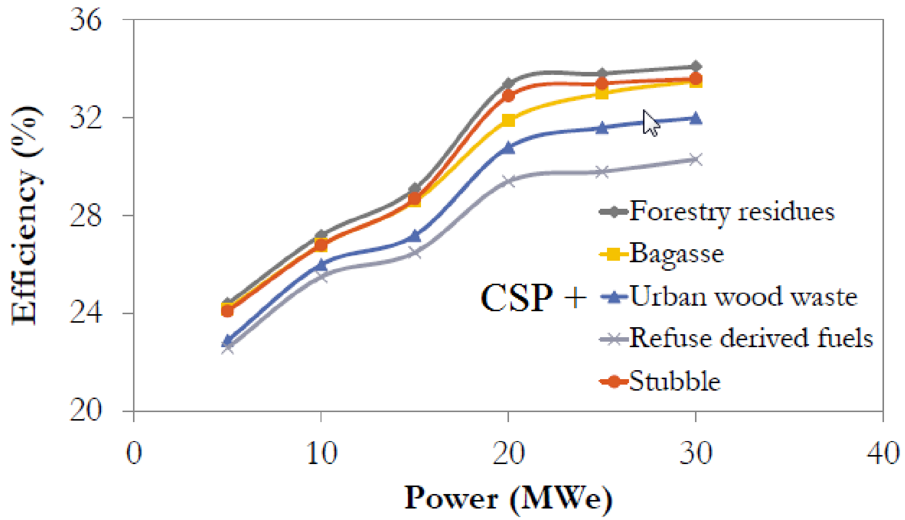

Net cycle efficiency of CSP-biomass hybrids with power output for different biomass feedstock / CSP combinations [9]

CSP-Biomass Hybrid Systems

Costs of CSP-biomass hybrid systems

- Costs
  ➔ Installation costs lower than standalone CSP with same nominal capacity
  Example for 40 MW_{el} plant @ 3.5 M$/$MW_{el}$: $140M
  ➔ cost reduction of up to 50% [10]

- Locations for CSP-biomass hybrids:
  ➔ Many, with high DNI and biomass availability
  ➔ hybrids make CSP commercially viable also in countries with low electricity price

- CSP integration effect on biomass plant?
  ➔ hybridization reduce biomass demand (i.e. land usage for energy crops) by 14 – 29% [11]

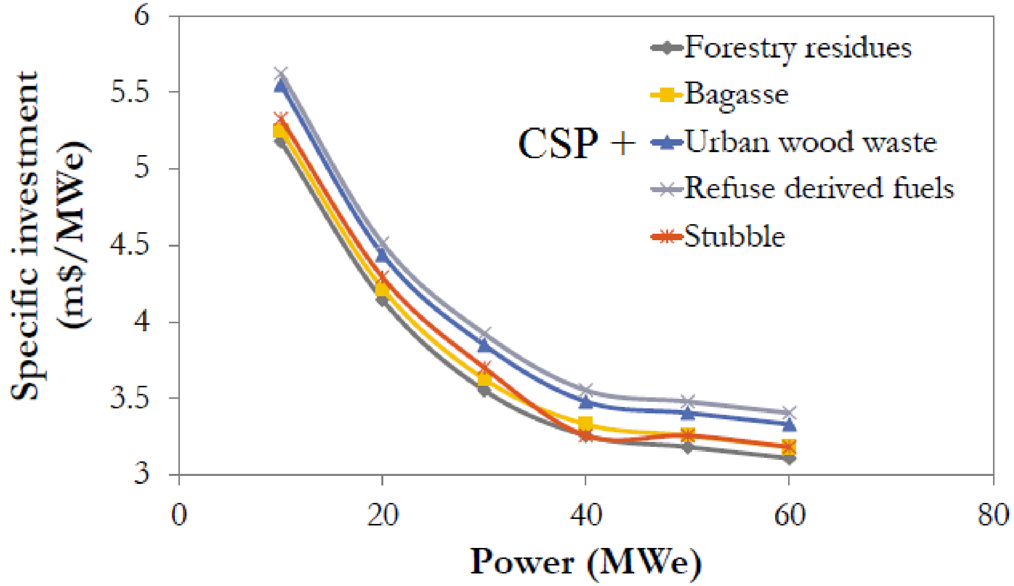

Variation of specific investment of solar-biomass hybrids with power output for different biomass feedstocks [9]

CSP-Biomass Hybrid Systems
Detail views of Termosolar Borges plant

CSP-biomass hybrids

- Detail views of Termosolar Borges hybrid plant [12], [13]:

a) left: 2 x 22 MW_{th} dual biomass and natural gas boilers

b) Parabolic trough solar field position at noon

c) Biomass (trunk wood) delivery to the plant

CSP Hybrid Systems
Overview

CSP-wind hybrids

- Hybridization / hybrid power plants?
  ➔ combine CSP with other RE
- Options:
  a) Combining conventional power cycle plants with CSP: Internal hybridization
  ⟶ Integration into existing plant infrastructure
  b) Combining standalone CSP with independent RE technologies: external hybridization
  ⟶ Compensate for temporal effects

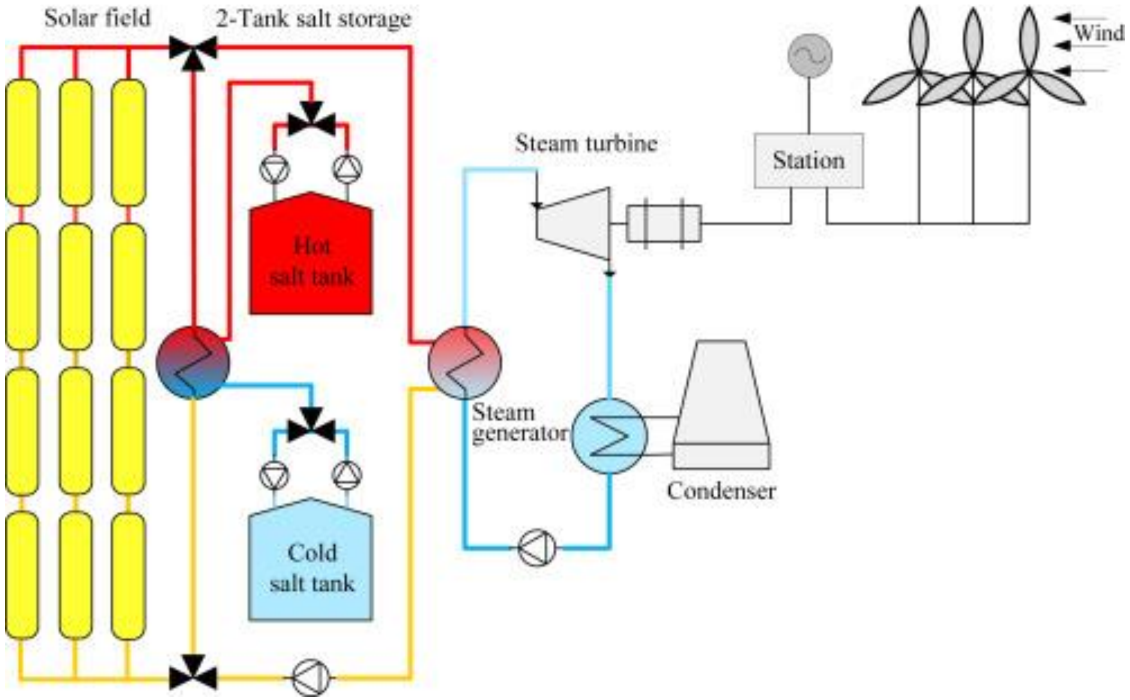

Exemplary hybrid of wind-CSP, i.e. a “light hybrid” power plant [2]

CSP-Wind Hybrid Systems

Exemplary study on CSP-wind hybrids

CSP-wind hybrids

- Feasibility studies were conducted for several locations
  - Arabian peninsula
  - Ontario
  - India
  - Italy
  - Spain
  - North African Countries
  -

    ➔ partially strong potential for complementarity between solar and wind power [14] [15]

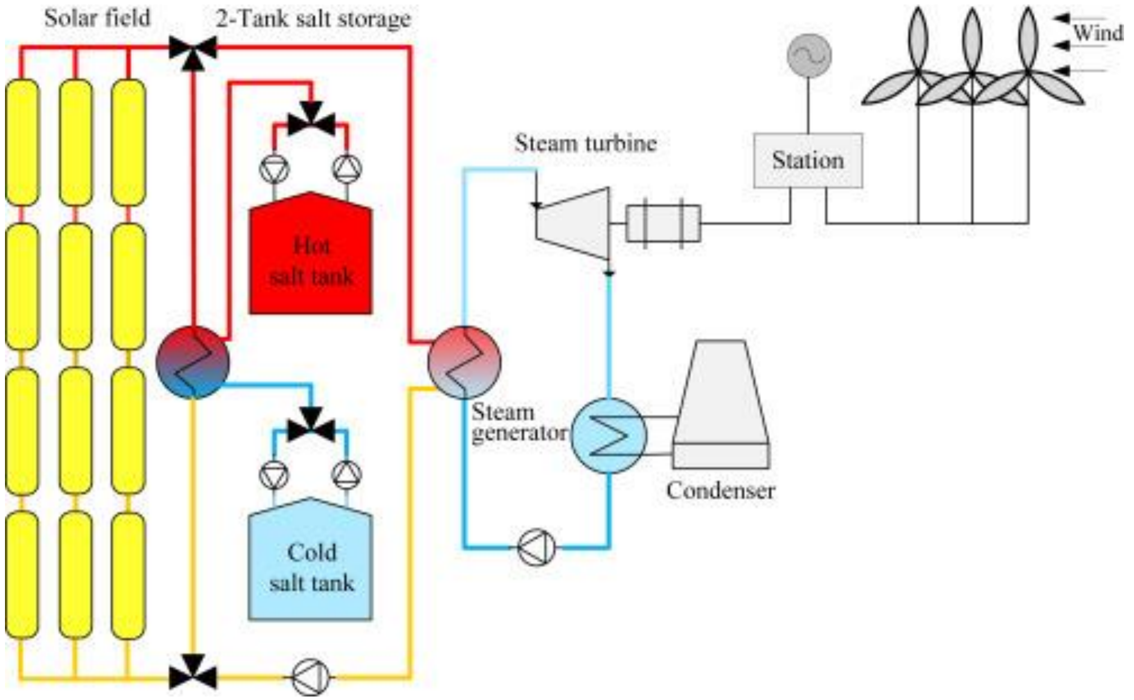

Exemplary hybrid of wind-CSP, i.e. a "light hybrid" power plant [2]

Fraunhofer ISE

CSP-Wind Hybrid Systems

Exemplary study on CSP-wind hybrids

- Configurations for co-locating solar and wind power plants in Texas were analyzed [16]
  ➔ deployment of hybrid plants with up to 67% of CSP would yield a positive return on investment
- Investigations for plants in Australia [10] show that CSP-wind hybrids have potential as several wind farms and CSP plants are co-located
  ➔ promising locations in South / West Australia (wind speeds > 7 m/s, DNI > 19.1 MJ/m^{2}d)
  ➔ excess electricity produced at night by wind farm can be utilized to charge TES of CSP plant
  ➔ However, 260% difference in day- and night-time electricity prices necessary for economic feasibility

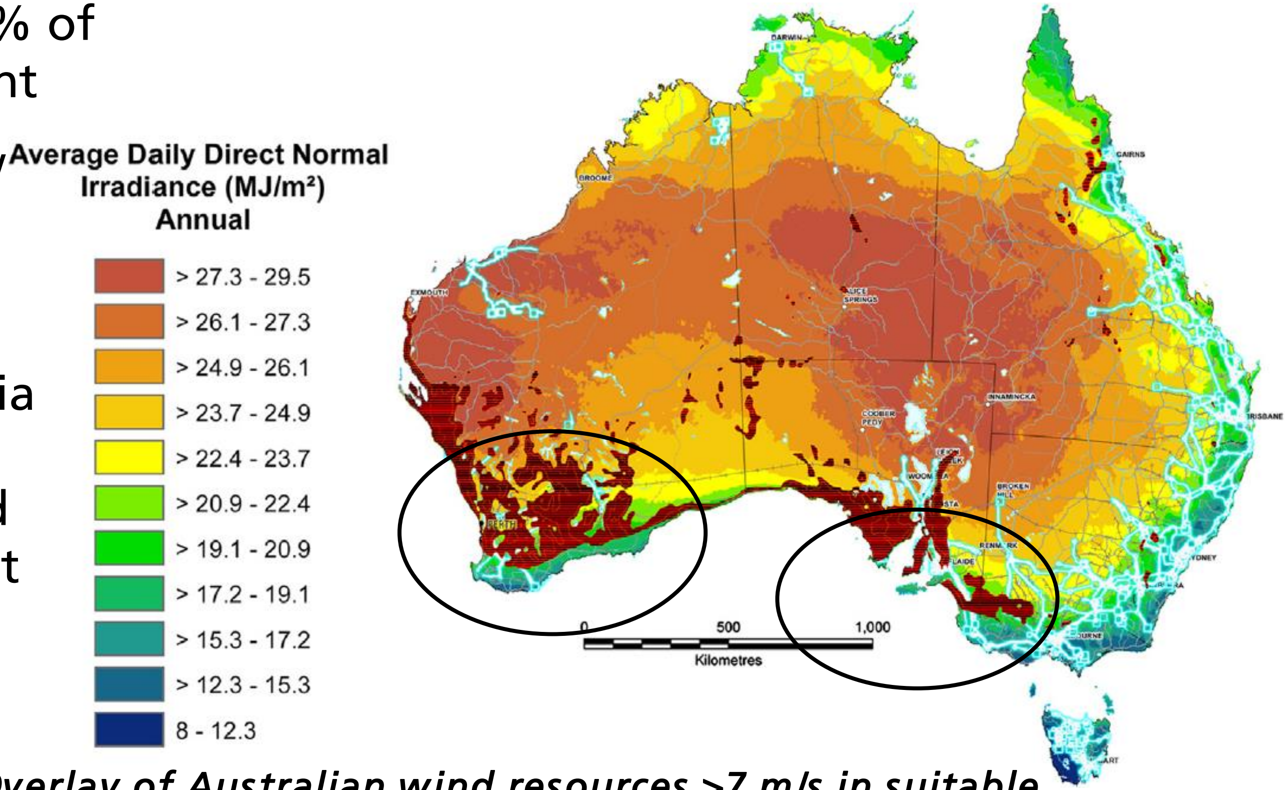

Overlay of Australian wind resources >7 m/s in suitable DNI areas >19.1 MJ/m2/day with transmission infrastructure [10]

CSP-Wind Hybrid Systems
Exemplary study on CSP-wind hybrids

- Study on the hybridization of CSP with wind farms in Andalucía by University of Jaén, Andalucía [17]
- Optimal locations for CSP-wind hybrids can overcome the spatiotemporal variability in standalone operation
- stable renewable energy base-load power possible

→ good seasonal balancing between CSP plant and wind farm

→ higher CSP capacity factor in summer and spring; higher wind capacity factor in winter and autumn

→ addition of TES to CSP plant enhances hybrid performance, especially in spring

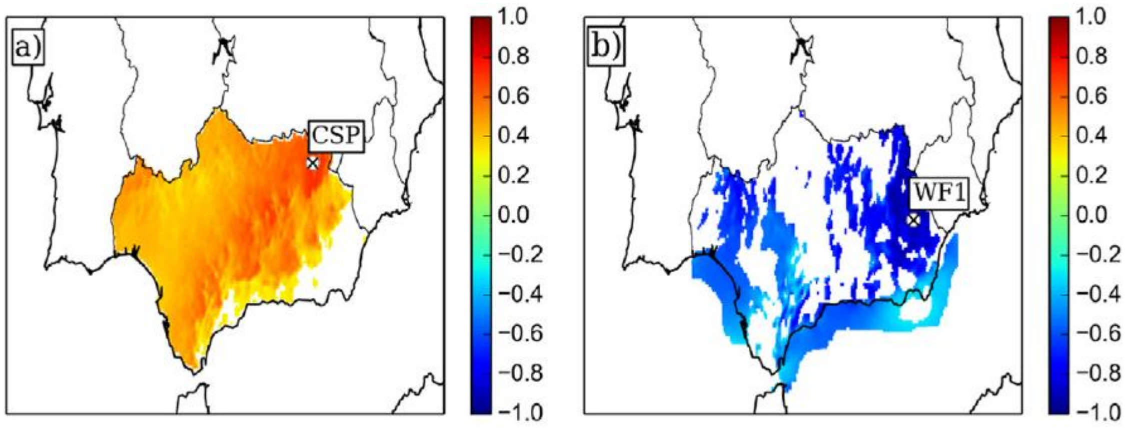

CSP (a) / wind (b) capacity factors during daylight hours [17]

CSP-Wind Hybrid Systems
Exemplary study on CSP-wind hybrids

- Study on CSP-wind hybrid plant performance at Texas Panhandle, USA [18]
  ➔ goal: determine suitability of CSP-wind hybrids to match utility electrical load vs. standalone wind farm
- Standalone wind farm generation is highest at night when electricity load is lowest and vice versa (see **Fig. a**)
- Best match for av. Annual utility electricity load (see **Fig. b**) :
  - 67 MW_{el} wind farm plus
  - 33 MW_{el} CSP plant with 6 h of TES
- But, LCOE of hybrid plant with TES is 2x standalone wind farm ($125/MWh CSP w. TES + wind vs. wind farm only @ $64/MWh)

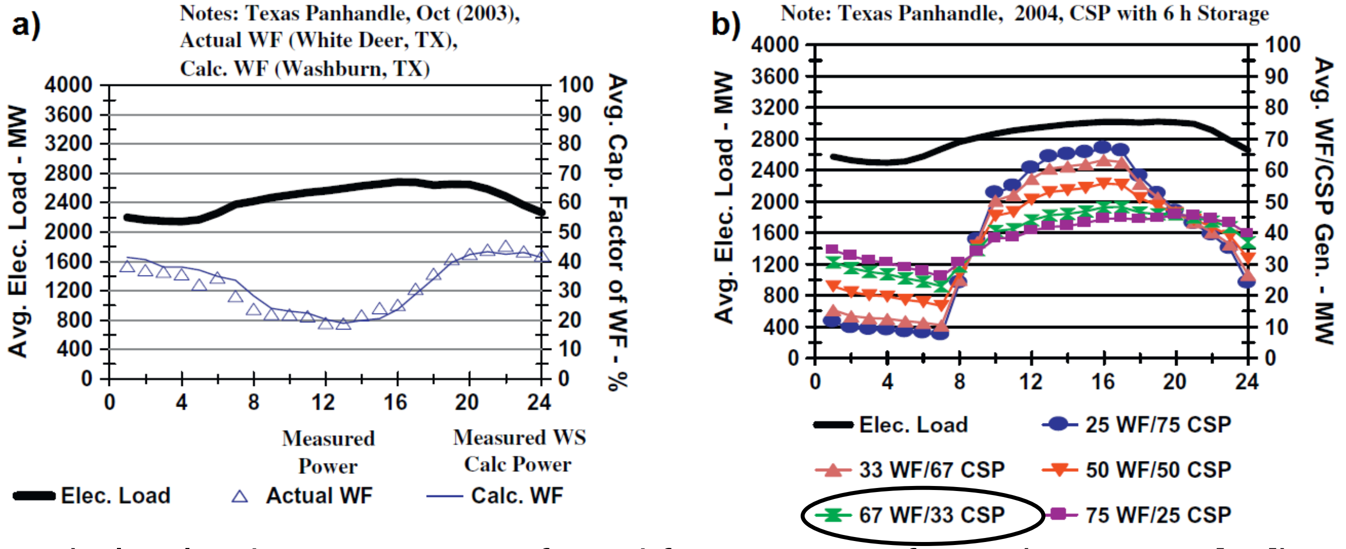

a) elec. load + comparison of wind farm capacity factor (Oct., 2003 [18])
b) annual utility loading vs. different ratios of wind + CSP with TES (2004)

Fraunhofer ISE

CSP-Wind Hybrid Systems
Study on CSP-wind hybrid system performance: Skyros / Greece

- Study on CSP/wind hybrid for Greek island [19]
  - CSP plant capacity of 10 MW_{el}
  - two Vestas V112 wind turbines á 3.3 MW_{el} each
  - ➔ Total capacity of 16.6 MW_{el}
- Mean annual efficiency:19.2%
- The COE of the CSP + wind hybrid: 400 €/MWh
- electricity costs on Skyros > 400 €/MWh in 2012/2013 (77% thereof: diesel costs)
  ➔ COE of hybrid plant is lower than of presently operating power generation plant
  ➔ Promising option for energy autonomy of remote locations (islands)

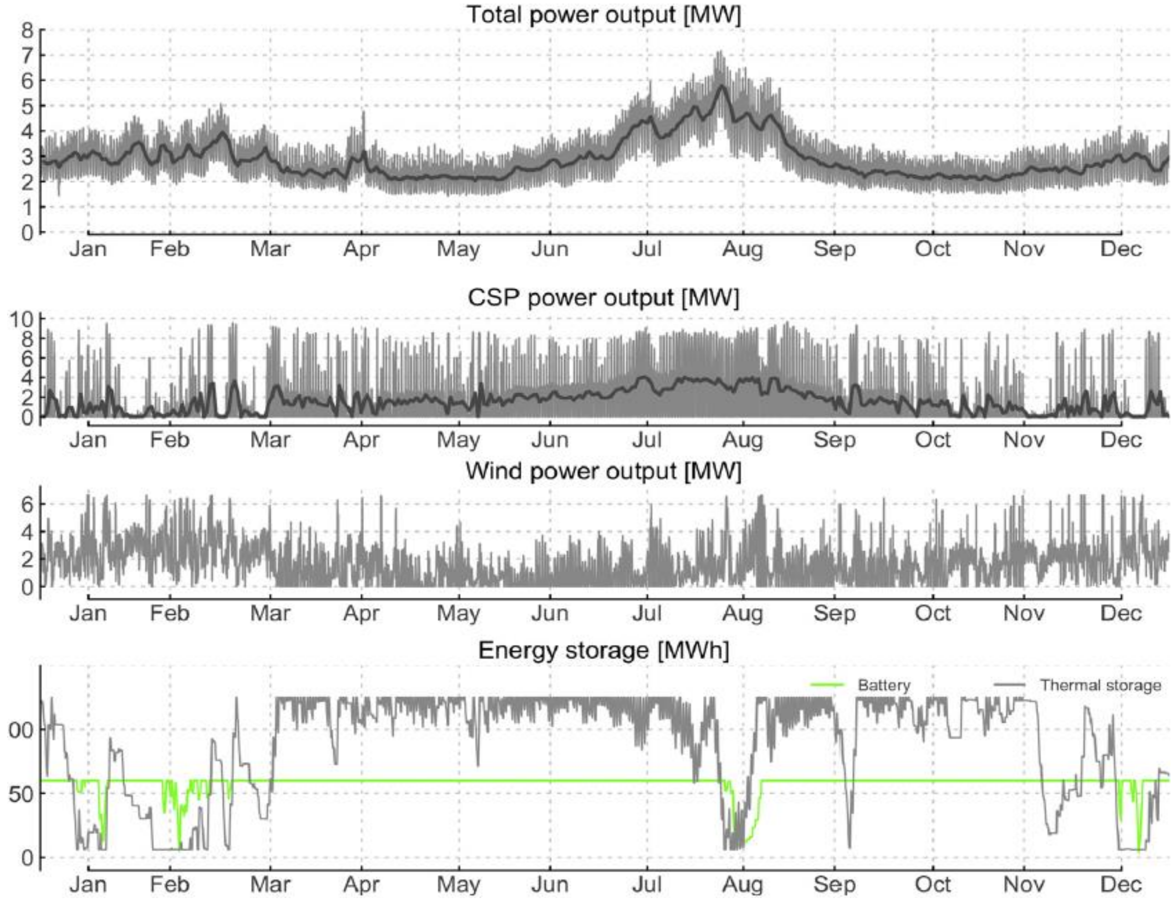

Performance of CSP-wind hybrid with el./th. storages [19]

Fraunhofer ISE

CSP-PV Hybrid Systems
Overview

CSP-PV hybrids

- Hybridization / hybrid power plants?
  ➔ combine CSP with other RE
-

  Options:

  a) Combining conventional power cycle plants with CSP: Internal hybridization
  ⟶ Integration into existing plant infrastructure

  b) Combining standalone CSP with independent RE technologies: external hybridization
  ⟶Compensate for temporal effects
  ⟶Joint use of electric infrastructure

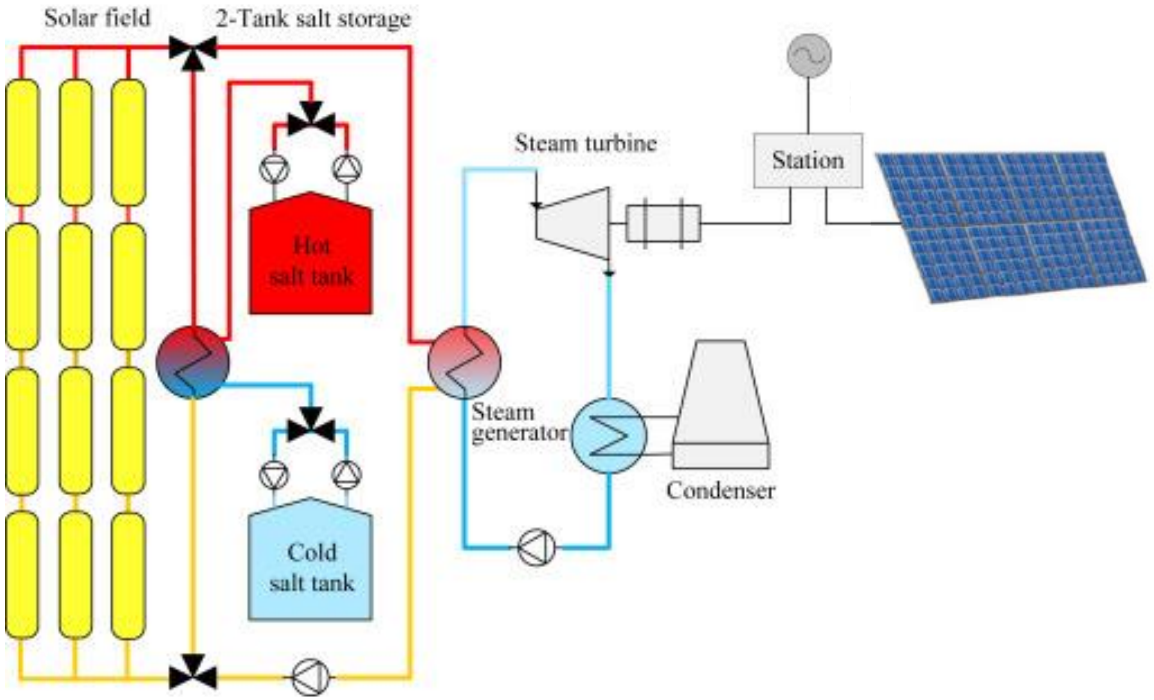

CSP hybridization with PV, adapted from [2]

CSP-PV Hybrid Systems
External hybridization

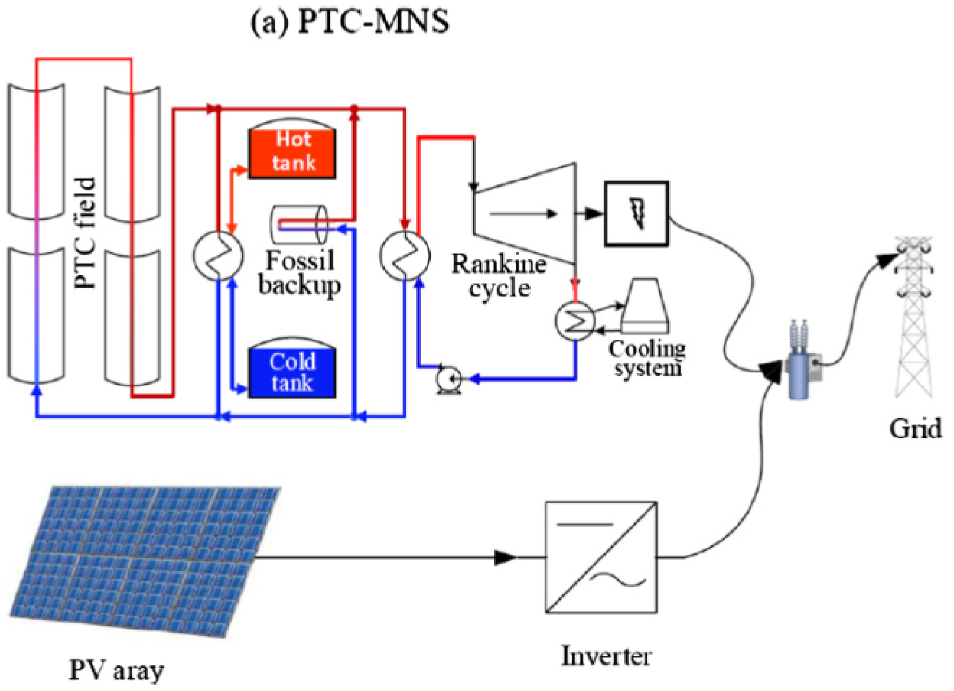

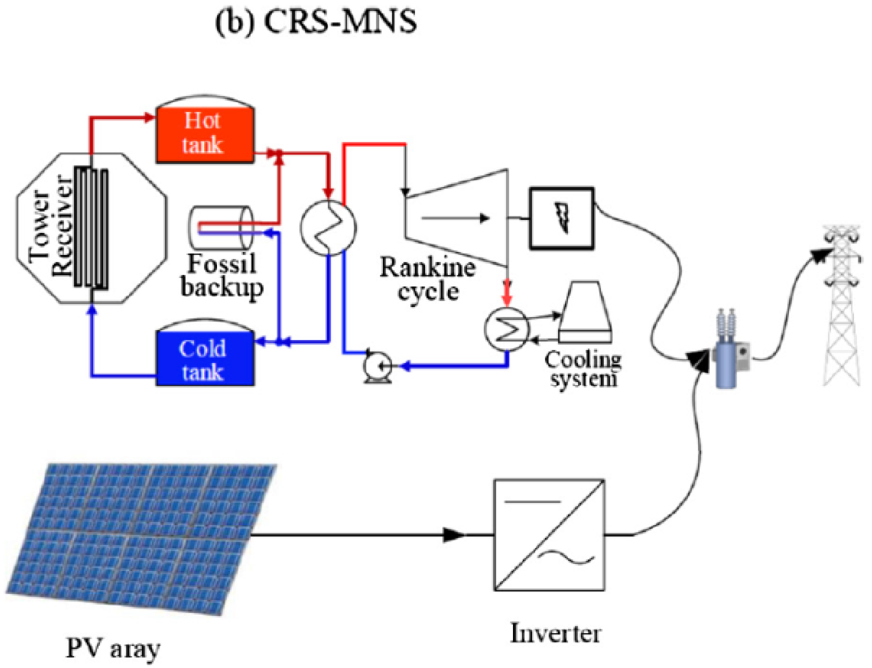

[20]

CSP-PV Hybrid Systems
Advantages of external hybridization

- Utilization of synergies
  - Share infrastructure (substations, transmission lines…)
  - Higher capacity factor
    - PV alone: 13%~19%
    - CSP with TES alone: > 50% → **Up to 90%**
- Reducing the overall LCOE

100 MW_{el} solar plants

PV plant without storage

Solar tower plant with large storage

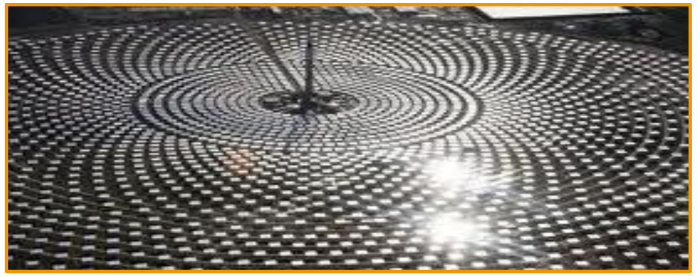

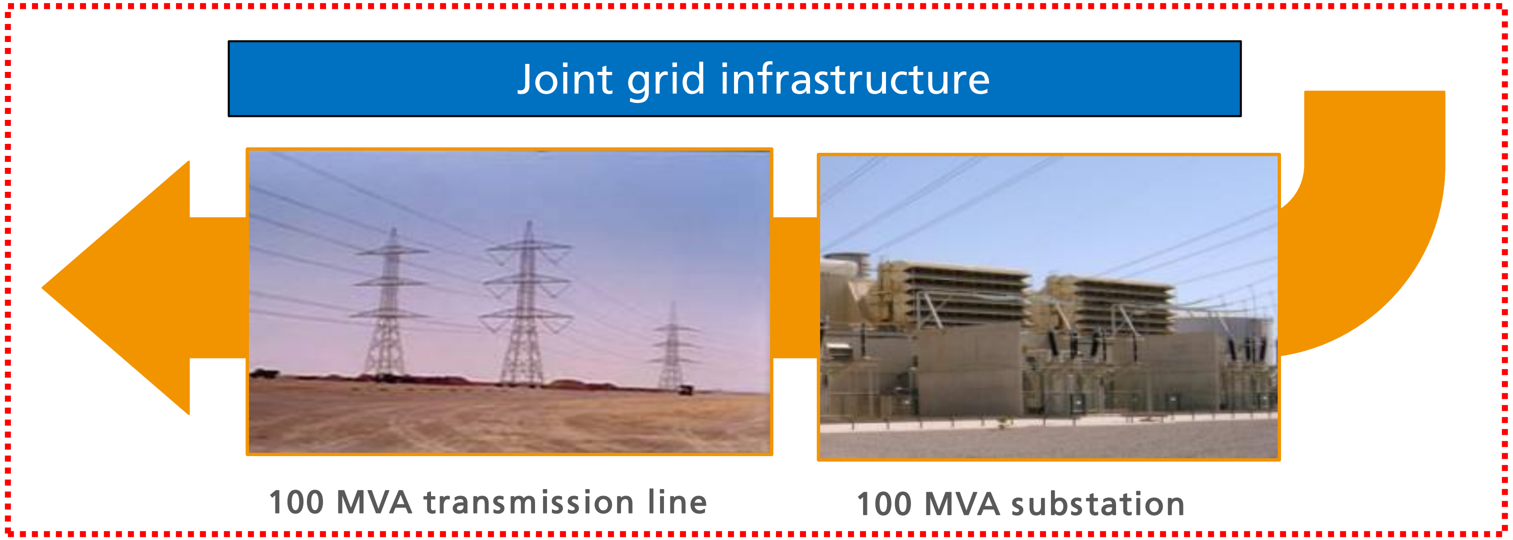

SFERA Fraunhofer ISE

CSP-PV Hybrid Systems
Advantages of external hybridization

- Combining cheap power production (PV) and dispatchable power supply (CSP)
  - Low cost of PV
  - Cheap thermal storage of CSP
  - 100% renewables possibility
- Adaption to demand
  - Stable output
  - Ramp up/down

[Image: Solar Reserve]

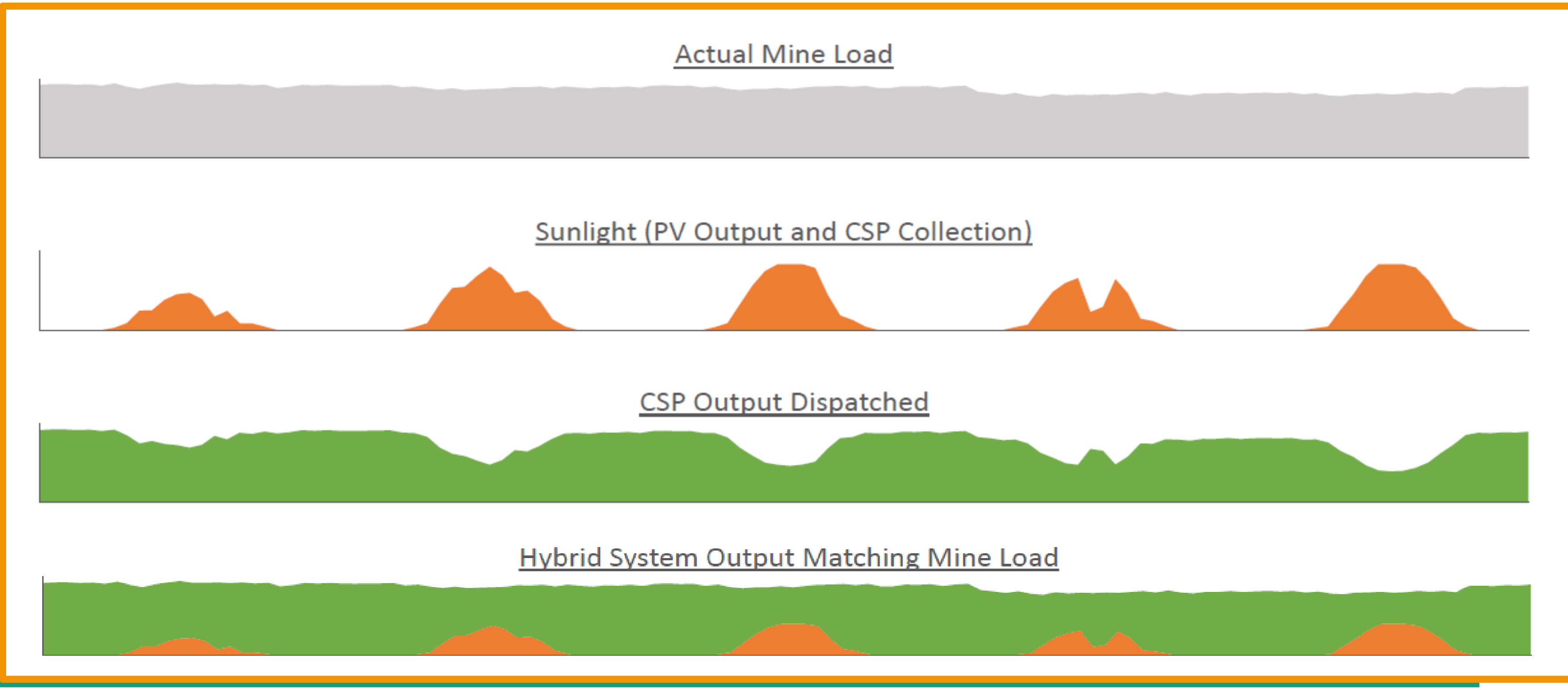

CSP-PV Hybrid Systems
Example 260 MWel unit in Chile

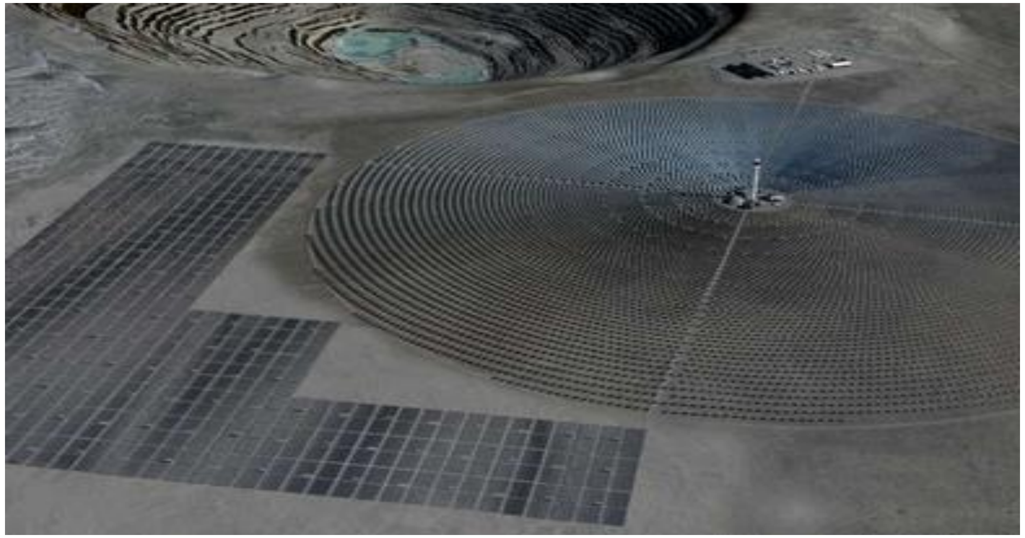

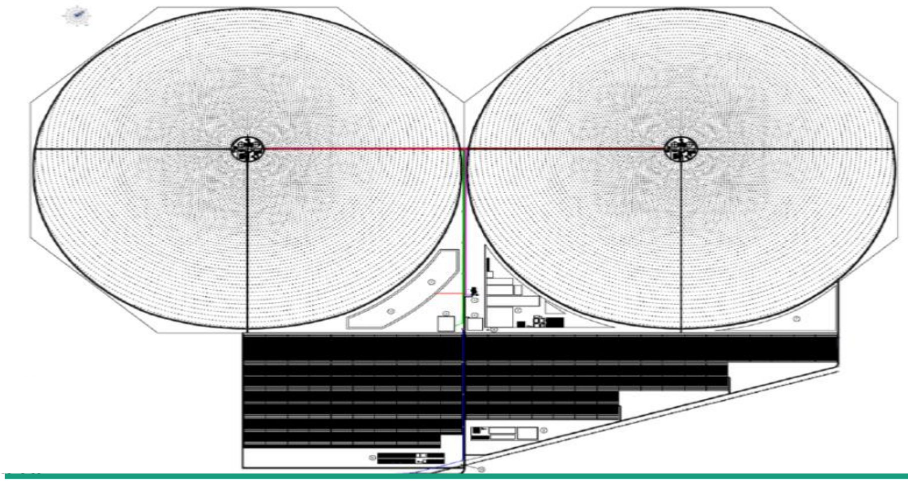

Copiapó (Chile)

- 2*130 MW_{el} capacity (CSP)
- 150 MW_{el} capacity (PV)
- 24 hours operation
- 14 FLH storage (CSP)
- 1,800 GWh_{el} annual pow. gen.
- < $0.10/kWh 30-year PPA
- Copiapó mine in the Atacama region
- 100% solar

[Images: Solar Reserve]

Fraunhofer ISE

CSP-PV Hybrid Systems
Scope of operation

- Stable baseload output
  - PV output↑, CSP output↓, baseload ~
- Output ramping up ↑, CSP output ↑
  - Response to the grid demand by CSP share
- Thermal storage is fully charged
  - defocusing parts of the collectors

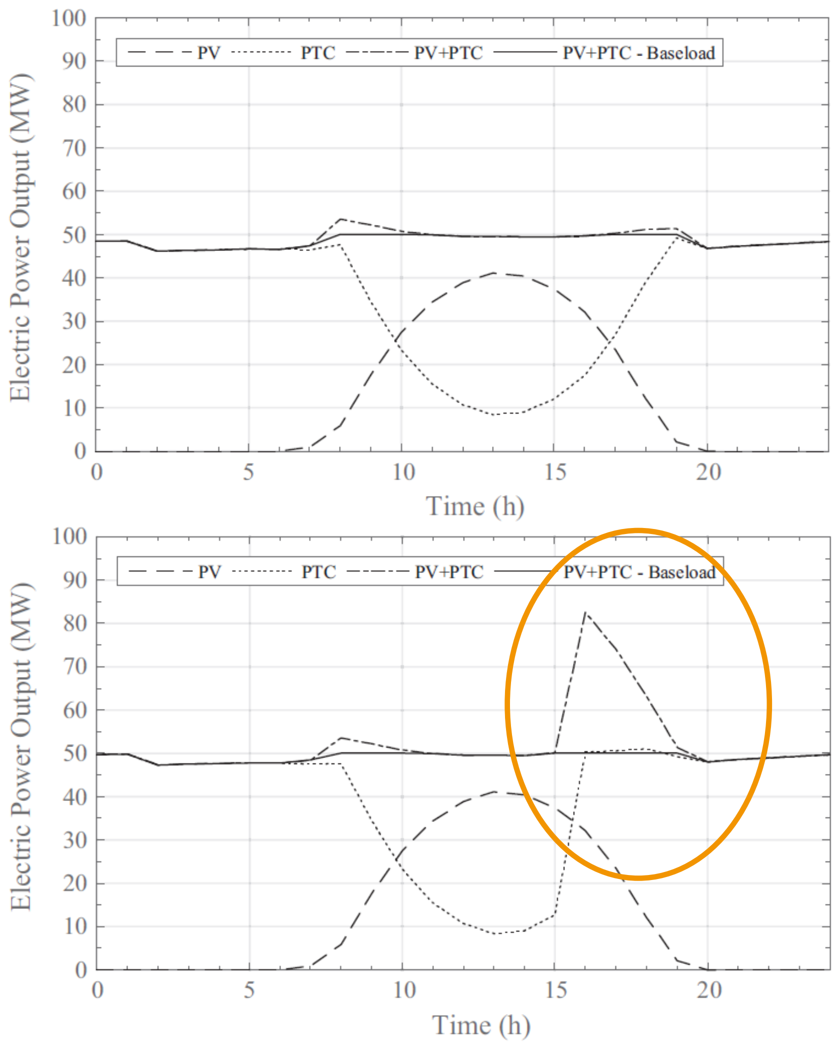

Dispatch modes of power production of the CSP + PV hybrid plant, (a) baseload production and (b) peak production. [20]

CSP-PV Hybrid Systems
Scope of operation

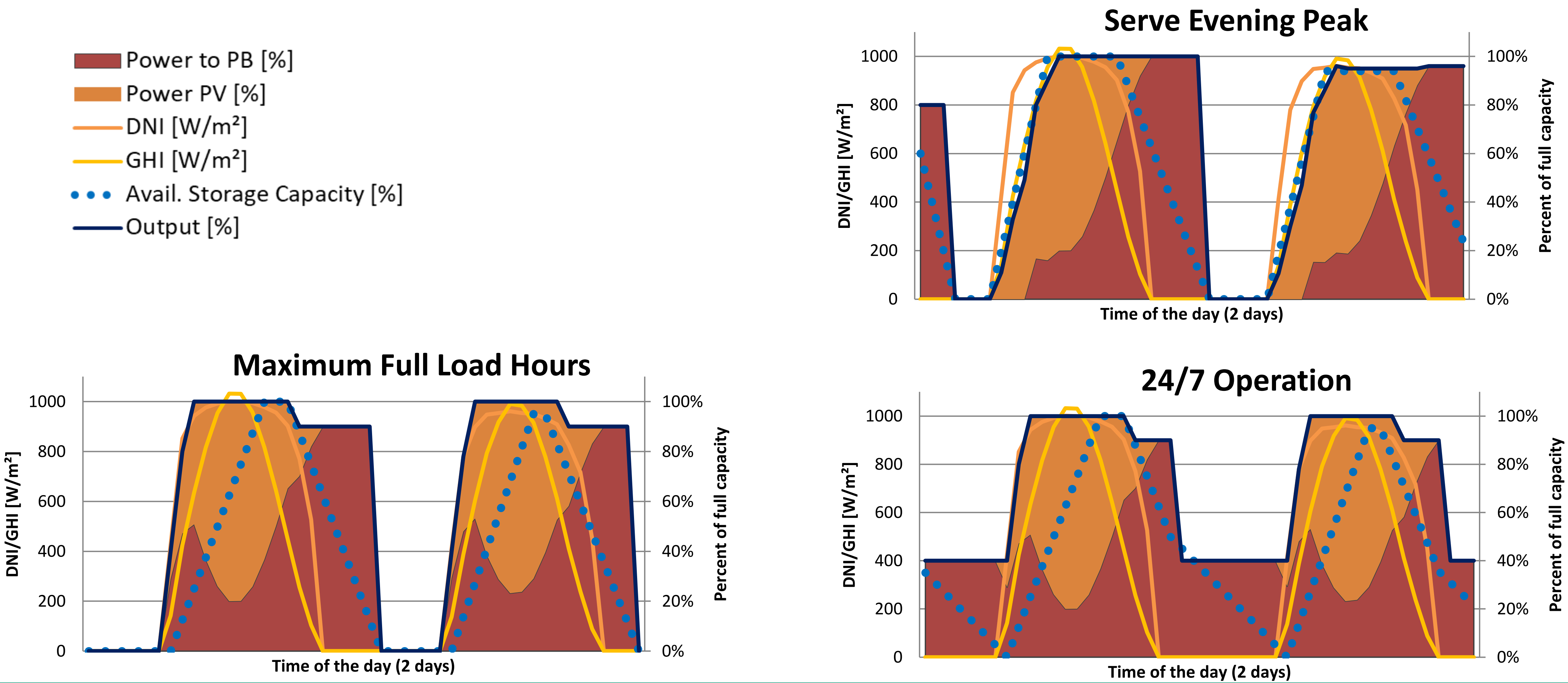

CSP-PV Hybrid Systems
Synergies in winter operation

- Utilization of GHI
  - CSP maybe unable to operate, PV to generate electricity
- Tilt of PV modules
  - Higher tilt angle for PV panels → generate more in the winter
  - The optimal inclination angle for the hybrid plant is considerably higher than the tilt angle for a PV-only plant.
  - → Hybrid PV array at a non-optimal condition
  - → Hybrid PV generating more power during winter months when CSP production decreases
  - →support a base-load production of electricity

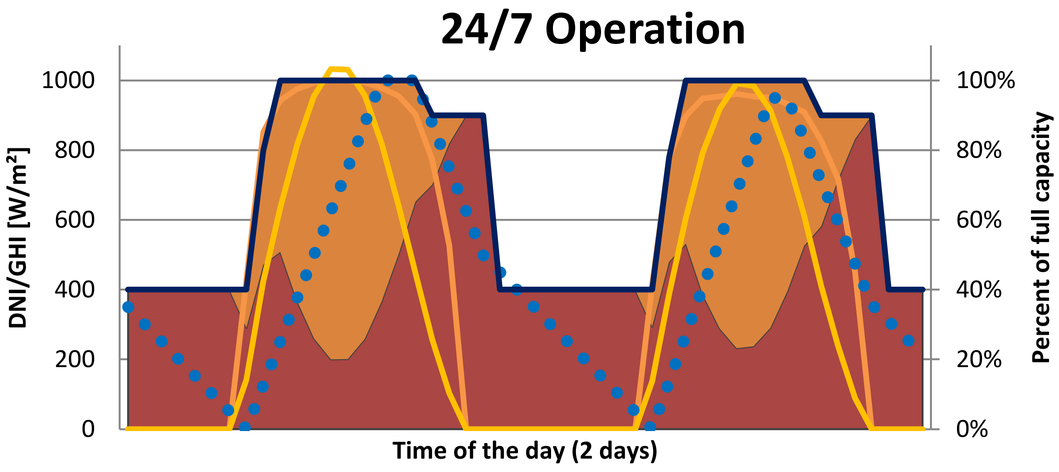

Fraunhofer ISE

CSP-PV Hybrid Systems
Hybridization on System Level or Plant Level?

- System Level:
  - PV, CSP independent at different sites:
    - PV Produces over day,
    - CSP dispatches to match overall loadcurve
    - 2x transmission line
    - Capacity factor each TL ~20% or lower (eg. Morocco 5/24h 19-23:59 CSP, 07:00-19:00 PV)
    - PV curtailed at peaks
    - Battery Storage at plant / at load center
    - Two operators, two strategies

- Share Grid:
  - PV, CSP independent at at close sites:
    - PV Produces over day,
    - CSP dispatches to match loadcurve
    - 1x transmission line
    - Capacity factor TL together ~40% or more (eg. Morocco >70% 18/24h 19-23:59 CSP, 07:00-19:00 PV)
    - PV curtailed at peaks
    - Battery Storage at plant / at load center
    - Two operators, two strategies

CSP-PV Hybrid Systems

Hybridization on System Level or Plant Level?

- Same operator:
  - PV, CSP dependant at at close sites:
    - PV Produces over day,
    - CSP dispatches to match loadcurve
    - 1x transmission line
    - Capacity factor TL together ~40% or more (eg. Morocco >70% 18/24h 19-23:59 CSP, 07:00-19:00 PV)
    - PV curtailed at peaks
    - Battery Storage at plant / at load center
    - One operator, one strategie

- Integrated System:
  - PV, CSP Combined in one plant:
    - PV Produces over day,
    - CSP dispatches to match loadcurve
    - 1x transmission line
    - Capacity factor TL together up to 90%
    - PV peaks (or even more) dumped battery storage and excess energy in heat storage
    - Battery Storage at plant / at load center
    - One operator, one strategy

CSP-PV Hybrid Systems
Recent concepts – internal integration

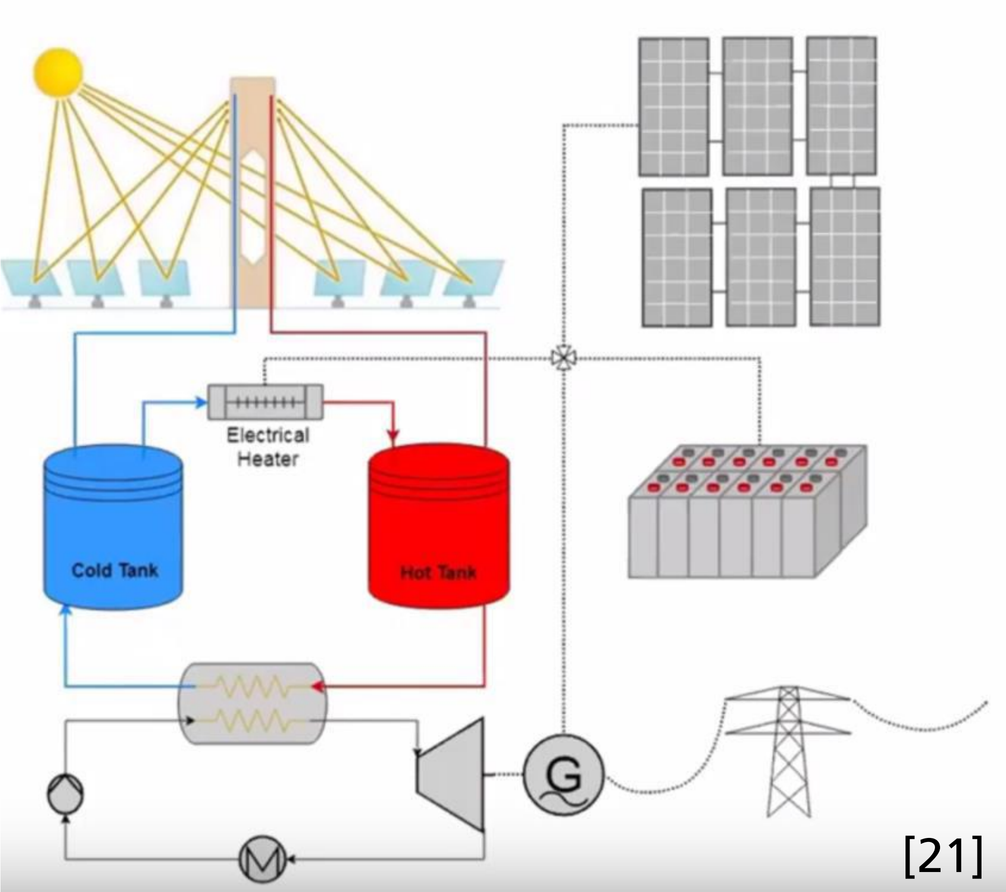

[21]

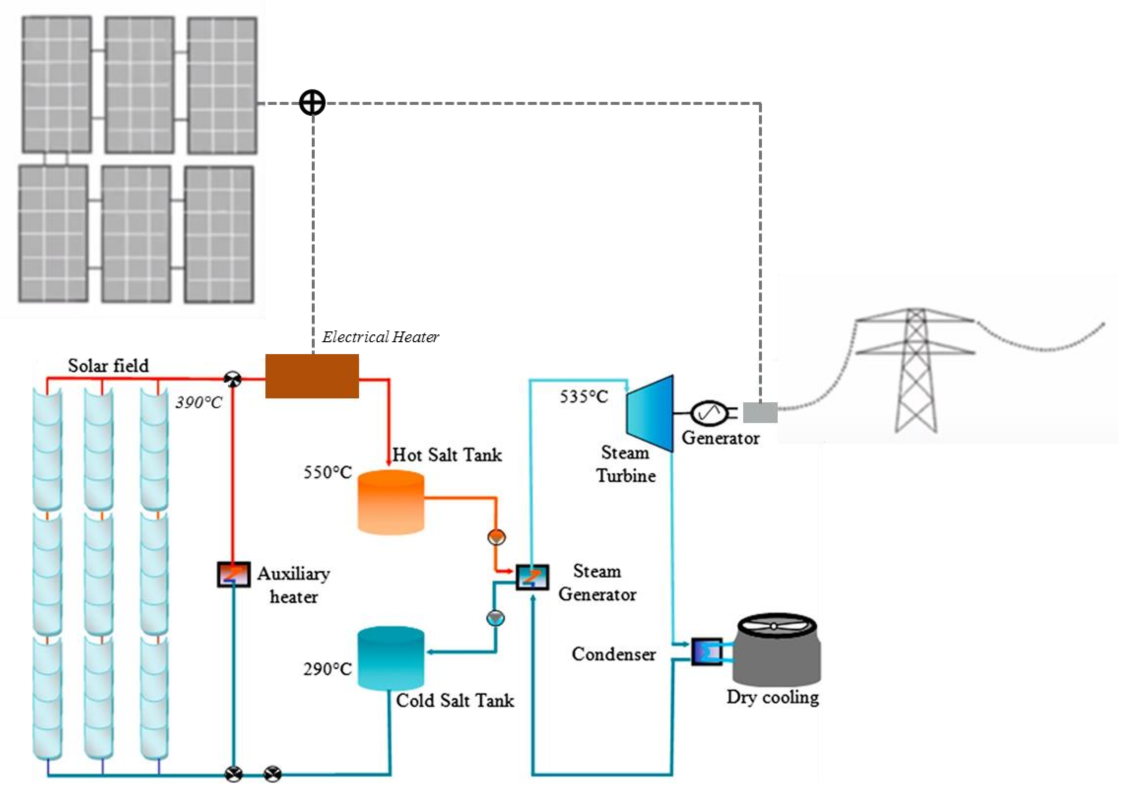

Adapted from [22]

CSP-PV Hybrid Systems
Recent concepts – internal integration

- 1 - PV production < 75 MW:
  - CSP+TES covers deficit
- 2 - PV production < 75 MW:
  - CSP operates at minimum (25%), PV surplus -> BES
- 3 - PV production >100 MW
  - CSP charges TES, PV surplus charges BES

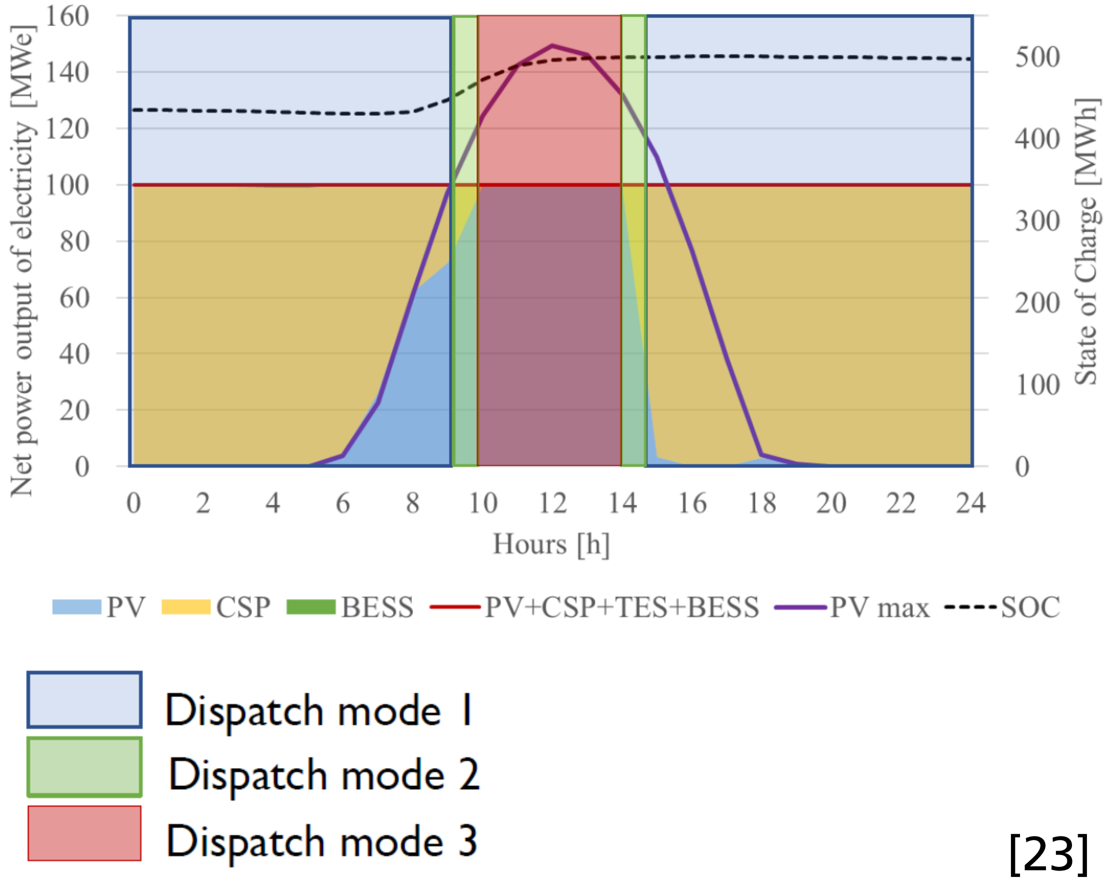

[23]

CSP-PV Hybrid Systems

Noor Midelt - PV providing high temperature heat

- Concept:
  - PV optimized for production over day with high (full) grid penetration
  - PTC field operates on oil 290-390°C with heat exchanger to salt storage
  - Electric excess energy heats the salt to 550°

Noor Midelt:

150 MW CSP + PV / 190 MW CSP + PV

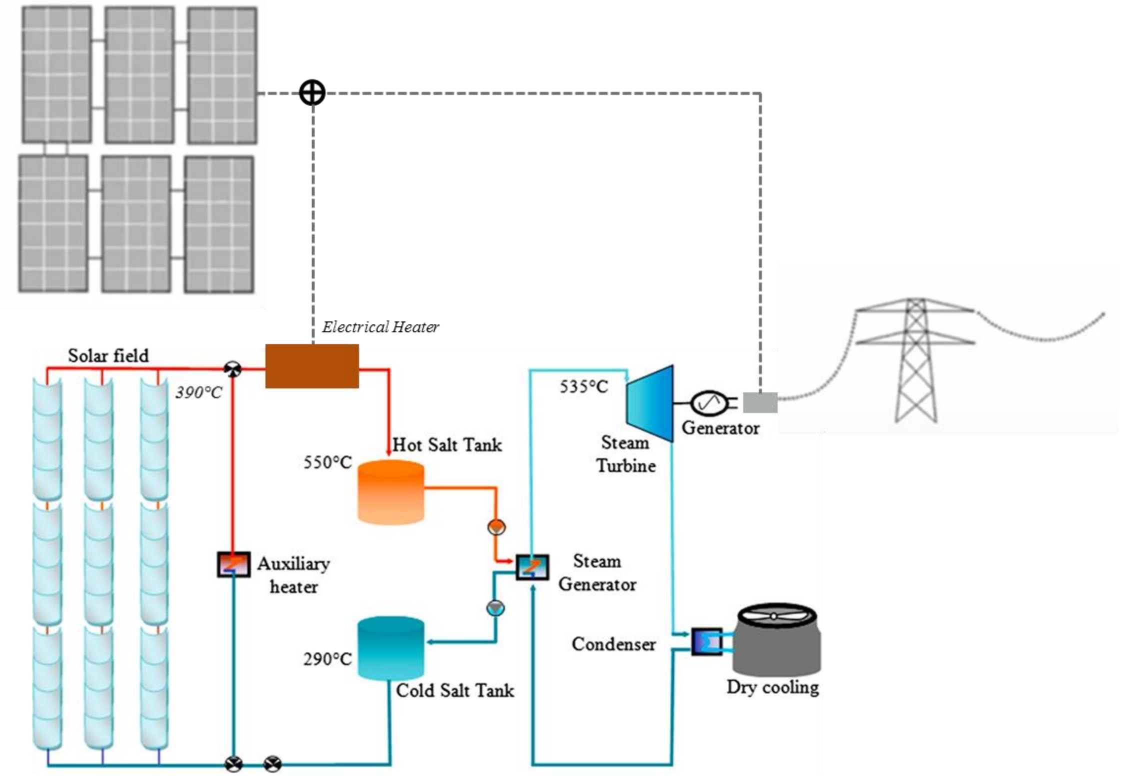

Adapted from [22]

Fraunhofer ISE

CSP-PV Hybrid Systems
Noor Midelt - PV providing high temperature heat

- But:
  - PV→Storage→Elektricity has LOW efficiency
  - Availability and cost of land becomes important
- Cost & risc [25]:
  - Not always lowest CAPEX leads to lowest LCOE
  - „Easily come down to 7 ct/kWh“
  - „In future 4-5 ct/kWh“
  - Only known technology → no risk in bankability

150 MW CSP + PV

190 MW CSP + PV

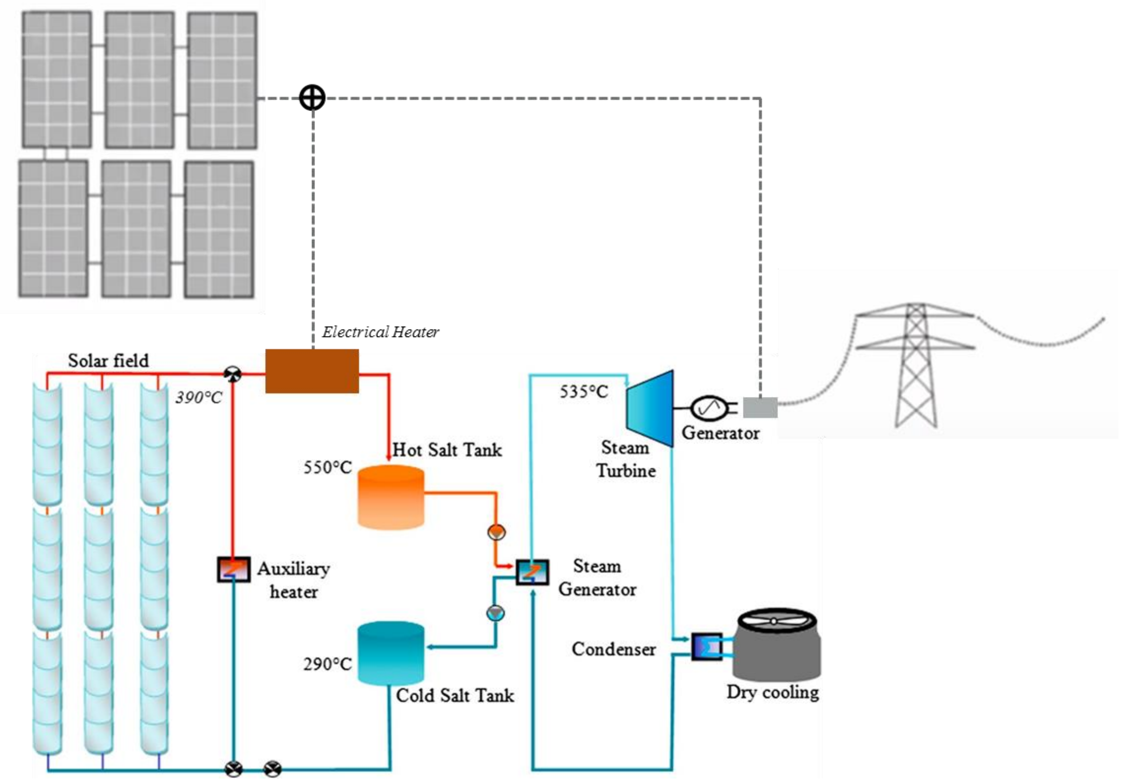

Adapted from [22]

Fraunhofer ISE

CSP-PV Hybrid Systems
Adapted tariffs give important incentives

- DEWA IV, PPA 35 years
  - Day tariff (PV): 24 US$/MWh
  - Day tariff (CSP): 29 US$/MWh
  - Peak tariff (CSP): 92 US$/MWh
- Noor Midelt, PPA 25 years
  - Peak hours tariff: 70 US$/MWh
  - Average tariff: 62 $/MWh

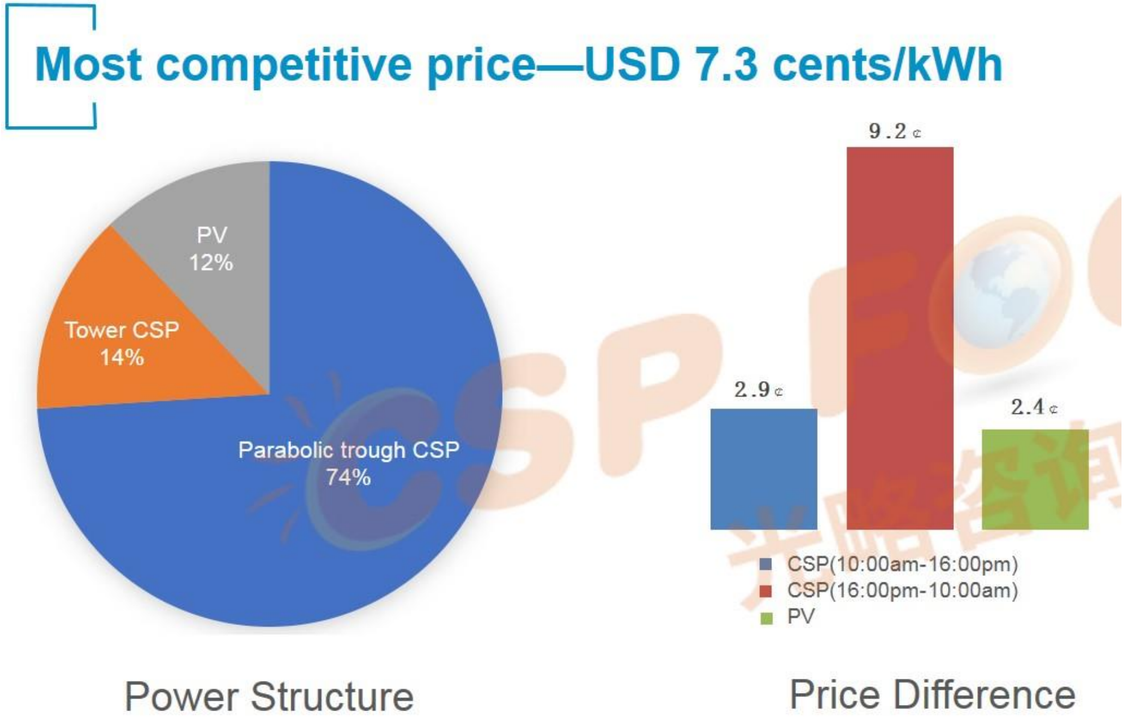

[24]

CSP-PV Hybrid Systems
Conclusions

- PV CSP plays a high potential, when
  - Fixed load curve
  - Stable demand for day and night
  - High night tarifs !!!

- CSP+PV expected to be main solution for high DNI sites with
  - CSP at minimum level for fast reaction
  - PV following passively
  - PV tilt optimized for winter (for non tracking PV)

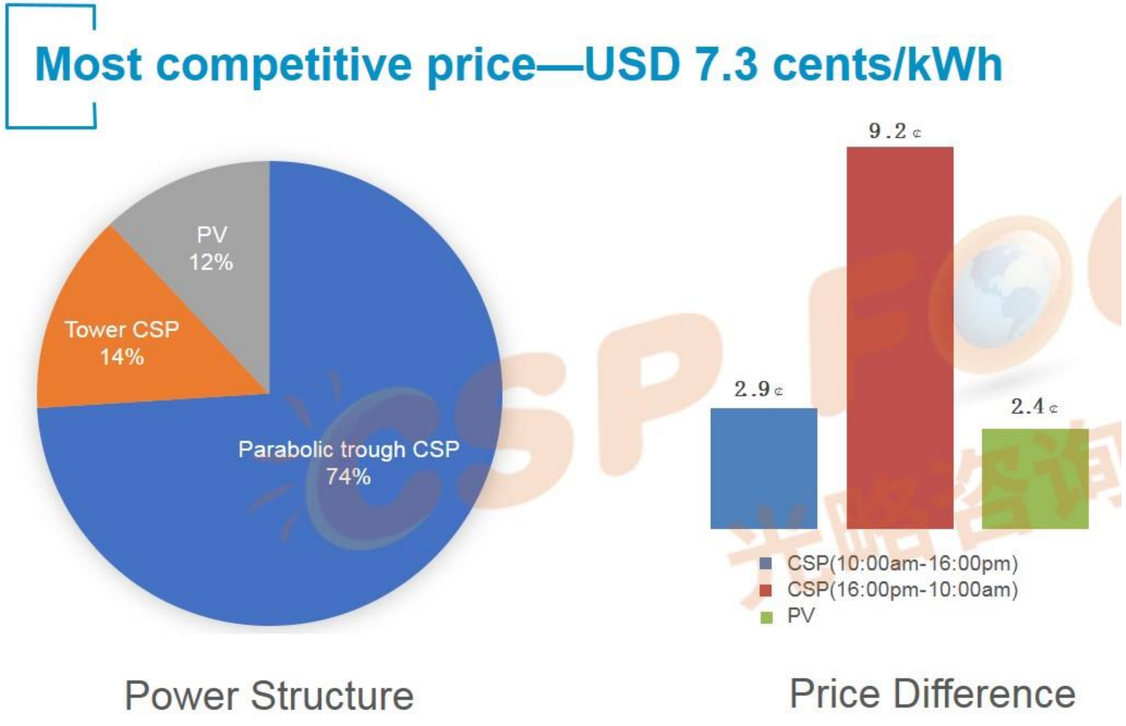

[24]

Thank you for your Attention!



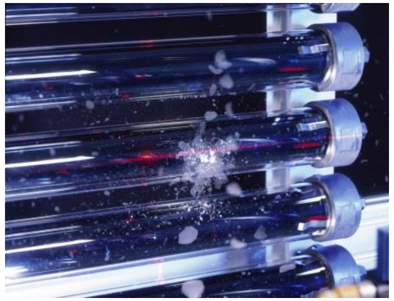
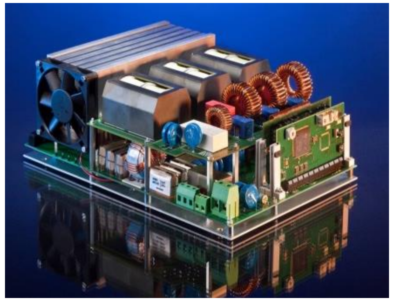
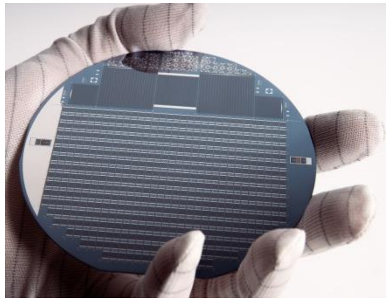


Fraunhofer Institute for Solar Energy Systems ISE

Gregor Bern

www.ise.fraunhofer.de

gregor.bern@ise.fraunhofer.de

Fraunhofer ISE

References

- [1] S. Pramanik, A review of concentrated solar power hybrid technologies, Article in Applied Thermal Engineering (2017). DOI: 10.1016/j.applthermaleng.2017.08.038
- [2] H.M.I. Pousinho, J. Esteves, V.M.F. Mendes, M. Collares-Pereira, C. Pereira Cabrita, Bilevel approach to wind-CSP day-ahead scheduling with spinning reserve under controllable degree of trust, Renew. Energy. 85 (2016) 917–927. doi:10.1016/j.renene.2015.07.022.
- [3] S.D. Oda, H.H. Hashem, A case study for three combined cycles of a solar-conventional power generation unit, Sol. Wind Technol. 5 (1988) 263–270. doi:10.1016/0741-983X(88)90023-9.
- [4] E.J. Sheu, A. Mitsos, A. a. Eter, E.M. a. Mokheimer, M. a. Habib, A. Al-Qutub, A Review of Hybrid Solar–Fossil Fuel Power Generation Systems and Performance Metrics, J. Sol. Energy Eng. 134 (2012) 041006–041006. doi:10.1115/1.4006973.
- [5] M. Livshits, A. Kribus, Solar hybrid steam injection gas turbine (STIG) cycle, Sol. Energy. 86 (2012) 190–199. doi:10.1016/j.solener.2011.09.020.

References

- [6] C.S. Turchi, Z. Ma, M. Erbes, Gas Turbine/Solar Parabolic Trough Hybrid Designs, in: Proc. ASME Turbo Expo, ASME, 2011: pp. 989–996. doi:10.1115/GT2011-45184.
- [7] NREL Concentrating Solar Power Projects website: http://www.nrel.gov/csp/solarpaces/
- [8] J.H. Peterseim, U. Hellwig, A. Tadros, S. White, Hybridisation optimization of concentrating solar thermal and biomass power generation facilities, Sol. Energy. 99 (2014) 203–214. doi:10.1016/j.solener.2013.10.041.
- [9] J.H. Peterseim, A. Herr, S. Miller, S. White, D.A. O'Connell, Concentrating solar power/alternative fuel hybrid plants: Annual electricity potential and ideal areas in Australia, Energy. 68 (2014) 698–711. doi:10.1016/j.energy.2014.02.068.
- [10] J.H. Peterseim, S. White, A. Tadros, U. Hellwig, Concentrating solar power hybrid plants - Enabling cost effective synergies, Renew. Energy. 67 (2014) 178–185. doi:10.1016/j.renene.2013.11.037.
- [11] J.D. Nixon, P.K. Dey, P.A. Davies, The feasibility of hybrid solar-biomass power plants in India, Energy. 46 (2012) 541–554. doi:10.1016/j.energy.2012.07.058.

References

- [12] Termosolar Borges, la primera planta termosolar en el mundo hibridada con biomasa: http://www.madrimasd.org/blogs/energiasalternativas/2013/01/02/131822
- [13] Suministro de 50.000 toneladas de biomasa forestal a Termosolar Borges: http://prensa.comsa.com/suministro-de-50-000-toneladas-de-biomasa-forestal-a-termosolar-borges/
- [14] S. Jerez, R.M. Trigo, A. Sarsa, R. Lorente-Plazas, D. Pozo-Vázquez, J.P. Montávez, Spatio-temporal complementarity between solar and wind power in the Iberian Peninsula, in: Energy Procedia, 2013: pp. 48–57. doi:10.1016/j.egypro.2013.08.007.
- [15] C. Kost, B. Pfluger, W. Eichhammer, M. Ragwitz, Fruitful symbiosis: Why an export bundled with wind energy is the most feasible option for North African concentrated solar power, Energy Policy. 39 (2011) 7136–7145. doi:10.1016/j.enpol.2011.08.032.
- [16] Colorado Integrated Solar Project, NREL Concentrating Solar Power Projects website: https://www.nrel.gov/csp/solarpaces/project_detail.cfm/projectID=75

References

- [17] F.J. Santos-Alamillos, D. Pozo-Vázquez, J.A. Ruiz-Arias, L. Von Bremen, J. Tovar-Pescador, Combining wind farms with concentrating solar plants to provide stable renewable power, Renew. Energy. 76 (2015) 539–550. doi:10.1016/j.renene.2014.11.055.
- [18] B.D. Vick, T.A. Moss, Adding concentrated solar power plants to wind farms to achieve a good utility electrical load match, Sol. Energy. 92 (2013) 298–312. doi:10.1016/j.solener.2013.03.007.
- [19] F. Petrakopoulou, A. Robinson, M. Loizidou, Simulation and evaluation of a hybrid concentrating-solar and wind power plant for energy autonomy on islands, Renew. Energy. 96 (2016) 863–871. doi:10.1016/j.renene.2016.05.030.
- [20] A. Starke, J. M. Cardemil, R. Escobar, and S. Colle, “Assessing the performance of Hybrid CSP + PV plants in Northern Chile,” Proceedings of the SolarPACES 2015 International Conference (2015).
- [21] CSP MENA KIP - Assistance au déploiement d’un programme et au montage d’un premier projet CSP en Tunisie: Finalisation de la tâche 1 et lancement de la tâche 2 -Tunis –27 et 28 juin 2019

References

- [22] Trabelsi, Seif Eddine; Qoaider, Louy; Guizani, Amenallah (2018): Investigation of using molten salt as heat transfer fluid for dry cooled solar parabolic trough power plants under desert conditions. In: *Energ. Convers. Manage.* 156, S. 253. DOI: 10.1016/j.enconman.2017.10.101.
- [23] Zurita Villamizar, Adriana. (2017). Techno-Economic Analysis of a Hybrid CSP+PV Plant Integrated with TES and BESS at Northern Chile. Presentation at the SolarPACES conference 2017, Santiago de Chile
- [24] Shanghai Electric & CSP Focus. (2019). Introduction of Dubai 950MW CSP+PV Project by Shanghai Electric. CSP Focus MENA 2019, June 26-27, Dubai, UAE
- [25] Oliver Baudson, MD, TSK Flagsol– Audio: Panel - Flagship project update in Morocco, CSP Madrid 2018 Conference, 2018

RAYTRACING SOFTWARE AND DESIGN TOOLS FOR HELIOSTATS FIELDS

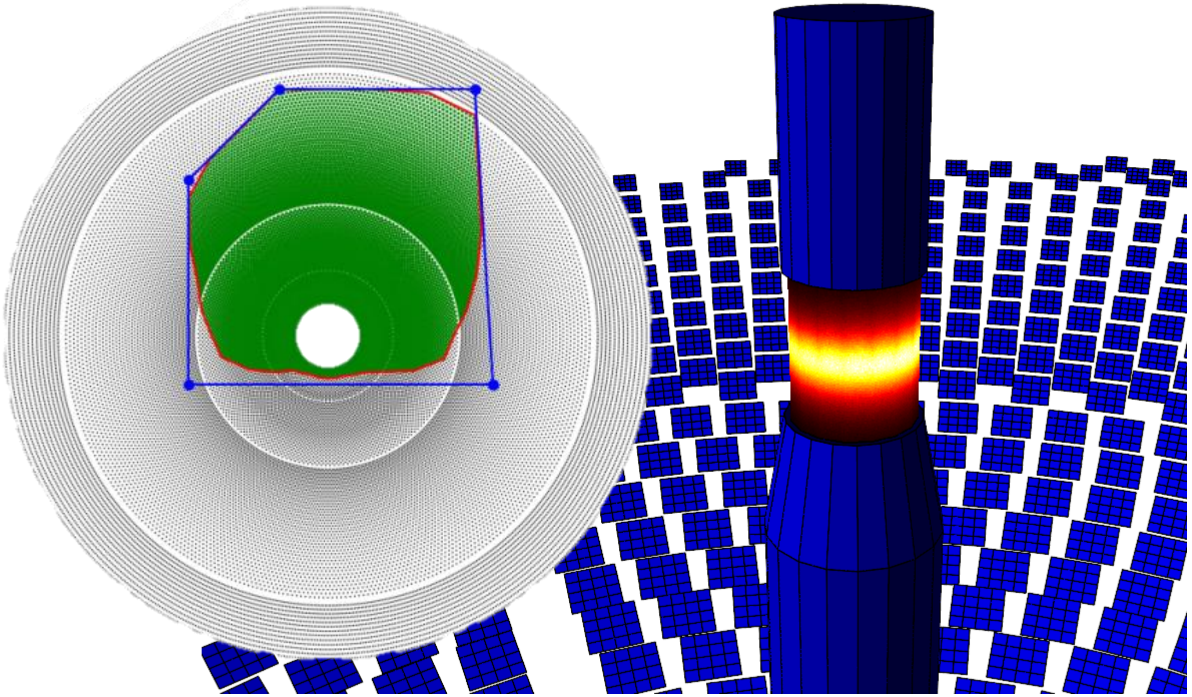

Gregor Bern, Peter Schöttl

Fraunhofer Institute for Solar Energy Systems ISE

SFERA III Workshop

Training on Central Receivers

Odeillo, July 9-12

www.ise.fraunhofer.de

AGENDA

- Raytrace3D
  - Basics
  - Simulation acceleration
  - Angle-dependent reflectance for soiling modeling
  - Individual heliostat assessment
  - Sky discretization for fast annual assessment
  - Coupling to dynamic receiver simulation
- Heliostat field design/optimization
  - Heliostat field layout algorithms
  - Heliostat selection based on polygon optimization

Raytrace3D
Principle

Monte-Carlo forward ray tracing

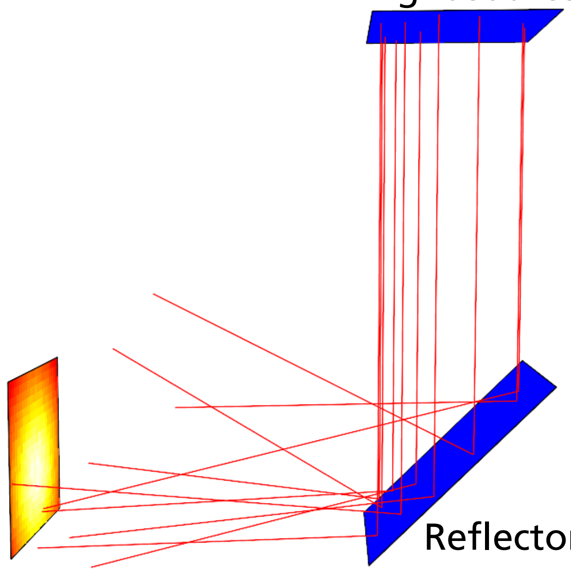

Features

- Comprehensive library of geometries/materials/light sources
  ➔ sophisticated modeling of solar applications
- Fully object-oriented
  ➔ readily extensible
- Number crunching in C++
  + Pre/Postprocessing in Python
  ➔ Fast and versatile
- Parallelized
  ➔ Run on simulation servers

Raytrace3D
Heliostat field losses

- Monte-Carlo ray tracing:
  Fraunhofer ISE tool *Raytrace3D*
  - Cosine losses
  - Shading
  - Absorption on heliostats
  - Blocking
  - Atmospheric attenuation
  - Spillage
  - Reflection from receiver
- Flux distribution
  on receiver surfaces [1]

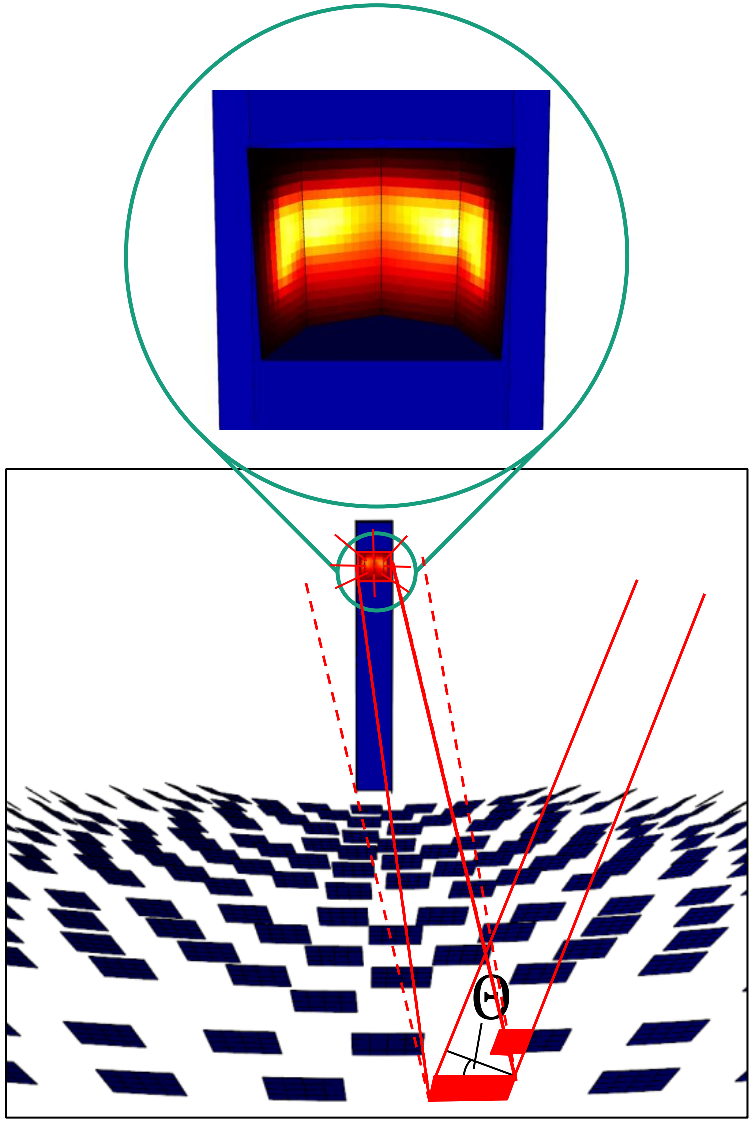

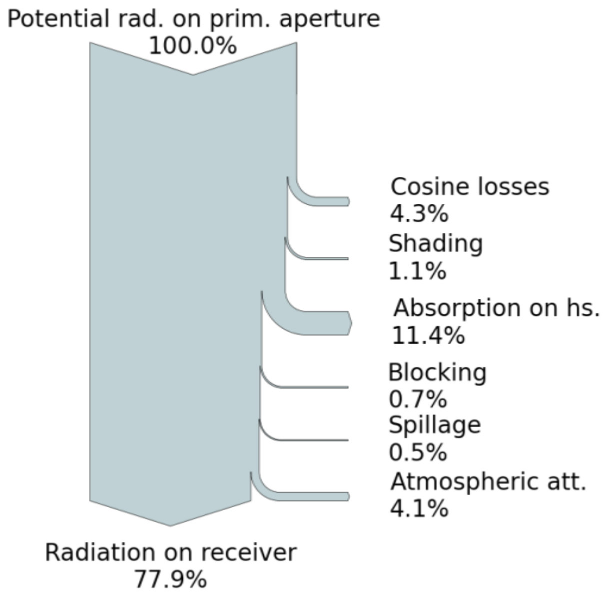

[1] P. Schöttl, G. Bern, D. W. van Rooyen, J. Flesch, T. Fluri, and P. Nitz, “Efficient modeling of variable solar flux distribution on Solar Tower receivers by interpolation of few discrete representations,” Solar Energy, vol. 160, pp. 43–55, 2018.

Fraunhofer
ISE

Raytrace3D
Graphical postprocessing

Gemasolar system
Fluxmaps depicted on receiver surfaces

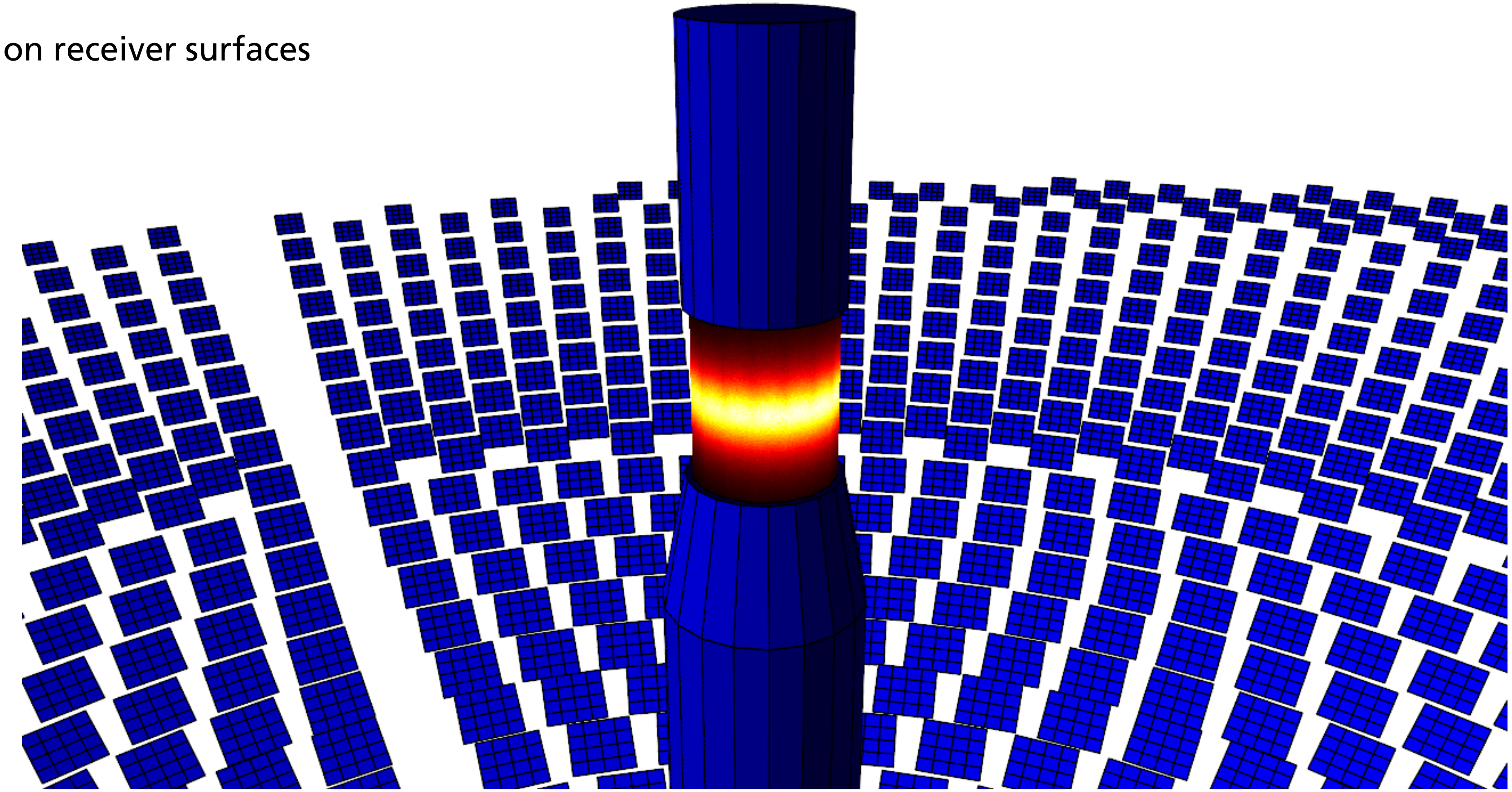

Raytrace3D

Simulation of solar towers

Solar Two

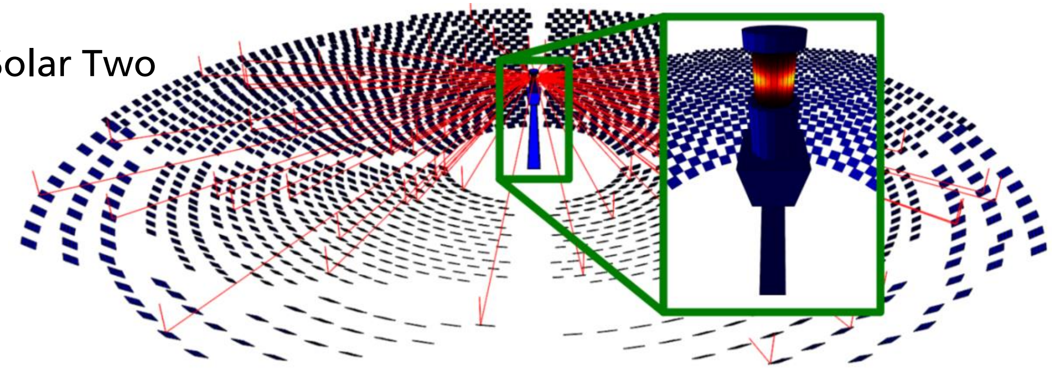

Gemasolar

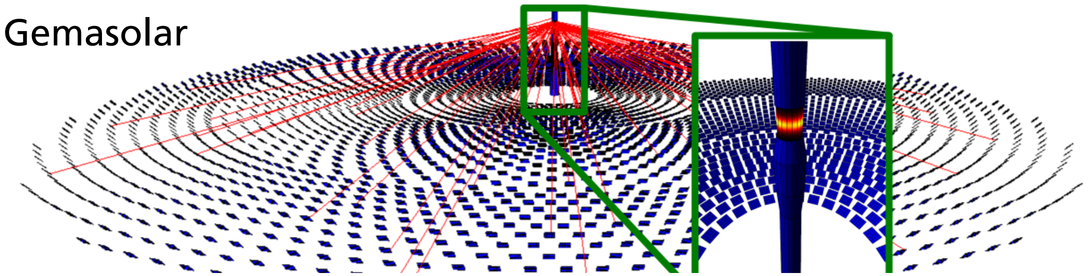

PS10

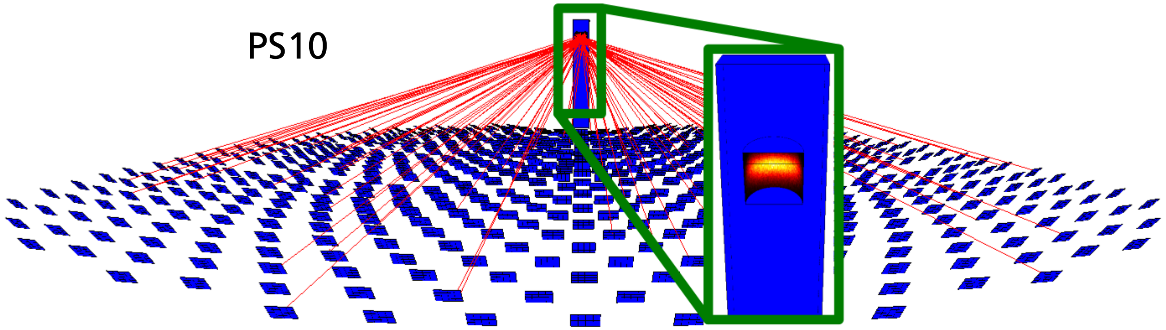

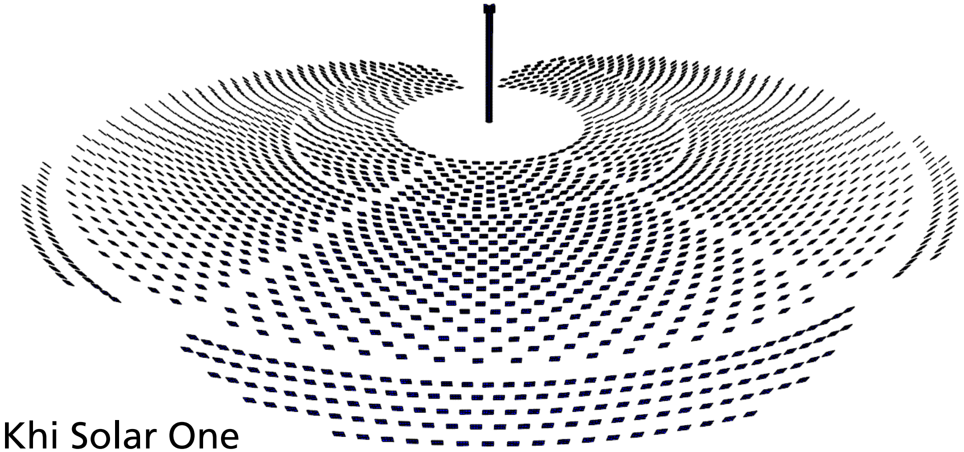

Khi Solar One

Ivanpah

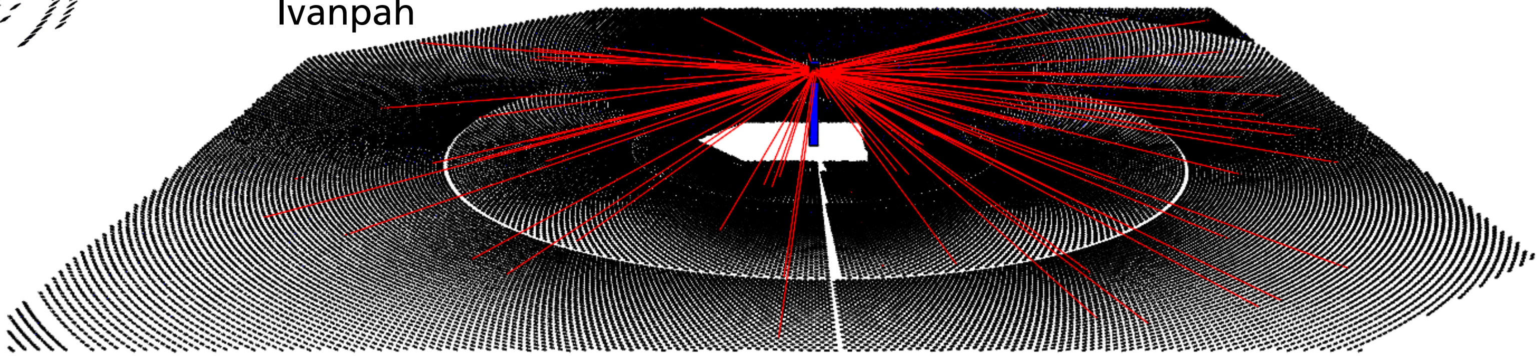

Raytrace3D concepts
Simulation acceleration

- Heliostats as light source
  - Creation of rays on heliostat surface
  - Trace back to sun → shading
  - Trace to receiver → blocking, …
  - ➢ No tracing of (useless) rays on ground
- Bounding volume hierarchy
  - Automatic creation of axis-aligned bounding boxes
  - Binary tree hierarchy
  - ➢ Logarithmic instead of linear search
- ➢ Massive acceleration (several orders of magnitude)

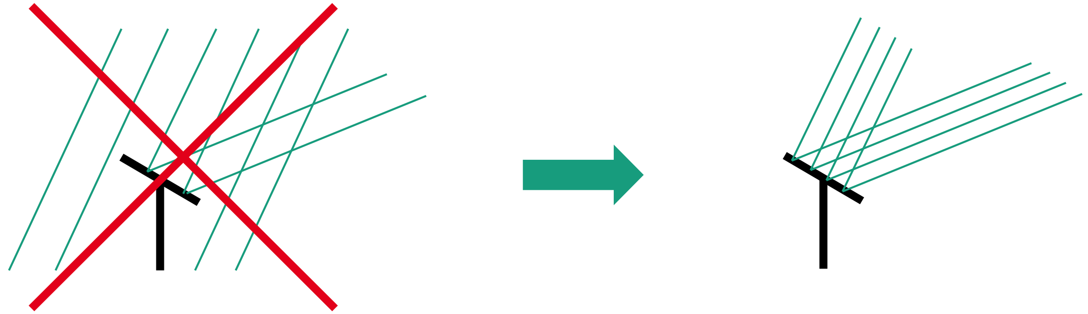

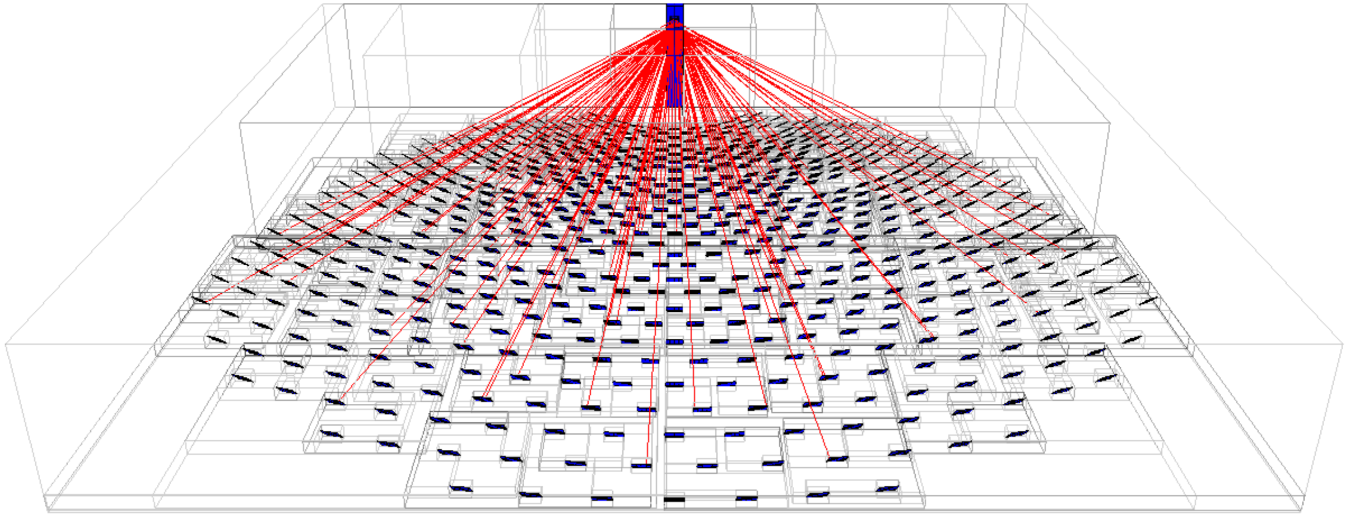

Raytrace3D concepts
Angle-dependent reflectance for soiling modeling

- Clean mirrors → weak incidence angle dependency of reflectance
- Soiled mirrors → strong incidence angle dependency of reflectance

- Raytrace3D: incidence angle dependent reduction of reflectance
- Reduction of solar yield

➢ Improved yield prediction

➢ Optimization of cleaning cycles

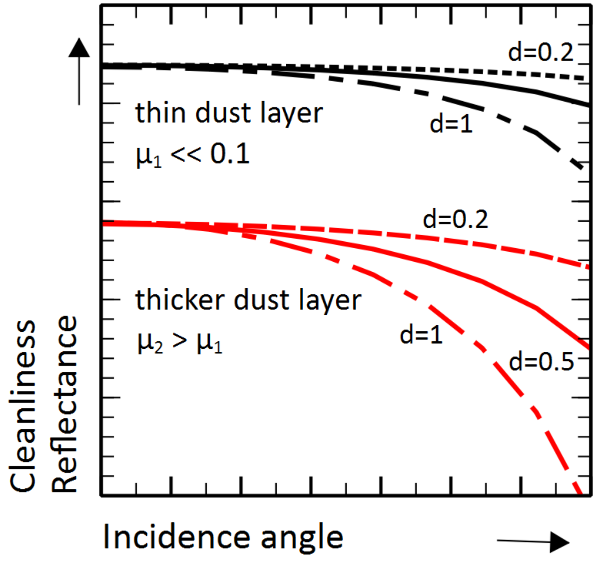

[2]

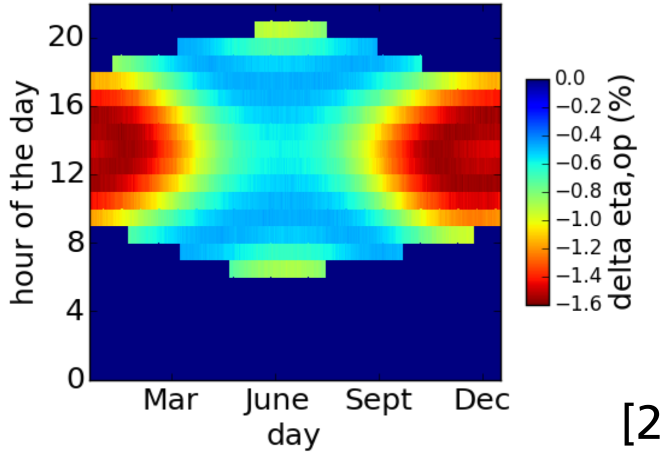

[2]

[2] A. Heimsath, P. Nitz, The effect of soiling on the reflectance of solar reflector materials - Model for prediction of incidence angle dependent reflectance and attenuation due to dust deposition, Solar Energy Materials and Solar Cells, vol. 195,pp 258-268, , 2019

Fraunhofer ISE

Raytrace3D concepts
Individual heliostat assessment

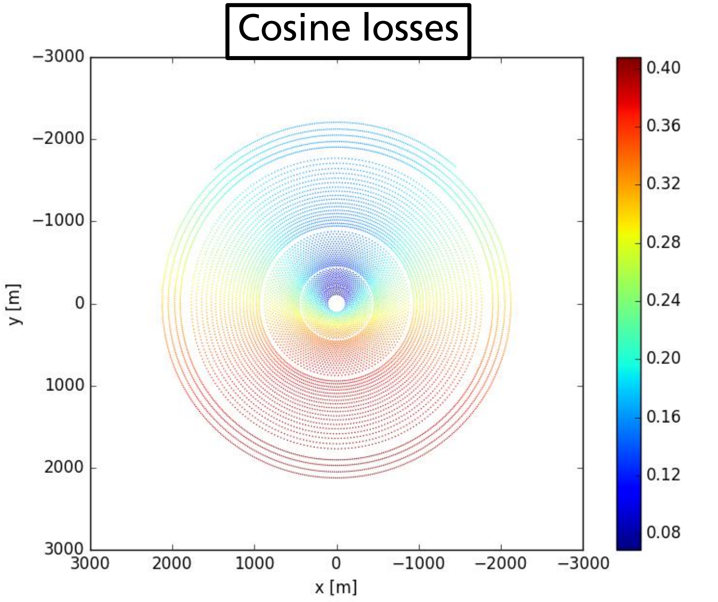

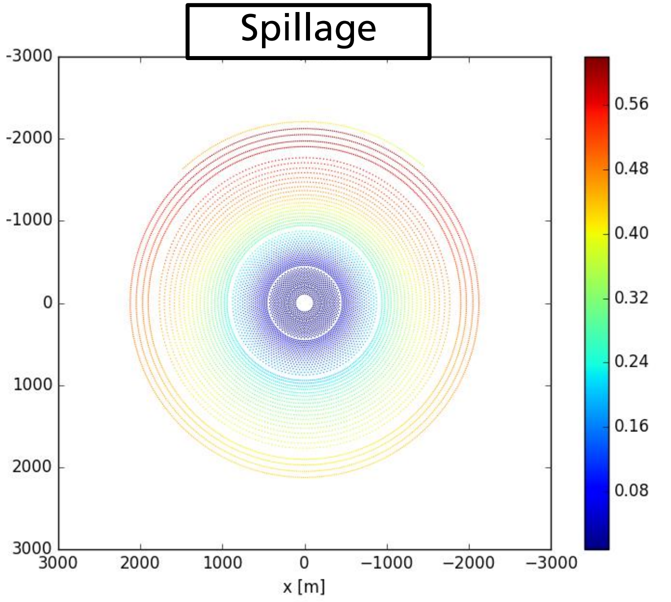

- Built-in routine for evaluating ray history
- Per-unit assessment of primary aperture (heliostats)
- Evaluation of different loss mechanisms (cosine, shading, …)
- (Optional) integration of secondary concentrator

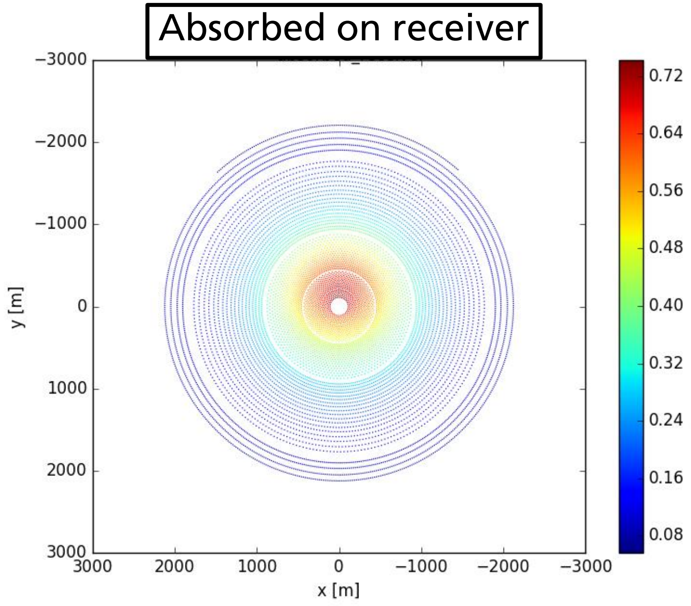

- ➢ Full insight in heliostat field loss mechanisms
- ➢ Input for field design

Raytrace3D concepts
Sky discretization for fast annual assessment [2,3]

- Uniform discretization of the sky hemisphere

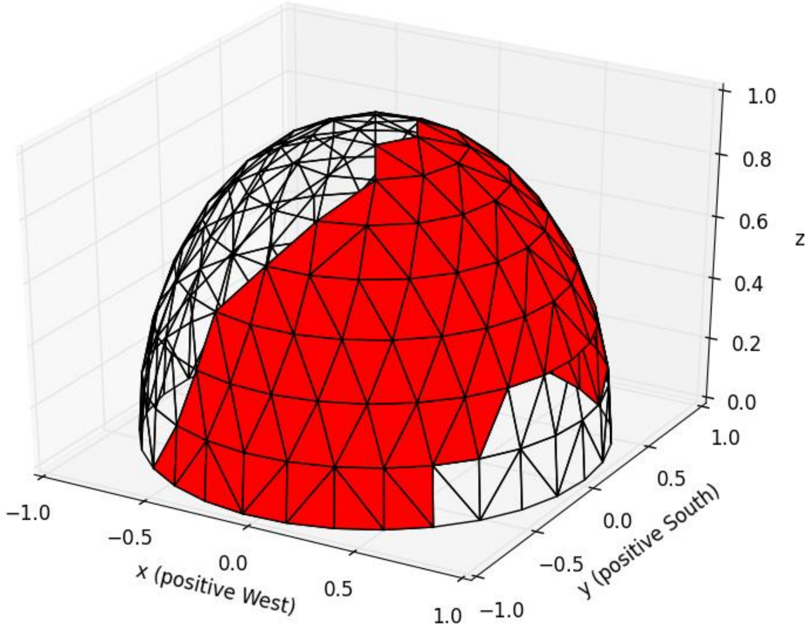

[3] P. Schöttl, G. Bern, D. W. van Rooyen, J. Flesch, T. Fluri, and P. Nitz, "Efficient modeling of variable solar flux distribution on Solar Tower receivers by interpolation of few discrete representations," Solar Energy, vol. 160, pp. 43–55, 2018.
[4] P. Schöttl, K. Ordóñez Moreno, F. C. D. van Rooyen, G. Bern, and P. Nitz, "Novel sky discretization method for optical annual assessment of solar tower plants," Solar Energy, vol. 138, pp. 36–46, 2016.

Fraunhofer ISE

Raytrace3D concepts

Sky discretization for fast annual assessment [2,3]

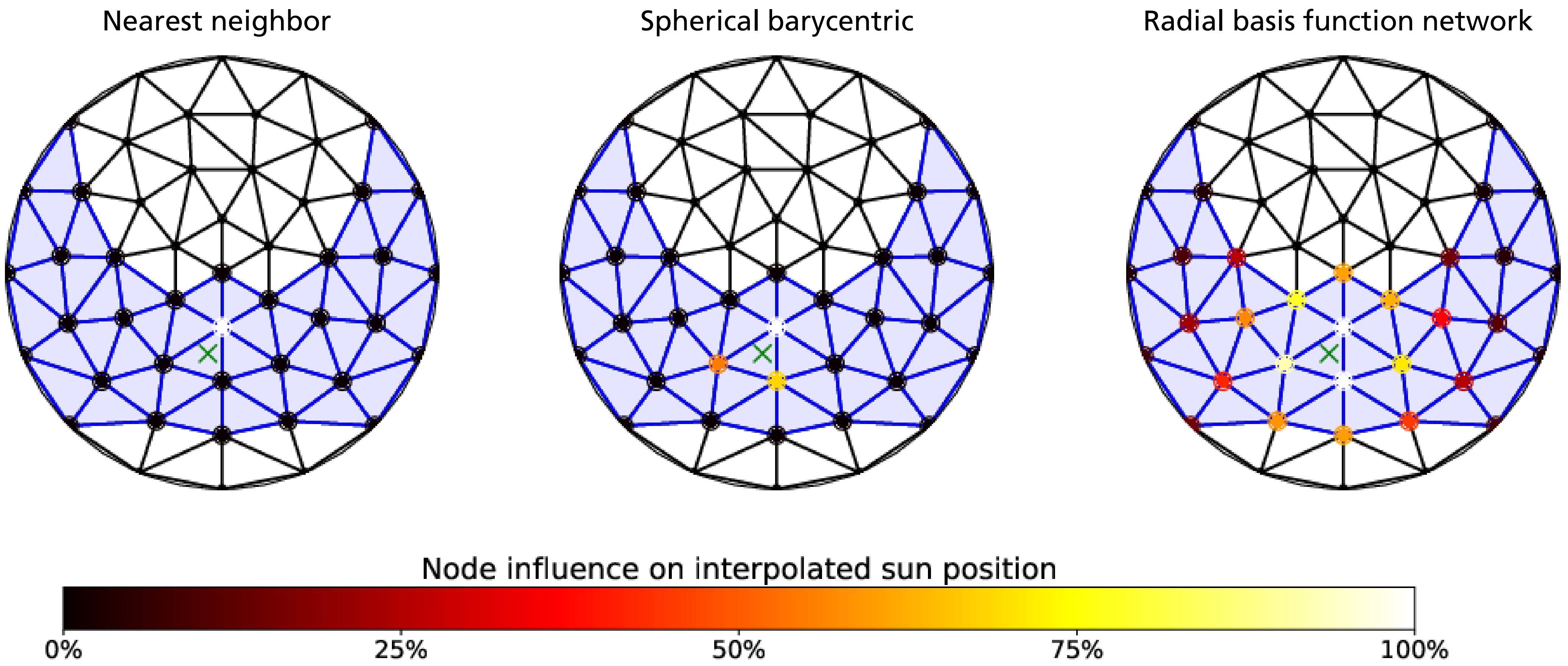

[3] P. Schöttl, G. Bern, D. W. van Rooyen, J. Flesch, T. Fluri, and P. Nitz, "Efficient modeling of variable solar flux distribution on Solar Tower receivers by interpolation of few discrete representations," Solar Energy, vol. 160, pp. 43–55, 2018.
[4] P. Schöttl, K. Ordóñez Moreno, F. C. D. van Rooyen, G. Bern, and P. Nitz, "Novel sky discretization method for optical annual assessment of solar tower plants," Solar Energy, vol. 138, pp. 36–46, 2016.

Fraunhofer
ISE

Raytrace3D concepts

Sky discretization for fast annual assessment [2,3]

- Uniform discretization of the sky hemisphere
- Linear barycentric interpolation
  + Radial Basis Function (RBF) correction

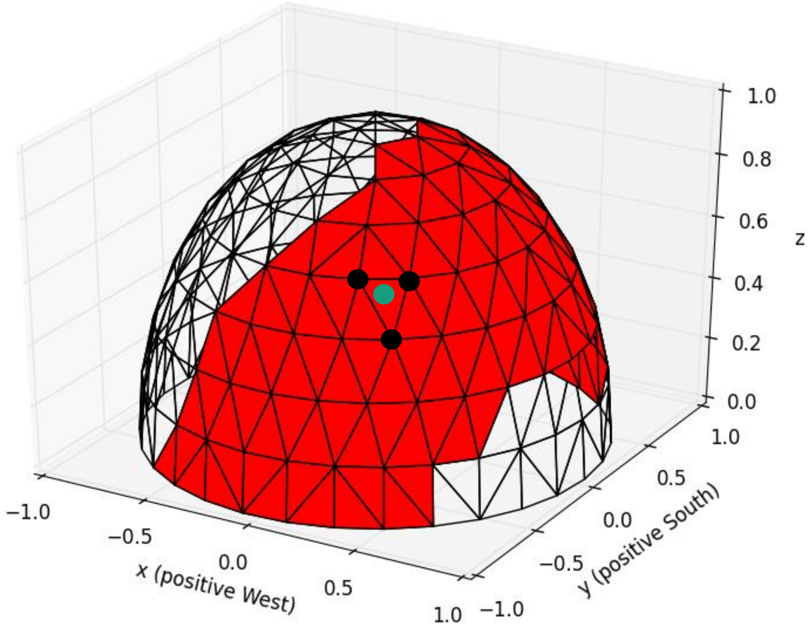

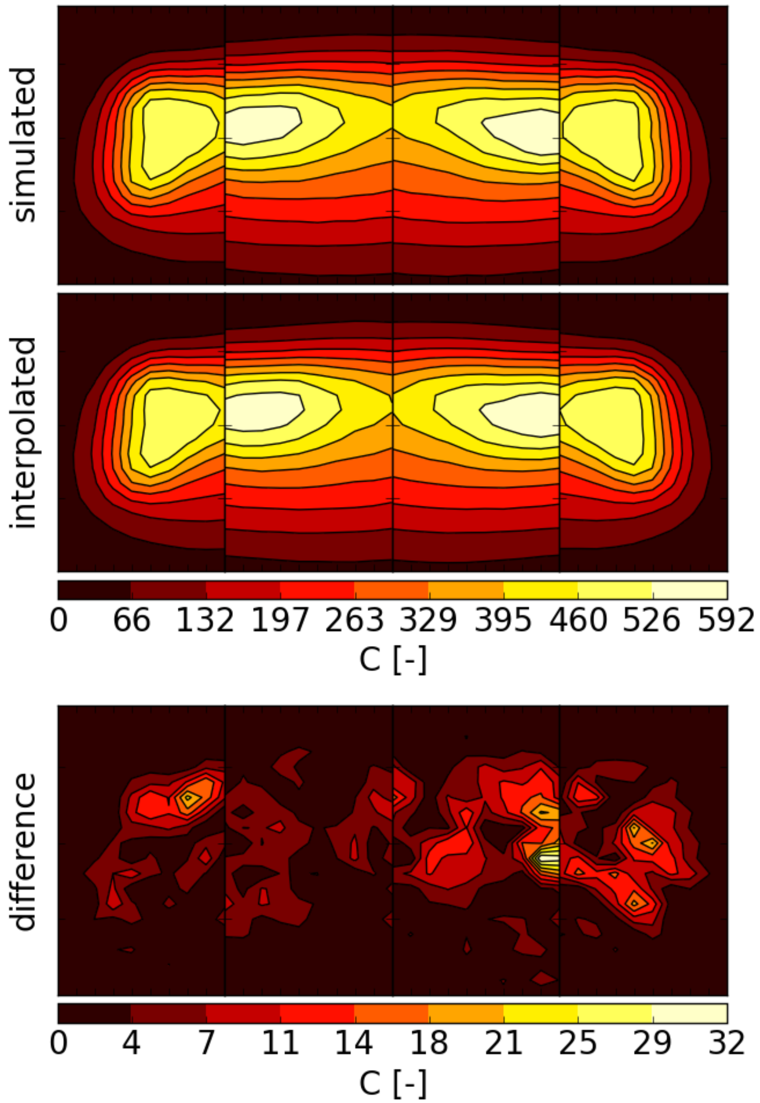

[3] P. Schöttl, G. Bern, D. W. van Rooyen, J. Flesch, T. Fluri, and P. Nitz, “Efficient modeling of variable solar flux distribution on Solar Tower receivers by interpolation of few discrete representations,” Solar Energy, vol. 160, pp. 43–55, 2018.
[4] P. Schöttl, K. Ordóñez Moreno, F. C. D. van Rooyen, G. Bern, and P. Nitz, “Novel sky discretization method for optical annual assessment of solar tower plants,” Solar Energy, vol. 138, pp. 36–46, 2016.

Fraunhofer ISE

Raytrace3D concepts
Coupling to dynamic receiver simulation

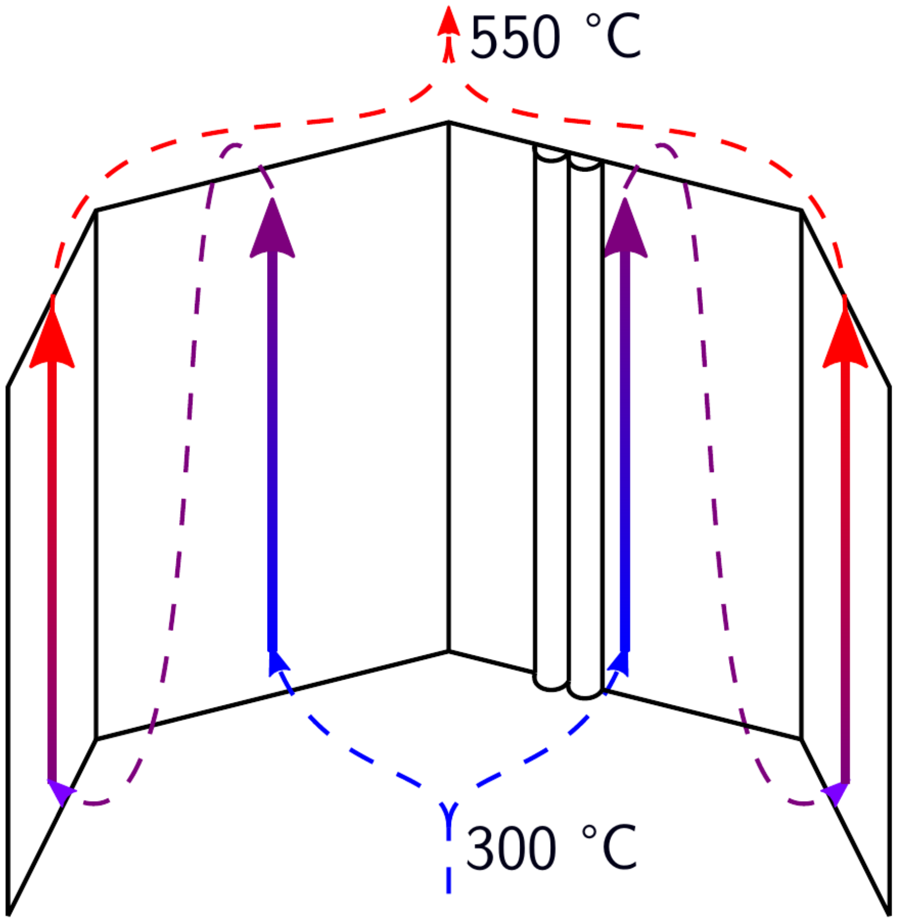

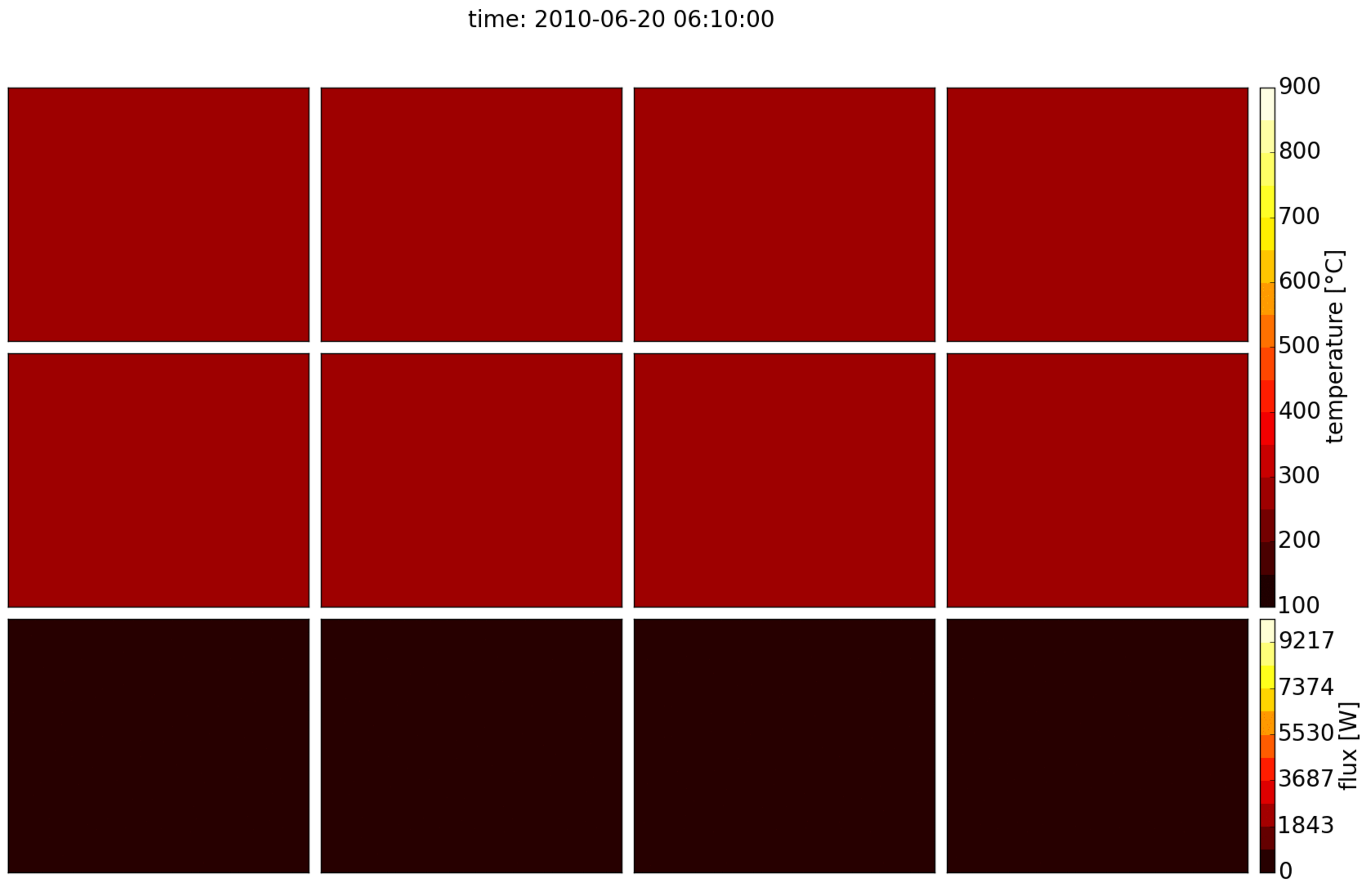

Top row: Temperature distribution [°C] in the fluid
Center row: Temperature distribution [°C] on the panel surface
Bottom row: Flux distribution [W] on the panel surface

Heliostat field design/optimization
Patterns-based algorithms

- Layout algorithms based on underlying pattern
- Base cases: radially staggered vs. cornfield
- Several free parameters
- Advantages:
  - Fast creation of large fields
  - Construction and maintenance easier in a regular layout
- Disadvantage:
  - Difficult to adapt to uneven terrain

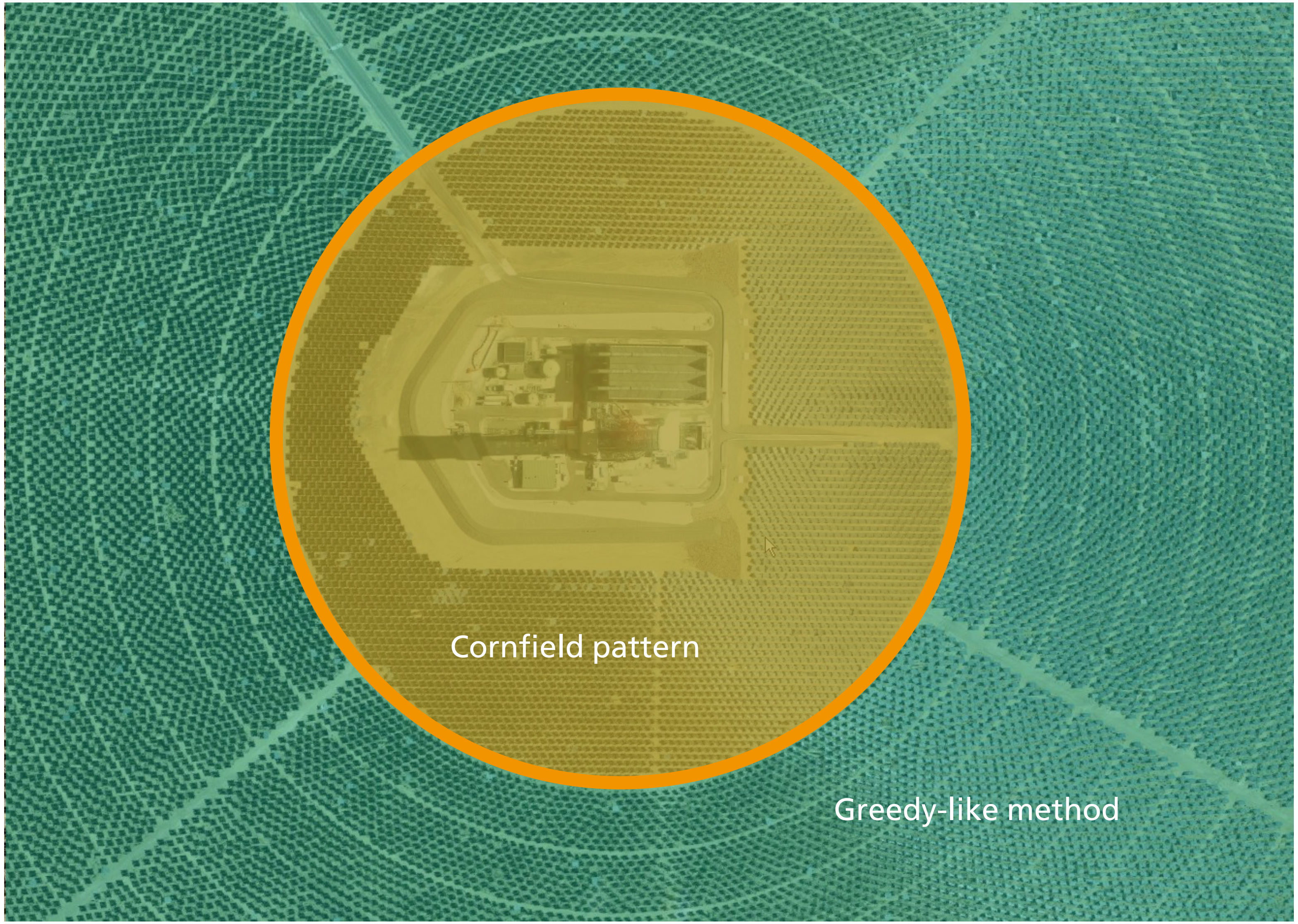

Part of Ivanpah field (source: Google Maps)

Heliostat field design/optimization
MUEEN layout

- Aim: no blocking
- Radially staggered
- Re-grouping for denser field
- Original algorithm [6] extended by Fraunhofer ISE [5]

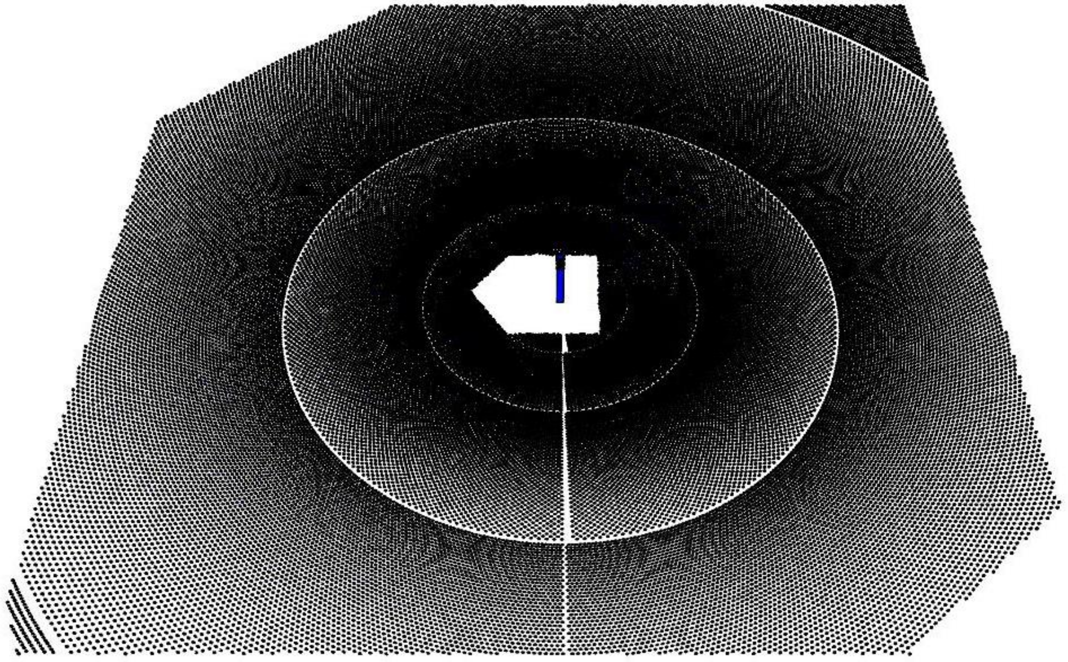

Re-modeling of Ivanpah heliostat field with *Fraunhofer ISE MUEEN* algorithm and field boundaries

[5] F.M.F. Siala and M.E. Elayeb, "Mathematical formulation of a graphical method for a no-blocking heliostat field layout," Renewable Energy, vol. 23, no. 1, pp. 77–92, http://linkinghub.elsevier.com/retrieve/pii/S0960148100001592, 2001.
[6] E. Leonardi, L. Pisani, I. Les, A. Mutuberria, S. Rohani, and P. Schöttl, "Techno-Economic Heliostat Field Optimization: Comparative Analysis of Different Layouts," Solar Energy, vol. 180, pp. 601–607, 2019.

Heliostat field design/optimization
CAMPO layout [7]

- Radially staggered
- Creation of densest possible field
- Azimuthal and radial stretching (local!) to reduce shading and blocking

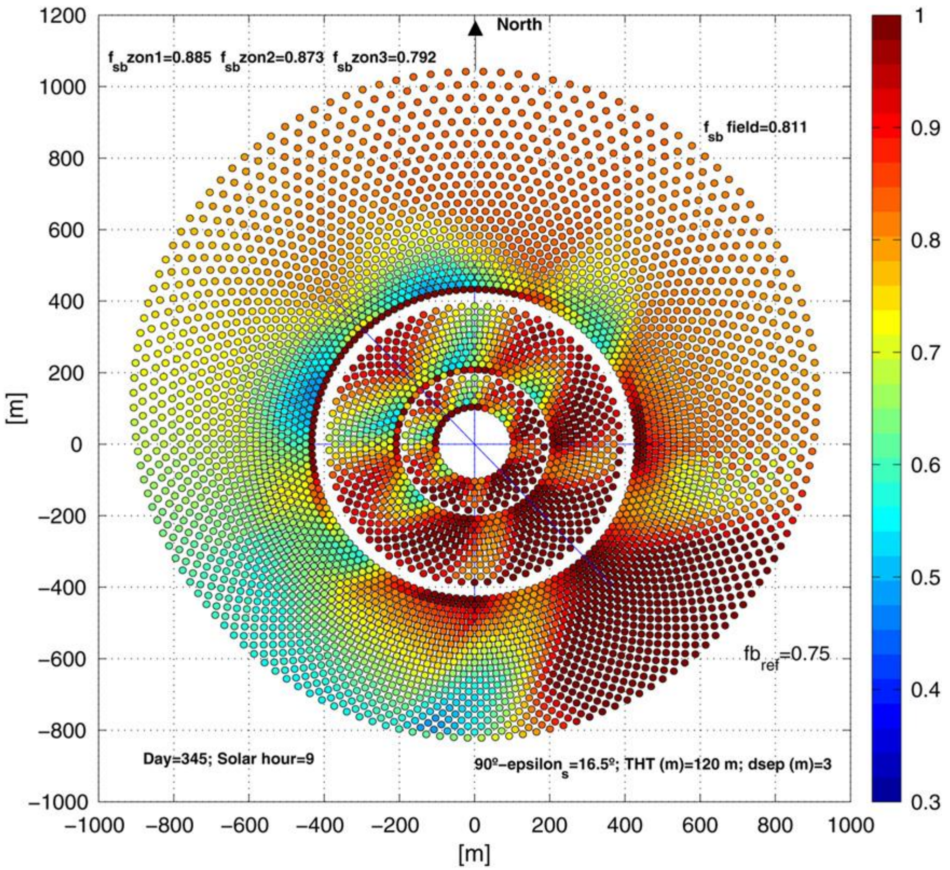

Field generated with CAMPO algorithm (plot from [7])

[7] F. J. Collado and J. Guallar, “Campo: Generation of regular heliostat fields,” Renewable Energy, vol. 46, no. 0, pp. 49–59, http://www.sciencedirect.com/science/article/pii/S096014811200198X, 2012.

Fraunhofer ISE

Heliostat field design/optimization
Biomimetic layout [8]

- Biomimetic phylotaxis disc pattern
  ➔ sunflower
- Angular distribution is related to the golden ratio $(1+\sqrt{5})/2$
- Optimization of free parameter

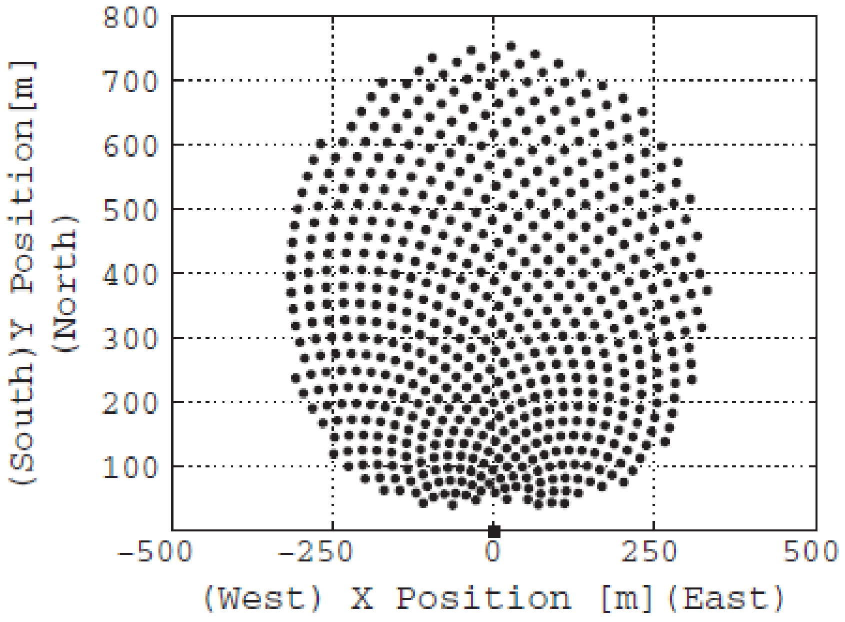

Field generated with biomimetic algorithm (plot from [8])

[8] C. J. Noone, M. Torrilhon, and A. Mitsos, “Heliostat field optimization: A new computationally efficient model and biomimetic layout,” Sol Energy, vol. 86, no. 2, pp. 792–803, http://www.sciencedirect.com/science/article/pii/S0038092X11004373, 2012.

Heliostat field design/optimization
Pattern-free algorithms

- No underlying pattern
- Heliostat placement based on some heuristic
- Advantages:
  - Easily applicable to uneven terrain
- Disadvantage:
  - Field creation very complicated and computationally intensive

Heliostat field design/optimization
Genetic algorithm [9]

- Random generation of initial heliostat base points
- Genetic algorithm (cross-over, mutation, selection) to optimize field

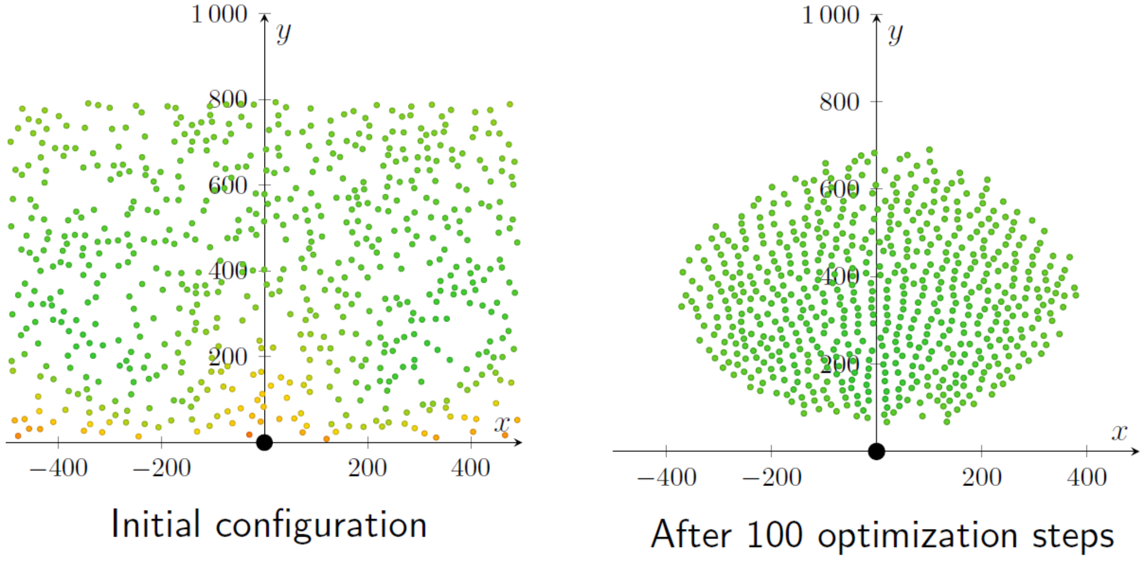

Field optimization with genetic algorithm (plot from presentation related to [9])

[9] P. Richter, M. Frank, and E. Abraham, “Multi-objective optimization of solar tower heliostat fields,” in Proceedings of European Conference on Mathematics for Industry (ECMI 2014), 2014.

Heliostat field design/optimization
Greedy algorithm [10]

- Iterative growth of the heliostat field
- Every new heliostat is placed at the currently best position in the available area
- Different implementations available

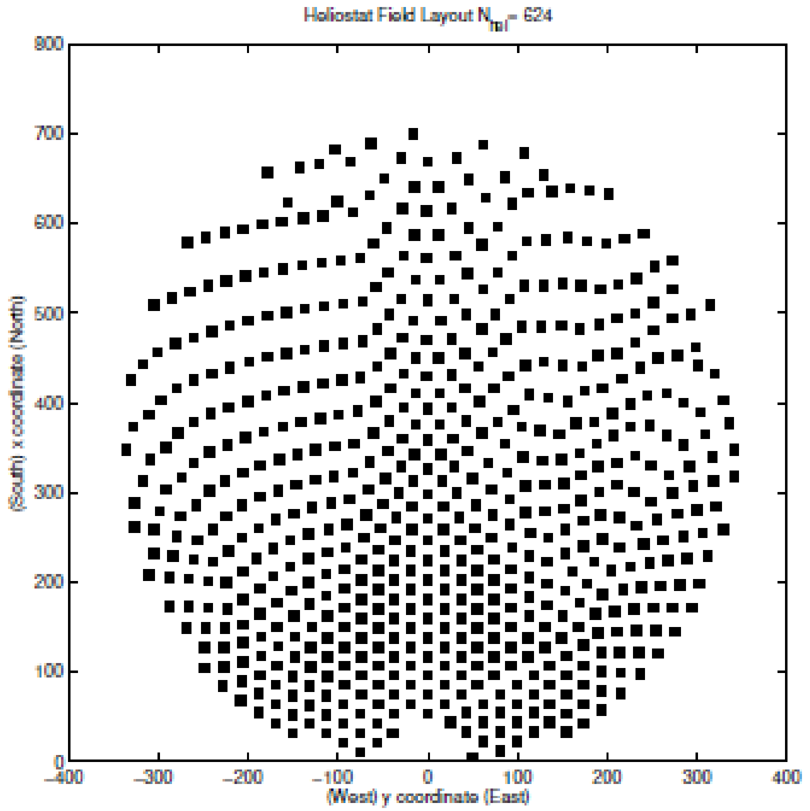

Field optimization with greedy algorithm (plot from [10])

[10] E. Carrizosa, C. Domínguez-Bravo, E. Fernández-Cara, and M. Quero, “A heuristic method for simultaneous tower and pattern-free field optimization on solar power systems,” Computers & Operations Research, vol. 57, no. 0, pp. 109–122, http://www.sciencedirect.com/science/article/pii/S0305054814003219, 2015.

Fraunhofer ISE

HELIOSTAT SELECTION BASED ON POLYGON OPTIMIZATION

- Motivation
- Problem Description
- Methodology
- Application
- Summary & Outlook

Motivation

- Heliostat field represents about 40% of CAPEX of entire plant [1]
- Typical loss composition for a 600 MW_{th} Solar Tower plant [3]

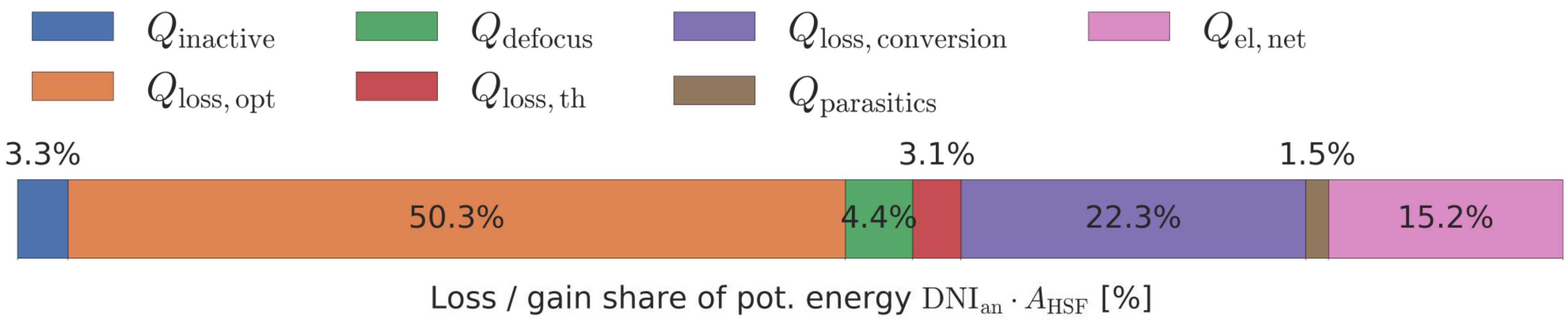

➢ Field design for **high annual efficiency** and **low cost** is crucial

[1] IRENA, "Renewable energy technologies: Cost Analysis Series - Concentrating Solar Power," 2012.

[3] Schöttl et al., "Performance Assessment of a Secondary Concentrator for Solar Tower External Receivers," submitted to 24th SolarPACES Conference, 2 – 5 October 2018, Casablanca, Morocco.

Fraunhofer ISE

Heliostat selection based on polygon optimization

Problem description: Heliostat Selection from Oversized Field

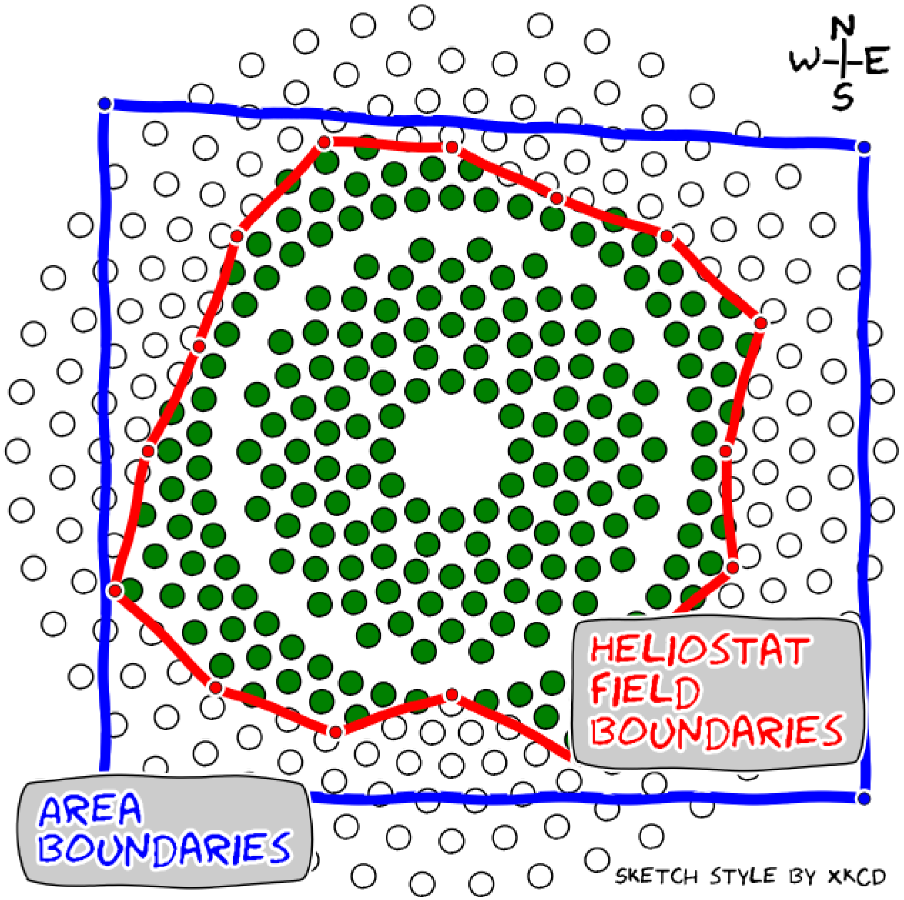

- Respect area boundaries
- Meet flux requirements
- Optimize for given objective function
- Coherent field, feasible w.r.t. construction and maintenance

HELIOSTAT SELECTION BASED ON POLYGON OPTIMIZATION

- Problem Description
- Methodology
  - Oversized Field
  - Polygon-Based Selection
  - Area Boundaries
  - Evolutionary Optimization Algorithm
- Application
- Summary & Outlook

Methodology
Oversized Field

Approx. 35k heliostats
in oversized field

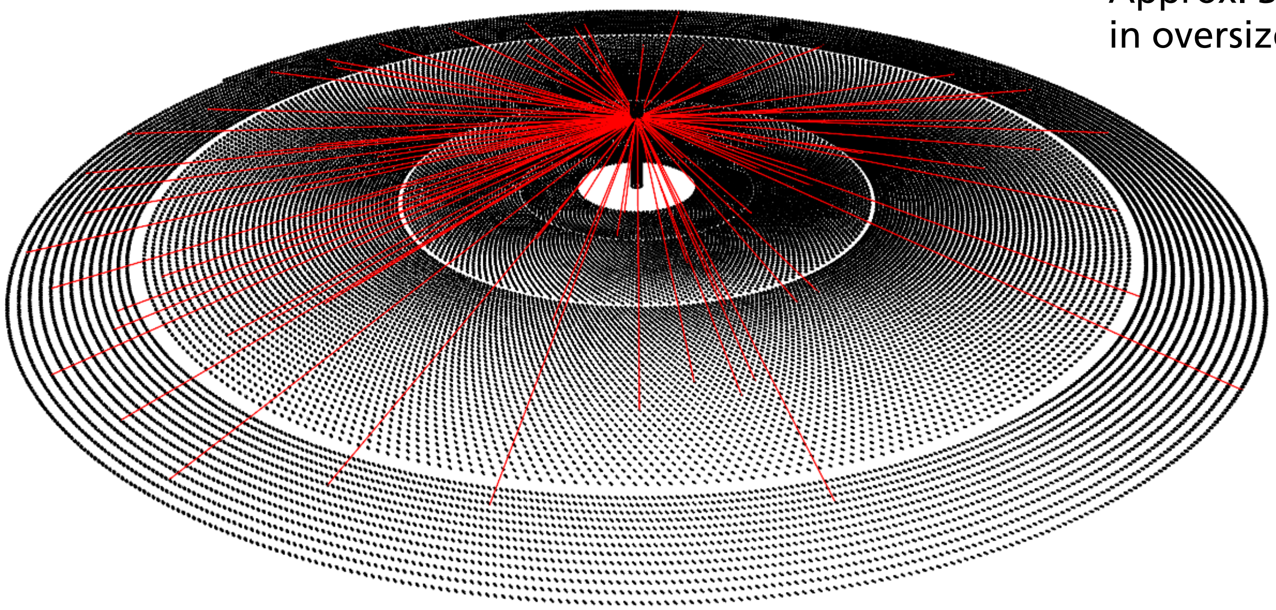

- Generation with **extended MUEEN algorithm [4]**
- Assessment with **Raytrace3D [5]**
- ➢ Not mandatory, any suitable tools can be used

[4] Siala and Elayeb, "Mathematical formulation of a graphical method for a no-blocking heliostat field layout," 2001.

[5] Branke and Heimsath, "Raytrace3D-Power Tower - A Novel Optical Model For Central Receiver Systems," 2010.

Fraunhofer ISE

Methodology
Polygon-Based Selection

- Equi-angular vertices
- Centered around tower base

- Only vertex radii as free parameters in optimization
- Coherent field boundaries
- Evaluation of objective function

  on entire field

- For polar field, limit angular range

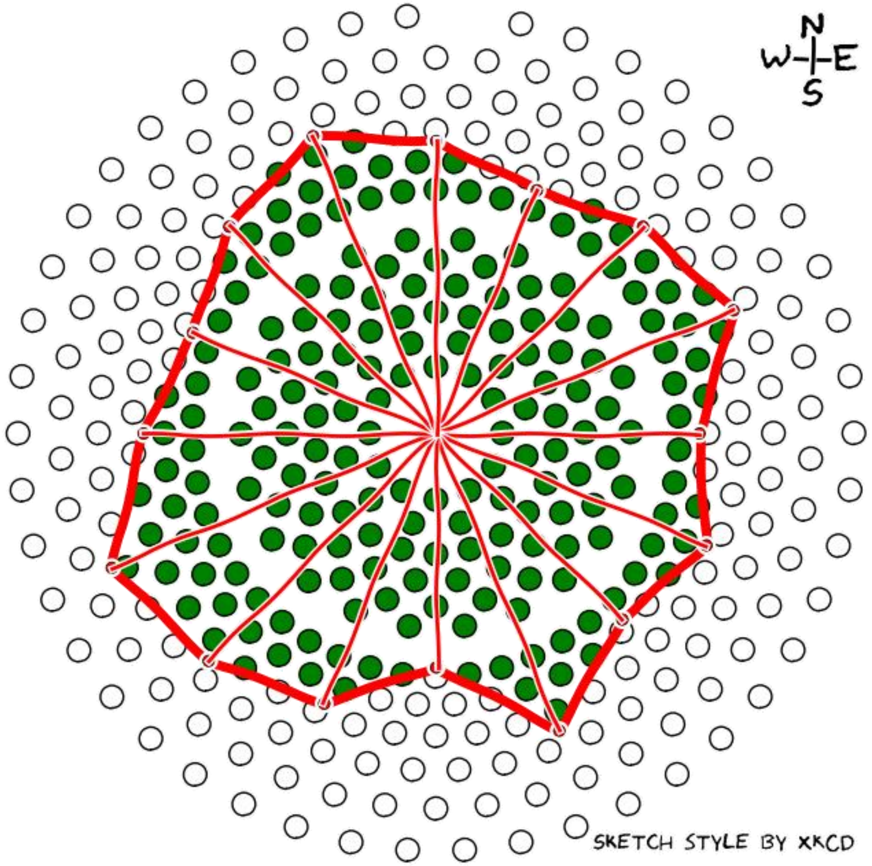

Methodology
Area Boundaries

- Yet another polygon
- Move relative to tower base
- ➢ Two additional degrees of freedom: Δx, Δy

Area boundaries are

- ~~Large, not constraining~~
- Large enough, constraining
- ~~Too small~~
- ~~Fixed position~~

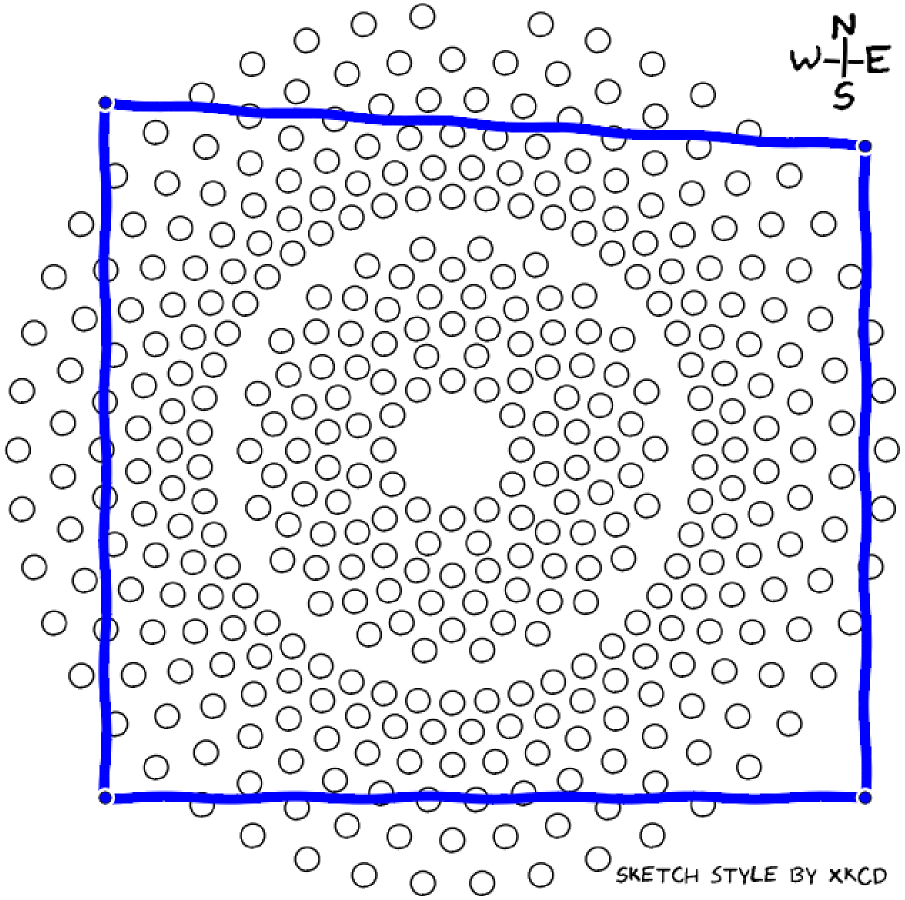

Methodology

Evolutionary Optimization Algorithm

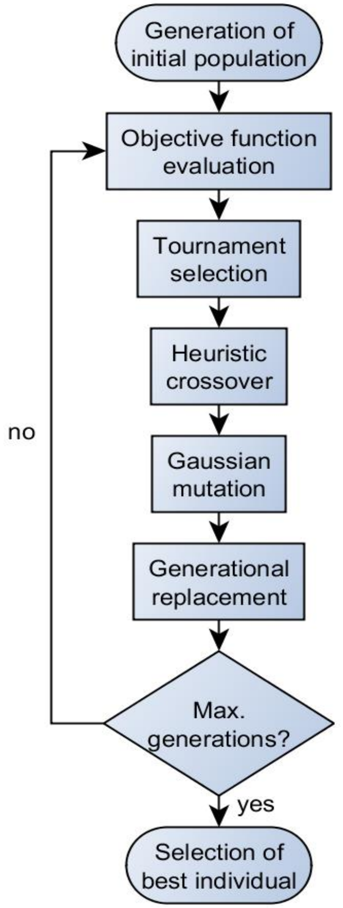

Problem-specific tweaks

- Penalty on not reaching required flux at design point
- Mutation range descreases with sigmoid function

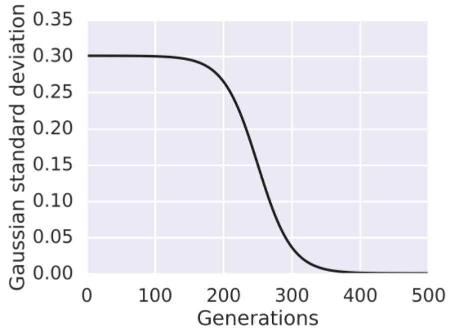

- Small tournament size of 3
- Full generational replacement, no elitism

➢ low selection pressure, no premature convergence

HELIOSTAT SELECTION BASED ON POLYGON OPTIMIZATION

- Problem Description
- Methodology
- Application
  - Base Scenario
  - Objective Function
  - Examples
- Summary & Outlook

Application
Base Scenario

Parameter	Value [6]
Site	Seville, Spain
Absorbed power at design point	55.27 MW
Tower height	100.5 m
External receiver diameter	14 m
External receiver height	12 m
Number of heliostats in oversized field	35000
Heliostat area (square)	8 m²
Minimum radial heliostat distance to tower	80 m
Design point	Winter solstice
Design DNI	850 W/m²

[6] Leonardi et al., "Techno-Economic Heliostat Field Optimization: Comparative Analysis of Different Layouts," Submitted to Solar Energy Journal, 2018.

Application
Objective function

Objective function maximizes yield per cost [6]:

- annual optical efficiency η_{an} of the entire field
- ground area A_{ground} being the convex hull of all heliostats
- cumulative mirror area A_{HSF} of all heliostats
- cost ratio $k = \frac{k_{ground}}{k_{HSF}}$ of ground area to mirror area
- Cumulative annual direct normal irradiance DNI_{an}

[6] Leonardi et al., "Techno-Economic Heliostat Field Optimization: Comparative Analysis of Different Layouts," Submitted to Solar Energy Journal, 2018.

Application
No Area Boundaries, Cost Ratio k=0%

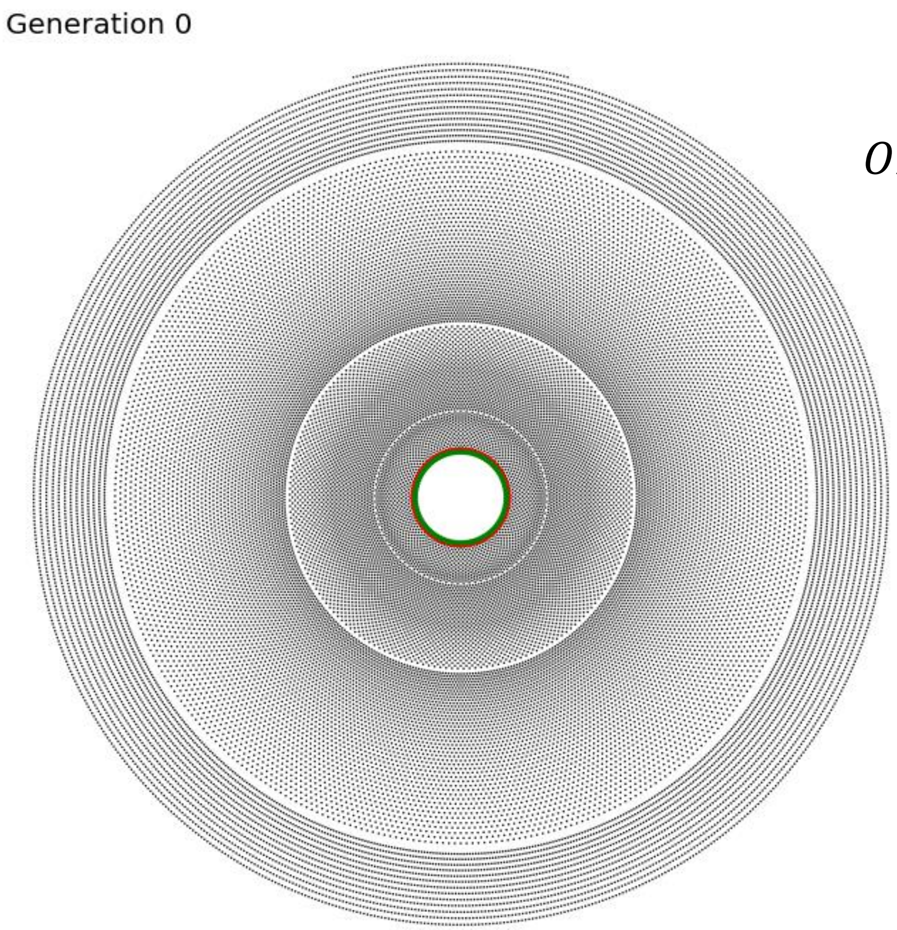

$$OF = \frac{\eta_{an}}{k \cdot \frac{A_{ground}}{A_{HSF}} + 1} = \eta_{an}$$

Animations showing best candidate every ten generations

Application

No Area Boundaries, Cost Ratio k=0%

$$OF = \eta_{an}$$

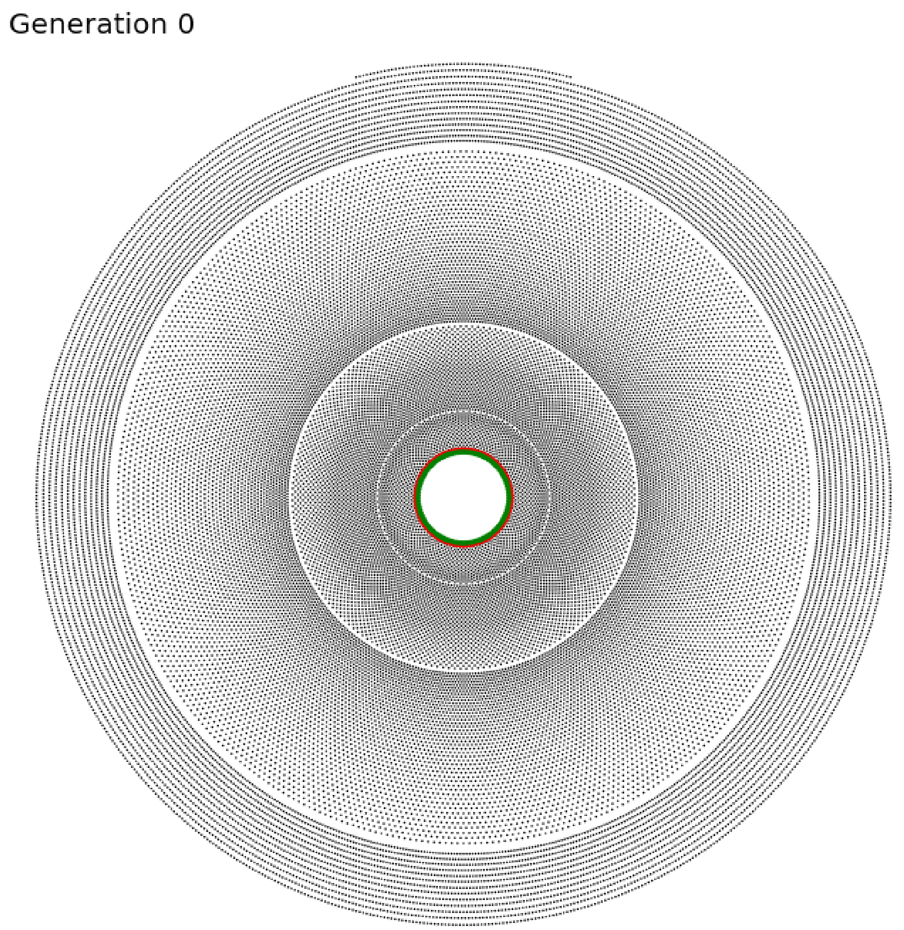

Application

No Area Boundaries, Cost Ratio k=0%

$$OF = \eta_{an}$$

G 10

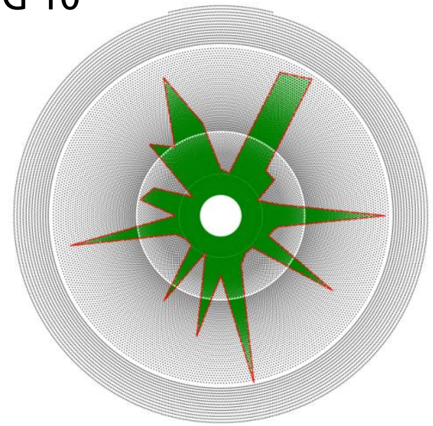

G 100

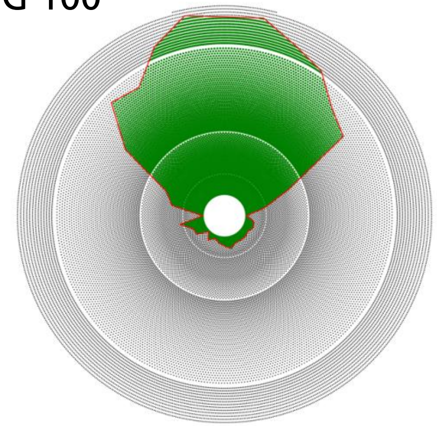

G 200

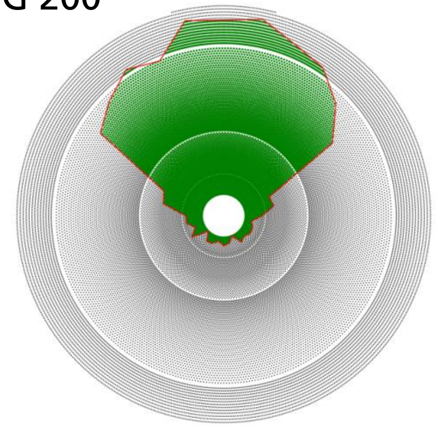

G 300

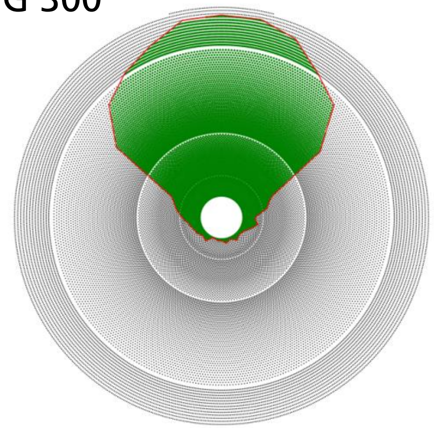

G 400

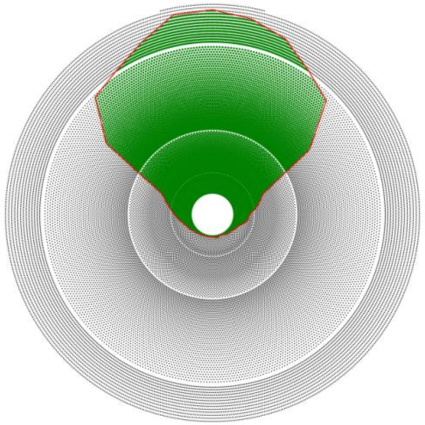

G 500

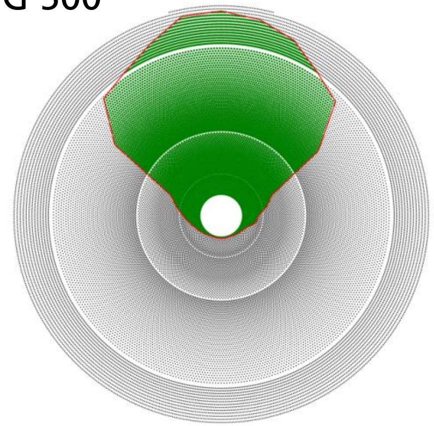

Application

No Area Boundaries, Cost Ratio k=4%

$$OF = \frac{\eta_{an}}{k \cdot \frac{A_{ground}}{A_{HSF}} + 1}$$

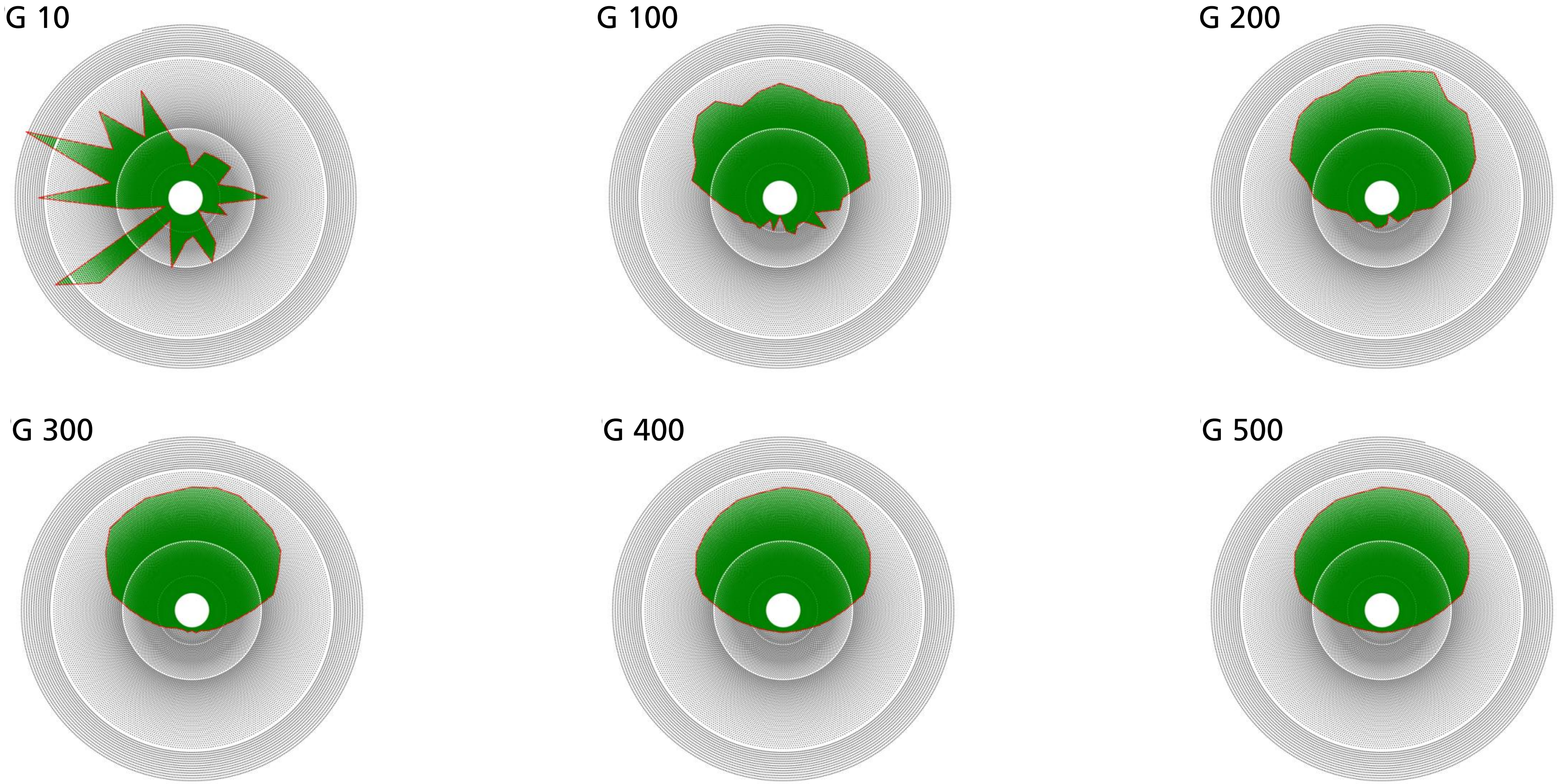

Application

Complex Area Constraints, Cost Ratio k=0%

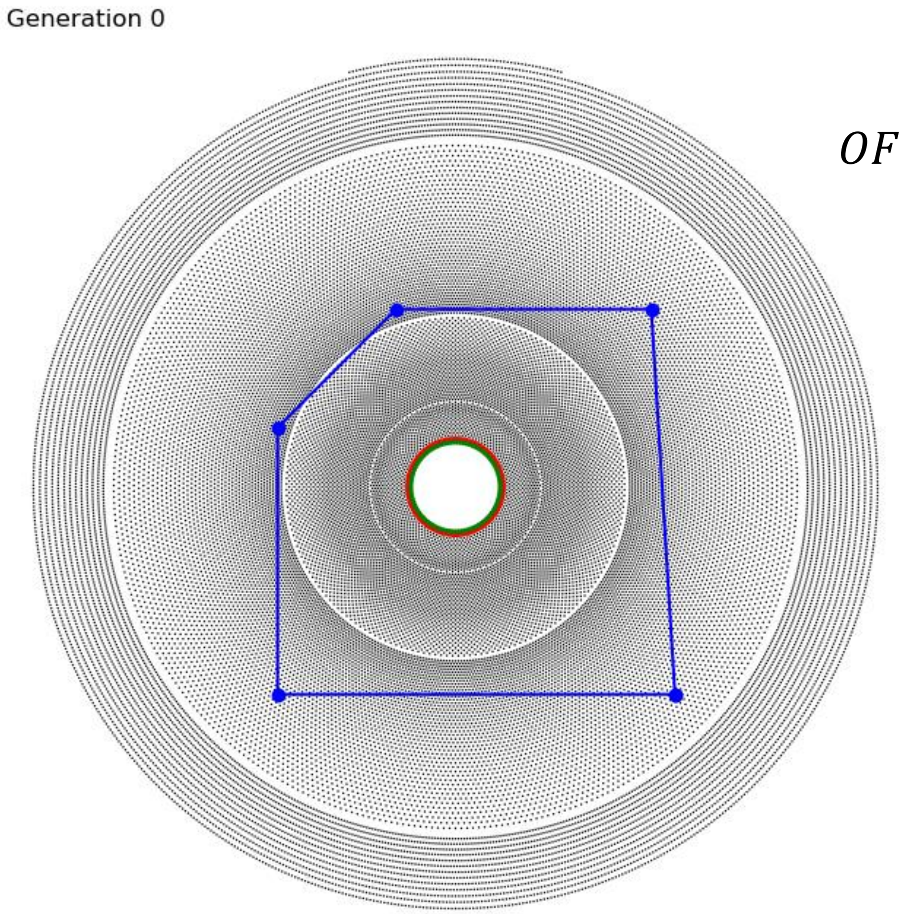

$$OF = \frac{\eta_{an}}{k \cdot \frac{A_{ground}}{A_{HSF}} + 1} = \eta_{an}$$

Application

Complex Area Constraints, Cost Ratio k=0%

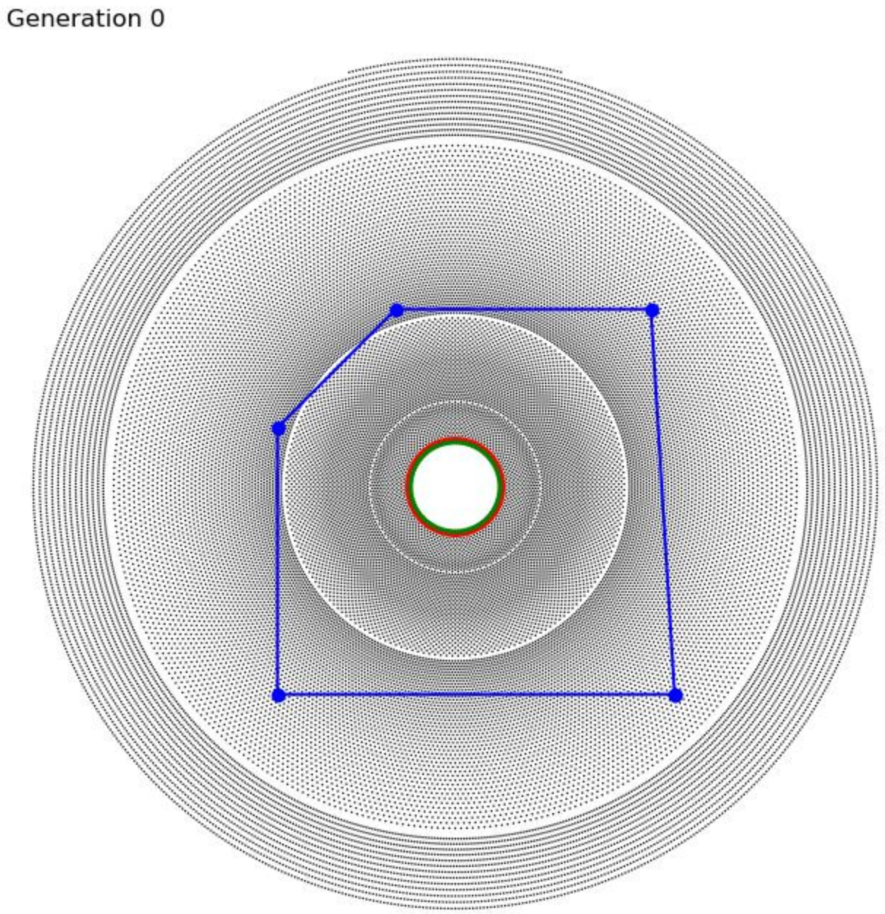

$$OF = \eta_{an}$$

Application

Complex Area Constraints, Cost Ratio k=0%

$$OF = \eta_{an}$$

G 10

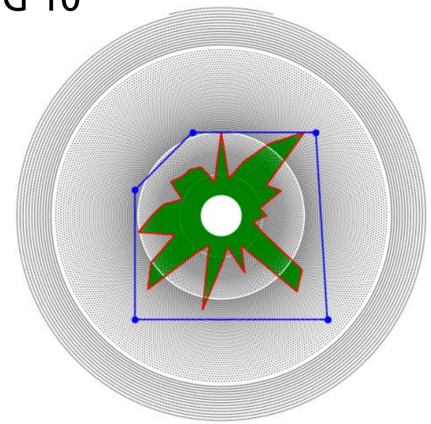

G 100

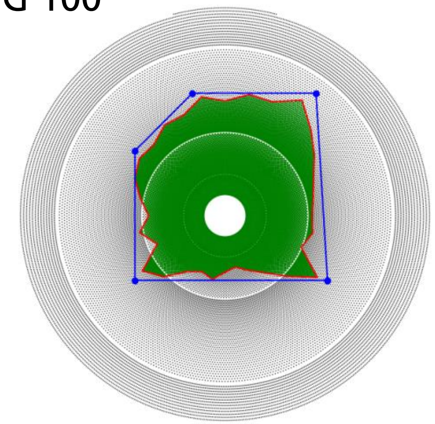

G 200

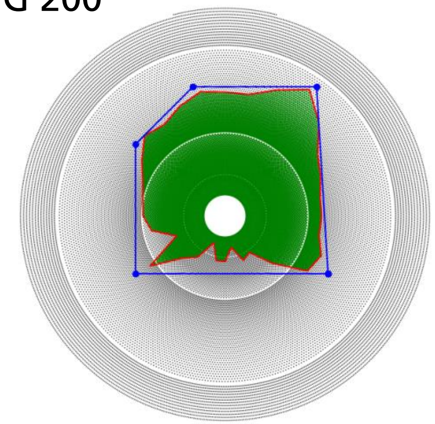

G 300

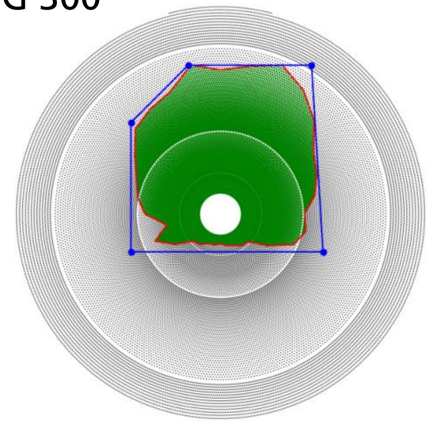

G 400

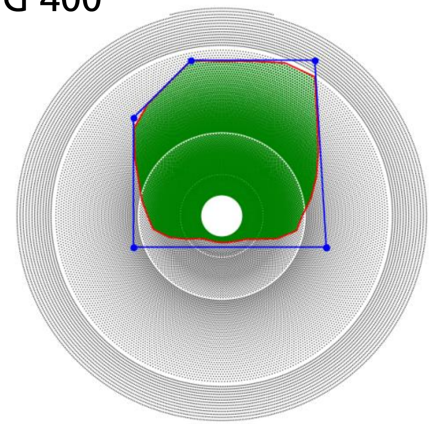

G 500

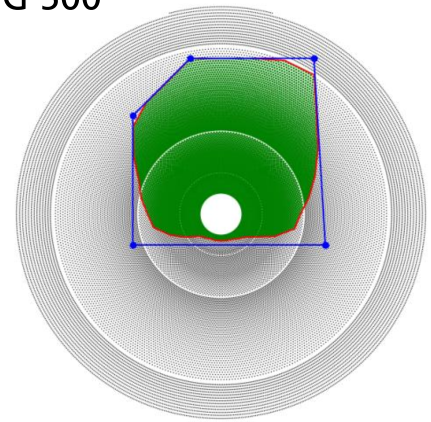

Summary & Outlook

- Method: solar field heliostat selection based on polygon optimization and boundaries
- Coherent fields
- Area boundaries
- Flexible objective function

➢ Quantitative comparison to other approaches

➢ Allowable flux limits in objective function

➢ Area boundaries with undercuts, holes and hilly terrain

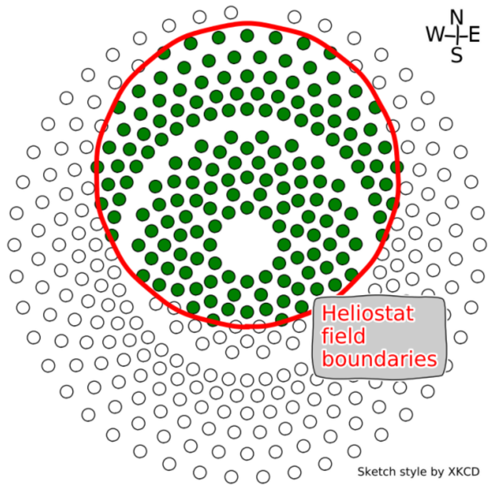

Ashalim Power Station, BrightSource Industries Israel (source: https://inhabitat.com/)

Thank you for your Attention!



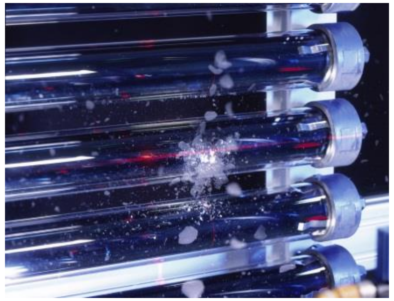
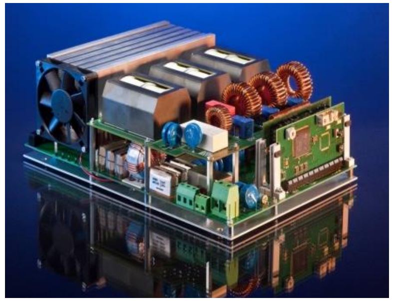
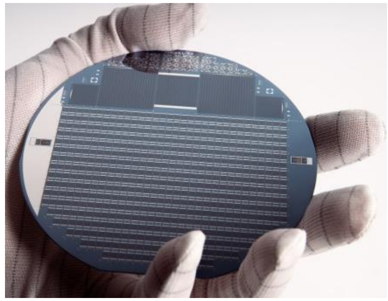


Fraunhofer Institute for Solar Energy Systems ISE

Gregor Bern, Peter Schöttl

www.ise.fraunhofer.de

gregor.bern@ise.fraunhofer.de
peter.schoettl@ise.fraunhofer.de

Fraunhofer ISE

Flux measurement for the Next-CSP project: Moving bar at Themis

SFERA-III Central Receivers Training
Odeillo, 10-12 July 2019

Benjamin Grange
benjamin.grange@promes.cnrs.fr

Solar Facilities for the European Research Area

Next-CSP project

- Installation at the Themis site
    - Tower of 104 m
    - 107 heliostats of 54 m² each
    - System between 83 m and 92 m height
    - ~70 tons

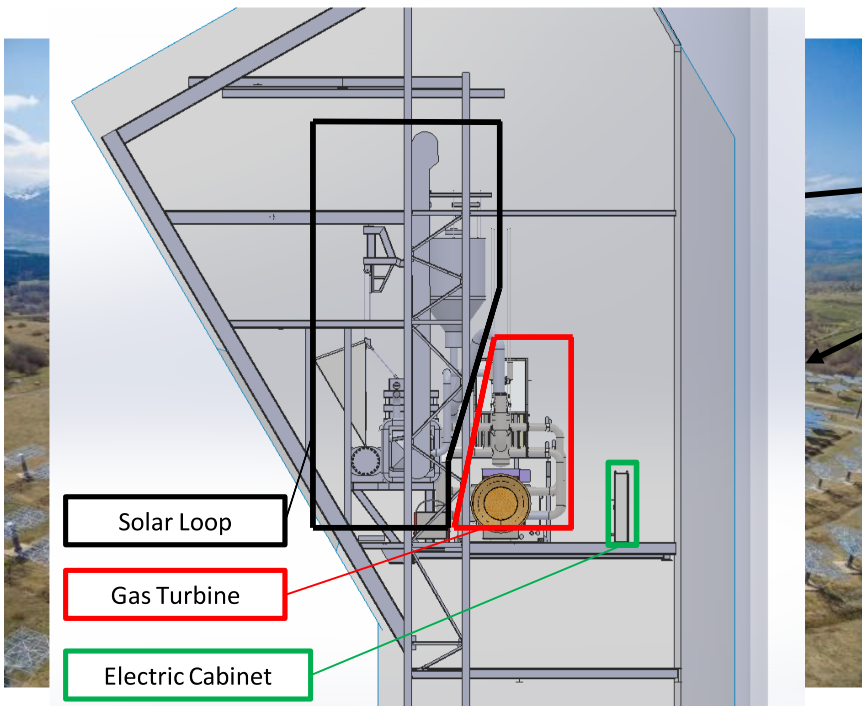

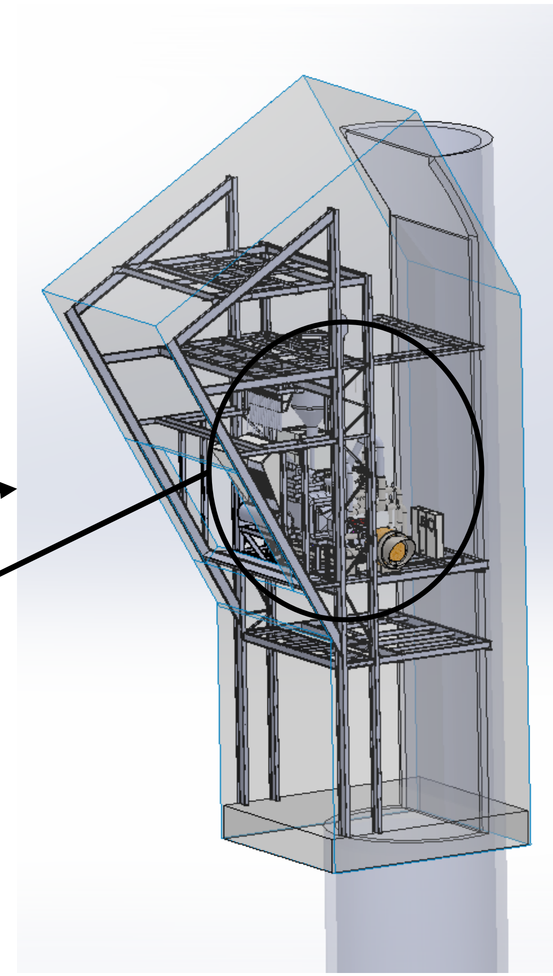

Next-CSP project

- Flux mapping at the aperture of the solar receiver → moving bar (fast motion to avoid melting the bar)

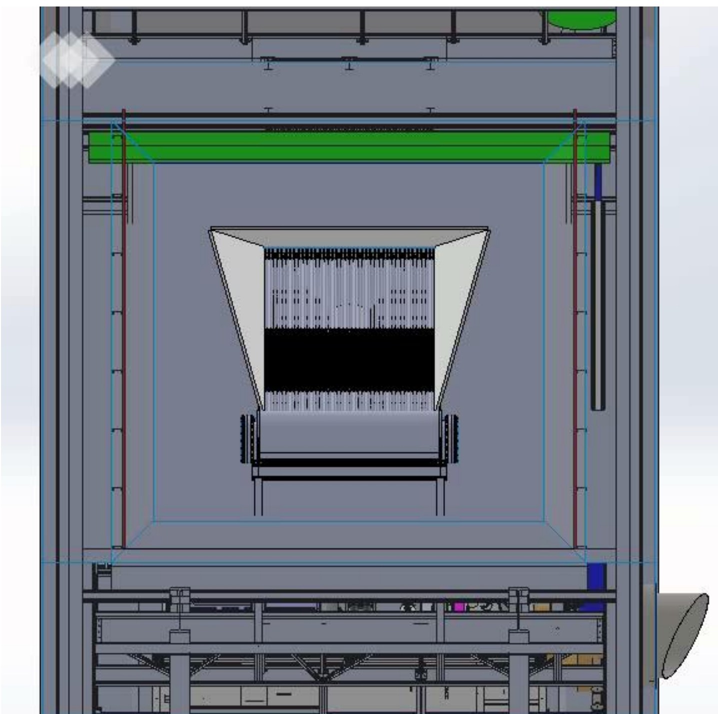

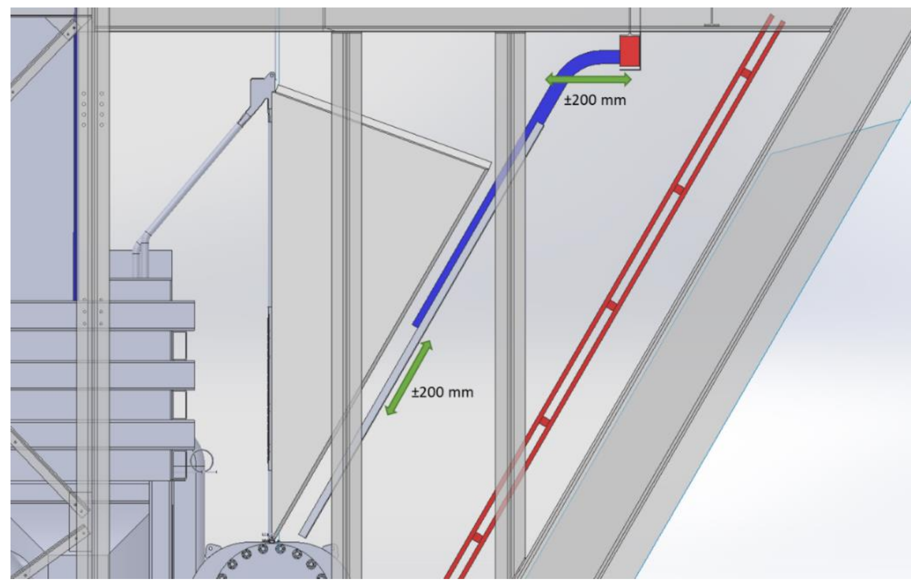

Flux measurement system

- Consists in:
  - High frame rate CMOS camera
  - Fast response heat flux sensor
  - Moving bar

- Advantage: Measure the flux distribution during solar receiver experiment

Flux measurement system

- CMOS camera installed in the solar field

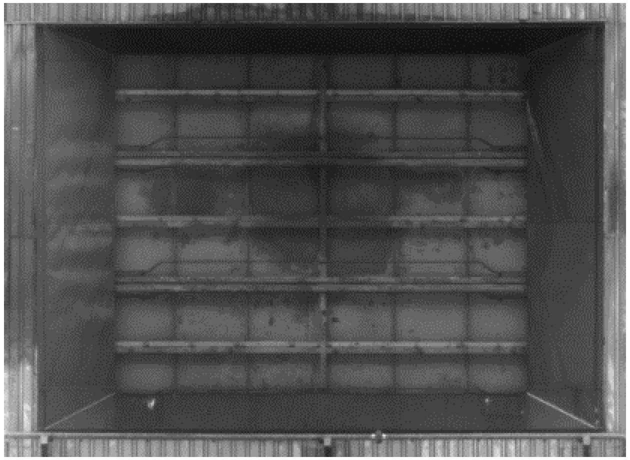

- Basler, sensor CMOS Sony IMX174, 1920*1200, monochrome
- High picture frame rate (up to 163 FPS)
- 16-bit dynamic
- Pixel of 2.34 x 2.34 mm

Flux measurement system

- Heat flux sensor installed on the moving bar

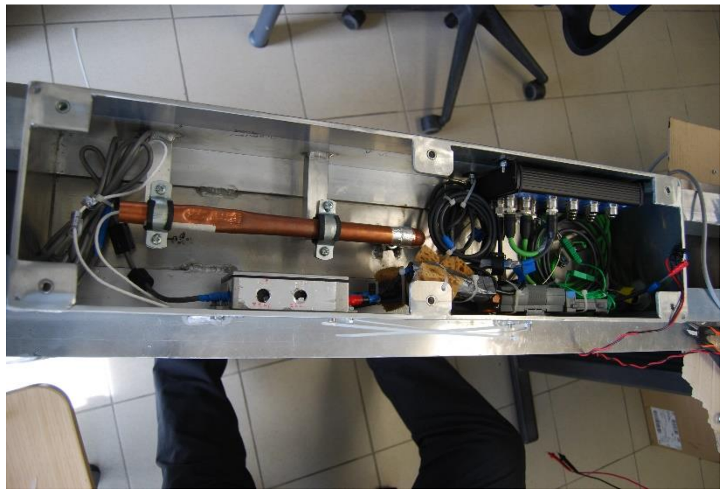

- Heat flux micro-sensor model HFM 6
- 17 to 300 μs response time
- Thermopile 4 mm in diameter, covered with Pyromark® film → α = 94%
- Accuracy of ± 3%
- High-speed A/D converter and data acquisition system ADDI DATA MSX-E3011

Flux measurement system

- Moving bar

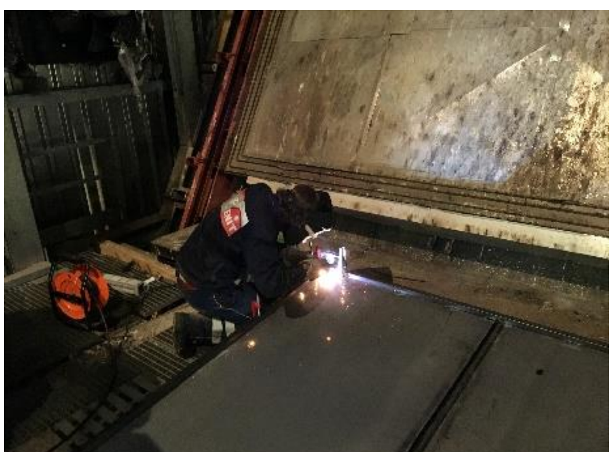

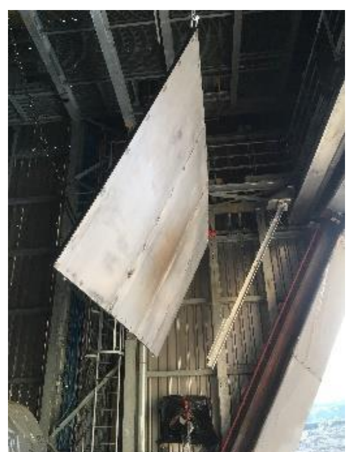

Flux measurement system

- Moving bar

Flux measurement system

- Moving bar

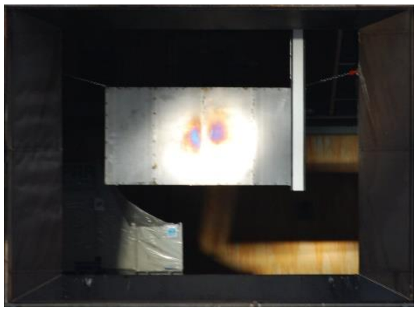
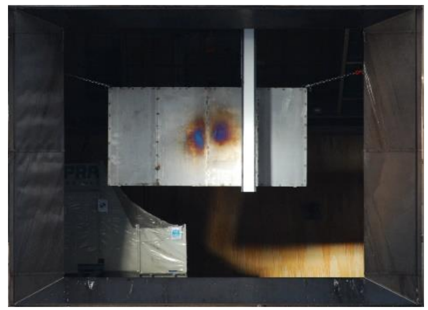
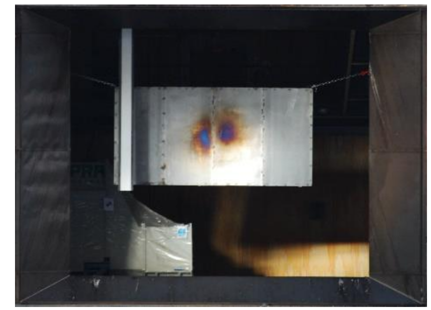

Flux measurement system

- View of the moving bar from the CMOS camera (colors added in ImageJ)
- Black stripes to be able to locate the bar in the concentrated solar flux

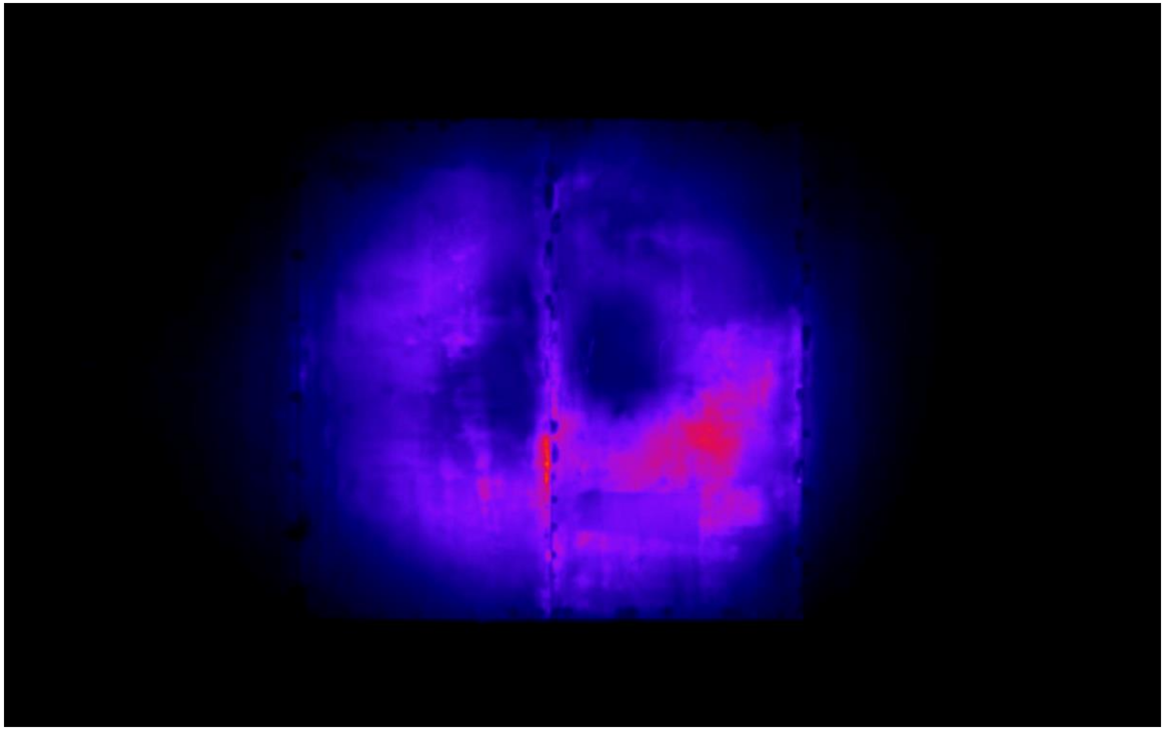

Flux measurement system

- Data processing (developed in the framework of the PEGASE project)
  - User interface

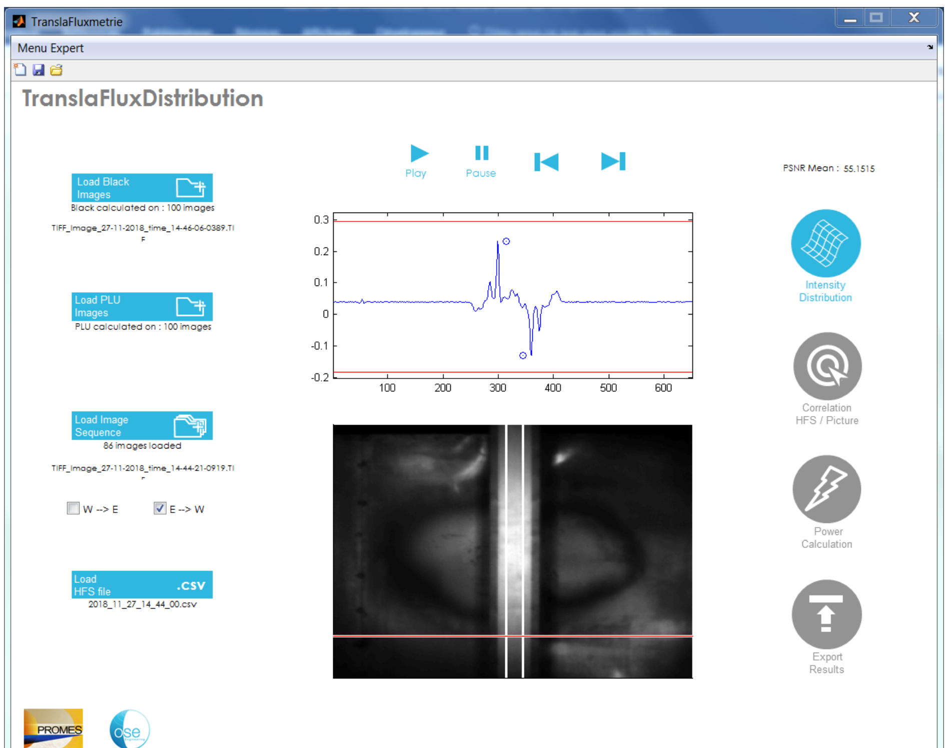

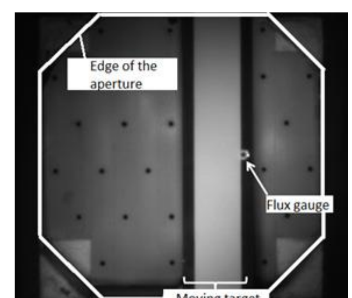

Flux measurement system

- Data processing
  - Flat-field correction (Same area of interest on the CCD matrix, same gain and shutter speed)
    - Lens covered with a tap → Black images → contain the electronic bias and noise generated by the A/D converter
    - Lens covered with a uniform brightness source → Flat-field images → contain the noise and distortion generated by each pixel when discharging their current and the optical defaults resulting from dust or scratches possibly remaining on the lens.

Flux measurement system

Flux measurement system

- Data processing
  - Flat-field correction

$$I_{net} = \frac{I_{raw} - I_{black}}{I_{flat} - I_{black}}$$

  - Background subtracted

$$I_{corr} = I_{net} - I_{back}$$

  - Gradient along x-axis (after normalization)

$$I_{grad-x} = grad_x(I_{corr-n})$$

  - Average value of normalized gradient along each column

$$Mean_{grad-x-n} = mean_y(I_{grad-x-n})$$

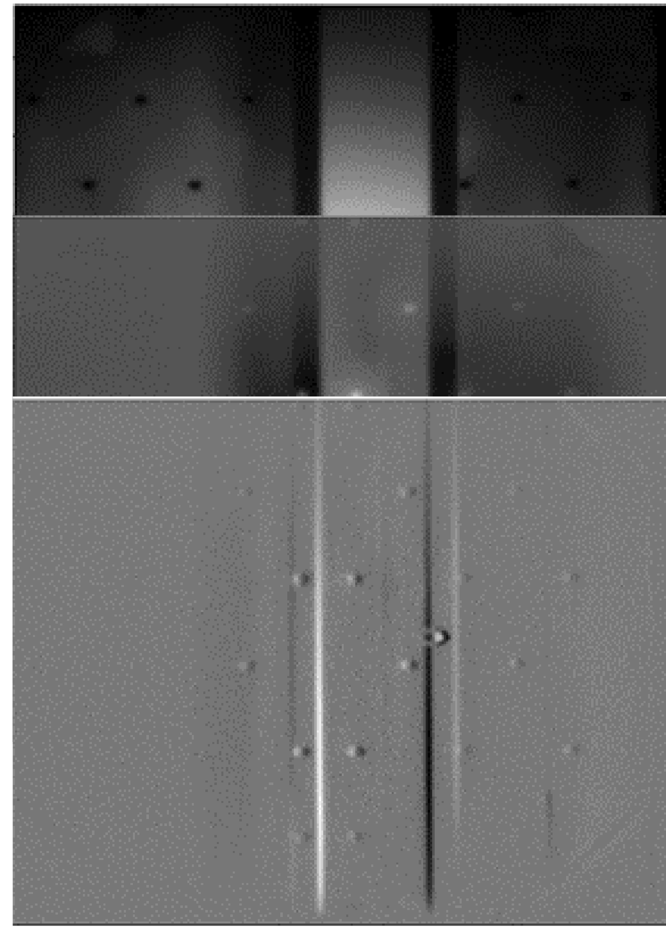

→ Spatial derivative approach

Flux measurement system

- Data processing
  - Mapping grey value

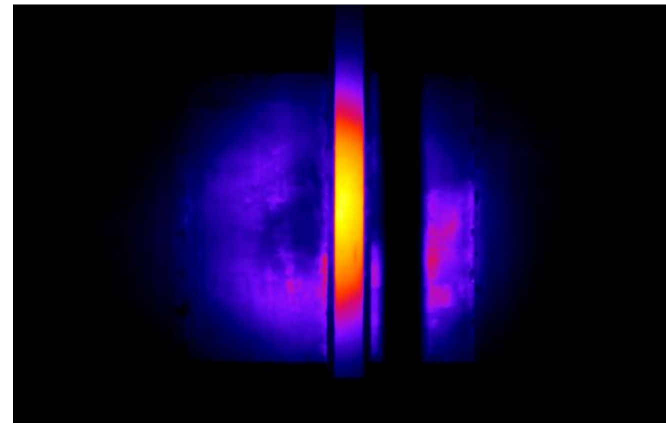

$$MeanValPixel(p) = \frac{1}{n}\sum_{i=1}^{n} ValPixel_p(i)$$

$$STD(p) = \frac{1}{n}\sqrt{\sum_{i=1}^{n}\left[ValPixel_p(i) - MeanValPixel(p)\right]^2}$$

  - *ValPixelp(i)* that deviate from the average by more than twice the *STD(p)* are rejected

$$MeanValPixel(p) - 2 \times STD(p) < ValPixel_p(i) < MeanValPixel(p) + 2 \times STD(p)$$

Flux measurement system

- Data processing
  - Calibration

$$\begin{cases} X_{flux}(n) = X_{max}(n) + dF_x \\ Y_{flux} = dF_y \end{cases}$$

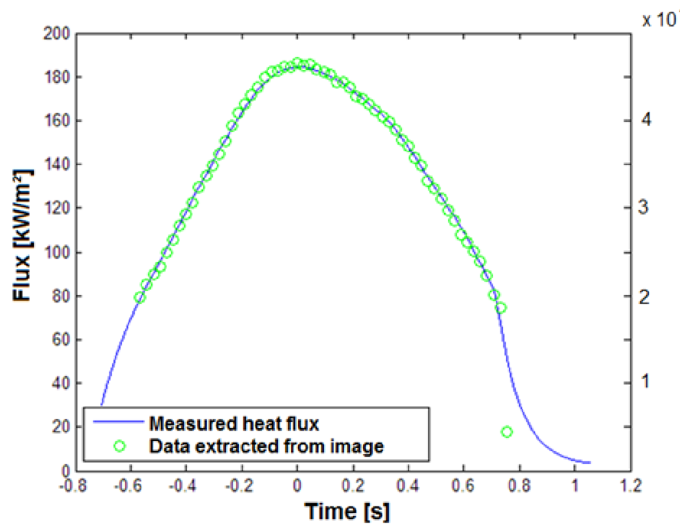

  - $ValPixel(x_n)=ValPixel(X_{flux}(n),Y_{flux})$

$$Cost(G) = \sqrt{\sum_{i=1}^{l} [G \times ValPixel(t_i) - F_{measured}(t_i)]^2}$$

Flux measurement system

- Data processing
  - Power calculation

$$P_{solar-in} = \sum_{cells} [Flux(cell_i) \times Area(cell_i)]$$

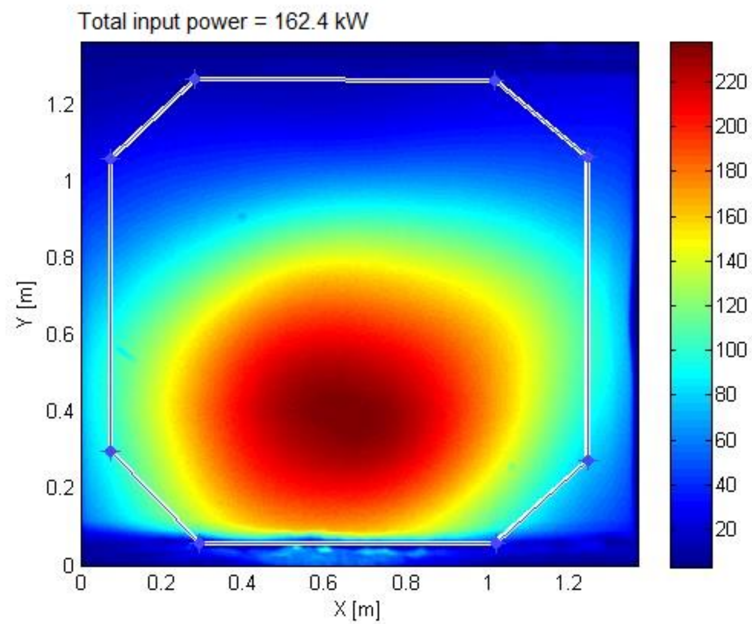

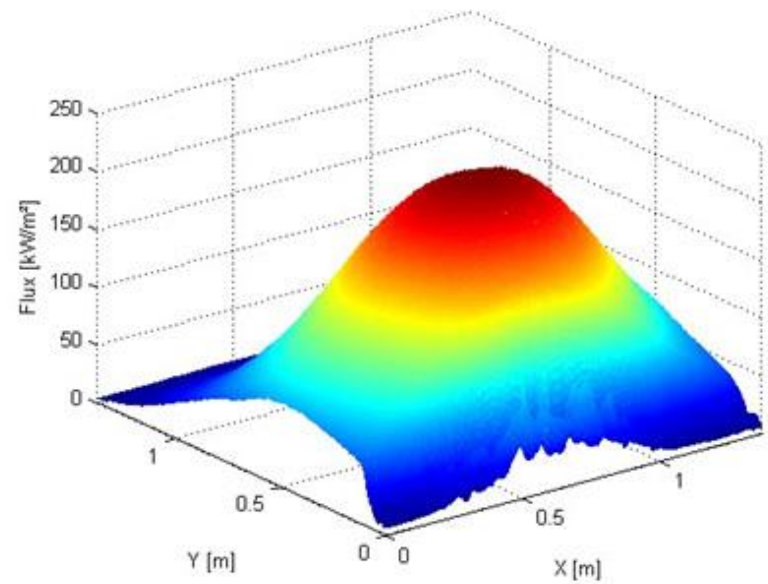

AIP Conference Proceeding: A. Ferriere, M. Volut, A. Perez, Y. Volut, In-situ measurement of concentrated solar flux and distribution at the aperture of a central solar receiver, 1734 130007 (2016), DOI: 10.1063/1.4949217

Thank you

This project has received funding from the European Union’s Horizon 2020 research and innovation program under grant agreement No 727762, project acronym NEXT-CSP.

http://next-csp.eu/

Flux measurements

Introduction

SFERA-III Central Receivers Training
Odeillo, 10-12 July 2019

Emmanuel Guillot
emmanuel.guillot@promes.cnrs.fr

PROMES

UPVD

Solar Facilities for the European Research Area

Solar Facilities for the European Research Area

The SFERA-III project has received funding from the European Union's Horizon 2020 research and innovation programme under grant agreement No 823802.

http://sfera3.sollab.eu/

Intro to flux measurements

1. Flux measurements?
2. Direct methods
3. Indirect methods

Flux measurements?

- Measuring the thermal energy
- 2 Parameters:
  - **Power**:

kW, MW, or MWth…

  - **Power density**:

1 kW/m2 = 1 sun = 0,1 W/cm2

Flux measurements?

Flux density →

Spectral radiance	$L_{e,\Omega,\nu}$ [nb 3] or $L_{e,\Omega,\lambda}$ [nb 4]	watt per steradian per square metre per hertz *or* watt per steradian per square metre, per metre	$W \cdot sr^{-1} \cdot m^{-2} \cdot Hz^{-1}$ *or* $W \cdot sr^{-1} \cdot m^{-3}$	$\mathbf{M} \cdot \mathbf{T}^{-2}$ *or* $\mathbf{M} \cdot \mathbf{L}^{-1} \cdot \mathbf{T}^{-3}$	Radiance of a *surface* per unit frequency or wavelength. The latter is commonly measured in $W \cdot sr^{-1} \cdot m^{-2} \cdot nm^{-1}$. This is a *directional* quantity. This is sometimes also confusingly called "spectral intensity".
Irradiance	E_e [nb 2]	watt per square metre	W/m^2	$\mathbf{M} \cdot \mathbf{T}^{-3}$	Radiant flux *received* by a *surface* per unit area. This is sometimes also confusingly called "intensity".
Spectral irradiance	$E_{e,\nu}$ [nb 3] or $E_{e,\lambda}$ [nb 4]	watt per square metre per hertz *or* watt per square metre, per metre	$W \cdot m^{-2} \cdot Hz^{-1}$ *or* W/m^3	$\mathbf{M} \cdot \mathbf{T}^{-2}$ *or* $\mathbf{M} \cdot \mathbf{L}^{-1} \cdot \mathbf{T}^{-3}$	Irradiance of a *surface* per unit frequency or wavelength. The terms spectral flux density or more confusingly "spectral intensity" are also used. Non-SI units of spectral irradiance include Jansky = 10^{-26} $W \cdot m^{-2} \cdot Hz^{-1}$ and solar flux unit (1SFU = 10^{-22} $W \cdot m^{-2} \cdot Hz^{-1}$).
Radiosity	J_e [nb 2]	watt per square metre	W/m^2	$\mathbf{M} \cdot \mathbf{T}^{-3}$	Radiant flux *leaving* (emitted, reflected and transmitted by) a *surface* per unit area. This is sometimes also confusingly called "intensity".
Spectral radiosity	$J_{e,\nu}$ [nb 3] or $J_{e,\lambda}$ [nb 4]	watt per square metre per hertz *or* watt per square metre, per metre	$W \cdot m^{-2} \cdot Hz^{-1}$ *or* W/m^3	$\mathbf{M} \cdot \mathbf{T}^{-2}$ *or* $\mathbf{M} \cdot \mathbf{L}^{-1} \cdot \mathbf{T}^{-3}$	Radiosity of a *surface* per unit frequency or wavelength. The latter is commonly measured in $W \cdot m^{-2} \cdot nm^{-1}$. This is sometimes also confusingly called "spectral intensity".

https://en.wikipedia.org/wiki/Radiometry (and not photometry)

Flux measurements?

- Measuring the thermal energy:
  - In total
  - In space
  - In time

MWSF H53 Flux data results

2D data

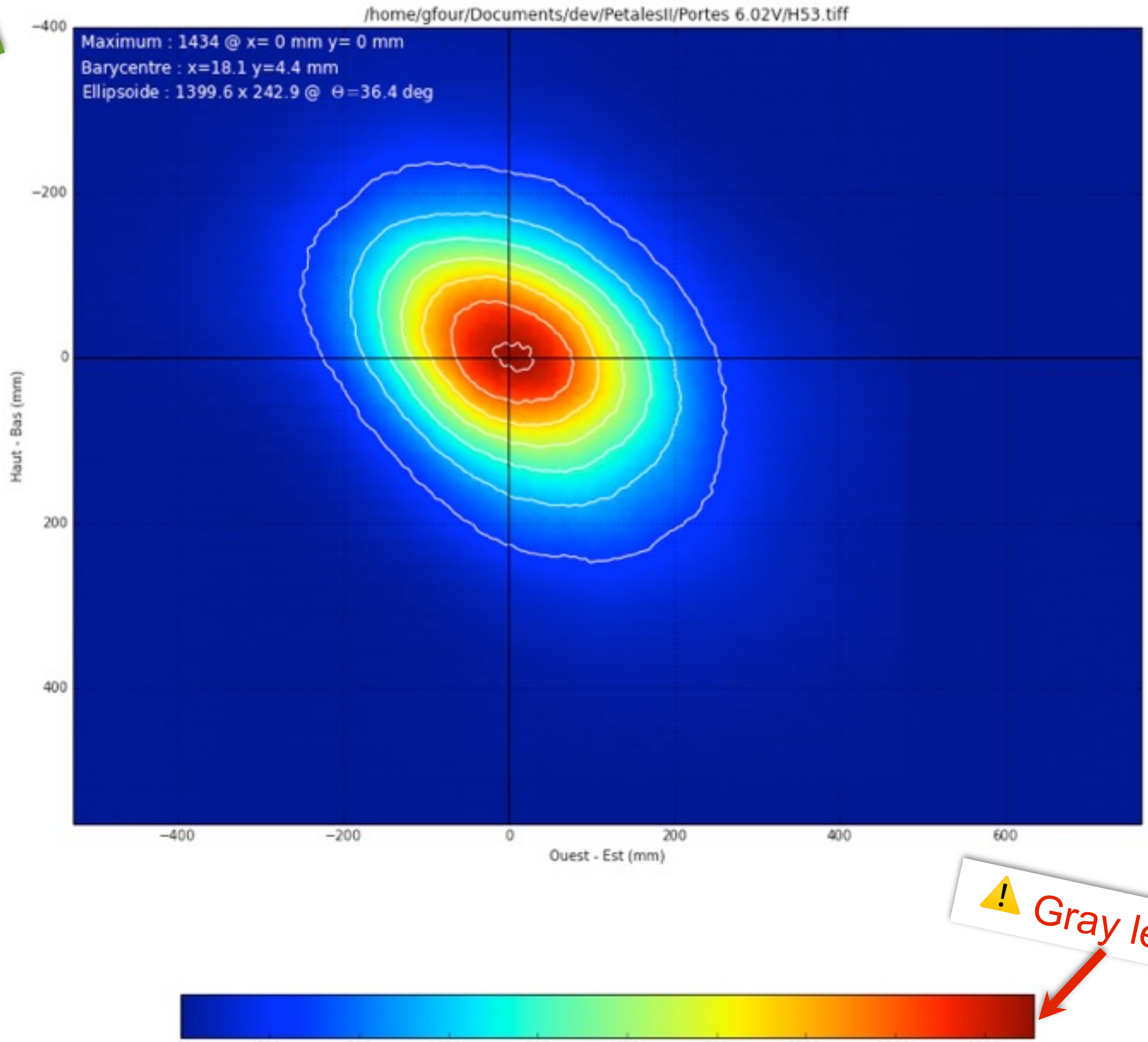

Gray levels

PETALES-C
+ Python

MWSF 2016

Flux final data results: focal volume exploration

3D data

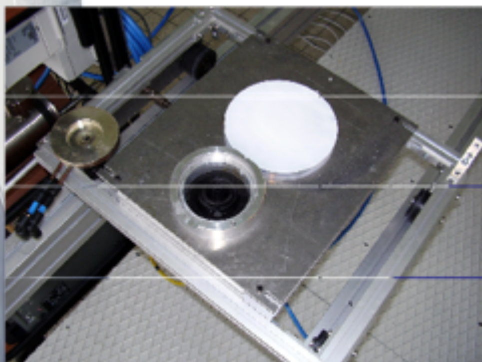

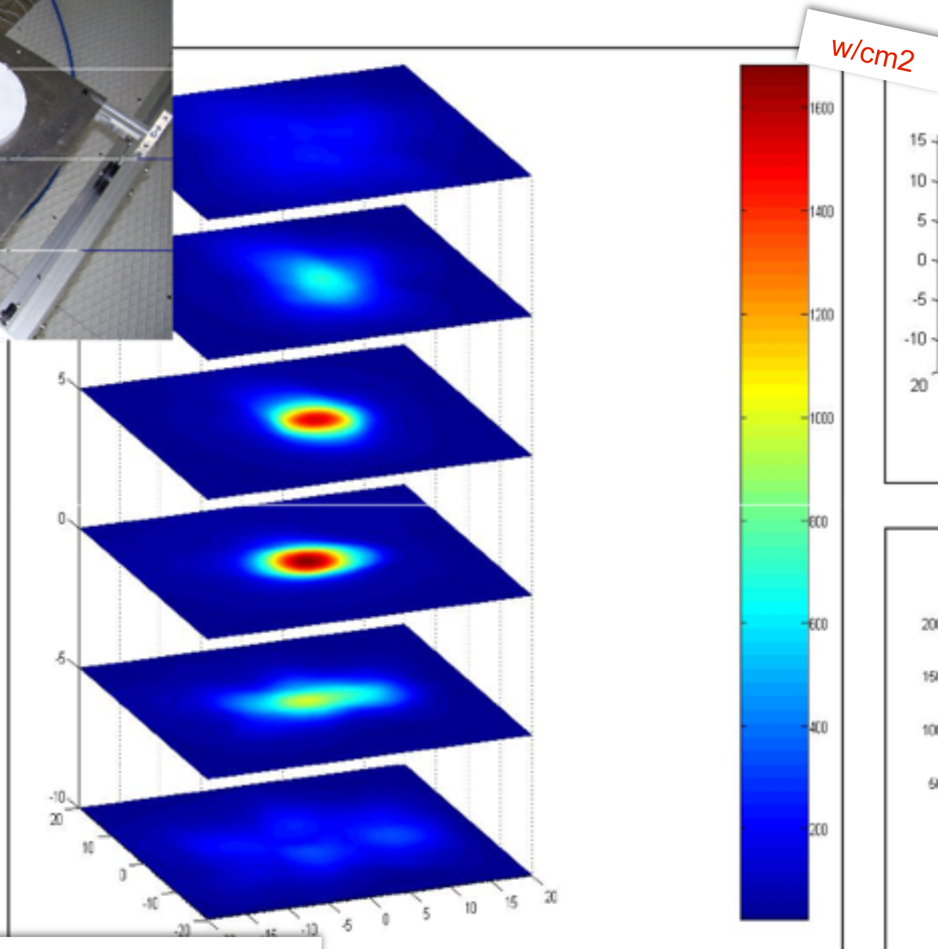

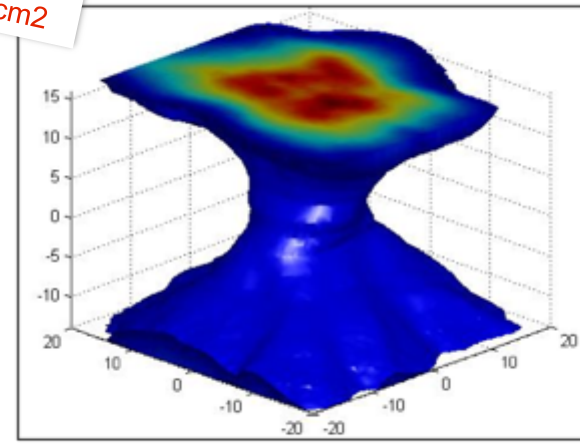

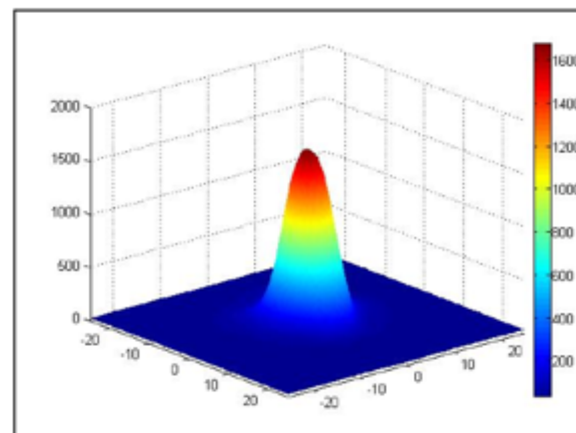

SolCal 20
LabView Perez
Analog Camera
C++ Giral
Matlab plots

CNRS-PROMES MSSF 2005

MWSF H16 Flux data results: tracking performance

2D+t data

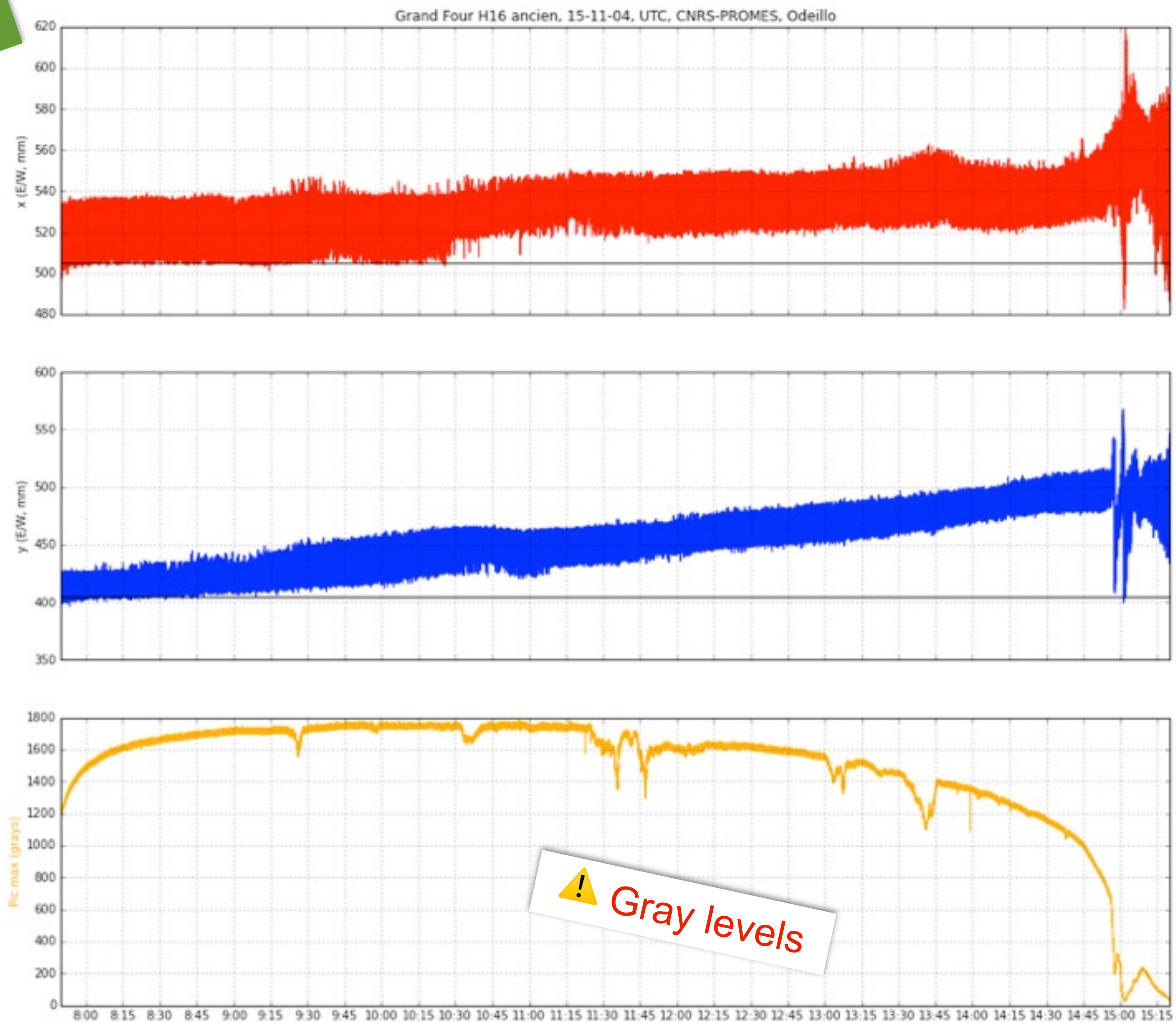

PETALES-C
+ Python

MWSF 2015

PSA flux data: tracking performance

2D+t data

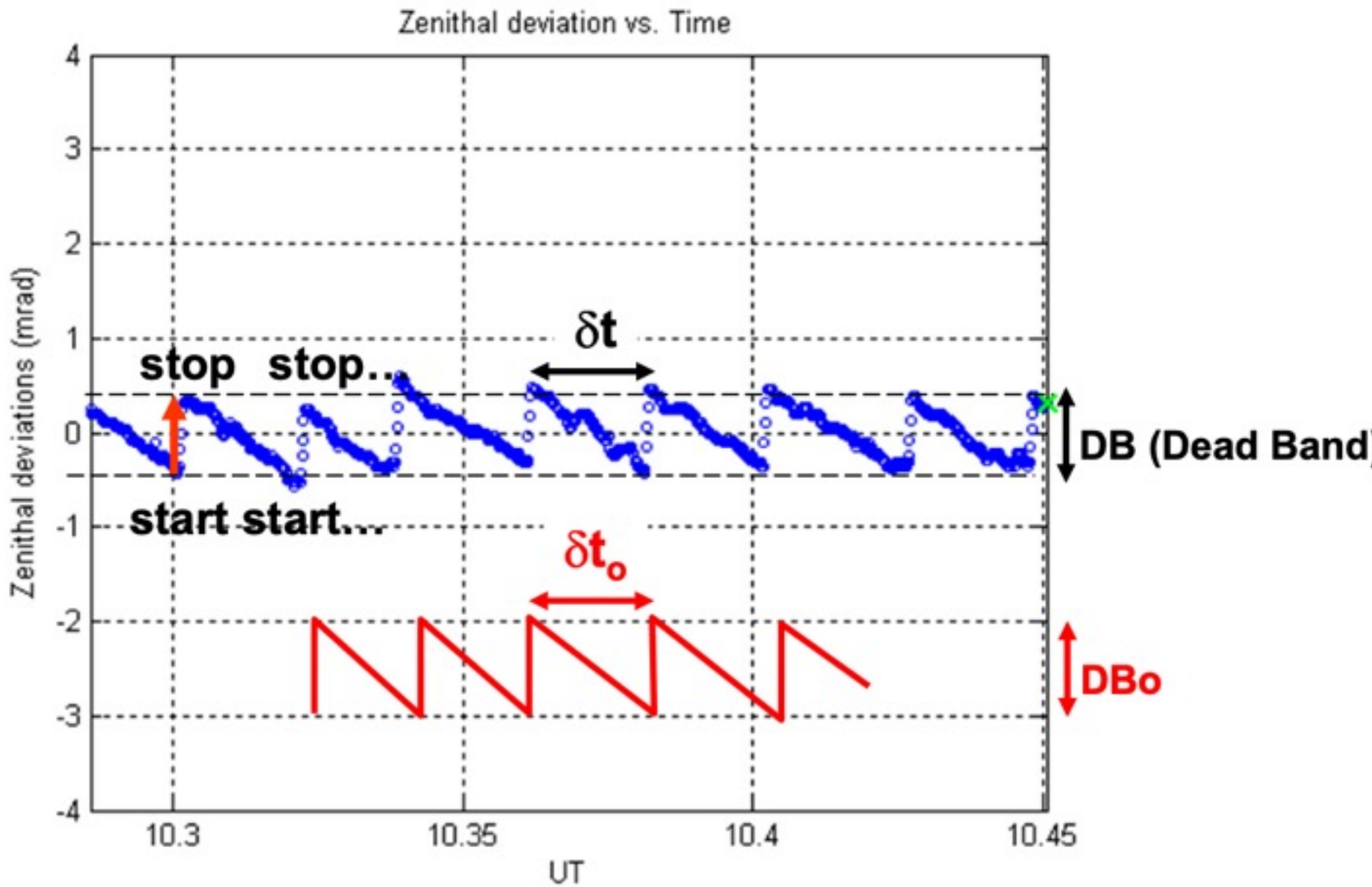

Expected pattern

Experimental pattern

Relevant parameters: δt, Db

Σdt -> daily energy saving

R. Monterreal

CIEMAT-PSA

Flux measurements: data reduction

- Spatial data reduction: defining the spot with reduced parameters instead of a picture
    - Peak value and location: maximum or barycenter
    - Gaussian standard deviations
    - Ellipsoid shape
    - Ellipsoid orientation
    - … ?

Flux measurements: data reduction

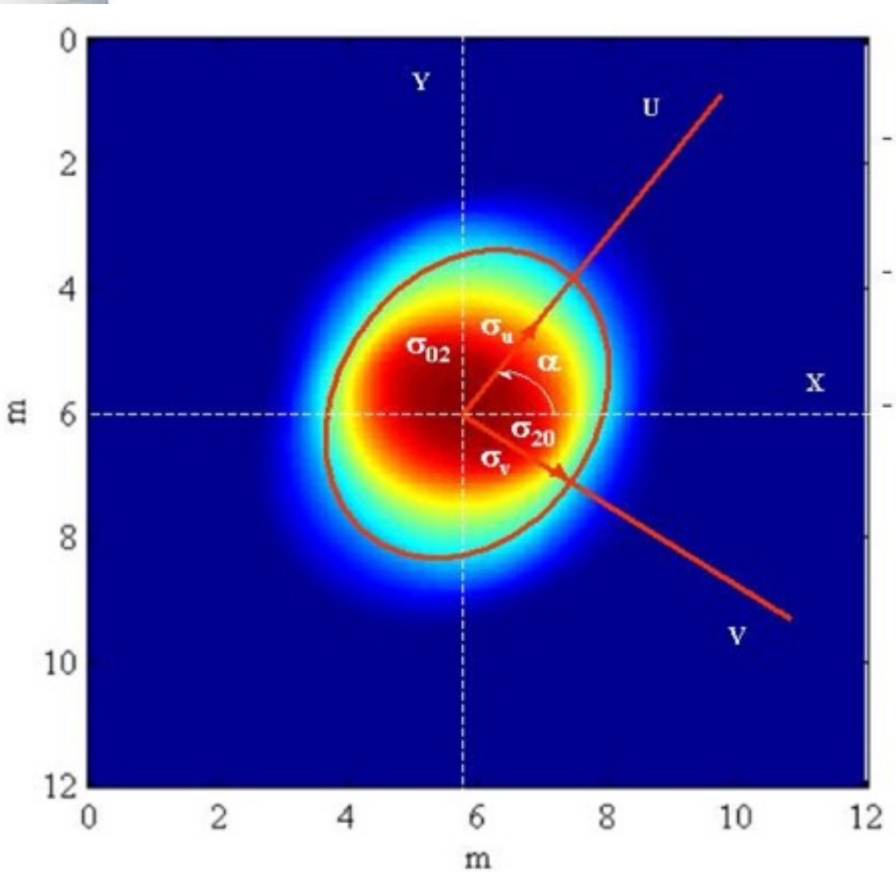

- **Image function *f(x, y)***: Bidimensional discrete function which represents the digital image generated by a CCD camera in nxm order matrix format.
- f(x, y) central moments:

$$\mu_{pq} = \int_{-\infty}^{\infty}\int_{-\infty}^{\infty}(x-\bar{x})^p (y-\bar{y})^q f(x,y)dxdy$$

for *p, q = 0, 1, 2... and* $\bar{x} = \frac{m_{10}}{m_{00}}; \quad \bar{y} = \frac{m_{01}}{m_{00}}$

In case of discrete function (digital picture):

$$\mu_{pq} = \sum_x \sum_y (x-\bar{x})^p (y-\bar{y})^q f(x,y)$$

R. Monterreal, CIEMAT-PSA

Flux measurements: data reduction

Our interest: p, q = 1, 2

$$\mu_{20} = \sum_x \sum_y (x-\bar{x})^2 f(x,y)$$

$$\mu_{02} = \sum_x \sum_y (y-\bar{y})^2 f(x,y)$$

$$\mu_{11} = \sum_x \sum_y (x-\bar{x})(y-\bar{y}) f(x,y)$$

$$\mathrm{var}(x) = \frac{\mu_{20}}{\sum\sum f(x,y)}; \quad \mu_x = \sqrt{\mathrm{var}(x)}$$

$$\mathrm{var}(y) = \frac{\mu_{02}}{\sum\sum f(x,y)}; \quad \mu_y = \sqrt{\mathrm{var}(y)}$$

$$\mathrm{cov}\,ar(x,y) = \frac{\mu_{11}}{\sum\sum f(x,y)};$$

$$C_{XY} = \begin{pmatrix} \mathrm{var}(x) & \mathrm{cov}\,ar(x,y) \\ \mathrm{cov}\,ar(x,y) & \mathrm{var}(y) \end{pmatrix};$$

$$\lambda_U, \lambda_V = EIG(C_{XY})$$

$$\mu_U = \sqrt{\lambda_U}$$
$$\mu_V = \sqrt{\lambda_V}$$

$$e = \frac{\mu_U}{\mu_V}$$
$$\alpha = \langle \hat{e}, \hat{u} \rangle$$

R. Monterreal, CIEMAT-PSA

Methods
for flux measurements

Flux measurements?

- 2 methods and set of instruments:
  - **Direct** methods

Sensors directly measure thermal power

  - **Indirect** methods

Several sensors and postprocessing required

Direct methods

Direct methods

- Gardon gages
- Calorimeters
- Other thermoeletric sensors
- (Pyroelectric sensors)
- (Photonic sensors)

Not (widely) used for CSP

=> local measurement = surface averaged

Gardon gauges

- Measuring heat flowing in a known material

=> measuring ΔT in a material

=> with a know conductivity

=> we can calculate the heat transfer

=> if we know the optical absorptivity

=> we can calculate the irradiance

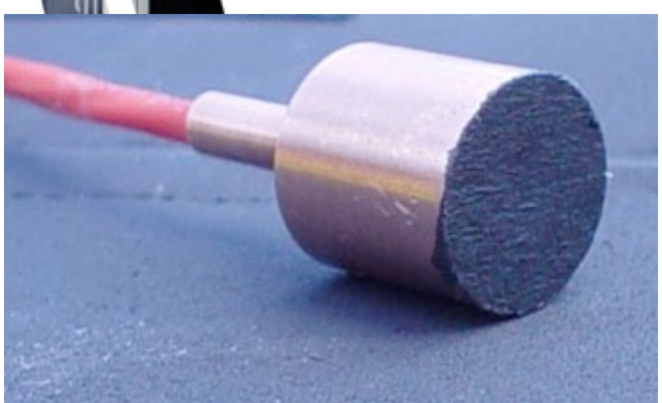

VATELL CORPORATION

Gardon gauges

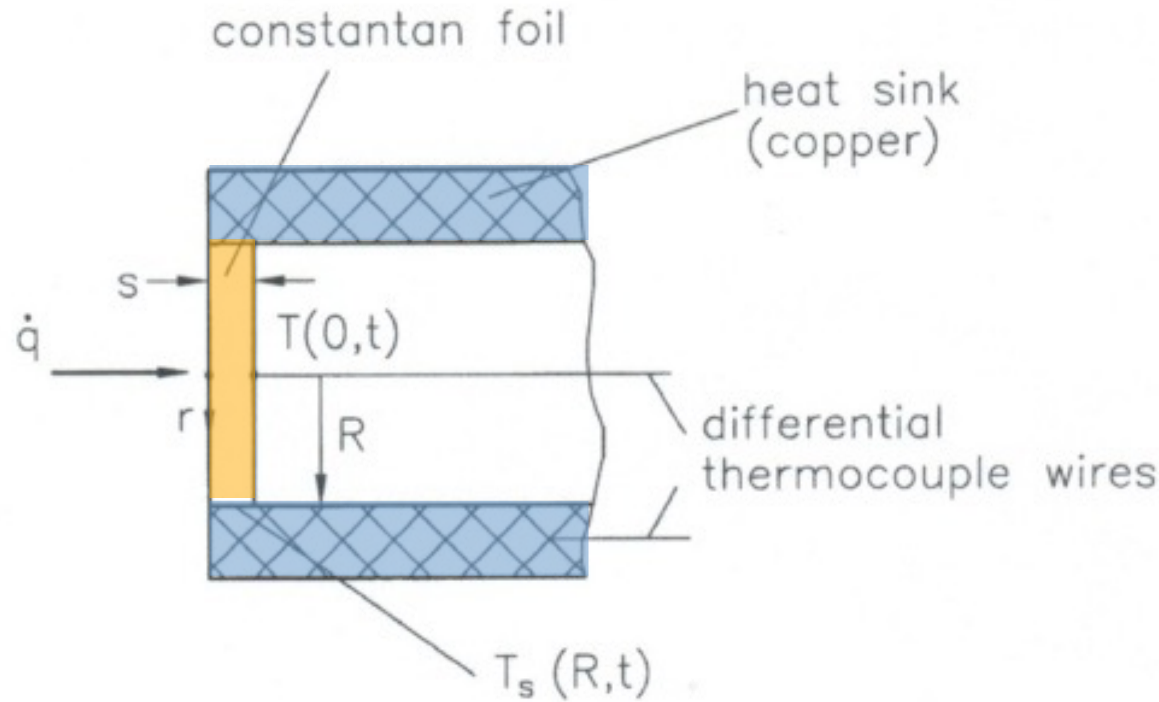

$$\vec{q} = -k\vec{\nabla}T$$

Gardon gauges

Advantages:

- Simple
- Small
- Accurate: 5-10 %
- Can have a window to protect from harsh conditions (dust, weather…)

Gardon gauges

- Widely used (and characterized):
  - Fire protection (0-50 suns)
  - Combustion (0-1000 suns)
  - CSP (0-5000 suns)
  - Plasma reactor (0-100 000+ suns)

Gardon gauges

Issues are well known (but not ± well corrected):

- Heat sink temperature dependance
- Absorptivity
- Convection losses
- Directionality
- (plus normal sensors signal issues, grounding…)

Gardon gauges

CIEMAT-PSA J. Ballestrin calibration:

graphite heated plate + reference sensor + spectral calculated correction for Zynolite coating

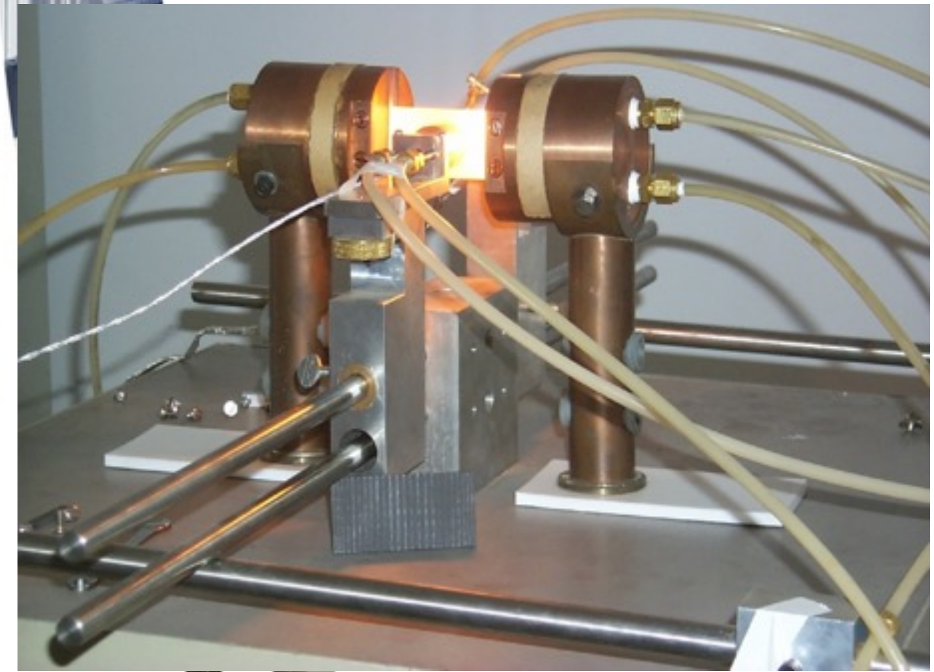

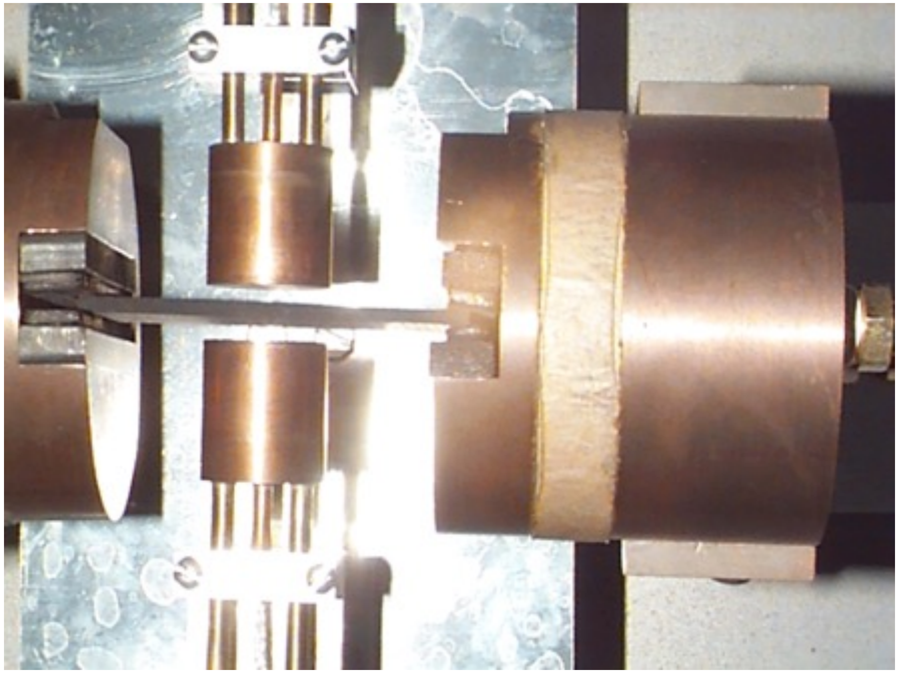

Gardon gauges

SFERA Flux Intercomp 2012 at Odeillo's MWSF

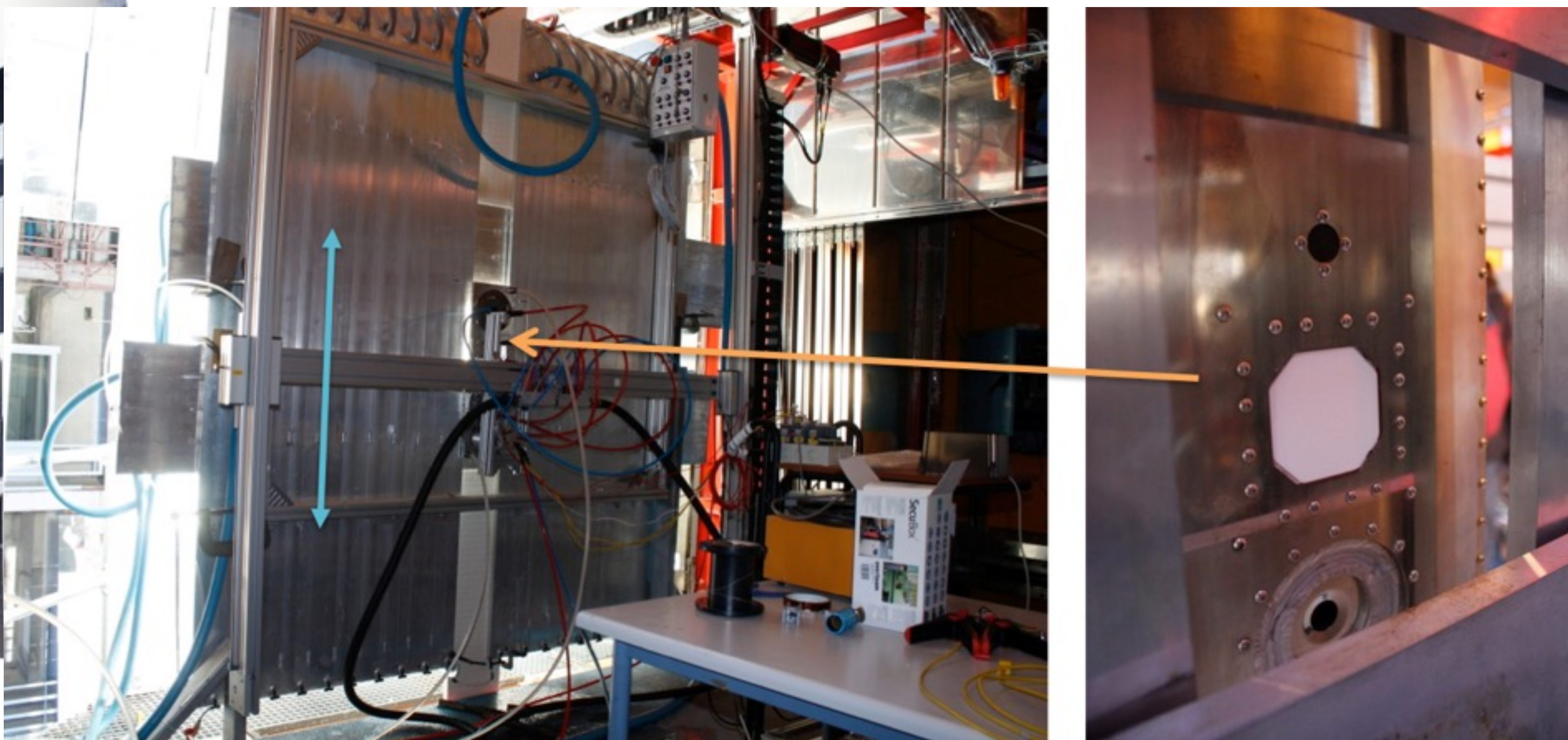

Thermoelectric sensors

Other thermoelectric sensors for:

- Faster speed: up to kHz rate
- Better signal range or sensibility
- Better or complete immunity to convection losses
- Lower price

Thermoelectric sensors

Usually, variations around the sandwich principle:

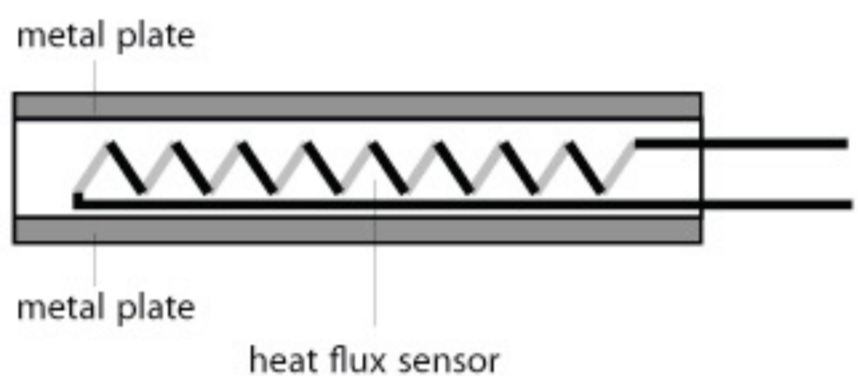

Hukseflux
Thermal Sensors

Thermoelectric sensors

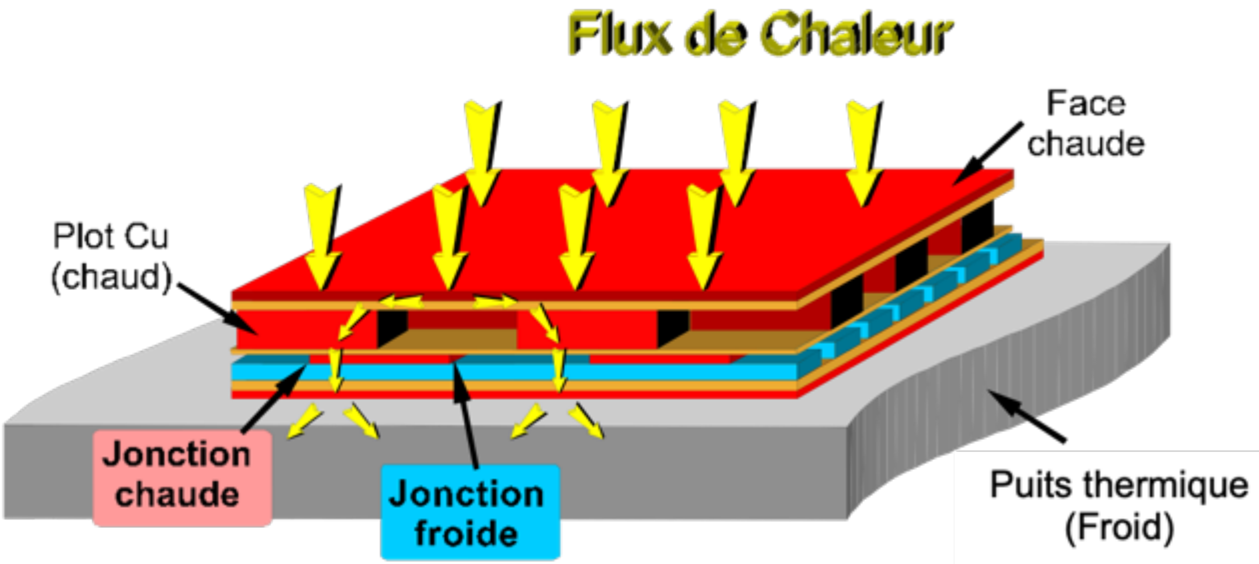

Captec

https://www.captec.fr/

Convection and T° self corrected

but low flux: < 500 suns

Calorimeters

Thermal energy is transferred to a fluid

=> measuring mass flow $\dot{m}$

=> measuring temperature change ΔT

=> knowing heat capacity c_p

=> calculate power P

$$P = \dot{m} \cdot c_\mathrm{p} \cdot \Delta T$$

Calorimeters

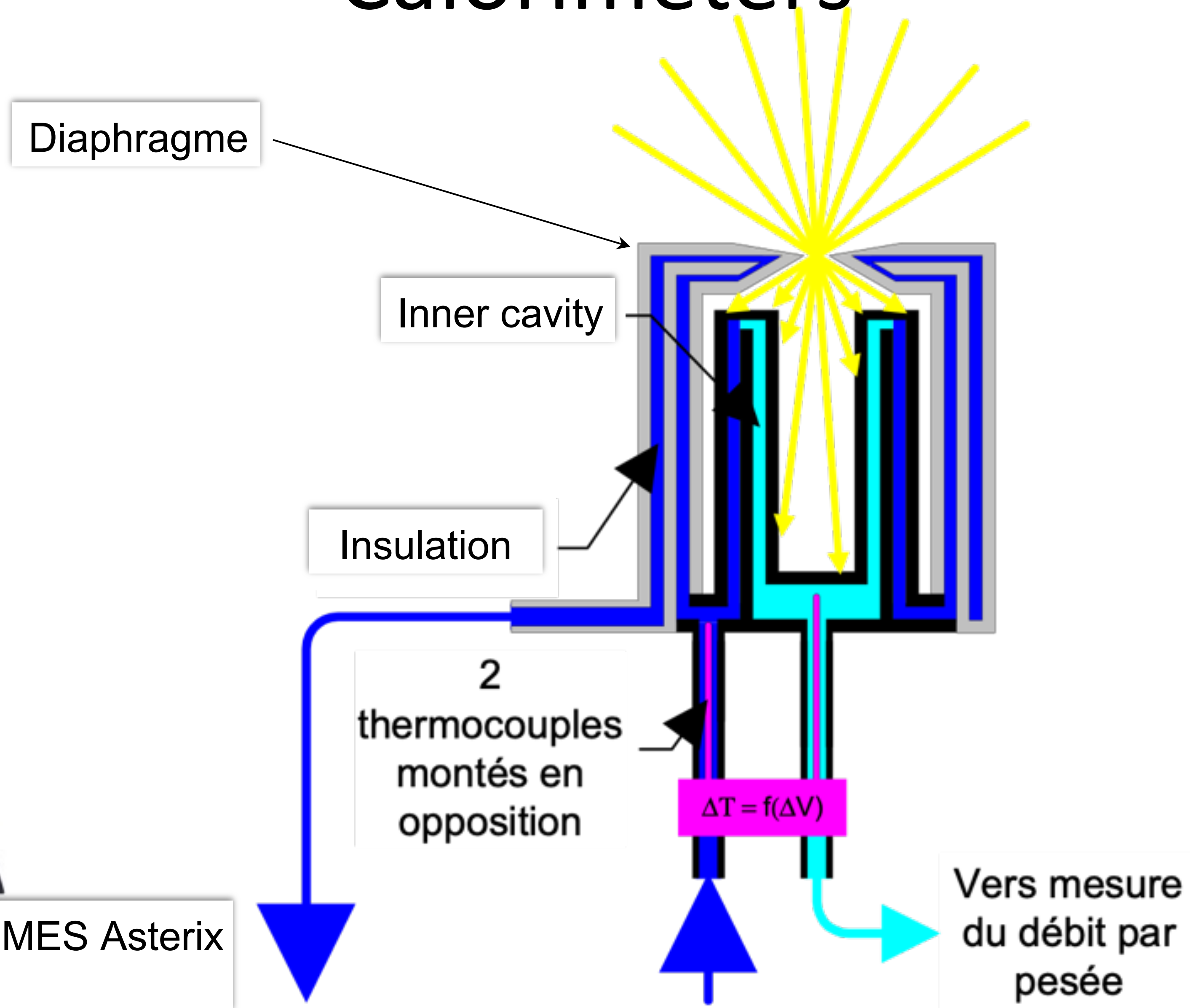

CNRS-PROMES Asterix
B. Rivoire

Calorimeters

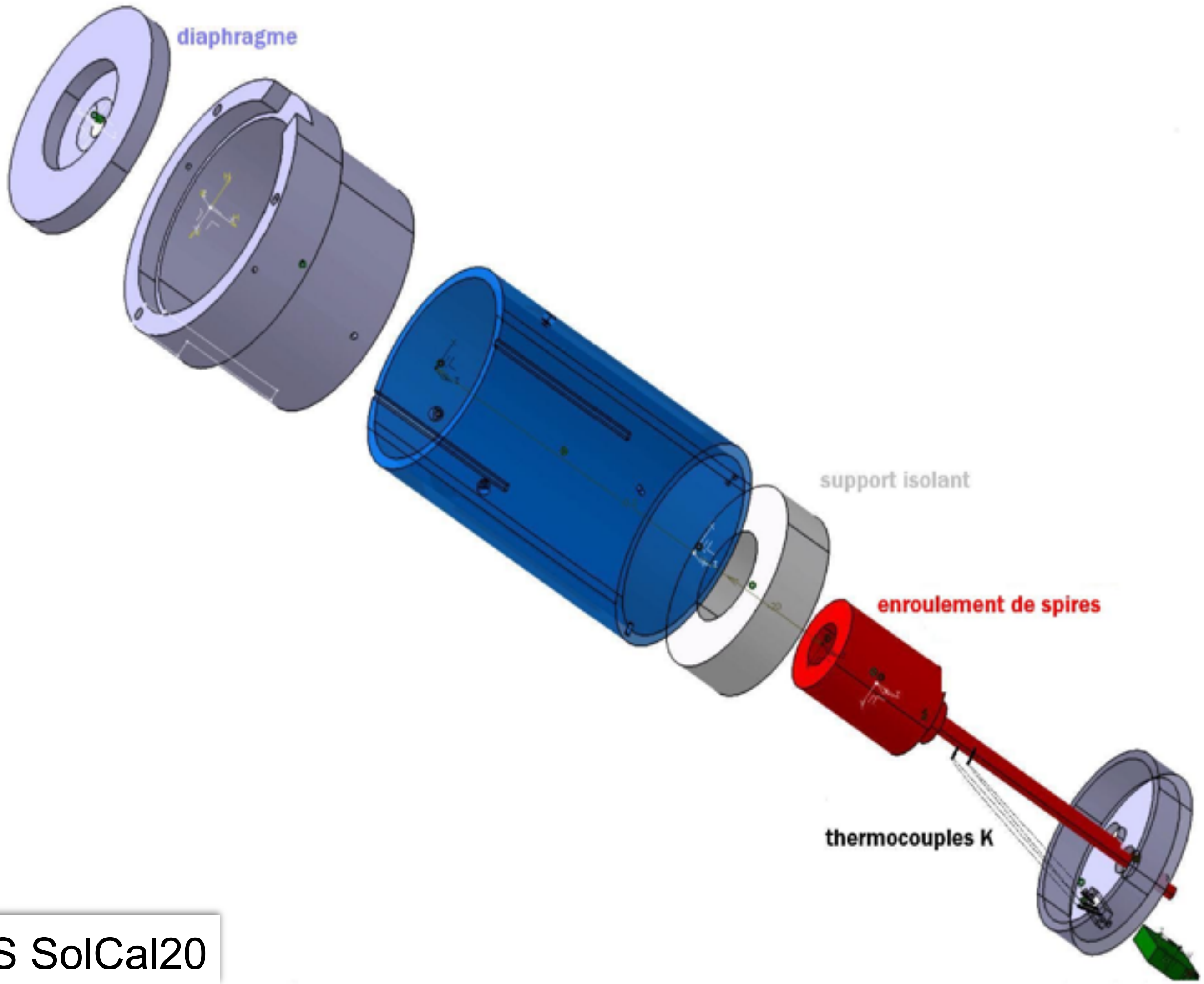

CNRS-PROMES SolCal20

Calorimeters

Measuring water **flow** with very high accuracy:

The best

- Weighting accumulated volume during a reference time
- Chronometer and reference volume(s)
- **Coriolis** flowmeter
- Other mass flowmeters (heat capacity…)
- Volumetric flowmeters

The «easiest»

Calorimeters

Calculating water **mass** from **volume**:

$$\rho = a_5 \bullet \left(1 - \frac{(T + a_1)^2 \bullet (T + a_2)}{a_3 \bullet (T + a_4)}\right)$$

ρ: density of water between 0 and 40 °C in kg/m³)

T: temperature of water in °C

a_1 = -3.983035 °C

a_2 = 301.797 °C

a_3 = 522528.9 °C^2

a_4 = 69.34881 °C

a_5 = 999.974950 kg/m³

For *pure* water…

Calorimeters

The best

Measuring **temperature** with very high accuracy:

- Thermistances RTD
- Thermistances PT100
- Differential thermocouple (E, J, K…)
- Normal thermocouples (E, J, K…)

The «easiest»

Calorimeters

What is the fluid heat capacity?

- Are we sure of our chemistry?
- Temperature correction

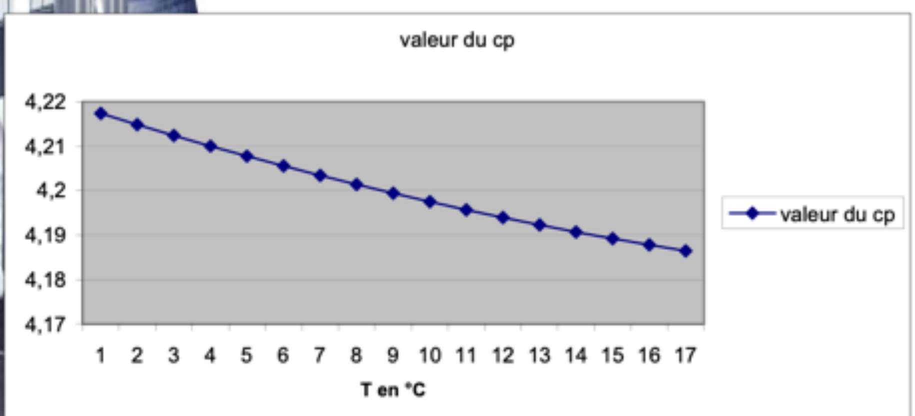

$$c_p = 4 \cdot 10^{-2} \frac{\mathrm{J}}{\mathrm{kg} \cdot {}^\circ\mathrm{C}^3} \cdot T^2 - 2.65 \frac{\mathrm{J}}{\mathrm{kg} \cdot {}^\circ\mathrm{C}^2} \cdot T + 4220 \frac{\mathrm{J}}{\mathrm{kg} \cdot {}^\circ\mathrm{C}}$$

c_p: mass heat capacity of the fluid in $\frac{\mathrm{J}}{\mathrm{kg} \cdot {}^\circ\mathrm{C}}$

T: mean temperature of the fluid *in* °C

For *pure* water…

Calorimeters

Optical absorptivity? have a cavity!!!

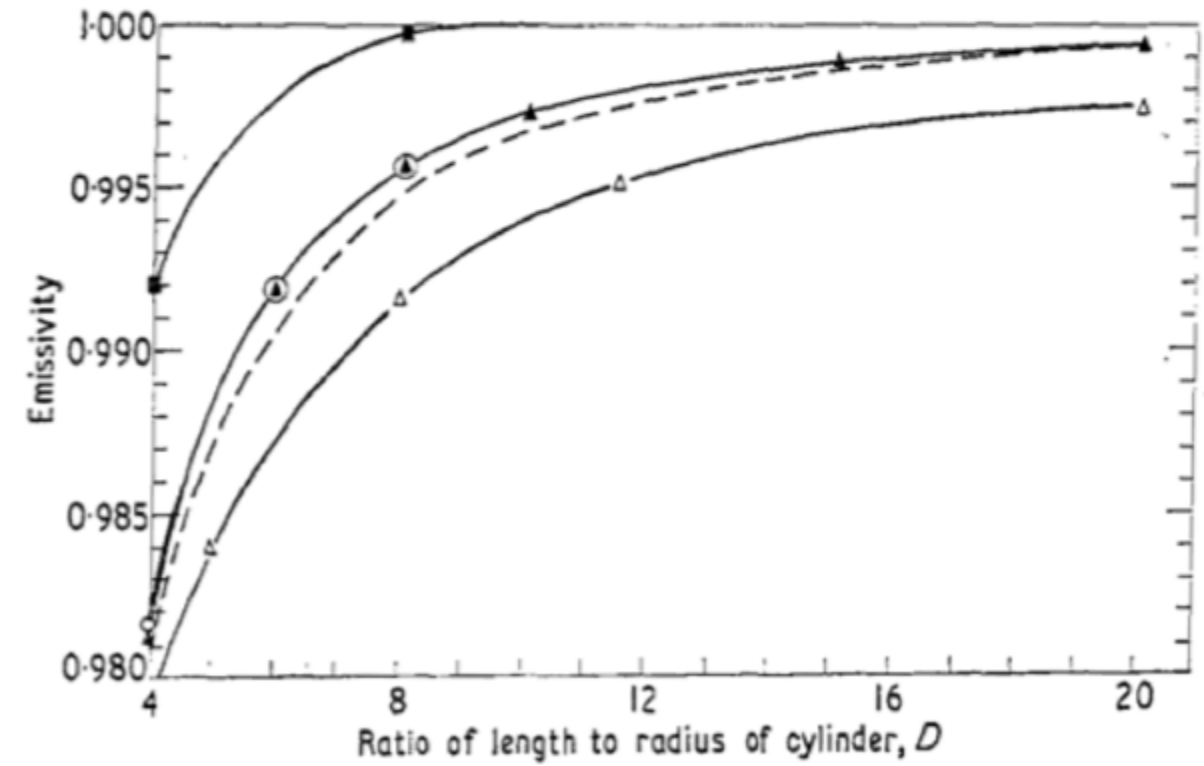

Calculated apparent cavity absorptivity with diffusive walls at **0.750**
(aka a poor old black paint…)

Direct method: flux mapping

⚠️ Only if fast enough!!!

- Using moving calorimeters

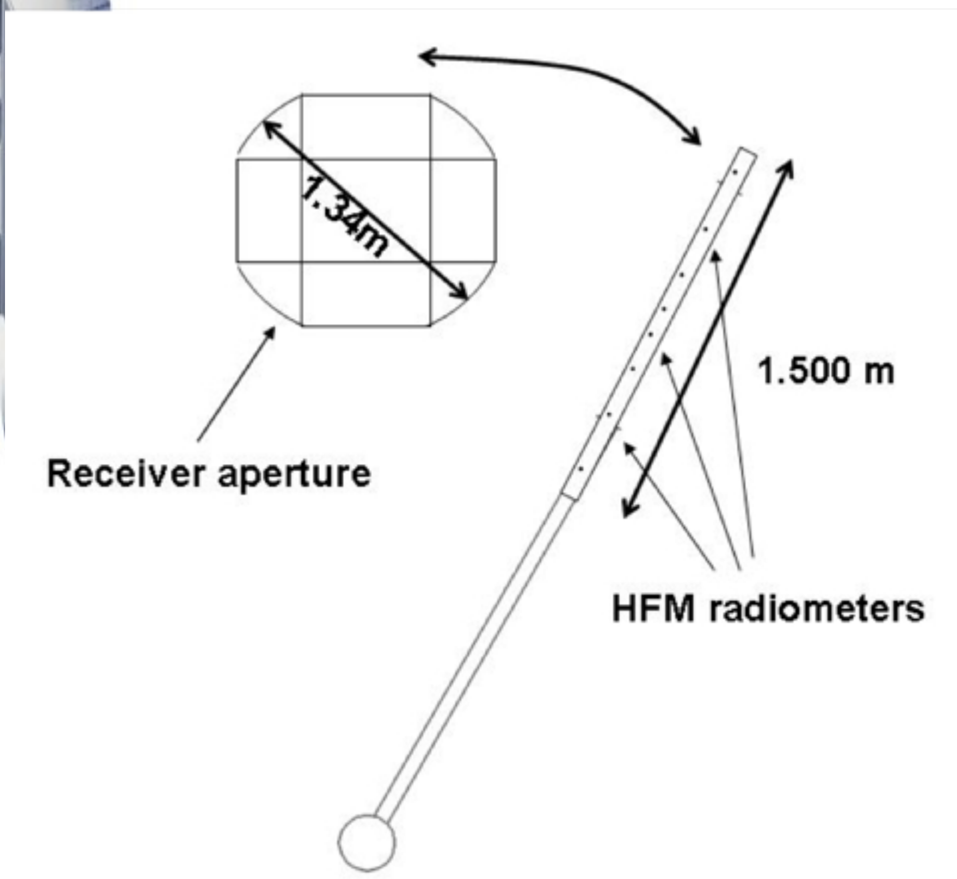

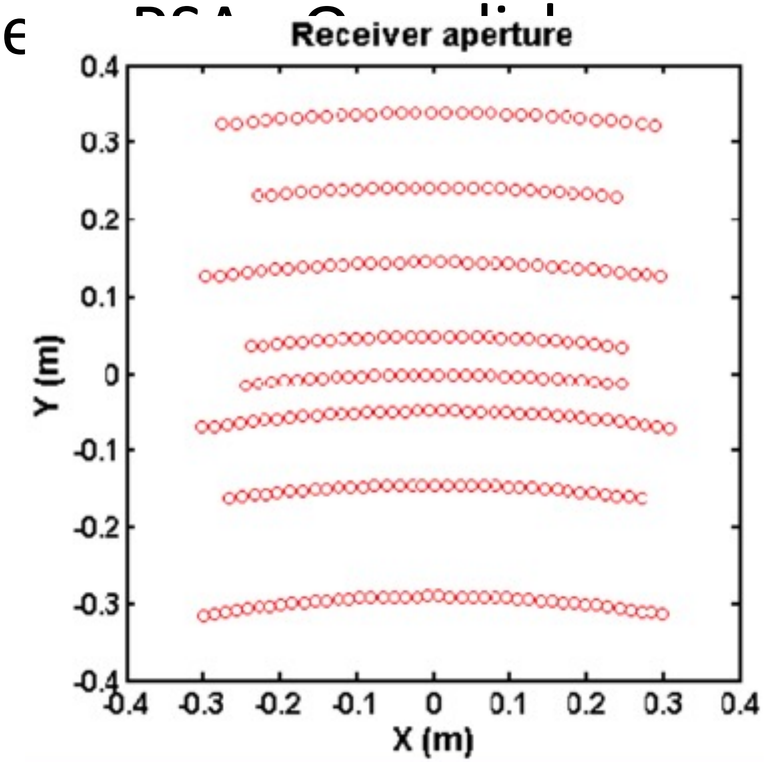

Discrete measurement location

Direct method: flux mapping

Interpolated data position → *Plotting results*

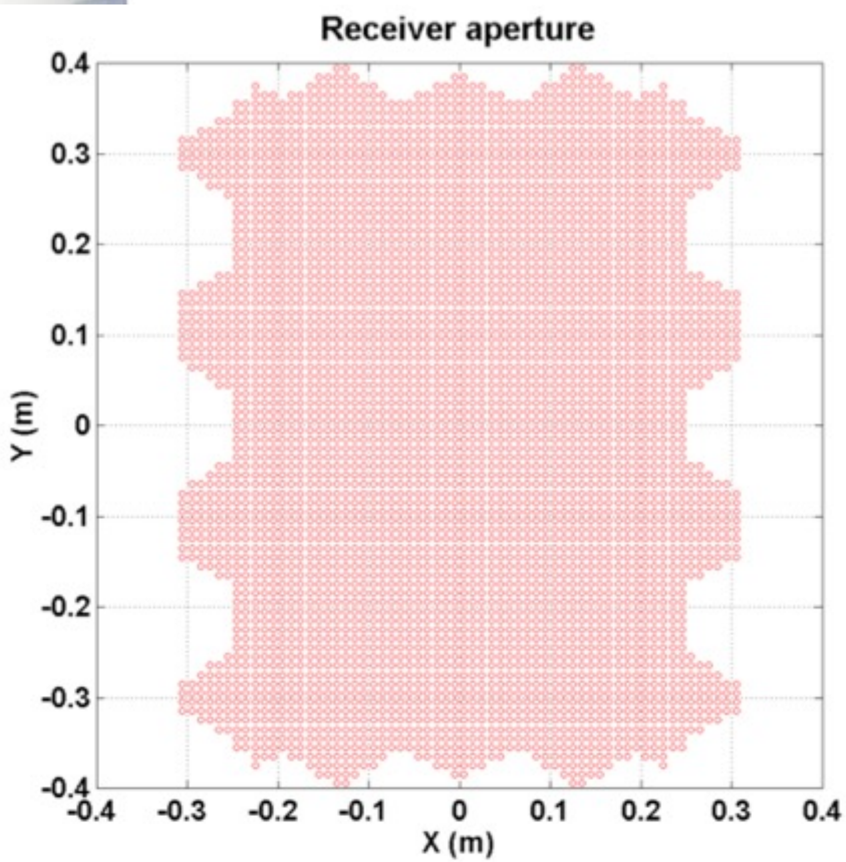

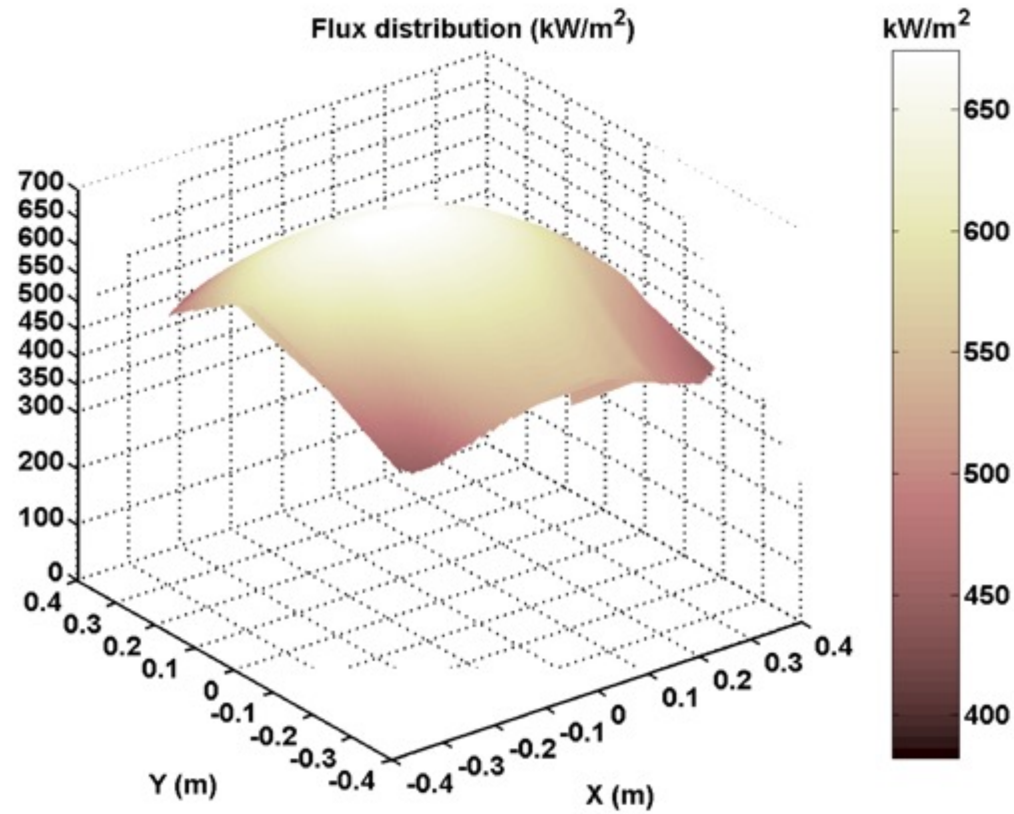

J. Ballestrin, CIEMAT-PSA, « one click flux map »

See also CNRS-PROMES « moving bar » at Themis (B. Grange presentation)

Direct sensors: the others

Pergamon

PII: S0038–092X(01)00105–0

Solar Energy Vol. 72, No. 3, pp. 187–193, 2002

0038-092X/02/$ - see front matter

www.elsevier.com/locate/solener

AN INSTRUMENT FOR MEASURING CONCENTRATED SOLAR-RADIATION: A PHOTO-SENSOR INTERFACED WITH AN INTEGRATING SPHERE

A. FERRIERE[†] and B. RIVOIRE
CNRS-IMP, Centre du four solaire Félix Trombe, BP 5, 66125 Odeillo, France

Received 19 October 2000; revised version accepted 5 November 2001

Communicated by LORIN VANT-HULL

Abstract—The expression of the intensity of light reflected by the internal surface of an integrating sphere with an input power provided by a concentrated solar beam is established using a model of multiple reflection of photons. This intensity appears to be proportional to the input power, and thus makes viable the utilization of a photo-sensor interfaced with an integrating sphere to build a solar fluxmeter. The major parameters of the design of the fluxmeter are then identified, and an optimized design is proposed. An example of a practical instrument is given, and its performance is measured and discussed. The sensitivity of the fluxmeter to the spectral distribution of the solar radiation requires a careful calibration of the gauge in order to achieve a measurement error less than ±5% of reading. © 2002 Elsevier Science Ltd. All rights reserved.

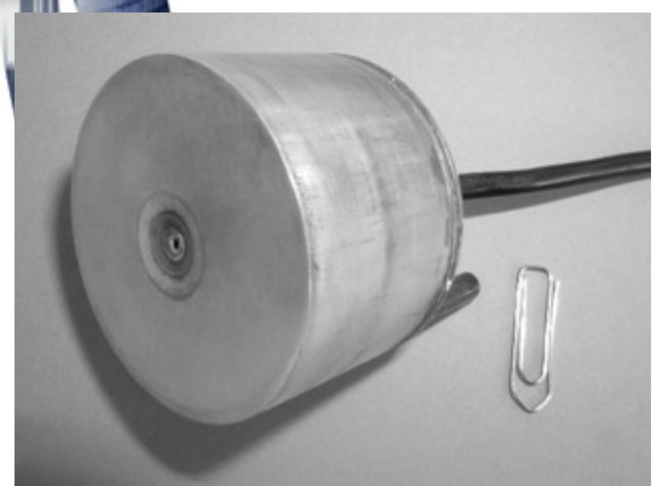

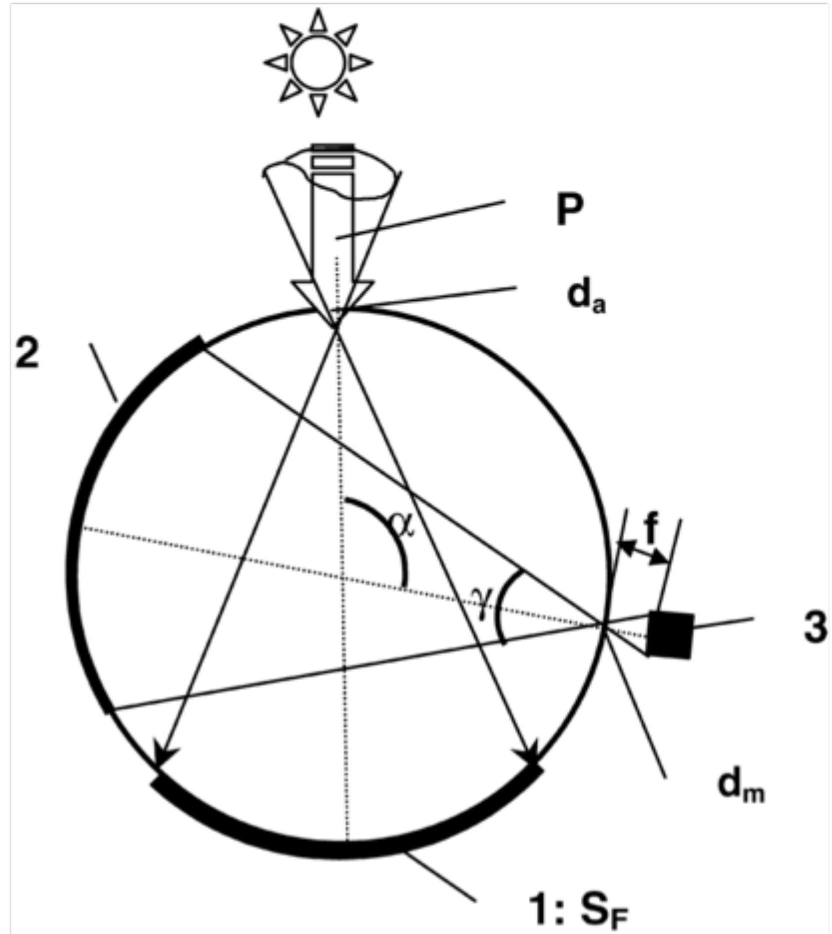

First characterization of the Odeillo Big Solar Furnace in 1970 with a fast moving instrument using a photodiode inside an integrating sphere

Direct sensors: the others

IPDH 10S Integrating sphere

ITDH 100P thermal detector head

Detector head connections

ITDH 100P on stand

Compact Photodiode Head IPDH-10C

Laser powermeters: be careful with the **spectrum** calibration!!!!!

Indirect methods

Indirect methods

- Camera based
- Ray tracing

Indirect method, camera based: main parameters

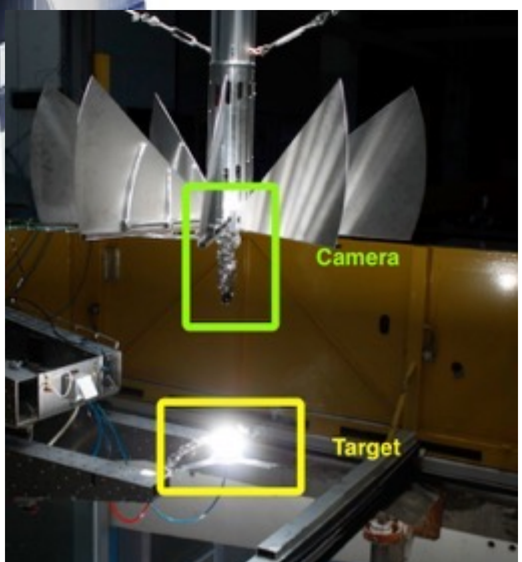

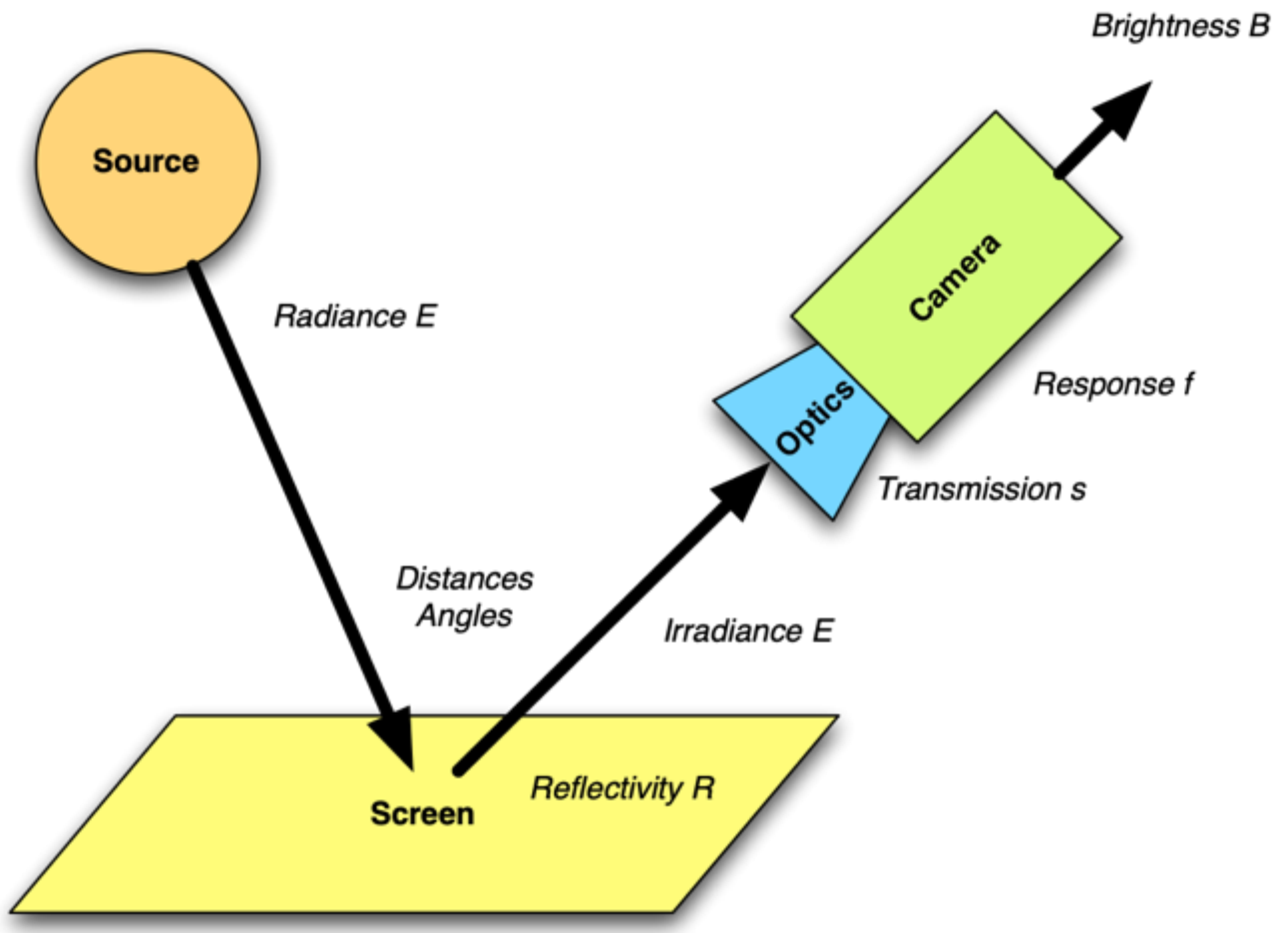

Simplified metrological model of the components required for camera based flux mapping. The calibrations, radiometric and spatial, are not included.

Indirect method, camera based: main parameters

The source, the Sun:

- Spectral issues
- Brightness distribution
- Apparent diameter (CSR)

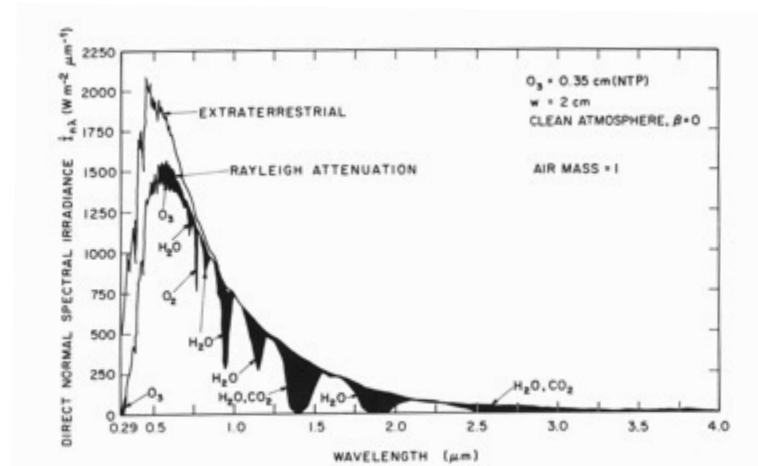

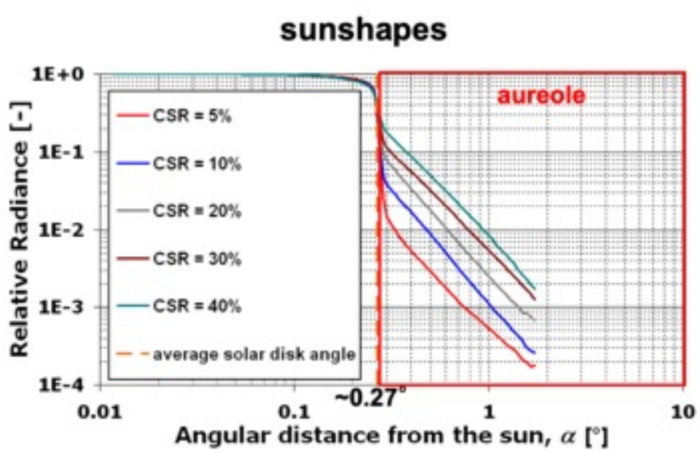

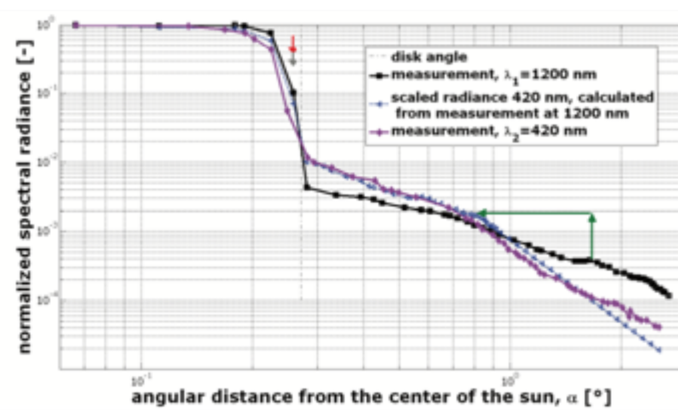

Indirect method, camera based: the target

Usual: PPG Amercoat 741 paint, smoked MgO…

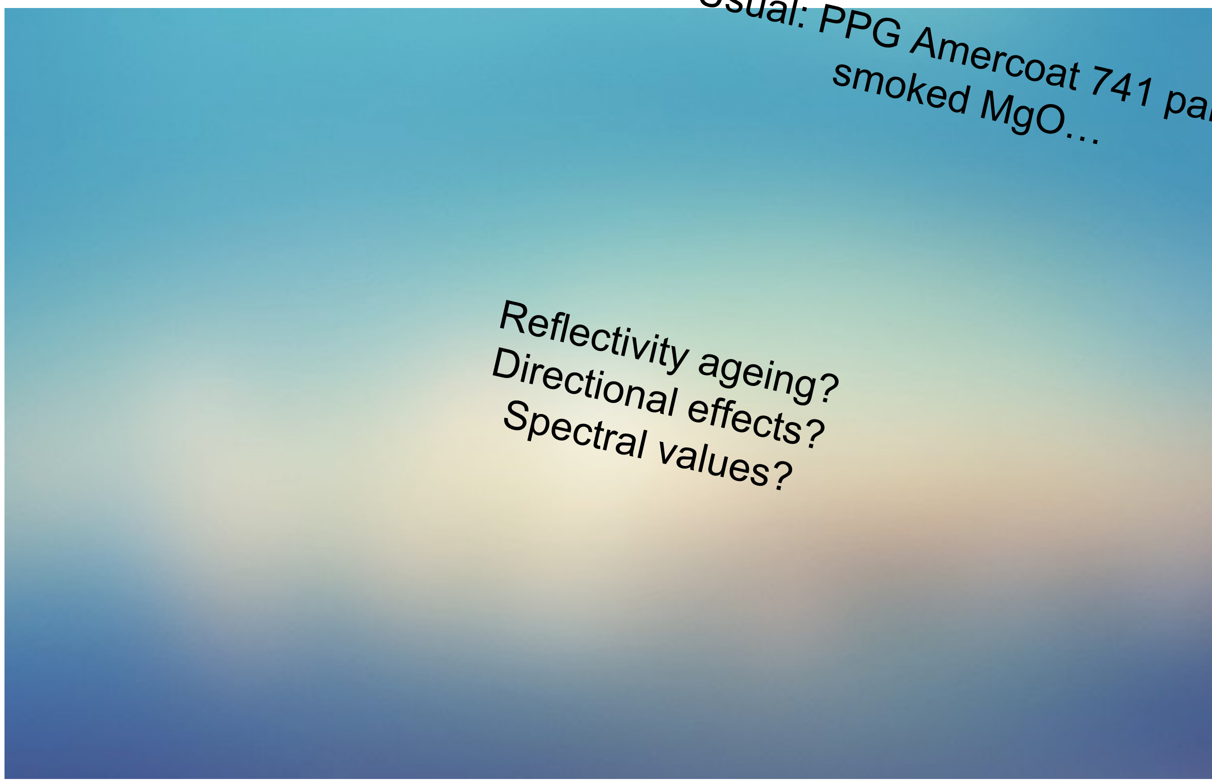

Target reflectivity **infield** characterization:
work in progress…

Indirect method, camera based: the lens and filters: spatial effects

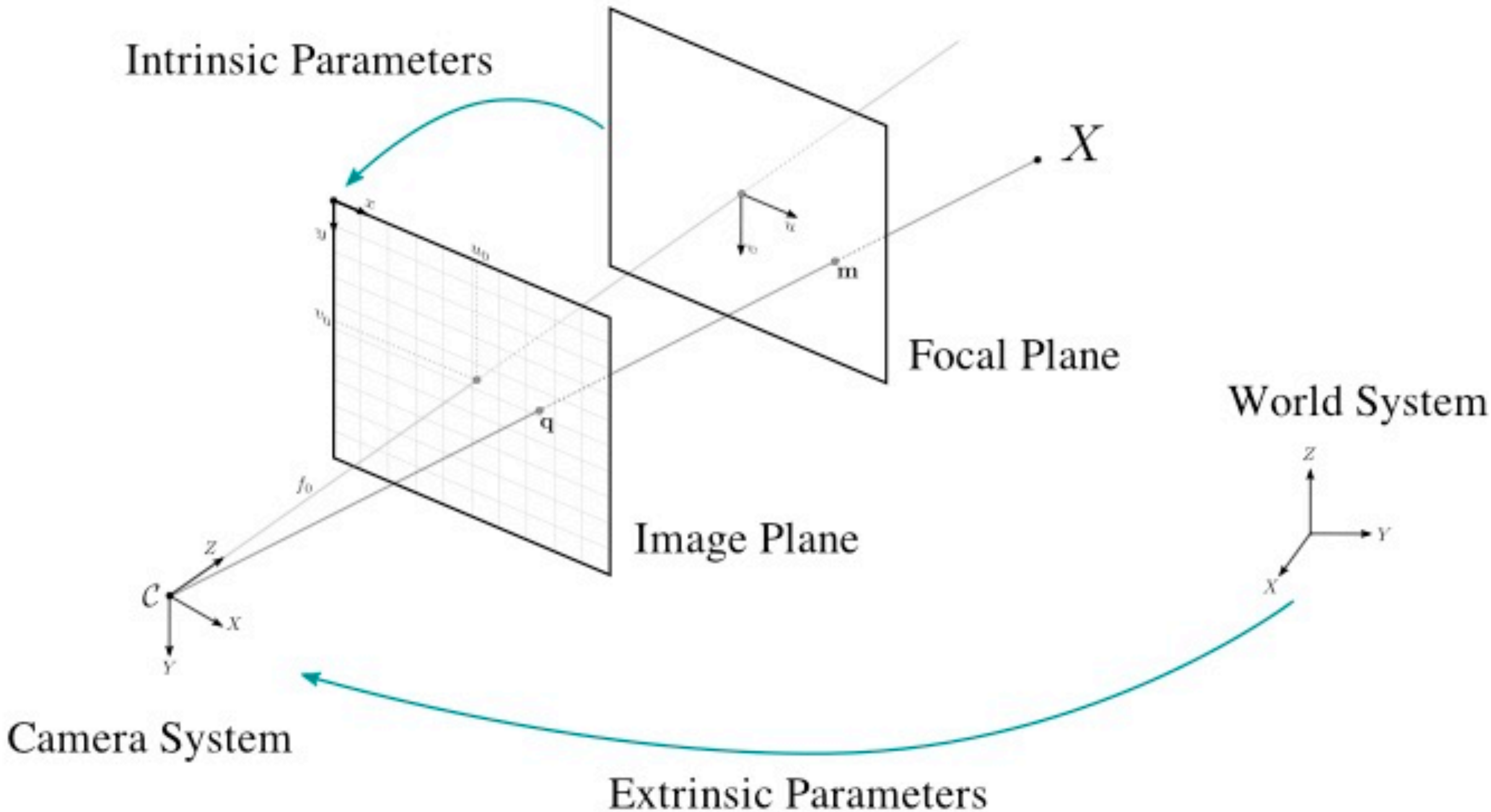

Indirect method, camera based: the lens and filters: intrinsic parameters

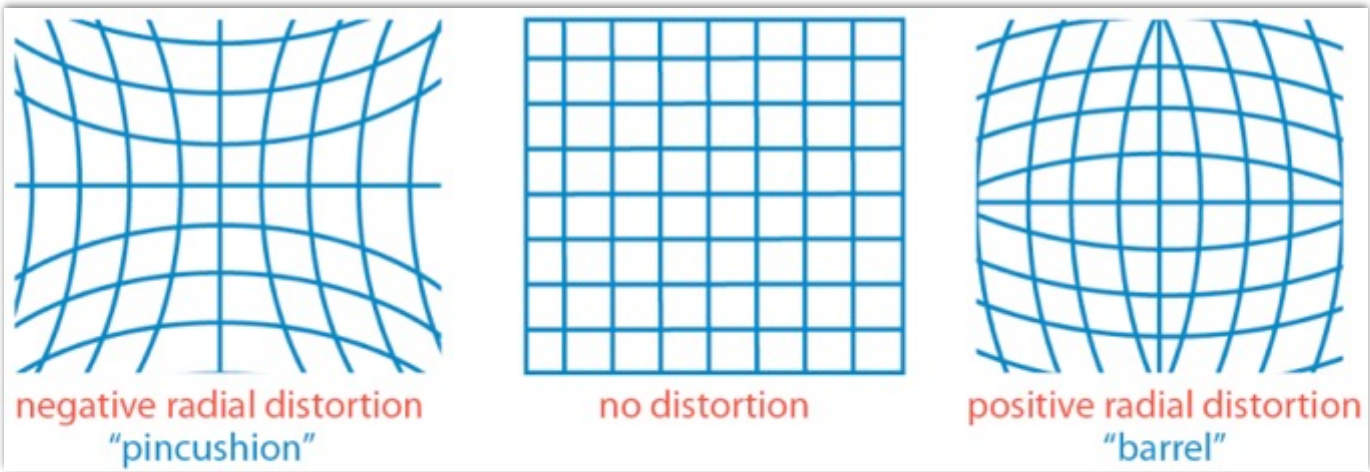

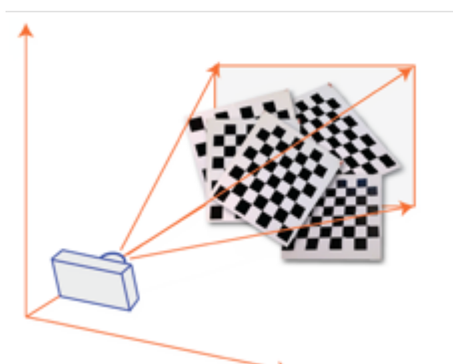

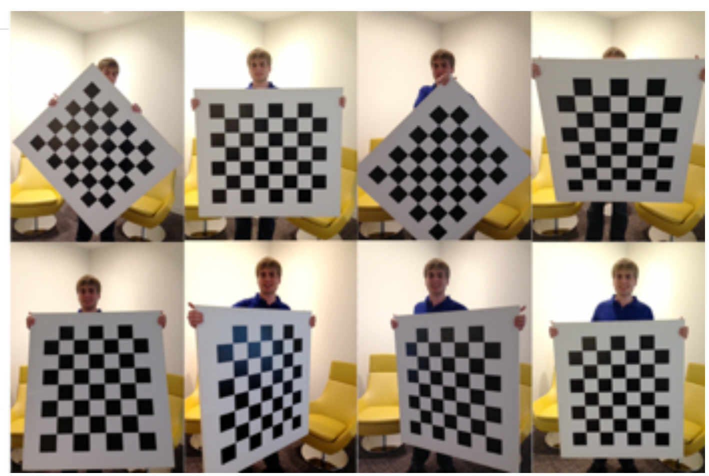

Indirect method, camera based: the lens and filters: extrinsic parameters

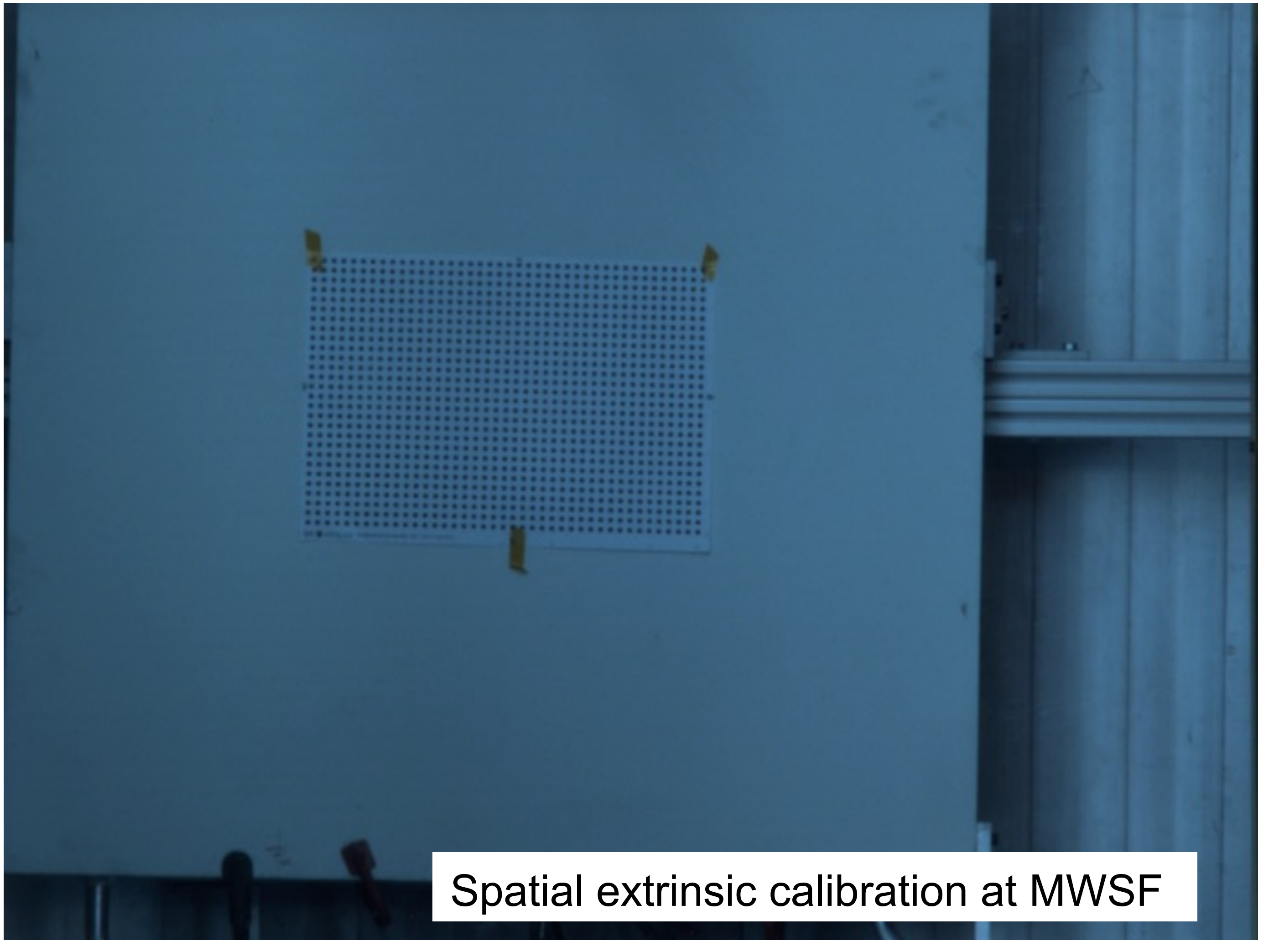

Spatial extrinsic calibration at MWSF

Indirect method, camera based: the lens and filters: radiometric calibration

Darker edges, especially with zoom lenses

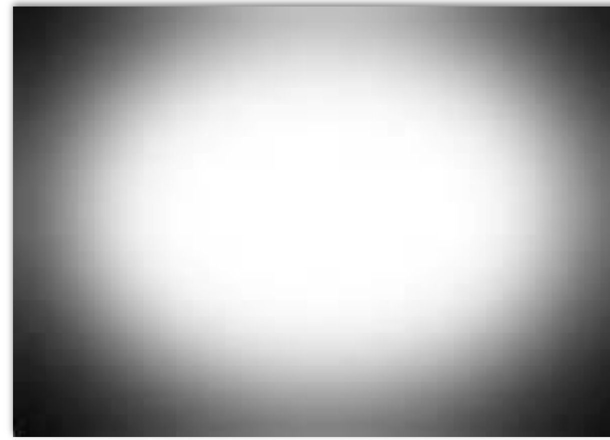

For normal lenses: calibration with a «flat field» picture from a flat box

Indirect method, camera based: main parameters

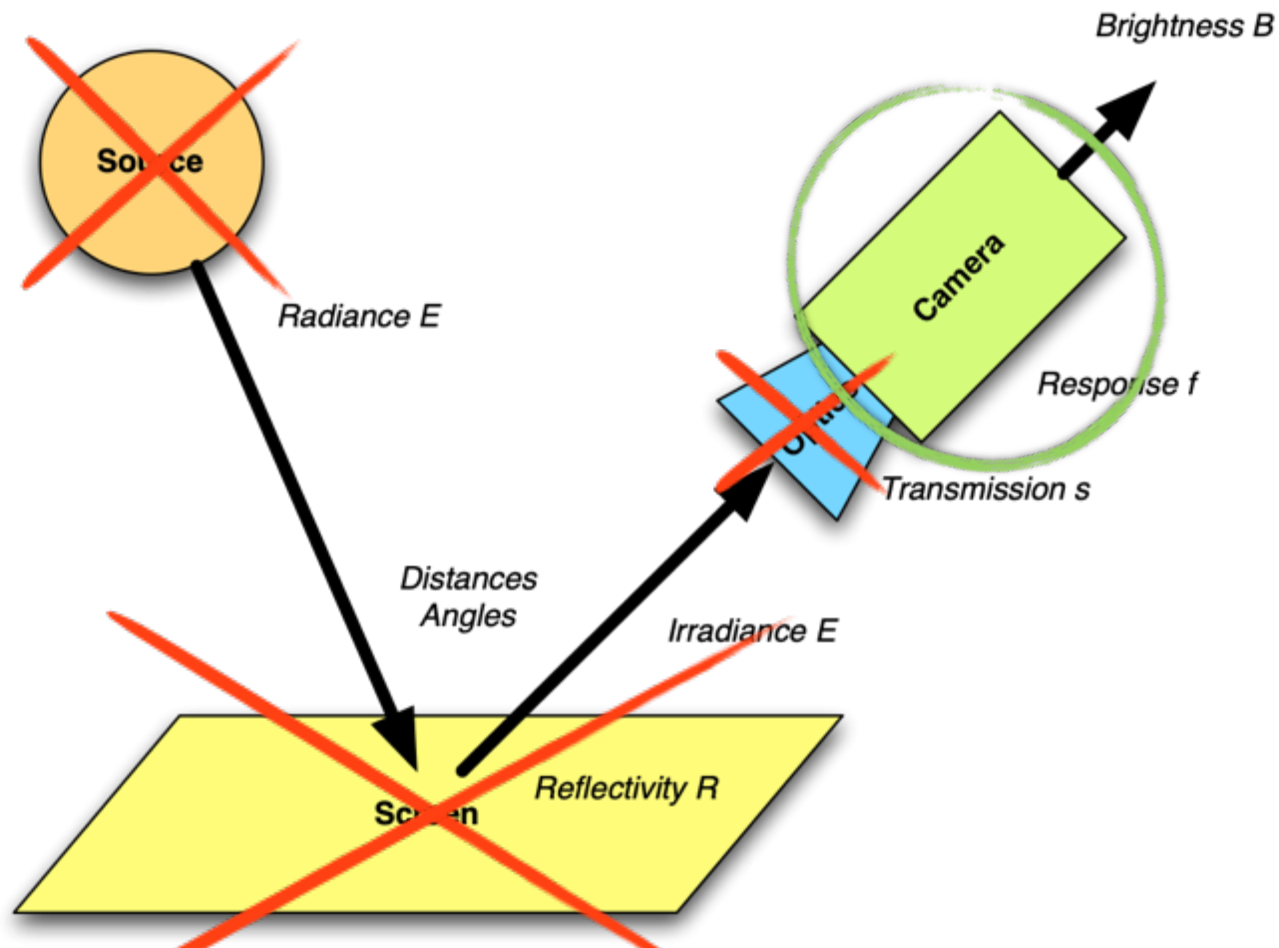

Simplified metrological model of the components required for camera based flux mapping.
The calibrations, radiometric and spatial, are not included.

Indirect method, camera based: camera parameters

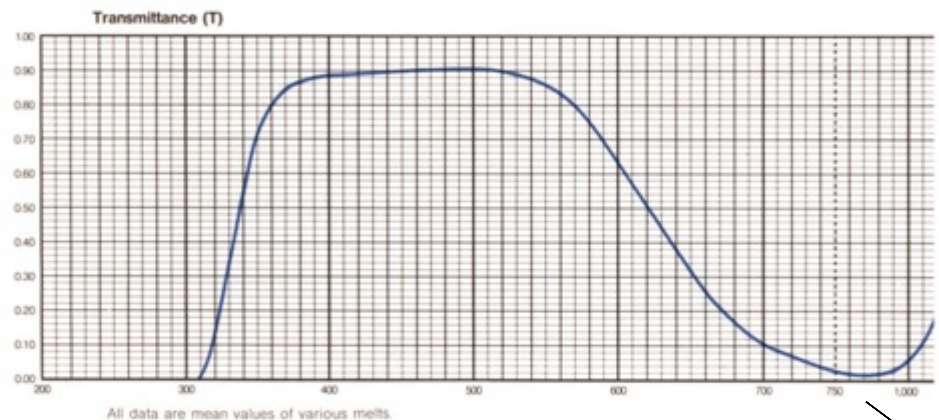

Transmission du filtre IR intégré : Hoya C500

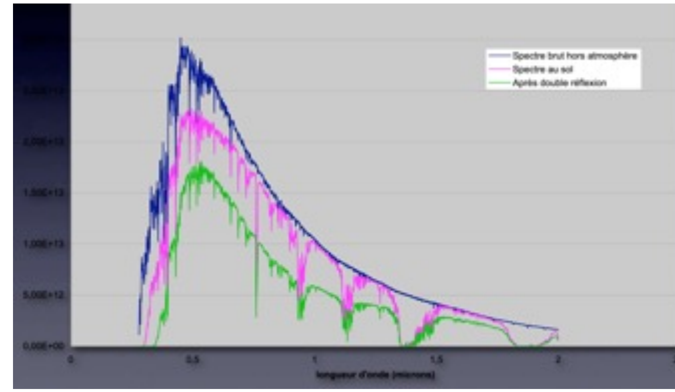

The sun, direct and at focus of CSP

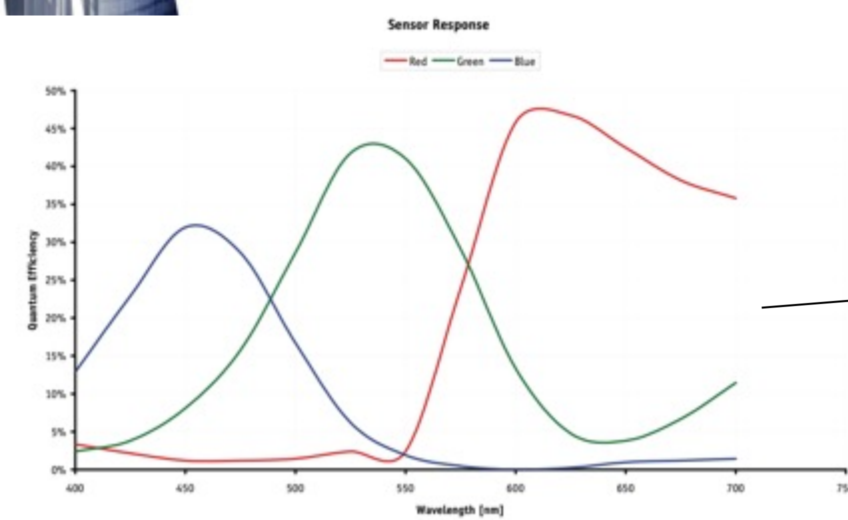

Sensibilité spectrale du détecteur Sony CCD ICX445AQA avec microlentilles EXview HAD

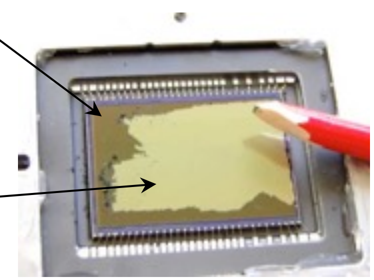

True esp. for all photonic sensors: careful with the absorption spectrum…

Indirect method, camera based: camera parameters

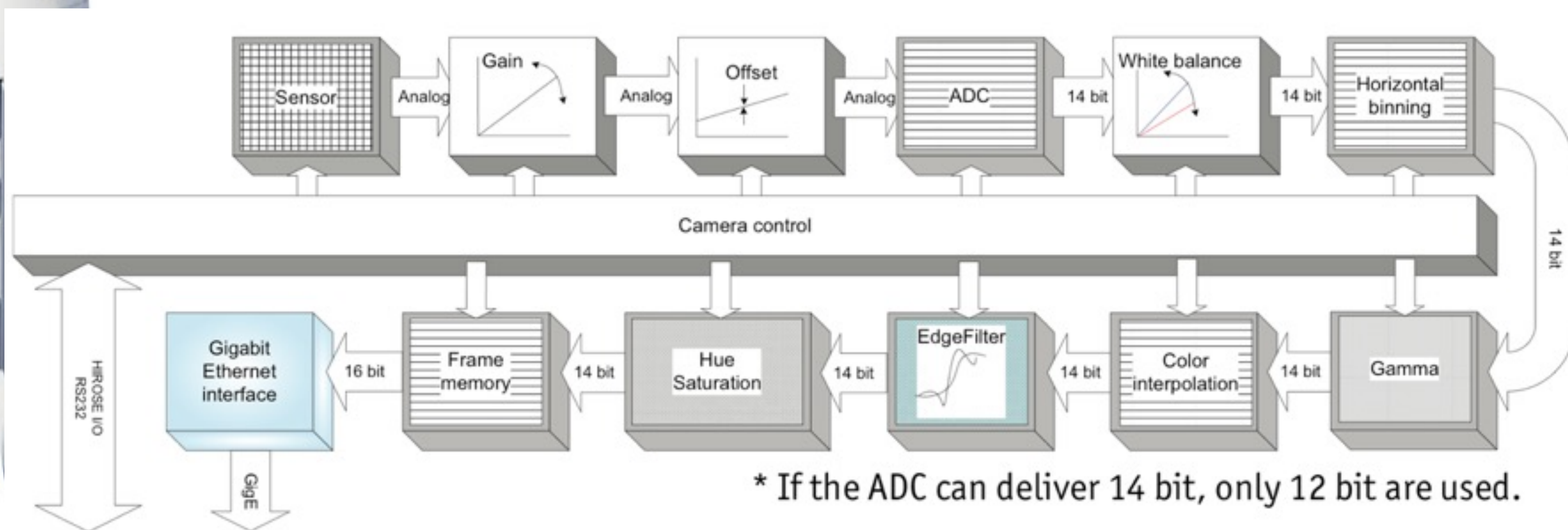

Inside a camera: data path.
And the settings.

Indirect method, camera based: camera parameters

- This was to take a picture.
- Now we need to calibrate its sensitivity using a reference «direct» sensor: calorimeter, radiometer…

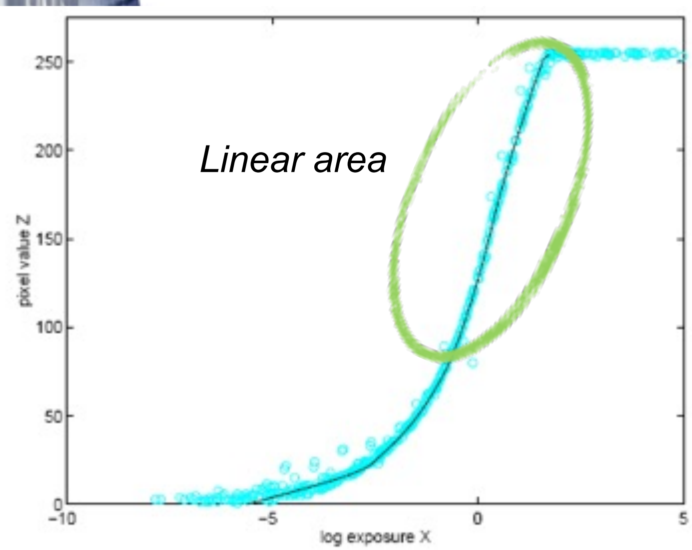

Si sensors are non 100% linear

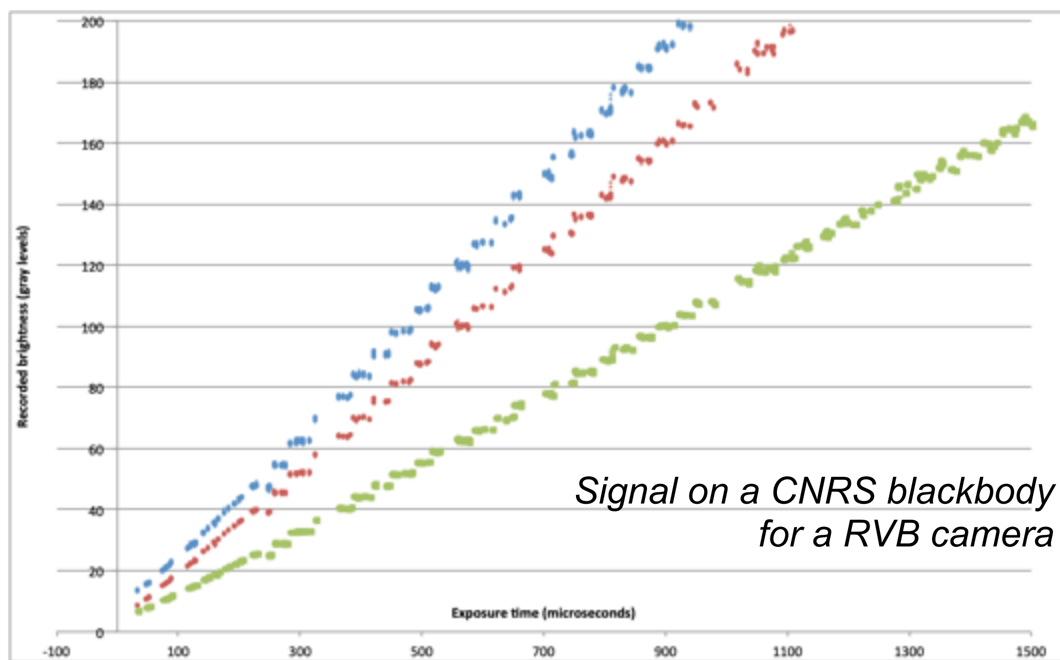

Indirect method, camera based: camera parameters

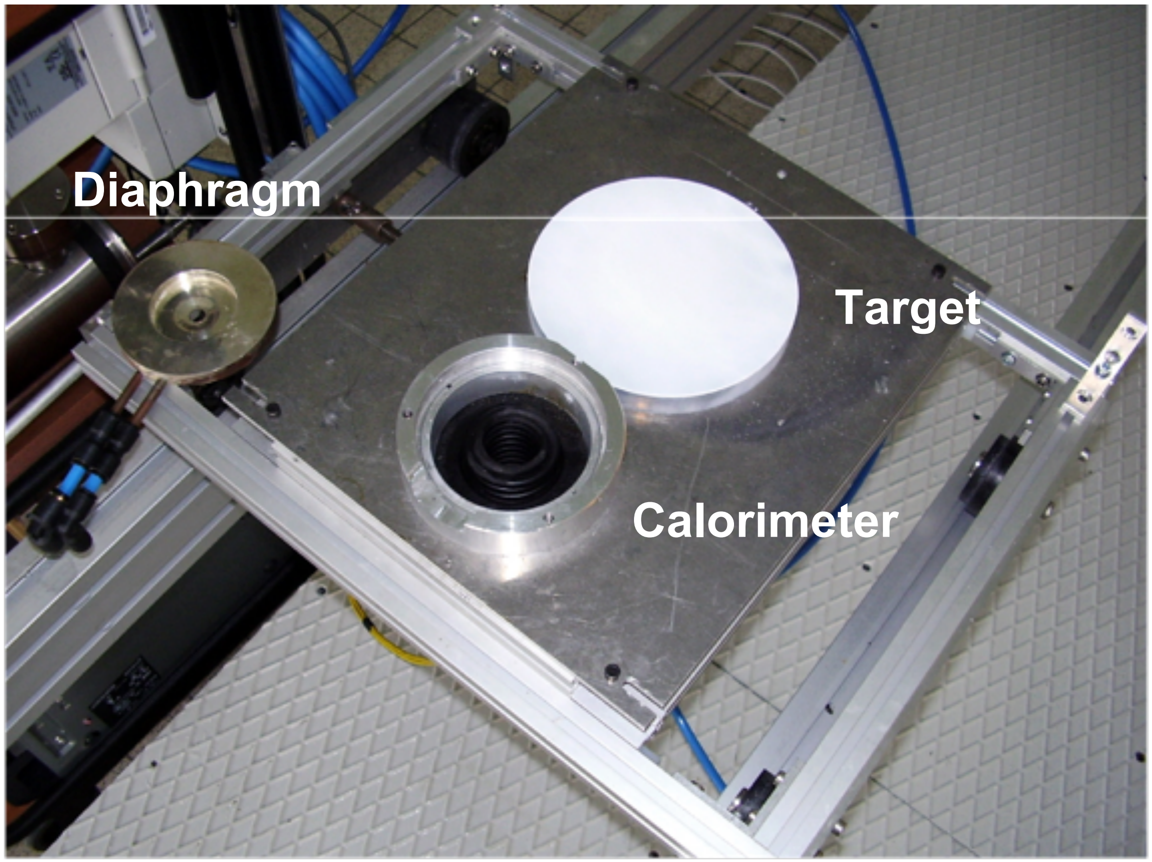

Setup at CNRS MSSF: measuring alternatively calorimeter and camera

Indirect method, camera based: camera parameters

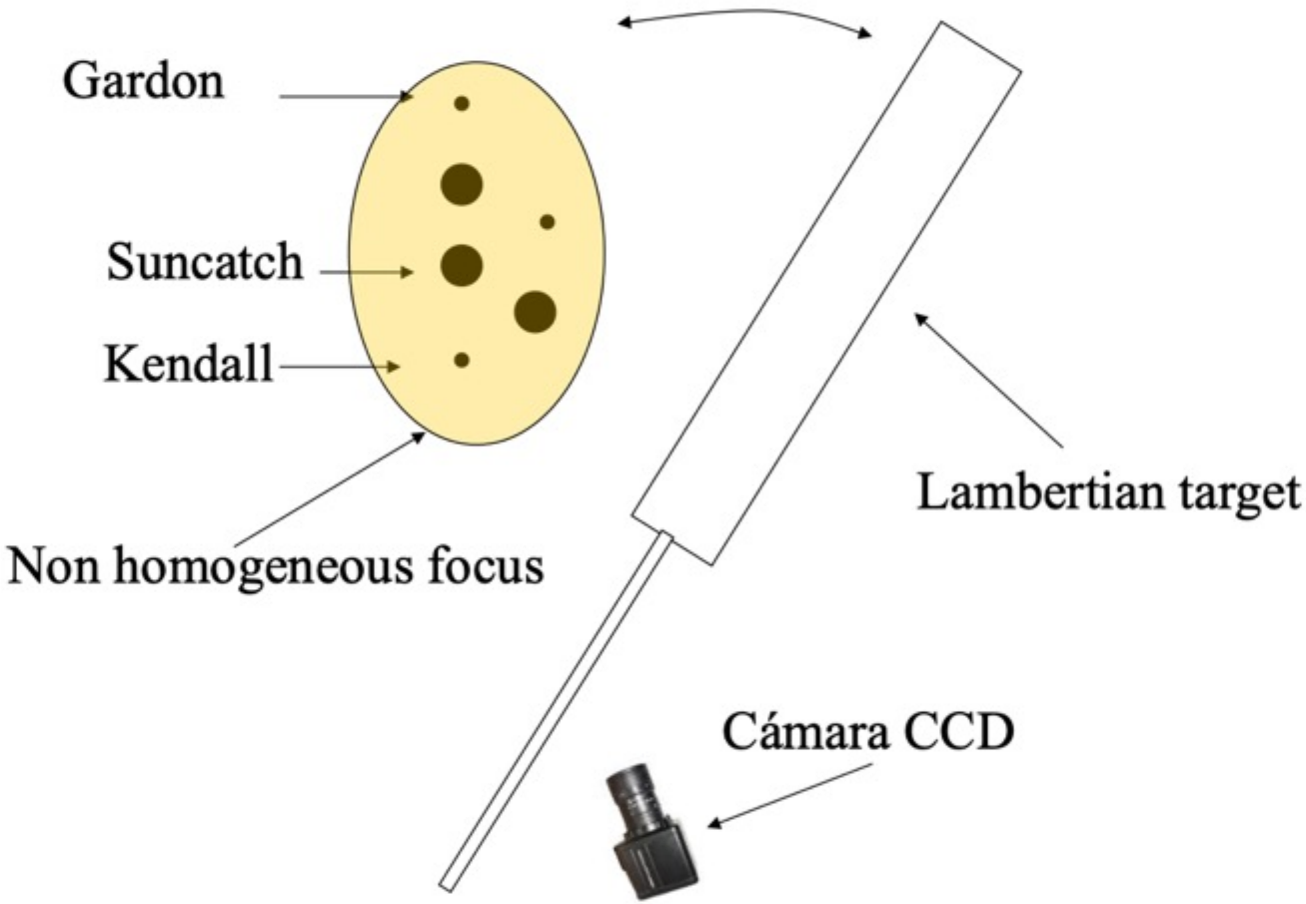

SFERA Intercomp 2012 setup

Indirect method, camera based: main parameters

Post processing:

- Spatial calibration
- Radiometric calibration
- DNI normalisation

=> a lot of 2D calculation of the gray levels

⚠ **numerical losses!!!!** *Typical pictures are 8 bits (per color), but we need at least 16 bits integer, and 32 bits floating point is by far the best.*

=> *Eventually TIFF format with metadata, but rather FITS or HDF5.*

Indirect method, camera based: Measurement process

Calorimeter data

+

Solar data x 2

+

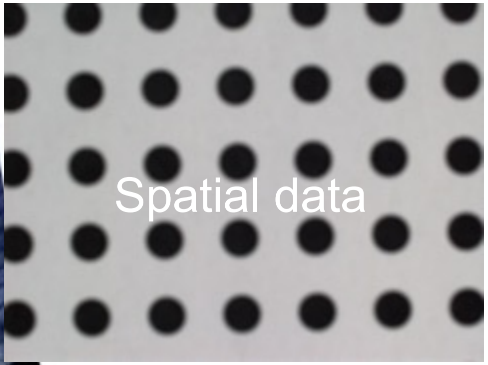

+

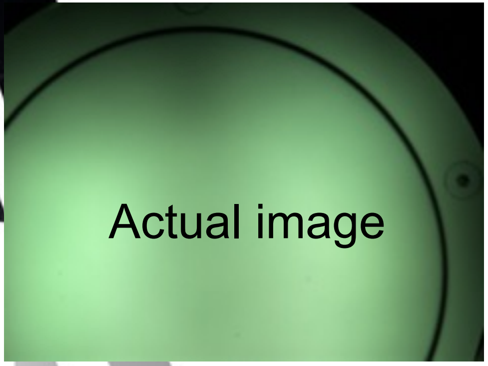

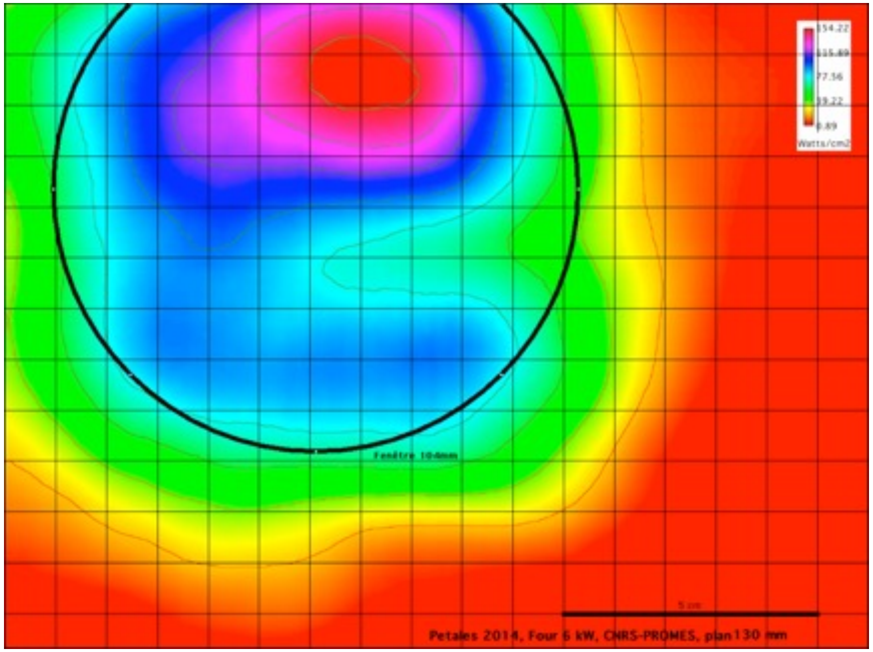

MSSF 6kW 2014

Indirect method, raytracing based

Caclulating fluxmaps:

- Need to know the source
- Need to know the optics: position, optical properties
- Choice of numerical or analytical models

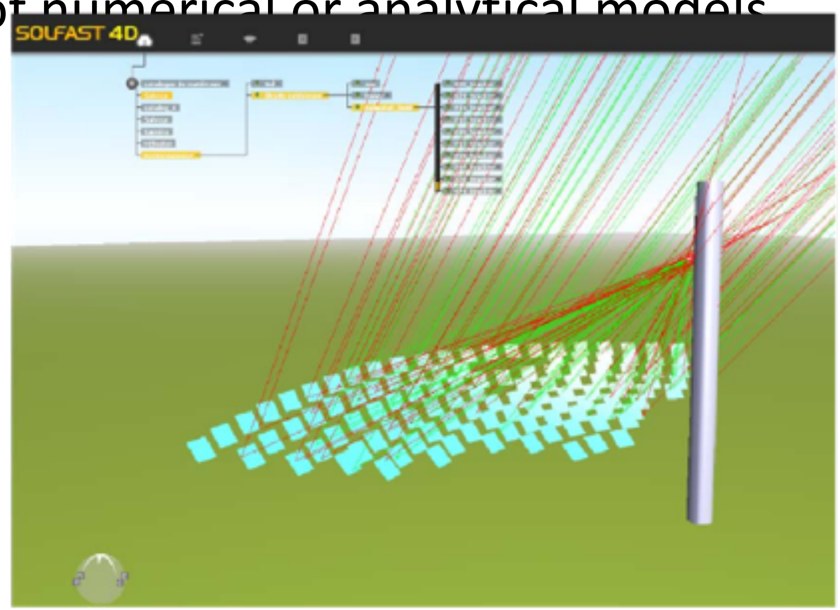

More information

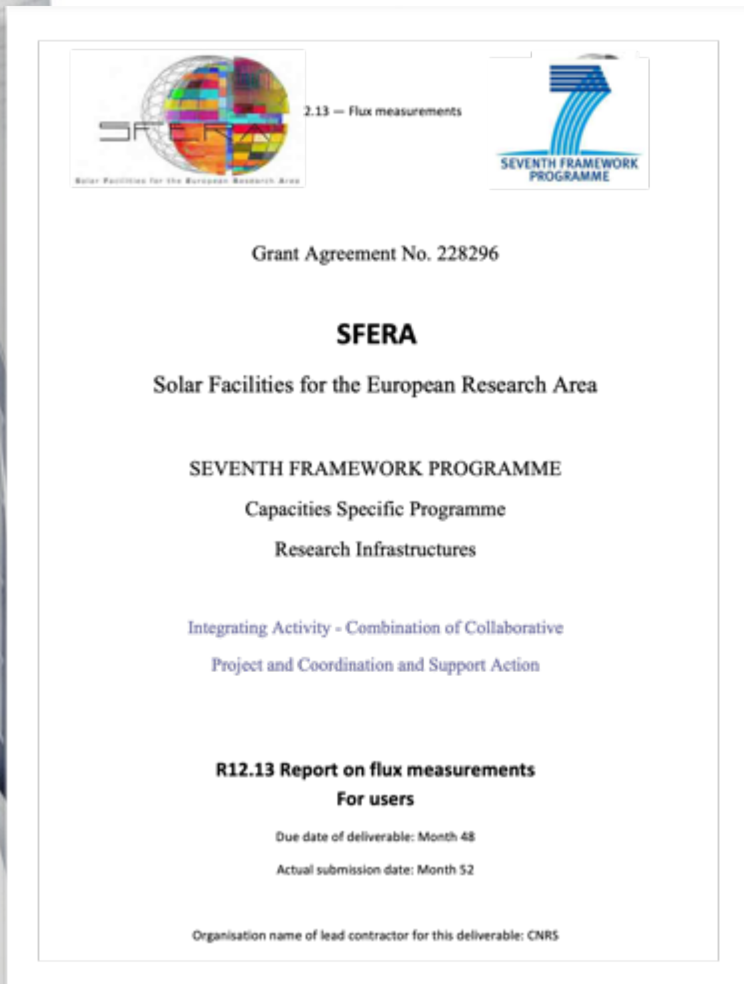
2.13 — Flux measurements

Grant Agreement No. 228296

SFERA

Solar Facilities for the European Research Area

SEVENTH FRAMEWORK PROGRAMME

Capacities Specific Programme

Research Infrastructures

Integrating Activity - Combination of Collaborative

Project and Coordination and Support Action

R12.13 Report on flux measurements
For users

Due date of deliverable: Month 48

Actual submission date: Month 52

Organisation name of lead contractor for this deliverable: CNRS


Grant Agreement No. 228296

SFERA

Solar Facilities for the European Research Area

SEVENTH FRAMEWORK PROGRAMME

Capacities Specific Programme

Research Infrastructures

Integrating Activity - Combination of Collaborative

Project and Coordination and Support Action

R12.4 Guidelines for Testing of CSP components

Due date of deliverable: Month 24

Actual submission date: Month 52

Organization name of lead contractor for this deliverable: DLR

http://sfera.sollab.eu

*SFERA «first», not SFERA-**III***

Measuring

SFERA-III Training Odeillo 2019

LABORATOIRE
PROCÉDÉS, MATÉRIAUX
et ENERGIE SOLAIRE
.UPR 8521 du CNRS.
conventionnée avec
l'université de Perpignan

PROCESSES, MATERIALS
and SOLAR ENERGY
LABORATORY

Emmanuel Guillot
CNRS-PROMES
Odeillo, France

PROMES

UPVD

Solar Facilities for the European Research Area

Solar Facilities for the European Research Area

The SFERA-III project has received funding from the European Union's Horizon 2020 research and innovation programme under grant agreement No 823802.

http://sfera3.sollab.eu/

Plan

- Measuring?
- Part I: Instrumentation
- Part II: Uncertainties
- [Part III: Quality]
- Measurement techniques

Special slide

Some tools should be

simply** defined and **usable

on these slides

Introduction

What is **measuring**?

- …

- …

- …

Introduction

What is **measuring**?

– Determine a **numeric** value of a **physical** parameter in a given set of **conditions**

➢ instrumentation

– With an evaluated **trust** of the numeric value

➢ uncertainties

– With an evaluated **trust** of the procedure

➢ quality

It is a science!

- Instrumentation + Uncertainties = **Metrology**

> ***Metrology*** *is defined by the International Bureau of Weights and Measures (BIPM) as*
> *"the* ***science of measurement****,*
> *embracing both* ***experimental and theoretical*** *determinations*
> ***at any level of uncertainty***
> *in any field of science and technology."*

Part I
Instrumentation

LABORATOIRE
PROCÉDÉS, MATÉRIAUX
et ENERGIE SOLAIRE
.UPR 8521 du CNRS.
conventionnée avec
l'université de Perpignan
PROCESSES,MATERIALS
and SOLAR ENERGY
LABORATORY

Emmanuel Guillot
CNRS-PROMES
Odeillo, France
emmanuel.guillot@promes.cnrs.fr

PROMES

UPVD

SFERA

Solar Facilities for the European Research Area

Instrumentation

MEASURING
IS
COMPARING

Instrumentation

Measuring: determine a numeric evaluation of a physical parameter with a process

- *Primary characteristics: time, length, mass…*
- *Derived characteristics: speed, surface, mass flow, viscosity, specific heat, hardness…*

…

Instrumentation

- Measuring: determine a numeric evaluation of a physical quantity with a process…

- …With comparison to a reference quantity

  => **Number** + **Unit**

What is the length of the car? 4,3 m

What is the temperature of the oil? 235 ° C

What is the DNI? 954 W/m2

Instrumentation

MEASURING
IS
COMPARING

The SI system of units

- 7 units to rule it all:
  - *Temperature* => kelvin (K)
  - *Time* => second (s)
  - *Length* => meter (m)
  - *Mass* => kilogram (kg)
  - *Luminous intensity* => candela (cd)
  - *Quantity of matter* => mole (mol)
  - *Electric current* => ampere (A)

The SI system of units

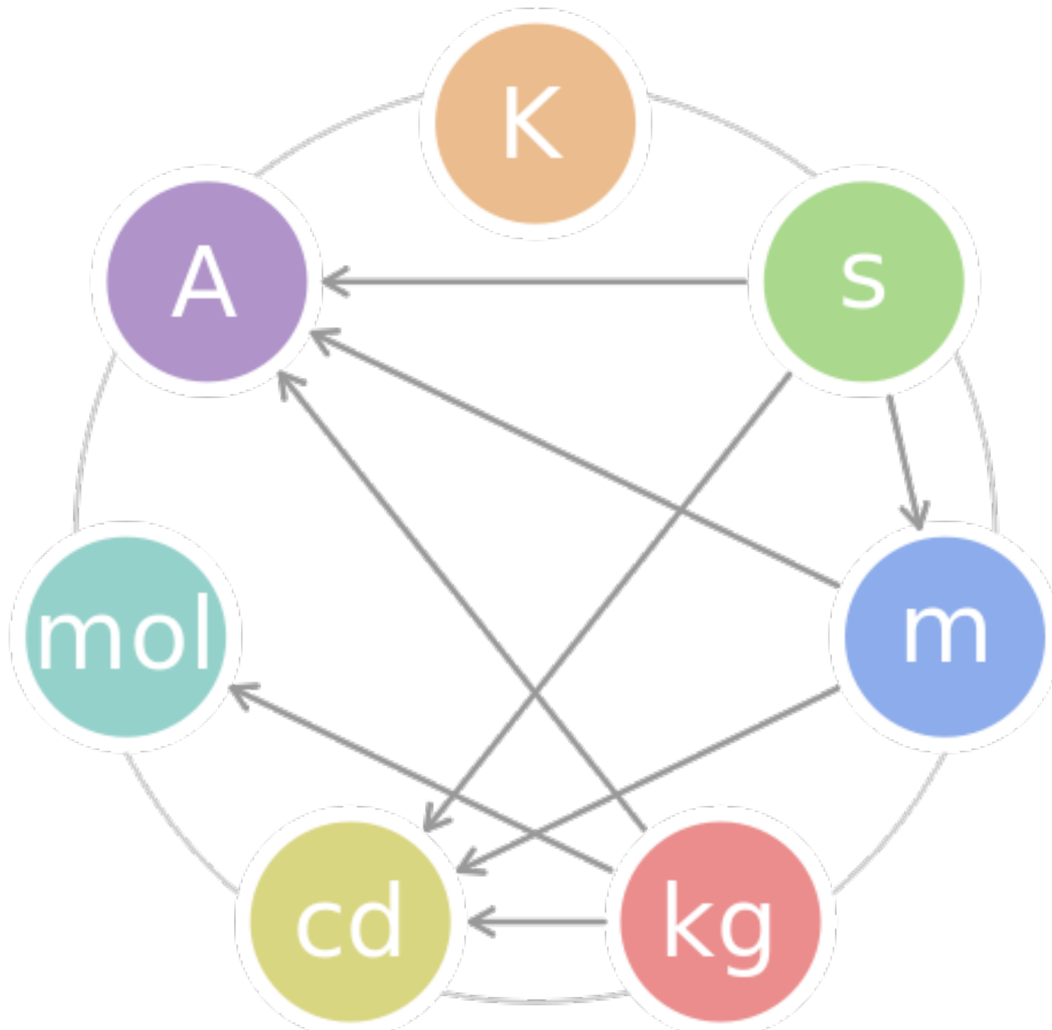

The SI system of units

- Definitions of the units? Universal!
  - It should be stable in time
  - With a repeatable procedure

⇒ Second = number of pulsations of transition state of Cesium

⇒ Meter = distance travelled by light in vacuum in 1 *second*

⇒ Mole = as many as many atoms in 12 mg of Carbon 12

⇒ …

⇒ Kilogram = mass of the International Prototype Kilogram

The SI system of units

- SI = Système International d'unités
- French Revolution: Universal for Mankind
  - including the measurement system
  - still many things in French by France based organizations

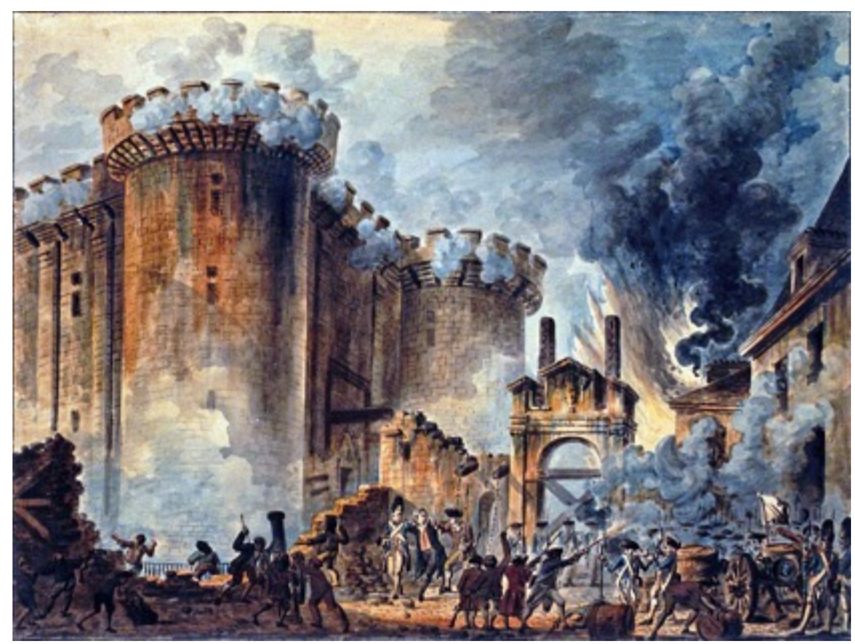

Traceability

MEASURING
IS
COMPARING

Traceability of units

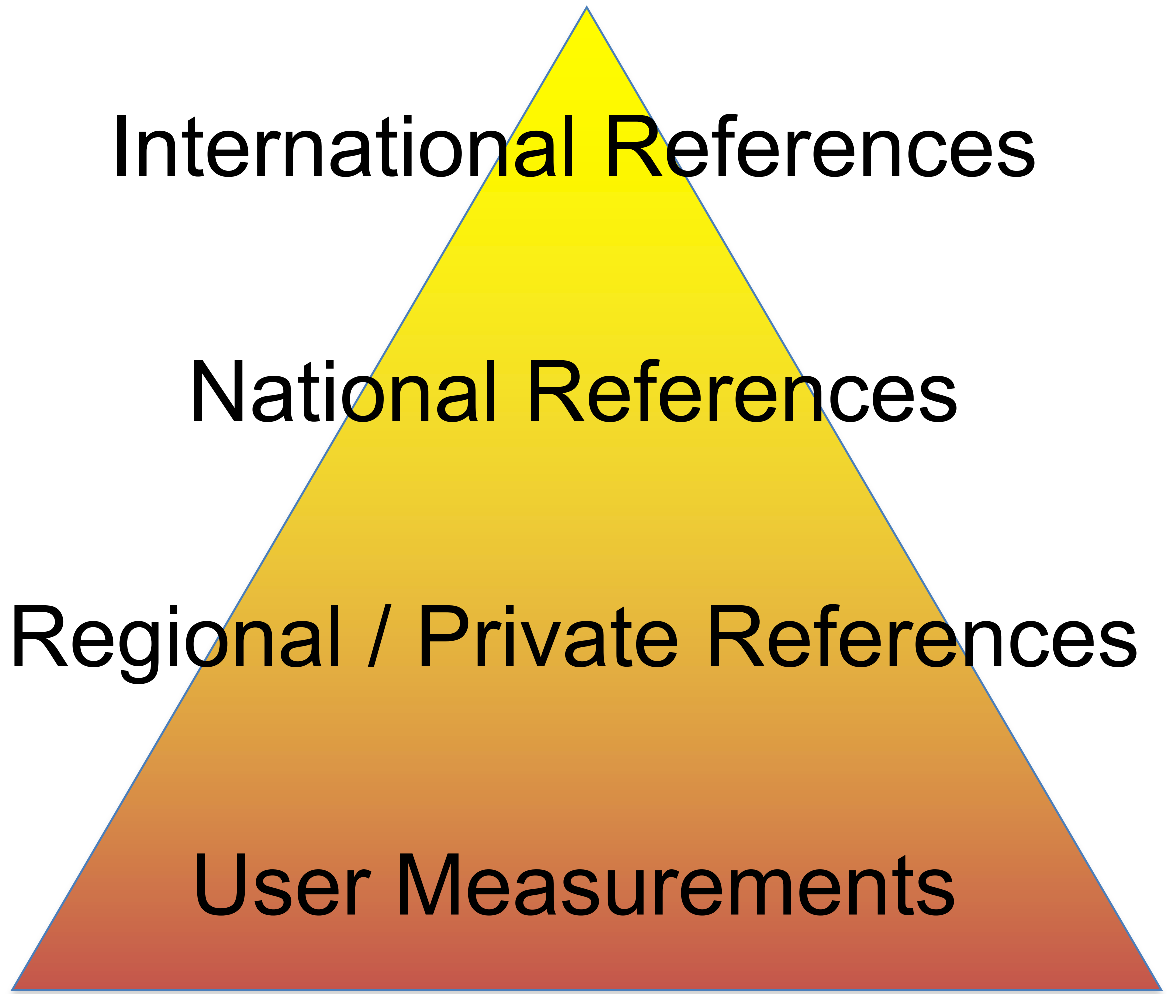

Comparison:
Process of Measurement

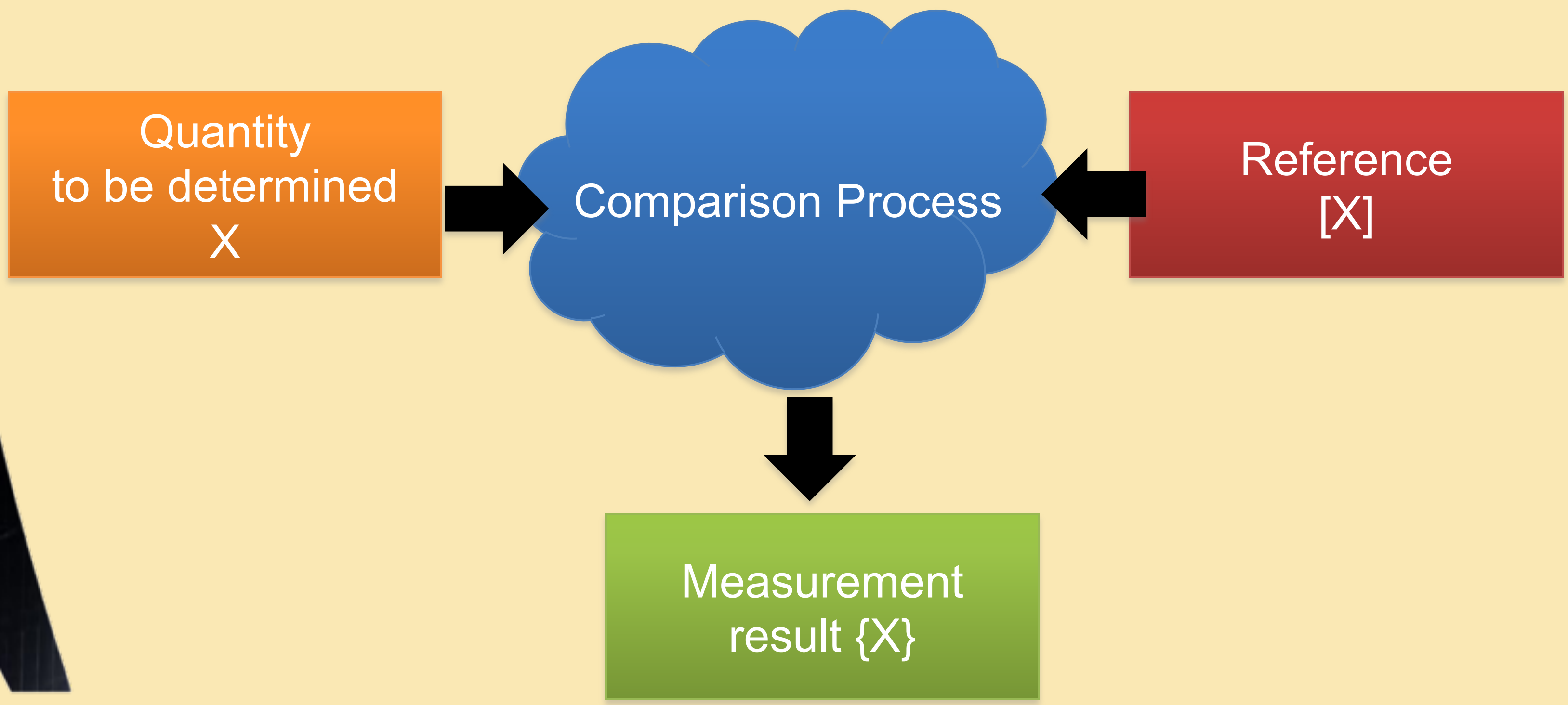

Process of measurement

Direct quantity

***Width* of a rectangle**

width

Process of measurement

Direct quantity

Width of a rectangle

width

Process of measurement

height

Example of indirect quantity

***Surface* of a rectangle**

S = h x w

width

Process of measurement

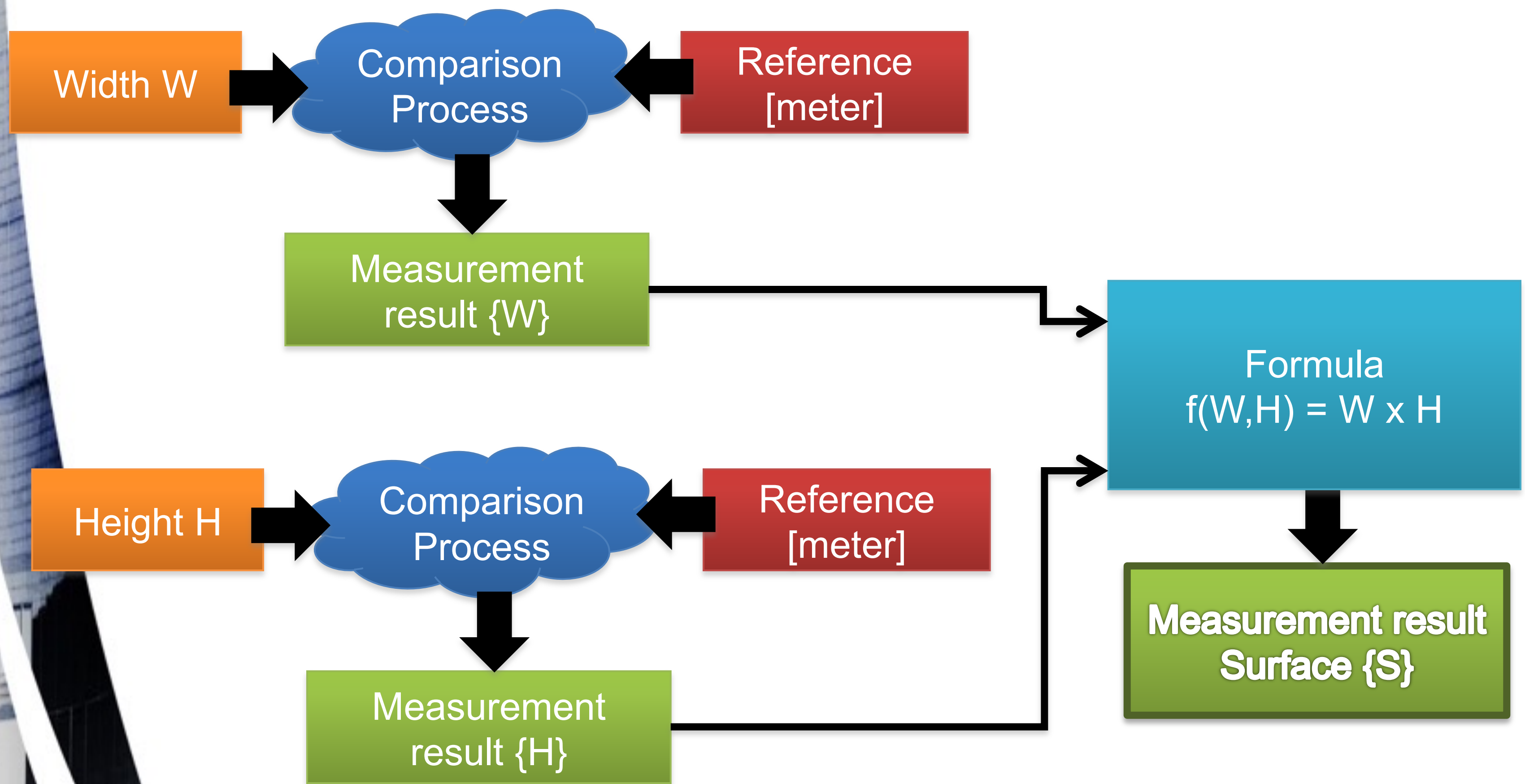

One observation of a measurement

- At the end, a numeric evaluation with a unit

The width of the rectangle is

13,45 cm

The surface of the rectangle is

127 cm^2

Part II
Uncertainties

LABORATOIRE
PROCÉDÉS, MATÉRIAUX
et ENERGIE SOLAIRE
.UPR 8521 du CNRS.
conventionnée avec
l'université de Perpignan
PROCESSES,MATERIALS
and SOLAR ENERGY
LABORATORY

Emmanuel Guillot
CNRS-PROMES
Odeillo, France

PROMES

UPVD

SFERA

Solar Facilities for the European Research Area

Reference

Guide to the expression of
Uncertainty in
Measurement

MEASURING
IS
COMPARING

But how good is the comparison?

How trustworthy is it?

Process of measurement

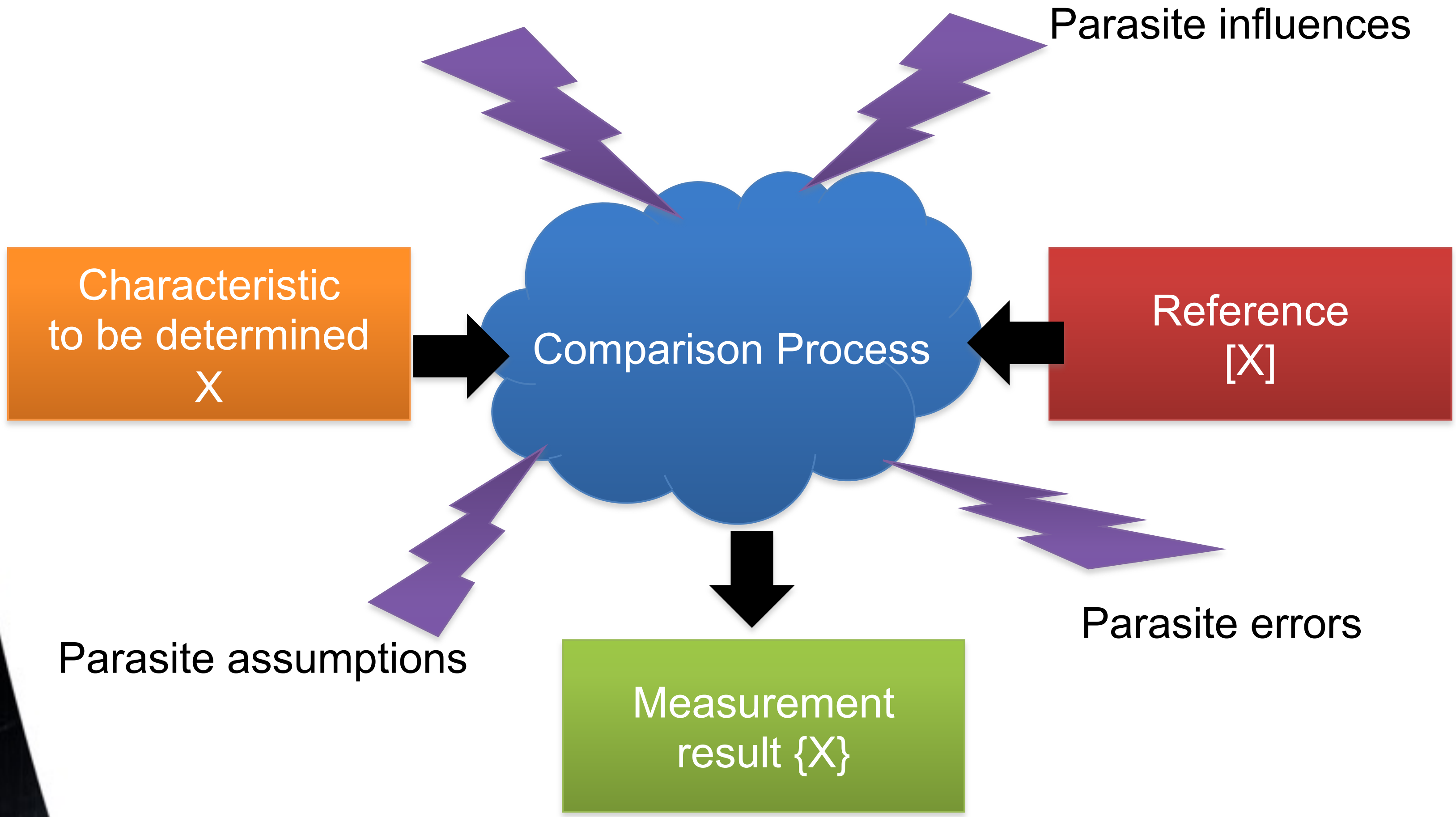

Uncertainties

Provide a **reasonable** *evaluation*
of how much **doubt** we have
about the numeric *evaluation* of the measurement

The Truth Is Out There

Uncertainty

Measurement = number + unit + uncertainty

the length of the truck is

12,5 m ± 0,1 m with 95 % confidence

Is a different measure significant?

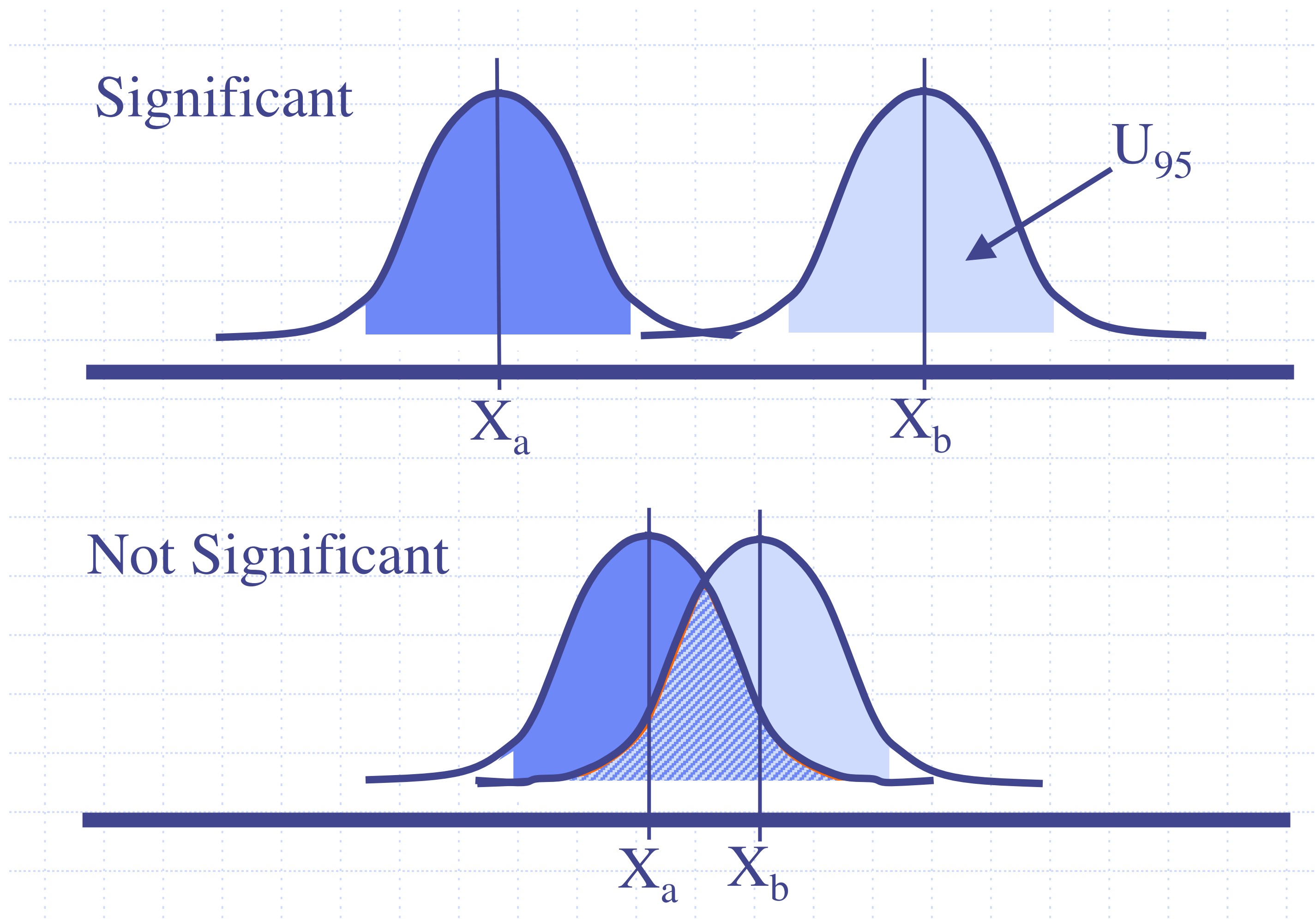

Conformity tests

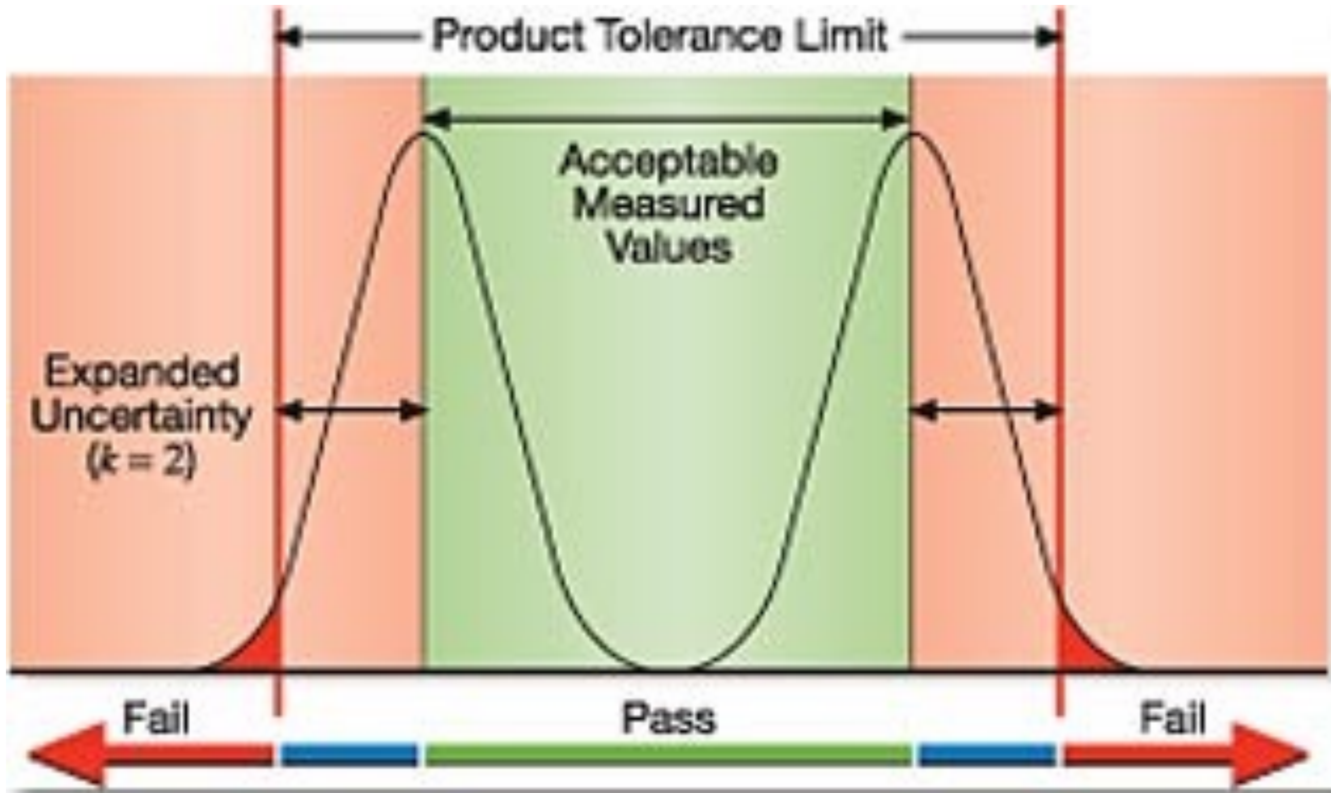

Conformity tests

CSP plant output depends on **receiver temperature**.

Evaluation of the **temperature** depends on:

- **Radiometric** measurements
- **Surface properties**

Evaluation of the radiometric depends on:

- **Atmospheric** conditions
- **Sensor and optical system** calibration

Evaluation of the **surface properties** depends on:

- Status of the **coating**

…

Modelisation of a measurement

{One observed value}

=

(True value)

+

(systematic error)

+

(random error)

Modelisation of a measurement

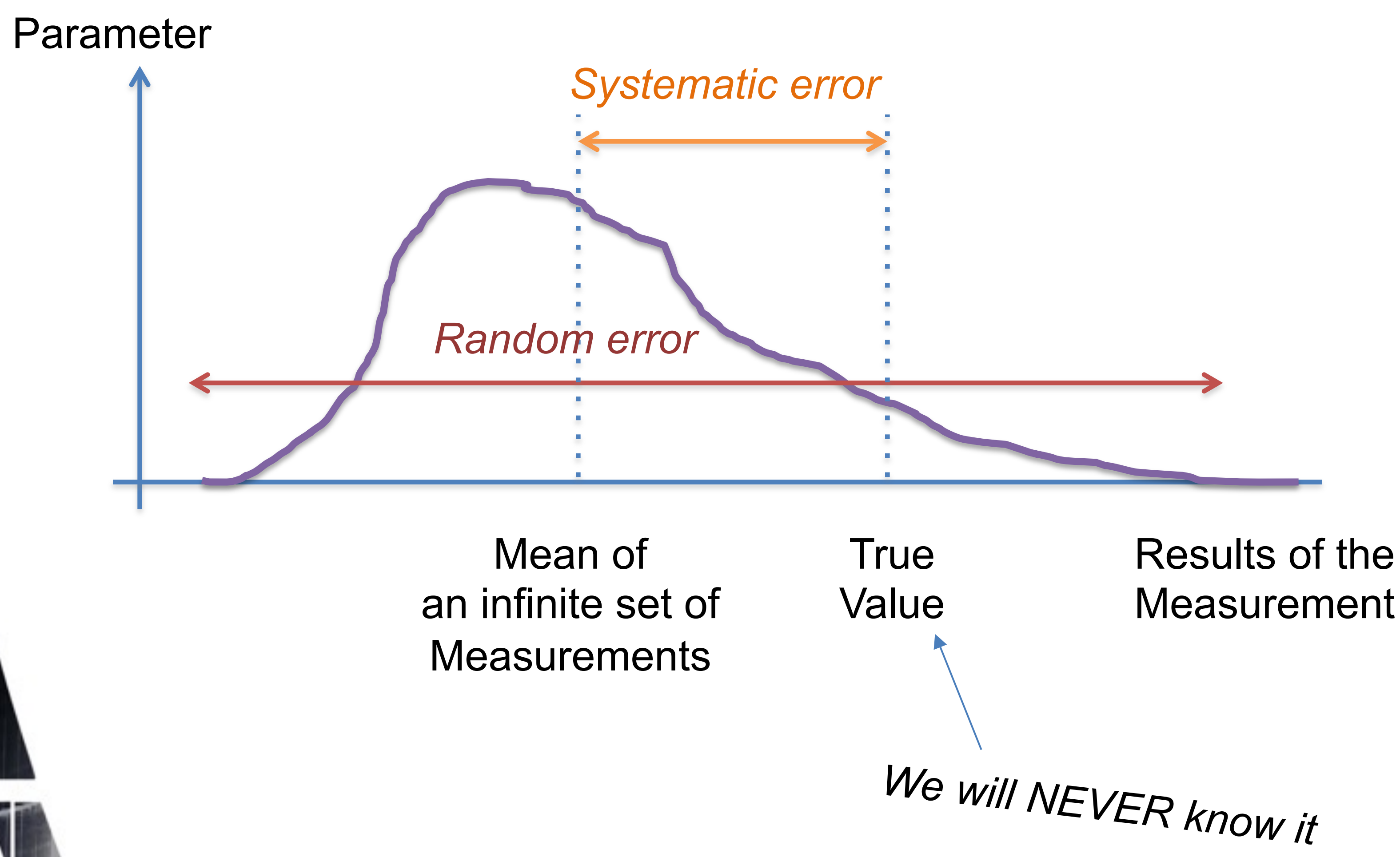

Systematic error

If a **systematic error** arises from a **recognized** effect of an influence quantity on a measurement result,

the effect can be quantified and, if it is significant in size relative to the required accuracy of the measurement,

a **correction** or **a correction factor** can be applied to compensate for the effect.

It is assumed that, after correction, the expectation or expected value of the error arising from a systematic effect is zero.

Systematic error

- Examples:
  - *While measuring a resistance, the connection wires => $R_{observerd} = R_{unknown} + R_{wires}$*
  - *The thermal expansion of a ruler => $L = L_0 + \alpha \cdot \Delta T$*
  - *A systematic bias observed during calibration of the sensor*

Random error

Random error presumably arises from **unpredictable or stochastic temporal and spatial variations** of influence quantities.

The effects of such variations give rise to **variations in repeated observations of the measurand**.

Although it is not possible to compensate for the random error of a measurement result, **it can usually be reduced by increasing the number of observations**; its expectation or expected value is zero.

Uncertainty evaluation

- Systematic errors can be **reduced** with a **correction**

  => *but we only have an estimate of the correction*

- Random error can be **reduced** with a **large number** of observations

  => *effect of the size of the set on the estimate knowledge??*

Uncertainty evaluation

- Method:
  1. Describe the measurement: list all the influence quantities
  2. Determine each influence quantity
  3. Determine the uncertainty for each quantity
  4. Calculate the combined uncertainty
  5. Calculate the expanded uncertainty

Uncertainty evaluation

1. Describe the measurement

Y is determined from N quantities Xi

$$Y = f\left(X_1, X_2, \ldots, X_N\right)$$

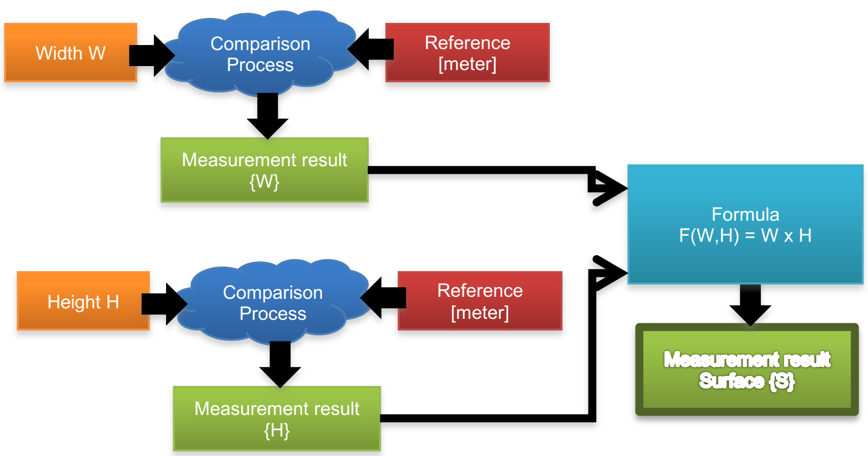

5Ms — Ishikawa — Fishbone

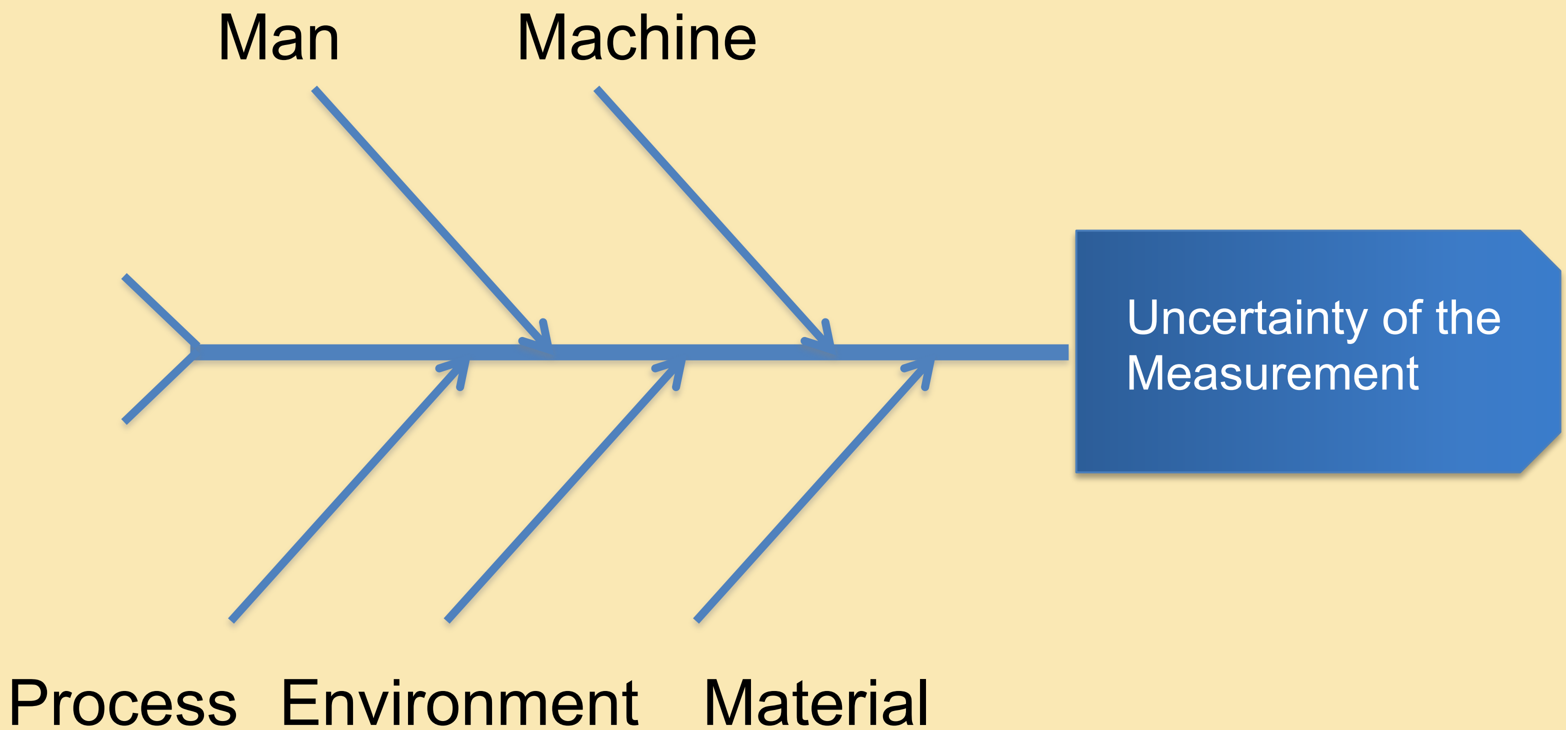

5M — Ishikawa — Fishbone

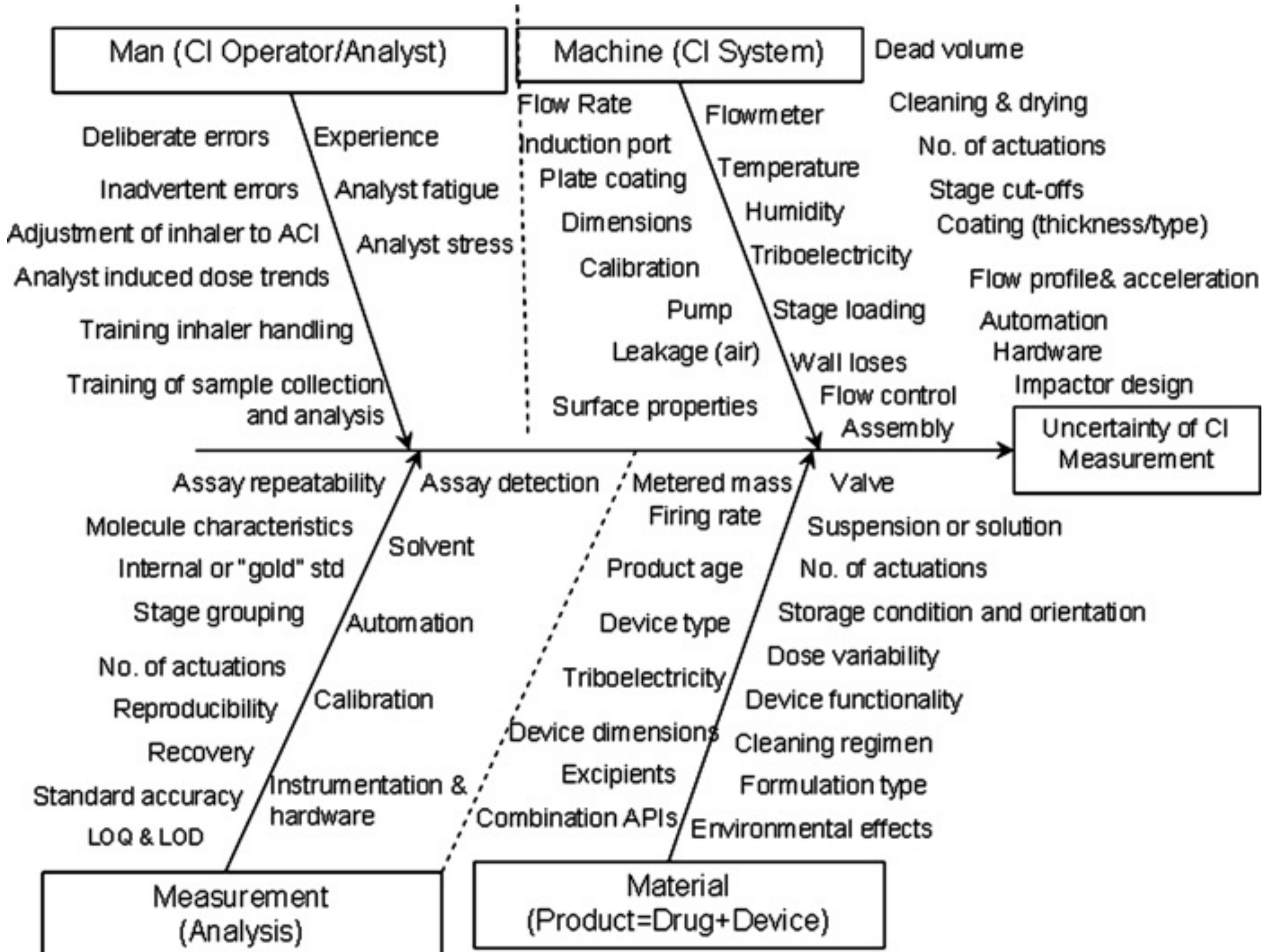

Uncertainty evaluation

- Method:
  1. Describe the measurement: list all the influence quantities
  2. Determine each influence quantity
  3. Determine the uncertainty for each quantity
  4. Calculate the combined uncertainty
  5. Calculate the expanded uncertainty

Uncertainty evaluation

3. Determine the uncertainty for each quantity

=> 2 cases:

- Repeated observations => TYPE A
- Other evaluation => TYPE B

GUM

Uncertainty Type A

If we have *n* repeated observations:

⇒ The best *estimate* of the quantity is the **mean**

$$\bar{q} = \frac{1}{n}\sum_{k=1}^{n} q_k$$

⇒ The best *estimate* of the **uncertainty** is

$$u = s_{\mathrm{p}} / \sqrt{n}$$ with $$s^2(q_k) = \frac{1}{n-1}\sum_{j=1}^{n}\left(q_j - \bar{q}\right)^2$$

Uncertainty Type B

If the quantity is not determined from repeated observations, the uncertainty is evaluated by **scientific judgement** based on **all of the available information** on the possible variability.

Examples:
- manufacturer's specifications
- data provided in calibration and other certificates
- uncertainties assigned to reference data taken from handbooks

Uncertainty Type B

⇒ Use the existing knowledge

⇒ Assume a distribution law of the variations

⇒ Calculate the uncertainty

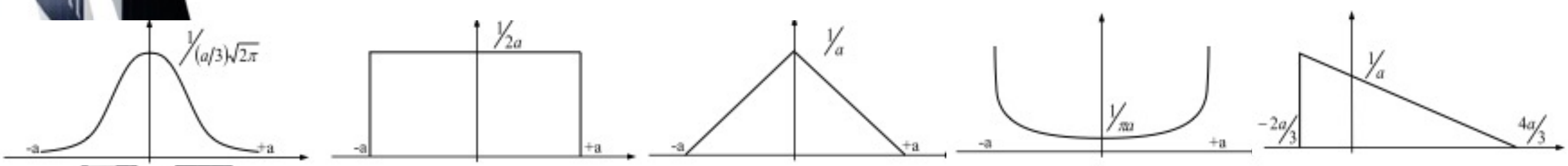

$\frac{a}{\sqrt{3}}$ $\frac{a}{\sqrt{6}}$ $\frac{a}{\sqrt{2}}$ $\frac{a}{\sqrt{4,5}}$

Uncertainty Type B

- For a numeric display ±a
- For a hysteresis ±a

$$u(\mu_t) = a/\sqrt{3}$$

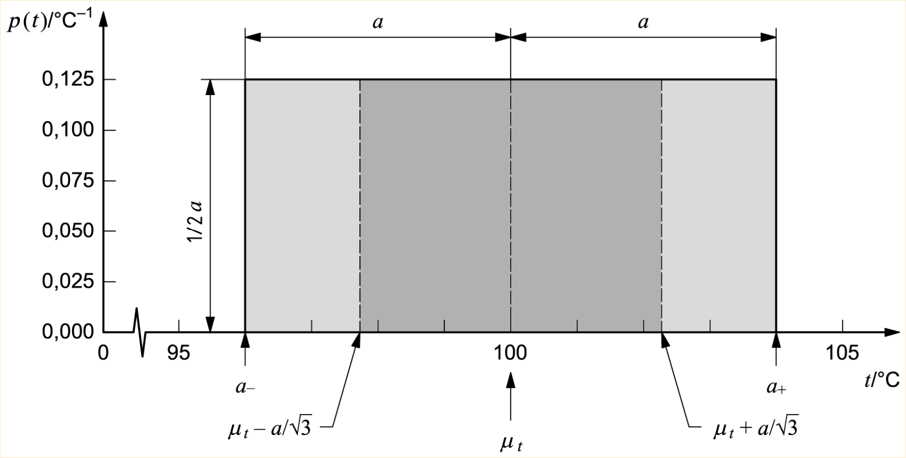

Uncertainty evaluation

- Method:
  1. Describe the measurement: list all the influence quantities
  2. Determine each quantity
  3. Determine the uncertainty for each quantity
  4. Calculate the combined uncertainty
  5. Calculate the expanded uncertainty

Combined uncertainty

- We have the law $Y = f\left(X_1, X_2, \ldots, X_N\right)$
- We have the X_i and their uncertainties

$u = s_{\mathrm{p}} / \sqrt{n}$

$u(\mu_t) = a / \sqrt{3}$

=> The combined uncertainty is (uncorrelated quantities)

$$u_{\mathrm{c}}^2(y) = \sum_{i=1}^{N} \left(\frac{\partial f}{\partial x_i} \right)^2 u^2(x_i)$$

The partial derivatives $\partial f / \partial x_i$ are equal to $\partial f / \partial X_i$ evaluated at $X_i = x_i$

Combined uncertainties

- Example:

  additive measurement of 2 quantities
  with equiprobable distributions

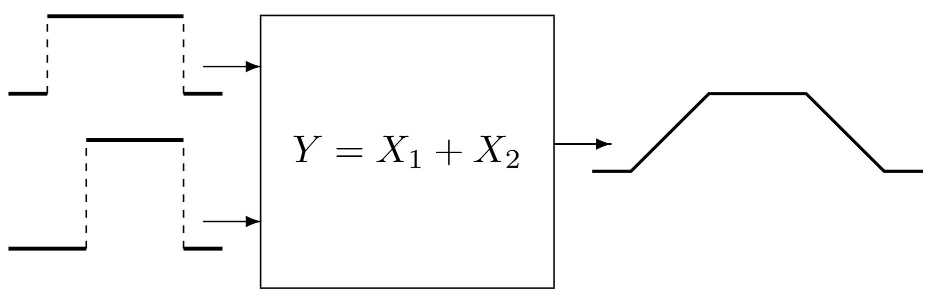

Combined uncertainties

$$u_c^2(y) = \sum_{i=1}^{N}\left(\frac{\partial f}{\partial x_i}\right)^2 u^2(x_i)$$

Sensitivity coefficients

Absolute uncertainty
NOT relative values

Uncertainty evaluation

- Method:
  1. Describe the measurement: list all the influence quantities
  2. Determine each quantity
  3. Determine the uncertainty for each quantity
  4. Calculate the combined uncertainty
  5. Calculate the expanded uncertainty

Expanded uncertainty

- u(Xi) describes the uncertainty
- But we would like to say: *the length is 12,5 m ± 0,1 m <u>with 95 % confidence</u>*

=> Expanded uncertainty ***U***

=> Coverage factor ***k***

$$U = k u_{\mathrm{c}}(y)$$

Expanded uncertainty

Assuming a few things (normal distributions…)

- For 95% confidence ***k* = 2**
- For 99% confidence ***k* = 3**

$$U = k u_c(y)$$

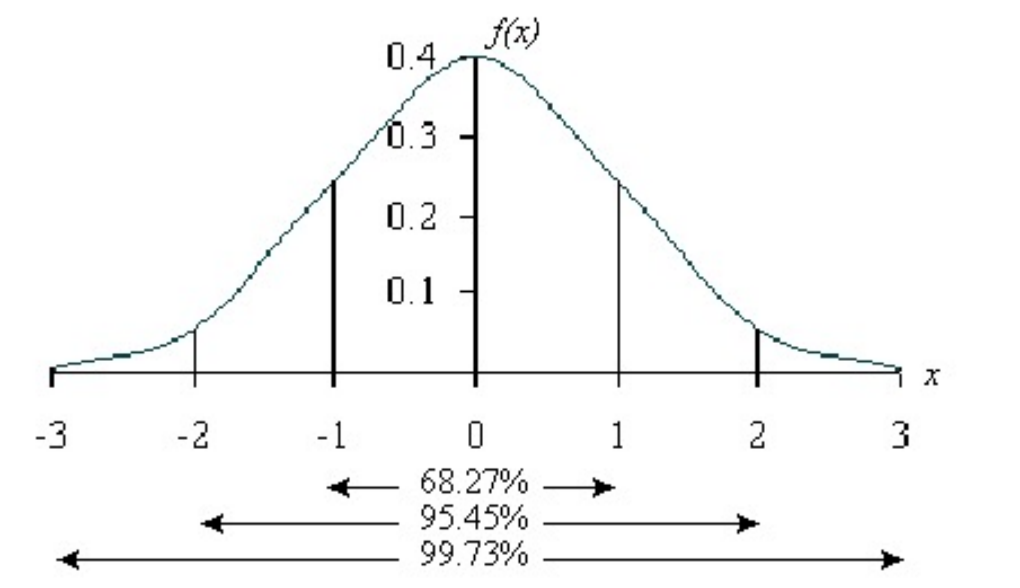

Assumptions for all these

- Normal distributions
- Large number of observations (70-100+)
- No **correlations** between quantities

Measurement techniques

LABORATOIRE
PROCÉDÉS, MATÉRIAUX
et ENERGIE SOLAIRE
.UPR 8521 du CNRS.
conventionnée avec
l'université de Perpignan

PROCESSES,MATERIALS
and SOLAR ENERGY
LABORATORY

Emmanuel Guillot

CNRS-PROMES

Odeillo, France

Solar Facilities for the European Research Area

Instrument properties

- Measurement range
- Linearity — *accuracy of response within range*
- Stability — *short and long term drift*
- Response time
- Accuracy
- Precision
- Hysteresis
- Quantization — *signal and sampling rate*
- Cost — *money, time, complexity*
- …

Measurement range

- How wide is the possible measurement range?
- Examples:
  - Size of a ruler
  - Starting and destruction speed of an anemometer
  - Freezing and boiling points of a thermometer

Linearity

- How many corrections to apply along the measuring range?

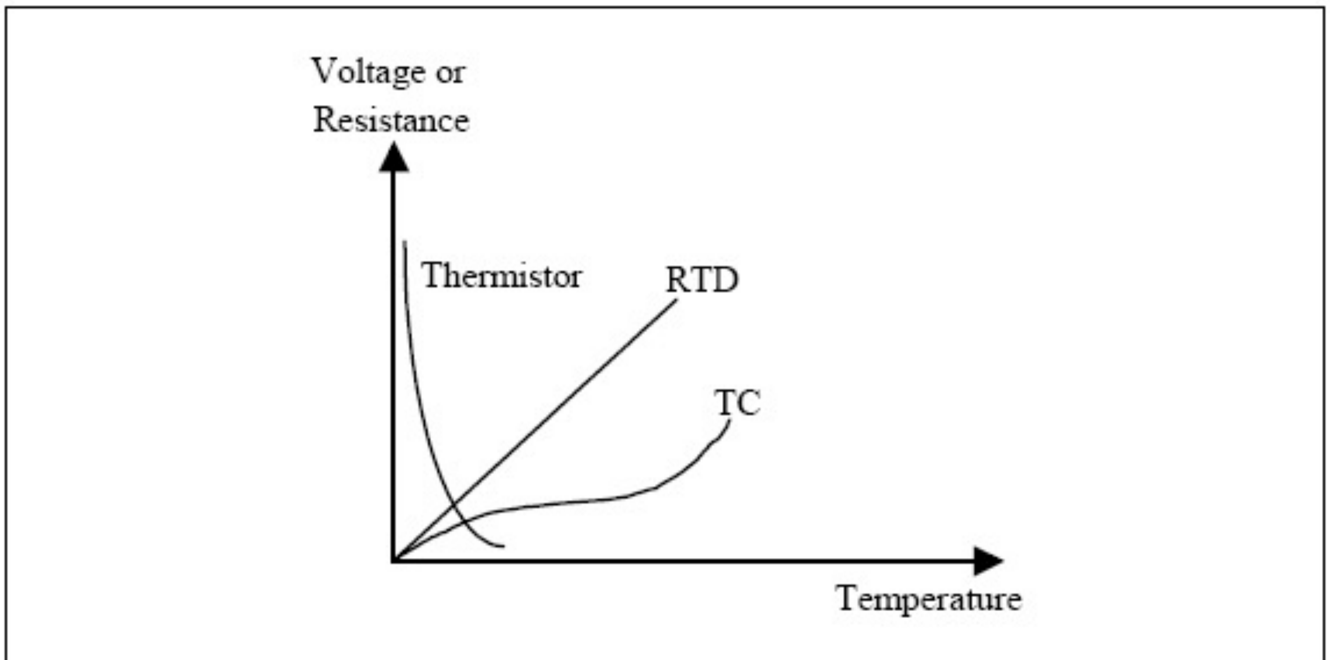

Figure 7-19. Comparison of TC, RTD, and thermistor

Stability

- How much drift of the measurement evaluation:
  - short term
  - long term

  - Example for a temperature measurement by thermocouple:
    - Short term drift: thermal sensitivity of the ADC
    - Long term drift: chemical alteration of the TC

Repeatibility and Reproductibility

Repeatability

Variability on an occasion

With-in run precision

Reproducibility

Variability on different occasions

Between-run precision

Response time

- How fast the output signal changes?

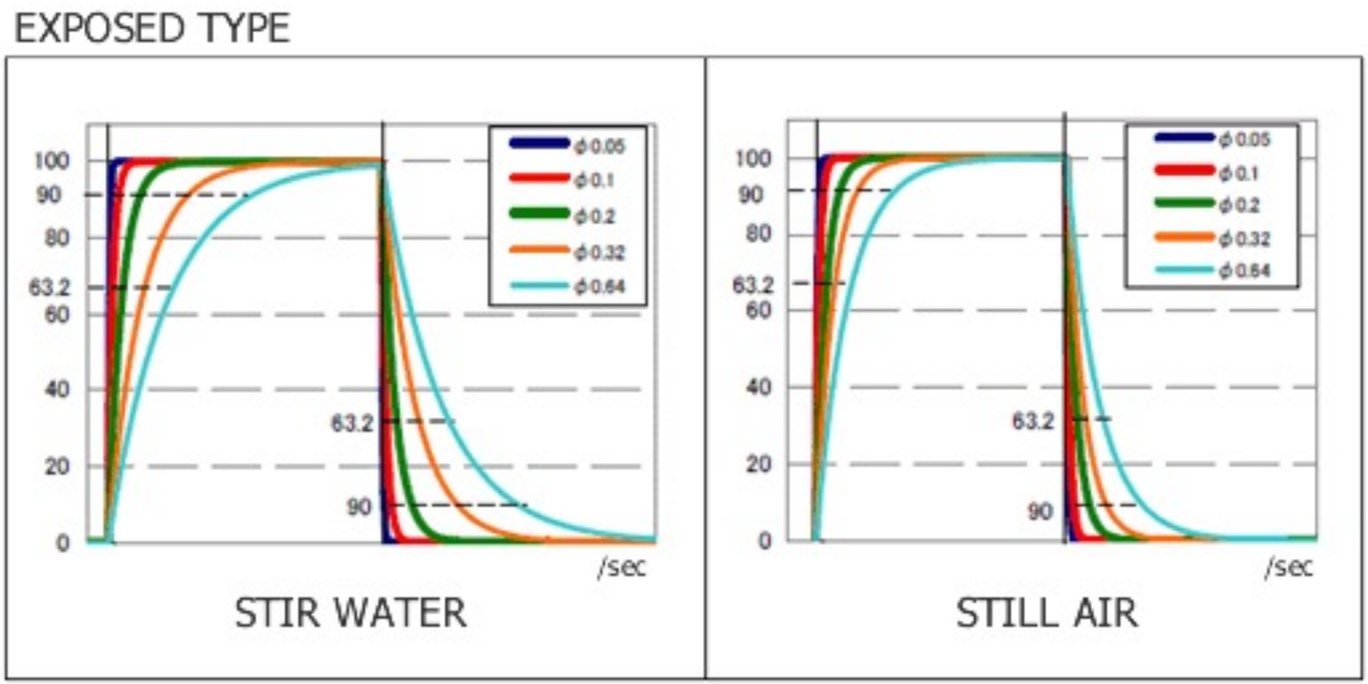

Thermocouples: Speed vs Diameter

Accuracy and Precision

Accuracy (Justesse)

The closeness of the experimental mean value to the true value.

High accuracy = Small systematic error.

Precision (Fidélité)

The degree of scatter in the results.

High precision = Small random error.

Accuracy and Precision

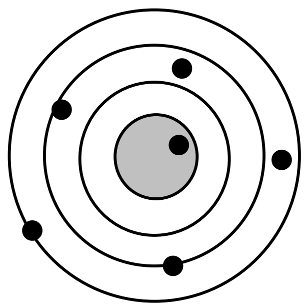

PRECISE

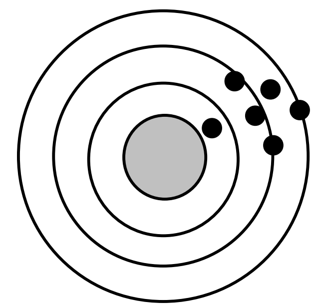

ACCURATE

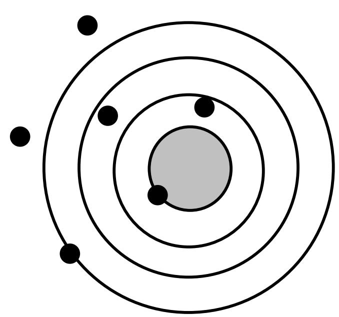

whatever…

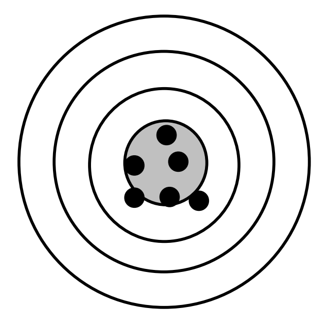

ACCURATE and PRECISE

Hysteresis

Does the output depends on past environment?

Ex: Meniscus

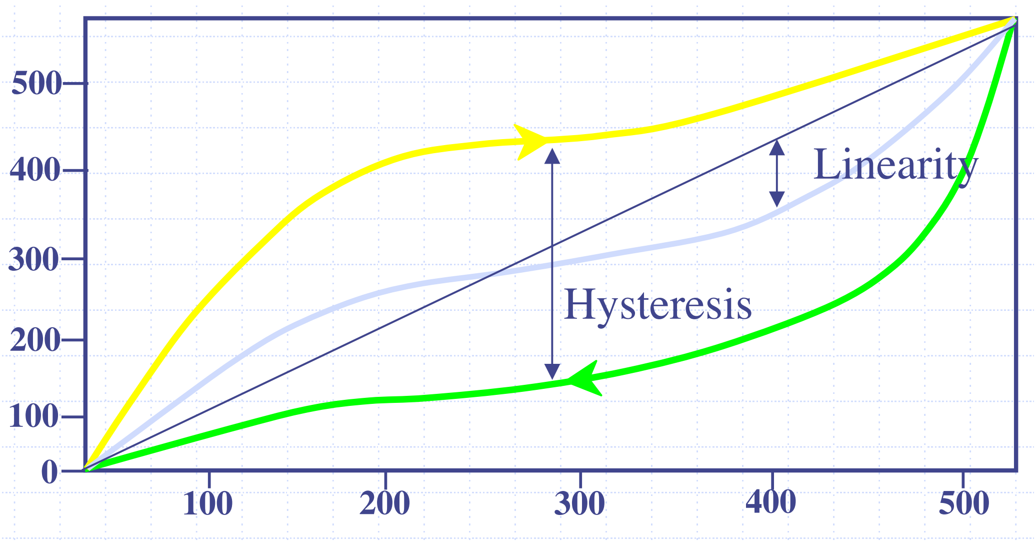

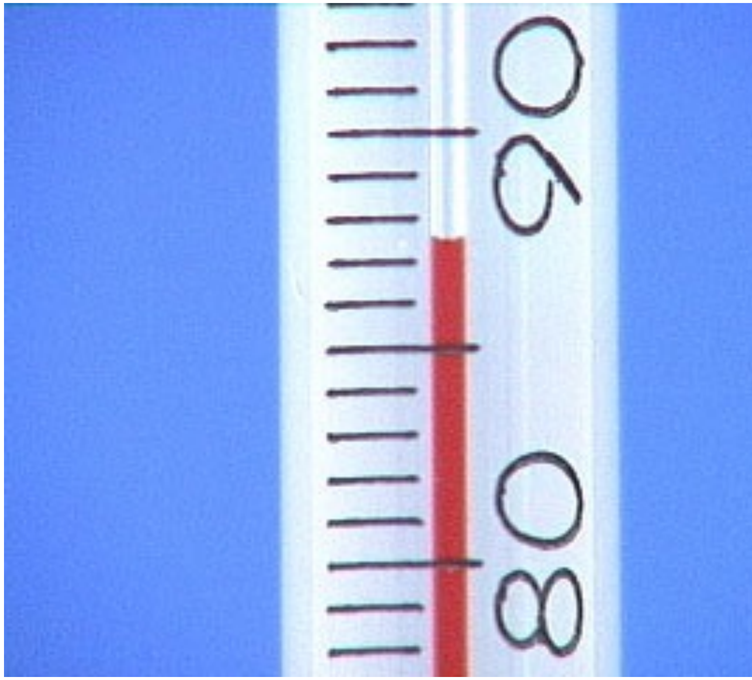

Quantization

Quantity of steps between the analog signal and the numeric value:

- Signal output
- Sampling rate

Eg: 16 bits = 65536 values for the Full Scale of the converter

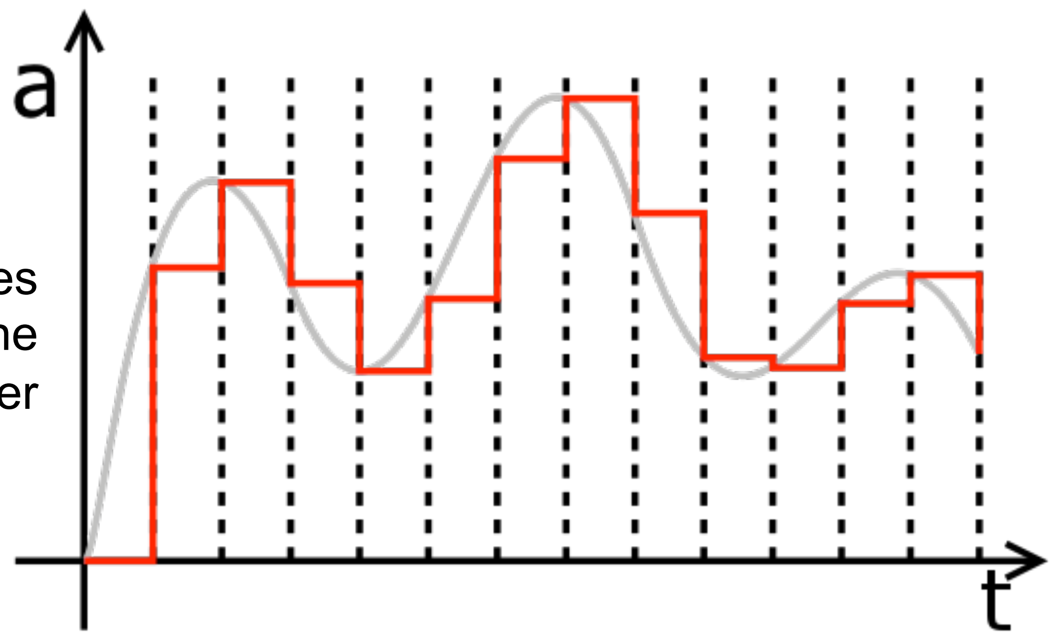

Eg: 1 ksps = 1000 values per seconds

Instrument properties

- Measurement range
- Linearity
- Hysteresis
- Stability
- Response time
- Quantization
- Accuracy
- Precision
- Repeatability
- Reproductibility
- Cost €€€-time
- …

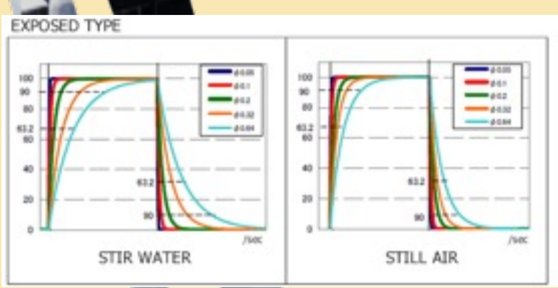

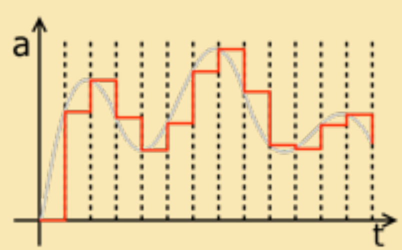

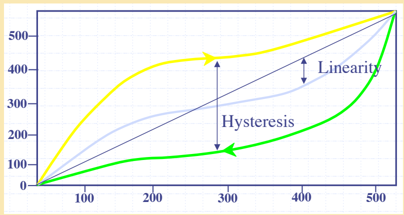

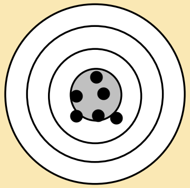

Choice of the instrument





width

***Width* of a rectangle**


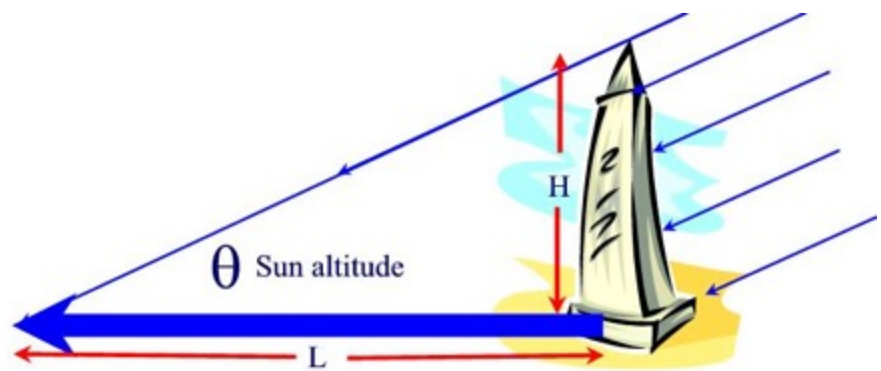

Instrument properties

There are **no perfect** sensor which has the perfect properties for all the measurements needs.

$\Rightarrow$ Need to adapt the technology and setup of the sensor to the actual requirement of measurement performance: “the size of the uncertainty”

$\Rightarrow$ **In order to save time and €€€**

$\Rightarrow$ **In order to be realistic with the environment**

Instrument properties

There are no perfect sensor which has the perfect properties for all the measurements needs.

⇒**A wished performance may be unreachable with the provided resources and the current state of the art of the Metrology**

⇒*Eg: measuring the irradiated surface temperature of a tower solar receiver at ±1 K @ 95% uncertainty: next to impossible in real field, at least for now… no ?*

Summary

LABORATOIRE
PROCÉDÉS, MATÉRIAUX
et ENERGIE SOLAIRE
.UPR 8521 du CNRS.
conventionnée avec
l'université de Perpignan

PROCESSES,MATERIALS
and SOLAR ENERGY
LABORATORY

Emmanuel Guillot
CNRS-PROMES
Odeillo, France

PROMES

UPVD

SFERA

Solar Facilities for the European Research Area

Measuring
is
Comparing

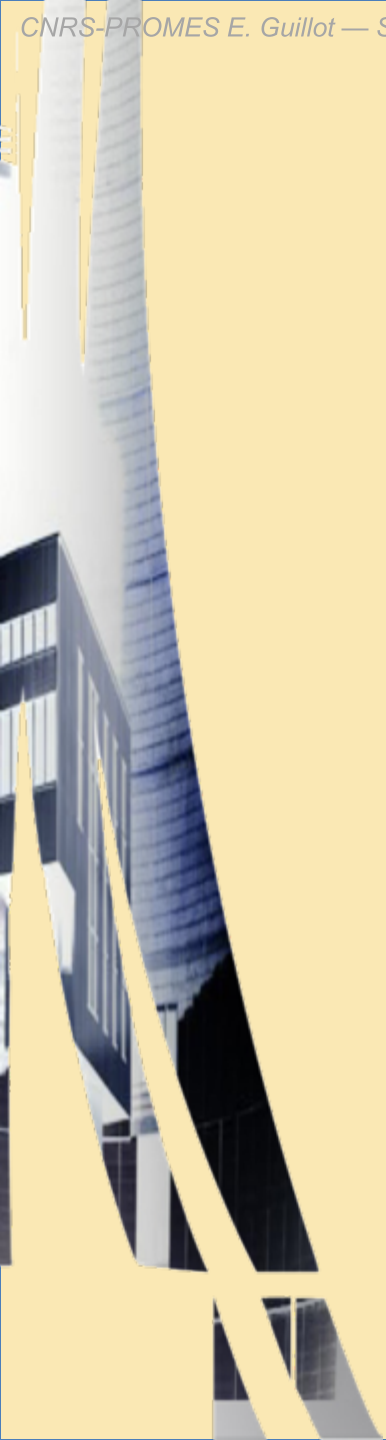

The Truth
is
Out there

Reference books about measurement *techniques*

- Béla G. Liptak

  CRC Press

  4th edition: 2005

  ISBN13: 978-084-931-0812

- Georges Asch

  Éditions DUNOD

  8th edition: 2017

  ISBN13: 978-210-076-0206

THE reference guide for uncertainties, terms

Bureau International des Poids et Mesures

http://www.bipm.org

http://www.bipm.org/en/publications/guides/gum.html

http://www.bipm.org/utils/common/documents/jcgm/JCGM_100_2008_E.pdf

http://www.bipm.org/utils/common/documents/jcgm/JCGM_104_2009_E.pdf

PROcesses, Materials and Solar Energy laboratory

PROMES

a CNRS laboratory

LABORATOIRE
PROCÉDÉS, MATÉRIAUX
et ENERGIE SOLAIRE
UPR 8521 du CNRS
conventionnée avec
l'université de Perpignan

PROCESSES,MATERIALS
and SOLAR ENERGY
LABORATORY

cnrs
www.cnrs.fr

UNIVERSITÉ
PERPIGNAN
VIA
DOMITIA

PROMES overview

A laboratory of the CNRS Institute of Engineering and Systems Sciences (INSIS)
+ agreement with University of Perpignan

Director: ***Alain Dollet***
alain.dollet@promes.cnrs.fr

Deputy Director: ***Marianne Balat-Pichelin***
marianne.balat@promes.cnrs.fr
Admin. manager: ***Naoual Autones***
naoual.autones@promes.cnrs.fr

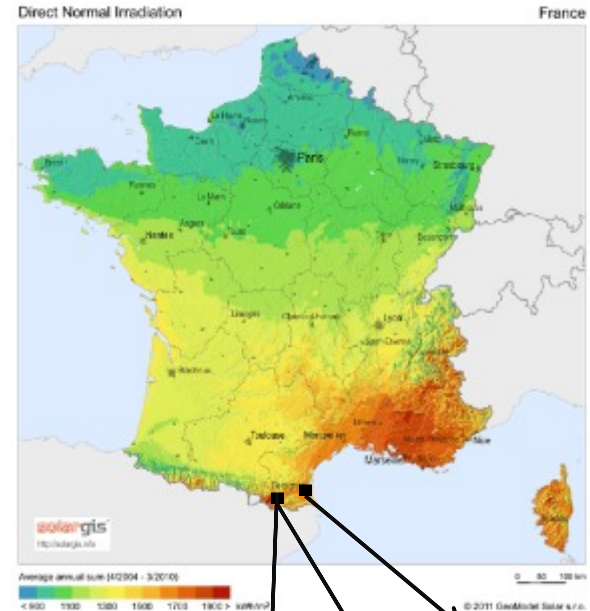

- ✓ **Staff:** about 150 people (incl. 60 students)
- ✓ **3 locations:** Perpignan, Odeillo & Targasonne
- ✓ **Original equipments:** solar furnaces (1.5 kW to 1 MW) & solar tower (5 MW)
- ✓ **Research Infrastructure** : National & European (SFERA 3 project, H2020)

CNRS
UNIVERSITÉ PERPIGNAN VIA DOMITIA
PROMES

PROMES overview

Mission

Development of Science & Technologies related to solar energy applications, mainly **concentrated solar energy**:

- ✓ ***Thermal conversion***: building heating and cooling
- ✓ ***Concentrated Solar thermal***: heat, power and fuel production
- ✓ ***Photovoltaic conversion***: new materials processing and concentrating PV (CPV)
- ✓ ***High temperature materials:*** *testing & evaluation*

PROMES overview

Large projects

- ✓ National Laboratory of Excellence in Solar Energy: "SOLSTICE"
- ✓ National Equipment of Excellence in Concentrated Solar Energy: "SOCRATE"
- ✓ European Infrastructure "SFERA3", "STAGE-STE",…
- ✓ Coordinator of H2020 projects:
  "Next-CSP" *Electricity from Gas turbine with particles*
  "PEGASE" *Electricity from Gas turbine with air receiver*
  "SolPart" *chemistry in suspended particles*

- ✓ Participates to H2020 projects:
  "RaiseLife" *improving CSP components*

PROMES Main Solar Facilities

Performances

Power : **from 1 kW to 5 MW**

Concentration: up to **16000 suns** (4000K)

Capacity to **modulate** power and flux density

Possibility to perform tests under vacuum and controlled atmosphere

Achievement of heating and cooling cycles, and very fast heating (<1s)

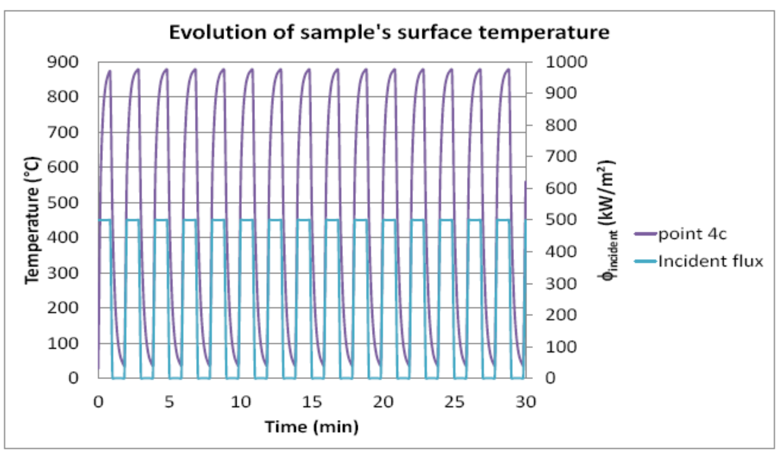

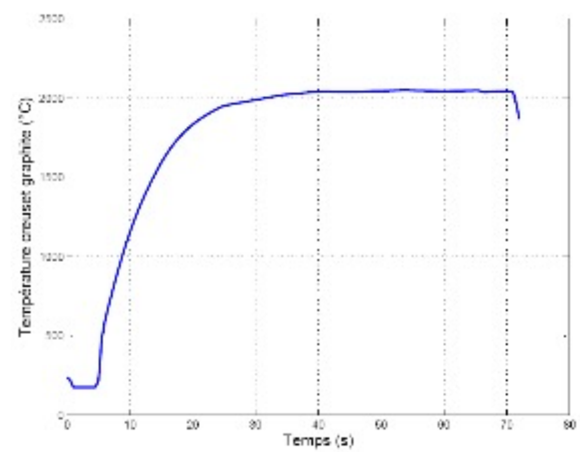

PROMES

15 Solar Facilities

- ✓ 12 Solar Furnaces (two reflections)
- ✓ 1 Dish, 50 kW (one reflection)
- ✓ 1 Parabolic trough, 150 kW (one reflection)
- ✓ 1 Solar Tower, 5 MW (one reflection)

P = 1000 kW

63 Heliostats, Parabola 54x40m,

Concentration ~ 10 000

PROMES Main Facilities

Small Solar Furnaces 6 kW, 2 kW and 1.5 kW

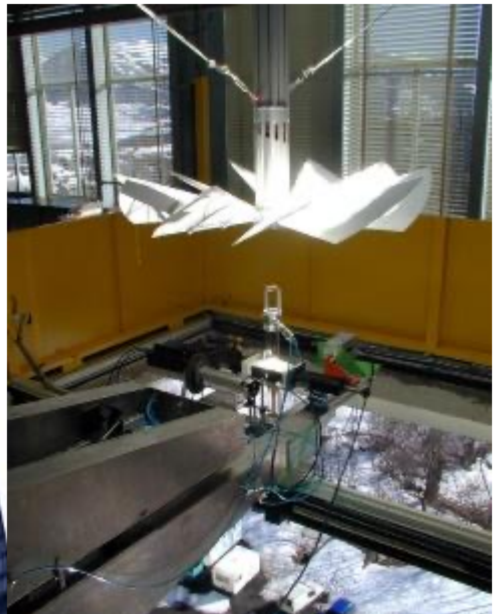

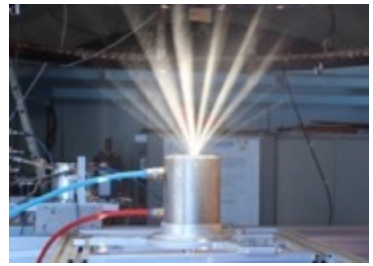

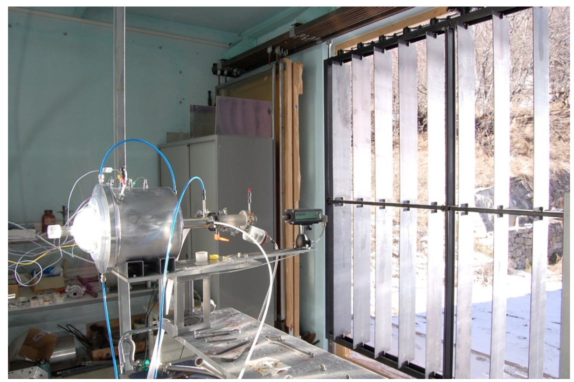

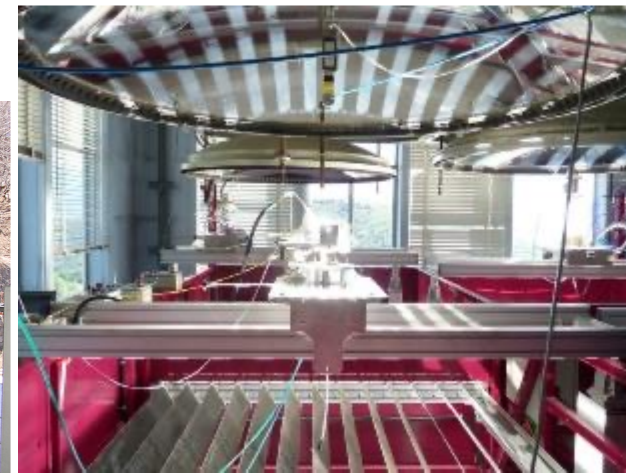

P = 6 kW
Spherical mirrors
D= 4m, S=12.5m²
f= 3.75m, d=5cm
Concentration ~ 6 000

P = 2 & 1.5 kW
Single mirror parabola
6 Units: D=2m, f=.85m, d=0.5-1cm
4 Units: D=1.5m, f= .65m, d=0.5-1cm
Concentration ~ 16 000

PROMES Main Facilities

The 1 MW Solar Furnace

P = 1000 kW
63 Heliostats
$S_{parabola}$=1830 m²
f=18 m
Concentration ~ 9 000

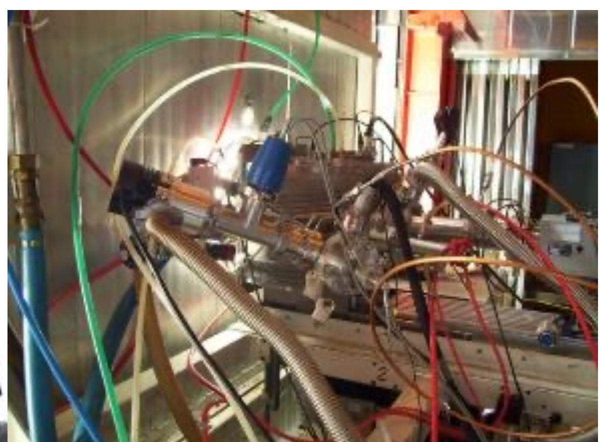

PROMES Main Facilities

Small solar plant (parabolic trough) Microsol-R

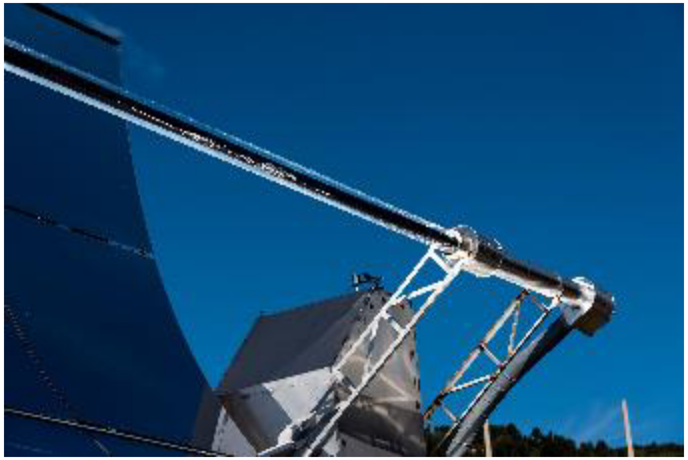

P = 150 kW
3 parabolic troughs
length: 12 m, aperture: 5,7 m
Concentration ~ 50

PROMES Main Facilities

THEMIS tower and heliostat field

P = 5000 kW
107 Heliostats 54 m²
2 focal experimental areas
Concentration ~ 2000

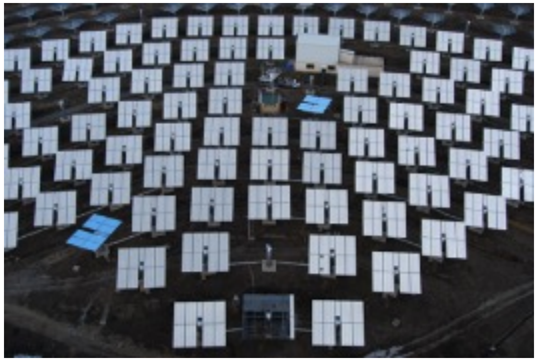

PROMES Main Facilities

Parabolic dish

P = 55 kW
Parabola d=8.5 m, 57 m², f=4.5 m
Concentration ~ 9500

Dish system configuration (Eurodish project) for electricity production from a Stirling Engine

Research teams

Domain 1 : Materials and extreme conditions

✓ **High Temperature Materials and Solar Fuels**

MHTCS team (L. Charpentier)

✓ **Photovoltaics, Plasmas, Thin Films**

PPCM team (L. Thomas)

✓ **Nanoscaled Systems and Structures :** Optical, Electronic, and Magnetic Properties

S2N team (H. Kachkachi)

Domain 2: Conversion, storage & transport of energy

✓ **Storage for Photochemical & Energetic Helioprocesses**

SHPE team (V. Goetz)

✓ **Thermophysics, Radiation & Fluid Dynamics for Solar Plants**

TRECS team (C. Caliot, A. Toutant)

✓ **Thermodynamics, Energetics and reactive Systems**

TES team (D. Stitou)

✓ **Systems control, instrumentation & characterization**

COSMIC team (S. Grieu)

✓ **Supervision, Solar Energy, Electrical Systems**

SEnSE team (T. Talbert)

cnrs
UNIVERSITÉ PERPIGNAN VIA DOMITIA
PROMES

R&D in the field of CSP & SF

Solar receivers
Materials design
(selective & HT)
Heat Transfer
New fluids

Concentrating systems
(optics)

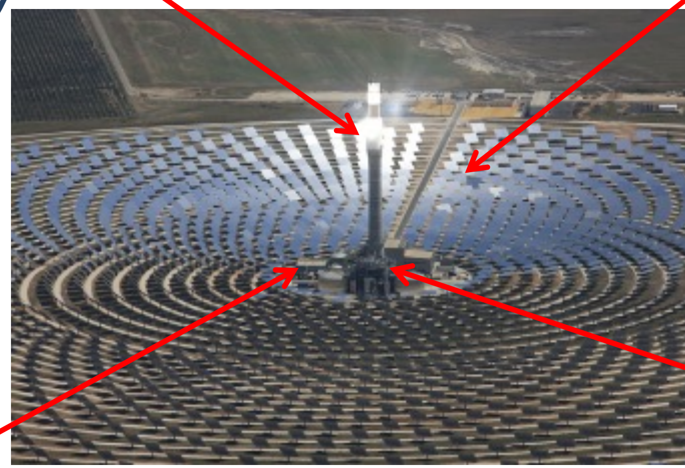

Storage
Thermal and thermochemical

Integration & Supervision

New applications:
Solar synthetic fuels
and thermochemistry

Solar resource assessment and forecasting

UNIVERSITÉ PERPIGNAN VIA DOMITIA

PROMES

From nano to commercial plants

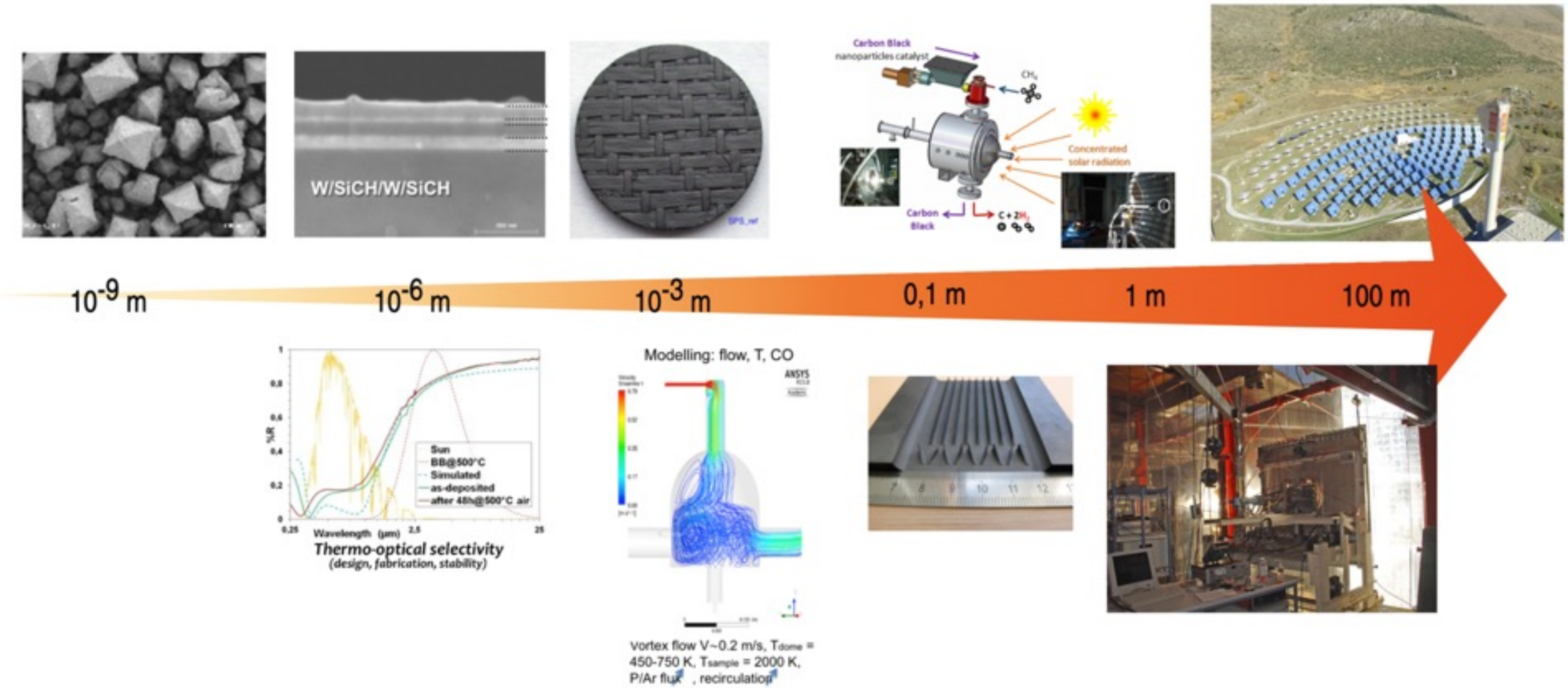

PROMES

R&D in the field of CSP & SF

❖ *Solar Receivers*

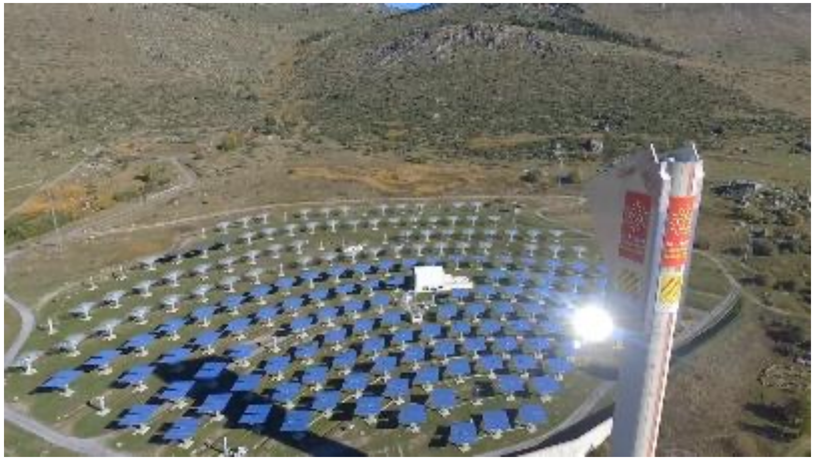

PEGASE project

- ✓ Hybrid solar gas turbine system
- ✓ Themis Solar tower facility (< 5 MWth) 550° C → 750° C → 1000° C
- ✓ Pressurized air (Brayton)
- ✓ Design (modeling), simulation & test of HT receivers (metallic, ceramic, …)

Funding until 2015: Public (Ministry of Research, Agencies) + private (EDF, TOTAL)

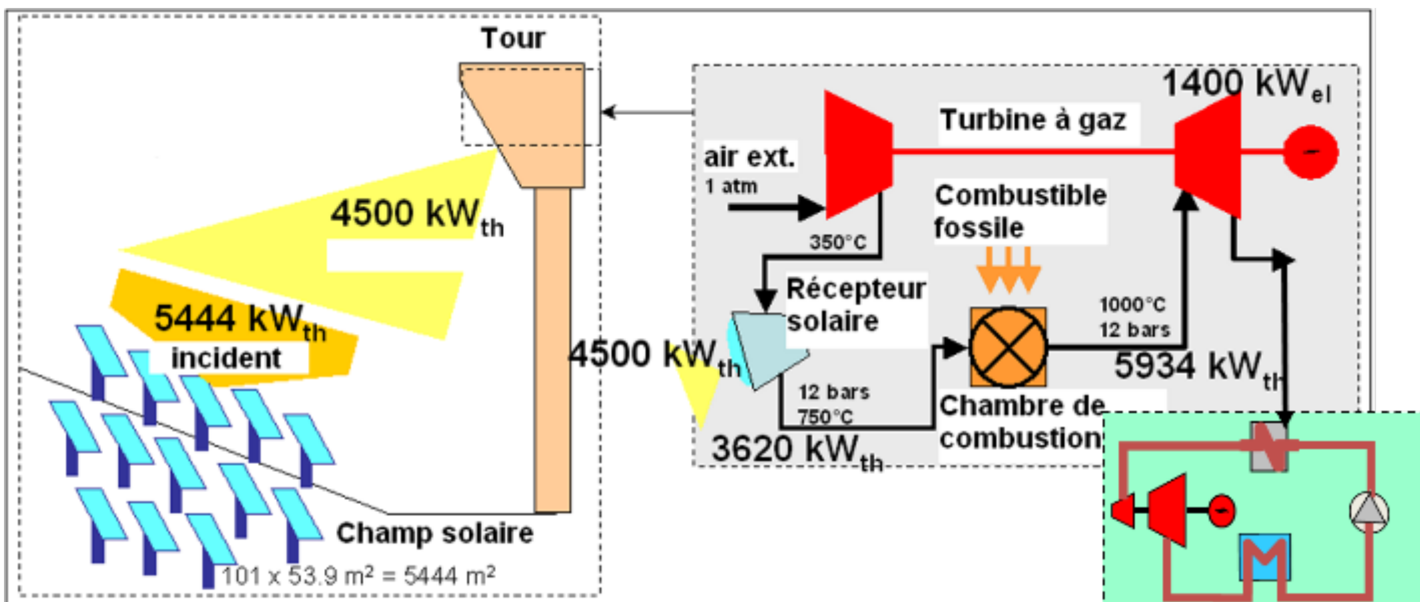

CNRS
UNIVERSITÉ PERPIGNAN VIA DOMITIA
PROMES

R&D in the field of CSP & SF

❖ *Solar Receivers (Heat transfer fluids)*

Next-CSP project

Particles receiver and thermal storage for CSP applications (→ *patented)*

Funding: EU H2020 1.8 M€, 2017-2020

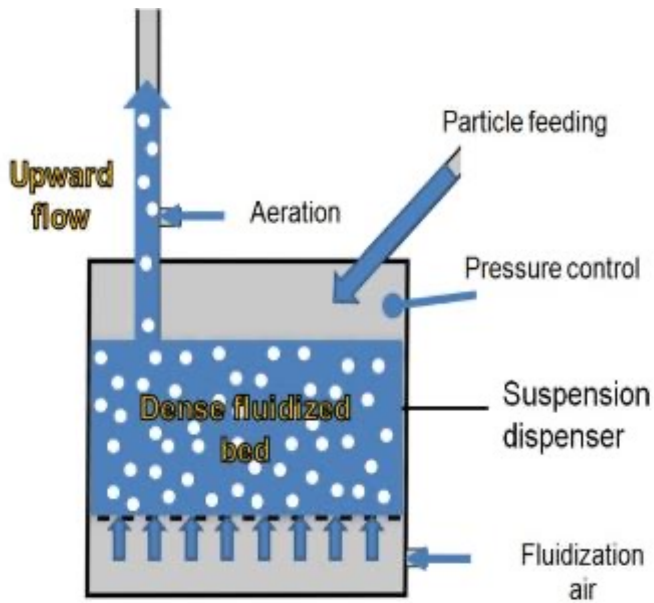

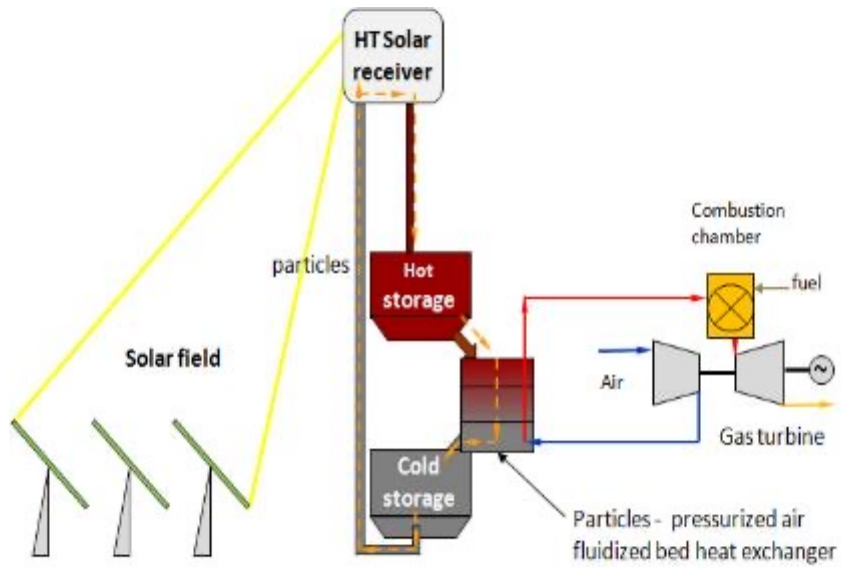

Particle-in-tubes solar receiver

R&D in the field of CSP & SF

❖ *Thermal storage (Sensible heat)*

✓ Shaped ceramic from various inorganic industrial wastes (abestos, flying ashes, …)

→ *Cofalit®, Start-up "Eco-Tech-Ceram"*

✓ Thermocline with cheap filler materials

✓ Modelling and experiments at lab and pilot scales

UNIVERSITÉ PERPIGNAN VIA DOMITIA

PROMES

R&D in the field of CSP & SF

❖ *Solar Fuels*

Solar fuels from thermochemical H_2O/CO_2 splitting cycles

✓ Metal oxide redox cycles

$$M_xO_y \rightarrow M_xO_{y-1} + ½O_2$$
$$M_xO_{y-1} + H_2O/CO_2 \rightarrow M_xO_y + H_2/CO$$

- Volatile oxides (ZnO/Zn, SnO_2/SnO…)

- *Solar reactors for thermal or carbo-thermal reduction*

- *Oxidation reactions (thermodynamics, kinetics, chemical yields)*

- Non-stoichiometric oxides (ceria, perovskites…)

- *Materials synthesis, doping, chemical reactivity over cycles (stability)*

- *Optimization of composition/morphology and solar reactor concepts*

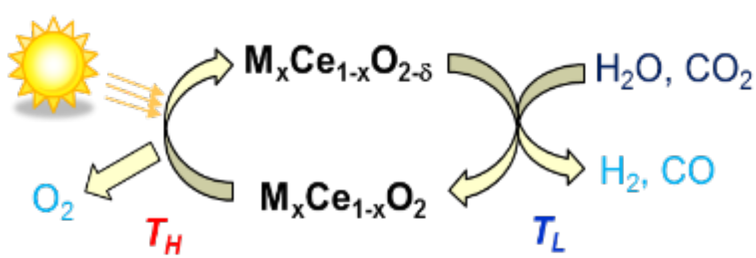

R&D in the field of CSP & SF

❖ *Solar Fuels*

Hydrogen/syngas production from hydrocarbon resources

✓ Methane decomposition (thermal / catalytic): $CH_4 \rightarrow C + 2H_2$

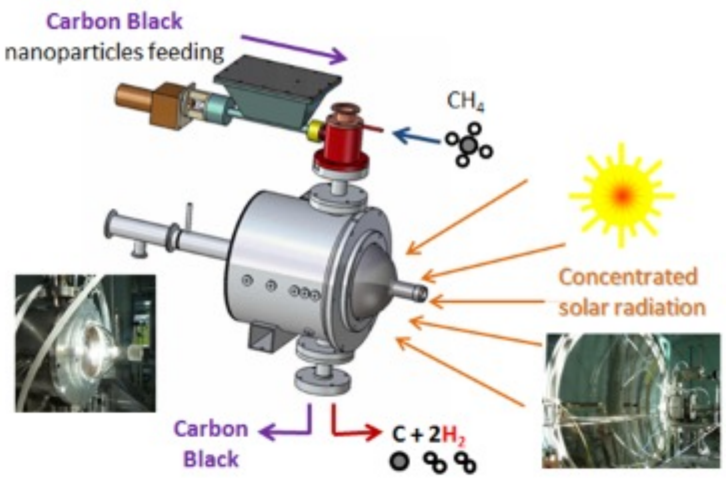

✓ Methane reforming for syngas production with oxygen carriers :

$CH_4 + MO \rightarrow M + CO + 2H_2$

$M + H_2O \rightarrow MO + H_2$

$= CH_4 + H_2O \rightarrow CO + 3H_2$

✓ Solar biomass gasification

→ *Testing of a continuously-fed tubular reactor for wood gasification*

R&D in the field of CSP & SF

❖ *Supervision & integration*

Solar resource assessment and forecasting

- ✓ Development of intra-hour forecasting models (GHI/DNI) based on the concept of time series, satellite data, or sky-imaging data
- ✓ Development and calibration of ground-based cameras equipped with ultra wide-angle lens (i.e. sky imagers) and High Dynamic Range (HDR) imaging
- ✓ Development of predictive strategies for optimal management (control) of photovoltaic (PV) and Concentrated Solar Power (CSP) plants

Electrical systems

- ✓ Development of electric energy conversion architectures (PV, CPV)
- ✓ Command and measurements systems in real time; fault detection strategies (PV) for smart-grids (cooperation with “La Compagnie du vent”)

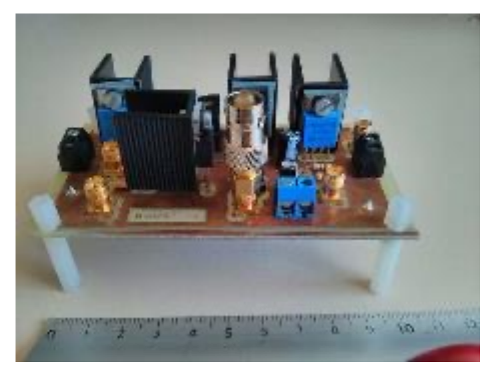

cnrs

UNIVERSITÉ PERPIGNAN VIA DOMITIA

PROMES

R&D in the field of High Temperature Materials

- ✓ Data implementation for DEBRISK code from CNES France for space debris mitigation: new oxidation laws in air plasma conditions and new thermo-radiative properties @ HT

- ✓ Participation to the IXV project (ESA, launched 11/02/2015) and Solar Probe Plus mission (NASA) to be launched in 2018: qualification of some parts of the instrumentation @ HT

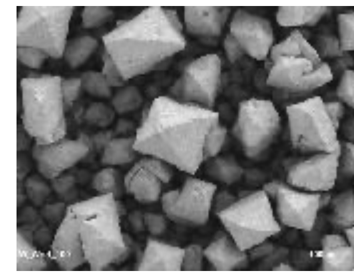

- ✓ HT characterization of new UHTC ceramics for future solar receivers (ANR project 2016-2019)

- ✓ Carbo-reduction by concentrated solar energy for future transportation using metal fuels in collaboration with PSA Peugeot-Citroën group

Solar metallurgy

Carbothermal reduction of MgO & Al_2O_3 at low pressure

Objectives:

✓ Regeneration of metallic oxides obtained by combustion processes for automotive applications (external combustion engine)

Methodology:

✓ **Feasibility and optimization of experimental parameters**
- Grain size/stoechiometry of reactants, reducing agent, P, T, duration…
- Conception of a reactor **Sol@rmet:** fluid mechanics, analysis of output gases to follow the reaction, condensation of the products

✓ **Qualitative and quantitative controls of the formed products**
- By-products, grain size and morphology…

✓ **Obtention of high yield and determination of technological issues to further develop the process**

cnrs

UNIVERSITÉ PERPIGNAN VIA DOMITIA

PROMES

Energetics and thermochemical systems

- Thermochemical processes for thermal energy storage & management
- Low grade heat energy conversion by thermo-hydraulic processes
- Optimization and economic models for energy

  - ✓ Autonomous reverse osmosis desalination by solar thermo-hydraulic process (DEPOTHS, SATT AxLR maturation project)
  - ✓ Solar cooling of autonomous telecommunication stations in desert areas using a thermochemical process (DACSOL project - SATT AxLR maturation project)

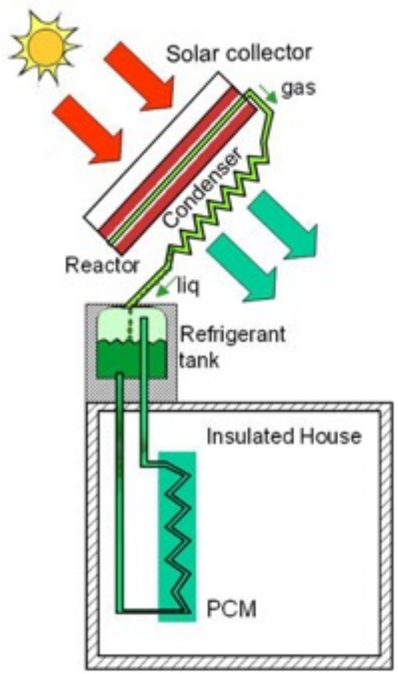

Detoxification of effluents with solar advanced oxidation processes

Solar outdoor oxidation performed on effluents collected at the outlet of water treatment plants (IRD-HSM, Sudoe Innovec Eau).

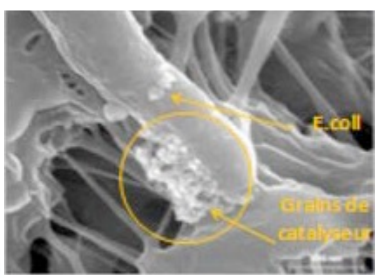

Modeling solar inactivation of E coli: coupling between mass transfer and membrane attack by free radicals (LBE INRA).

Félix TROMBE

Directeur de Recherches au C.N.R.S.

Directeur du Laboratoire de l'Energie Solaire du C.N.R.S. (Montlouis-Odeillo)

Président d'honneur de la Société Préhistorique de l'Ariège

50

1969 - 2019

Four Solaire d'Odeillo

Odeillo: 50 years

cnrs 80

Depuis 80 ans, nos connaissances bâtissent de nouveaux mondes

PROMES

UNIVERSITÉ PERPIGNAN VIA DOMITIA

CNRS: 80 years

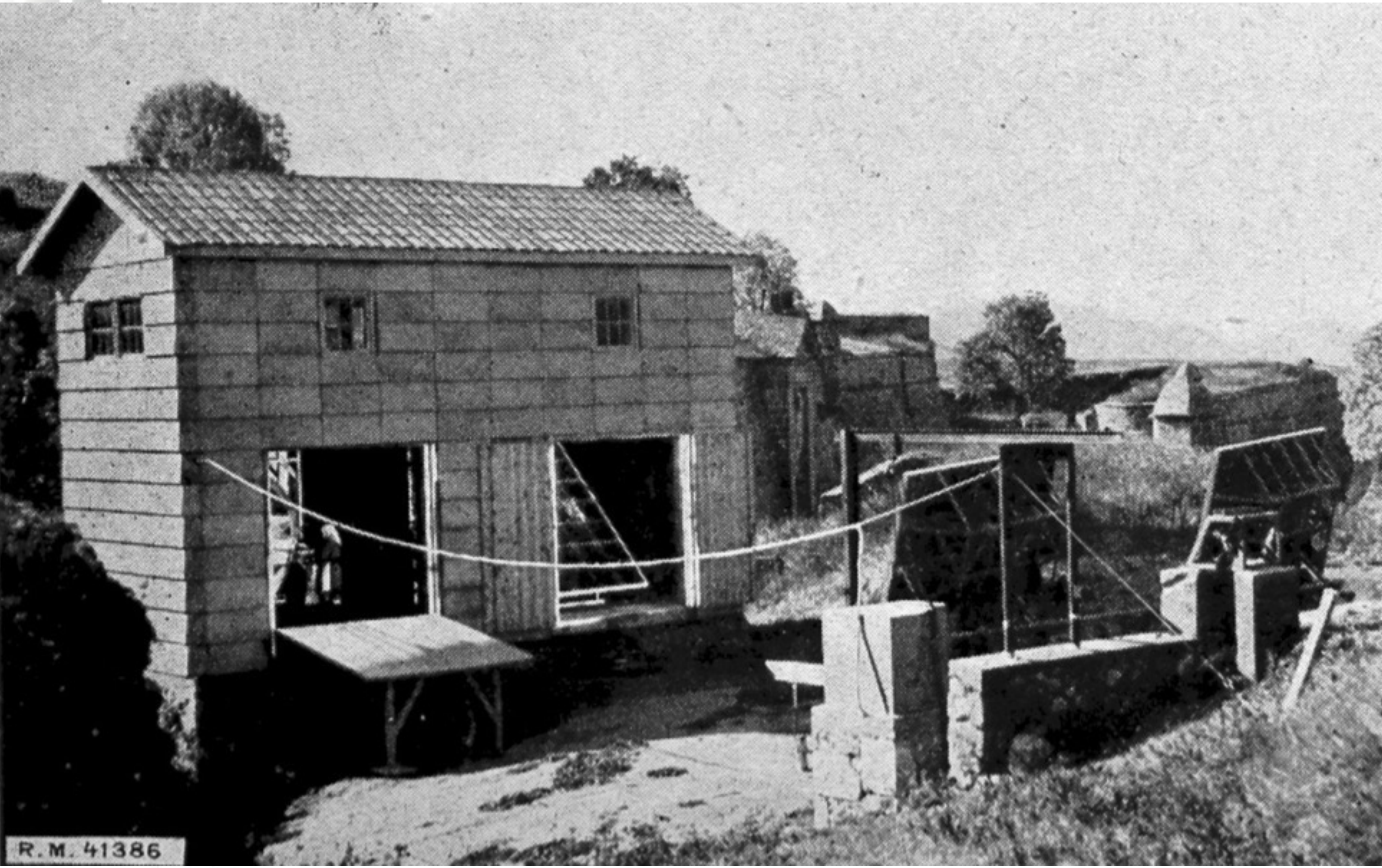

Mont Louis, 1949

70 years ago…

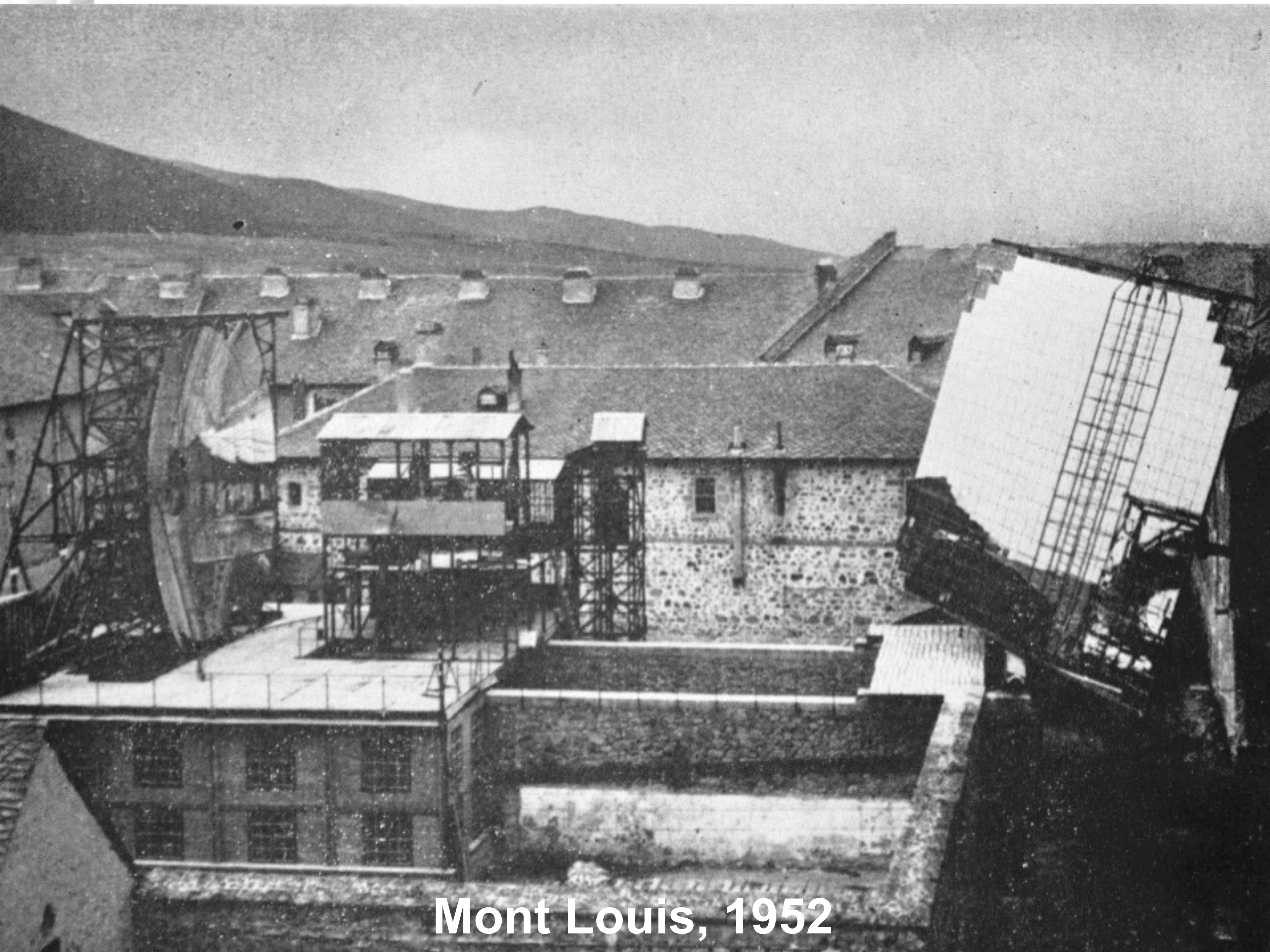

Mont Louis, 1952

https://www.promes.cnrs.fr

R&D in the field of CPV

CPV module characterization

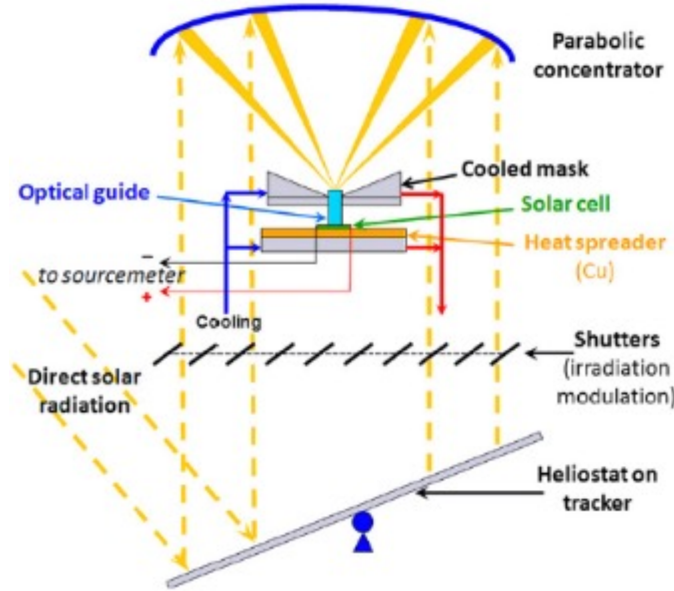

Solar cell characterization under ultra-high flux (up to 9000 suns)

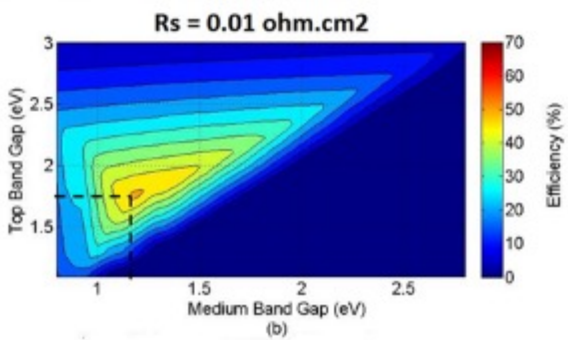

Modelling and optimization of multi-junction stacks

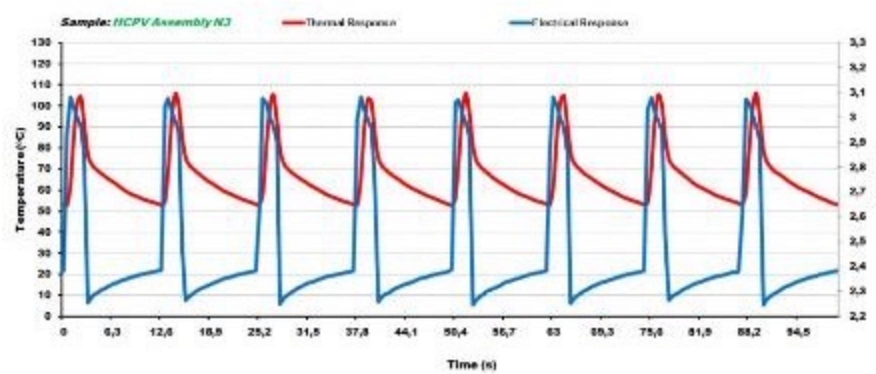

Accelerated ageing of SC

The Sol@rmet reactor - 2 kW solar furnace

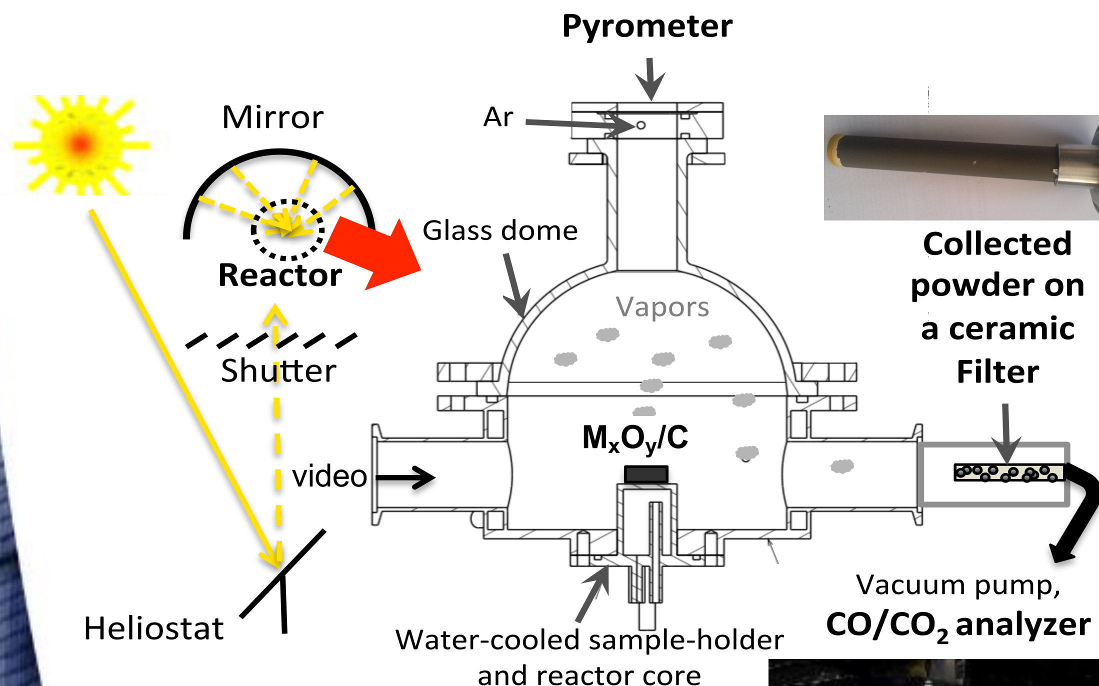

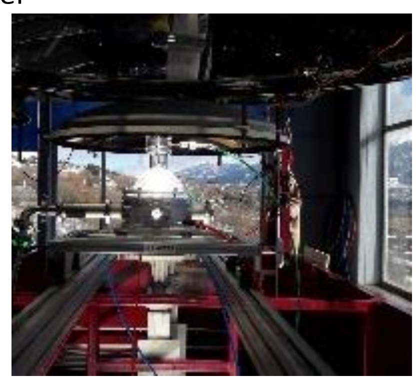

Modelling: flow, T, CO

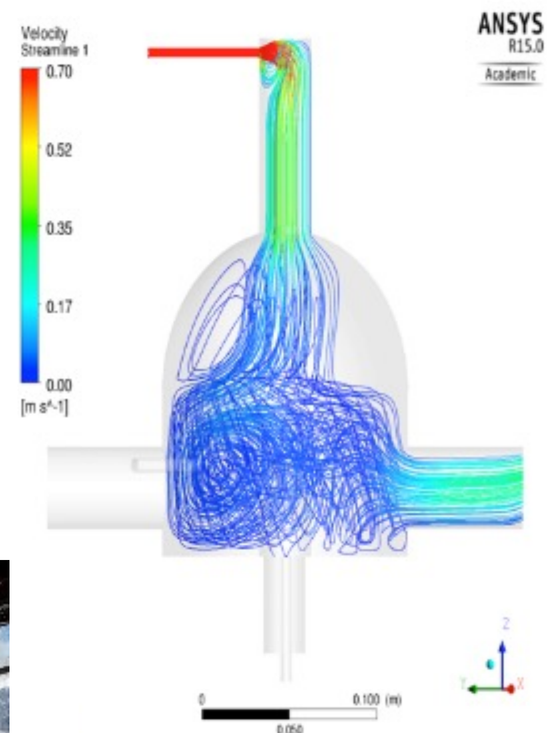

Vortex flow V~0.2 m/s, T_{dome} = 450-750 K, T_{sample} = 2000 K, P/Ar flux ↗, recirculation ↗

Air-tight reactor with direct solar irradiation
Measurement of T and reaction extent (CO/CO_2 analysis)

Ex: carboreduction of MgO @ 880 Pa

- Few Mg produced at 1700-2000 K contrary to thermodynamics
- @ 2200 K, 81% Mg (XRD with standards) with some recombination issues

Agglomerated powders obtained with « clean » micron-sized crystals (2-15 µm)

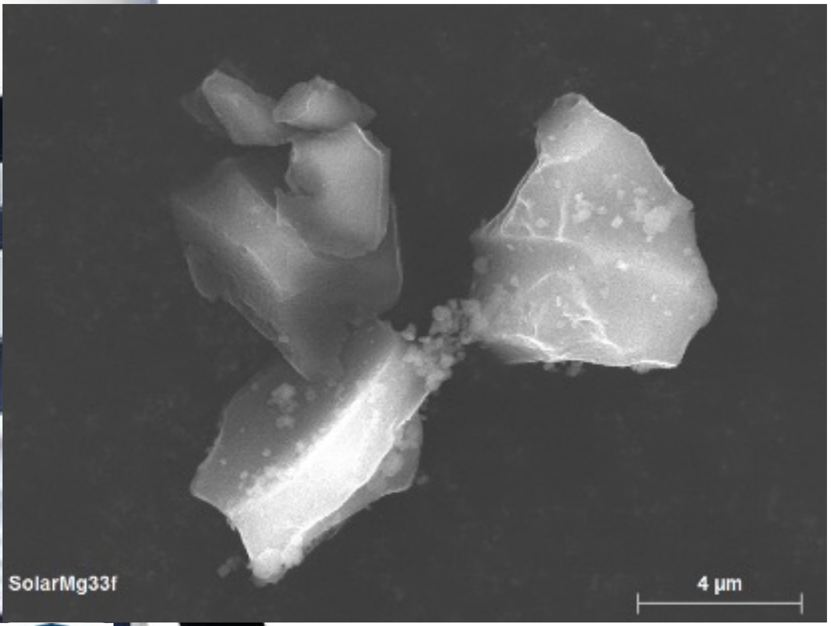

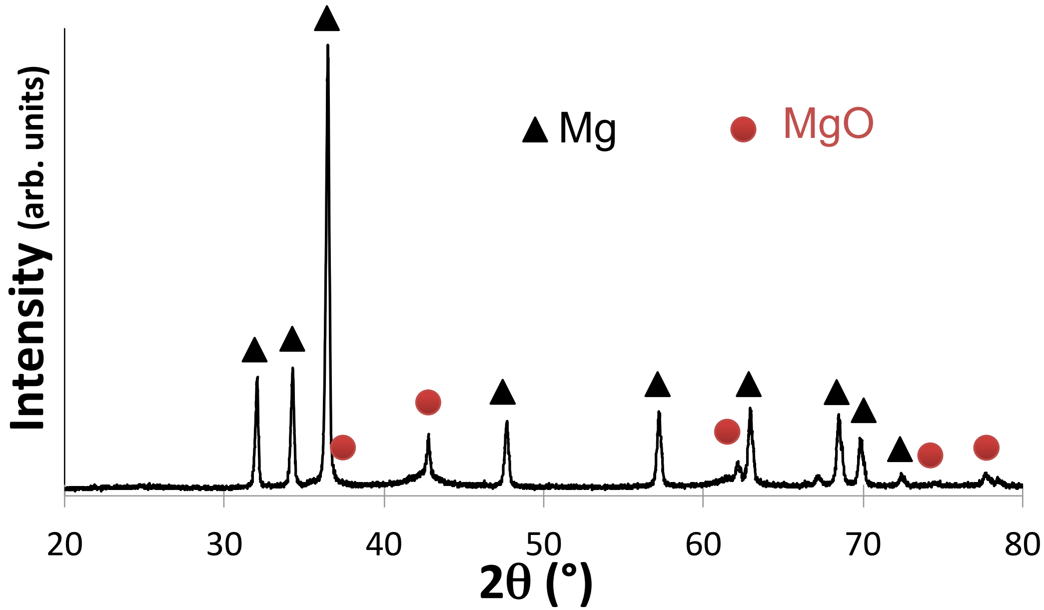

Perspectives:

- continuous process with less recirculation of gases and higher masses of reactant
- study of the condensation process of Mg (recombination with CO_2, temperature gradient in the reactor) at 880 Pa and at lower pressure

Electromagnetic energy conversion & magneto-optical properties in nano-structured media

Understanding & optimization of EM energy absorption, conversion & transfer

- ✓ *Channels for energy transfer (magnons, plasmons, excitons, phonons, hot electrons)*
- ➢ *Applications: Hyperthermia, photocatalysis, photovoltaics*

Microscopic study of plasmons & their interactions with other excitations in hybrid nanostructures:

- ✓ *Effect of material, size, shape, medium, spatial arrangement*
- ✓ *Effect of **magnetism** (intrinsic and/or external)*

Coll. A. Trügler, Univ. Graz

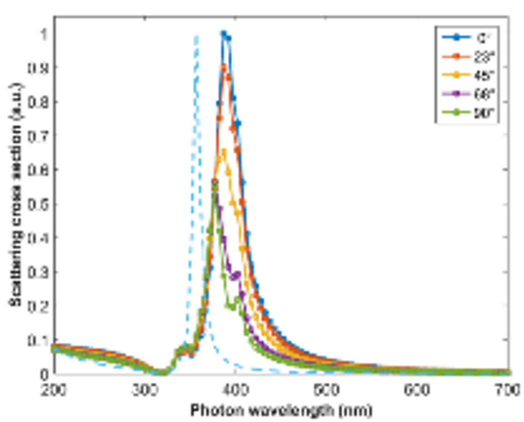

Spectra of Au-NP arrays

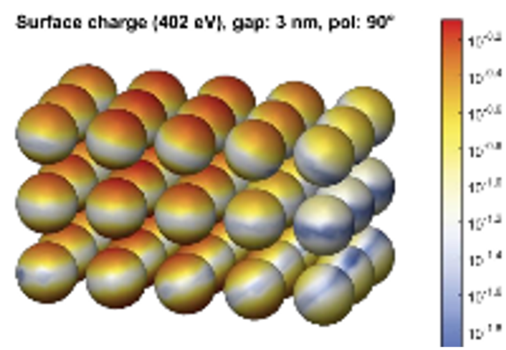

Plasmon coupling